DYSTROGLYCAN-DEPENDENT MODULATION OF
AQUAPORIN-4 DISTRIBUTION:
A NEW TARGET TO PREVENT BRAIN EDEMA

by

Geoffroy Pierre Jean-Claude Noël

Licence, Université Pierre et Marie Curie Paris VI, 2003
M.Sc., Université Claude Bernard Lyon I, 2005
Magistère, Ecole Normale Supérieure Paris, 2005

A THESIS SUBMITTED IN PARTIAL FULFILLMENT OF
THE REQUIREMENTS FOR THE DEGREE OF

DOCTOR OF PHILOSOPHY

in

The Faculty of Graduate Studies

(Anatomy)

THE UNIVERSITY OF BRITISH COLUMBIA
(Vancouver)

August 2010

ABSTRACT

Aquaporin-4 (AQP4) constitutes the principal water channel in the brain and is mainly clustered at the perivascular astrocyte endfeet. This polarized distribution is of major importance because it enhances water fluxes thereby modulating brain swelling in different pathophysiological conditions. Evidence points to a role of the dystroglycan (DG) complex in the localization of AQP4. To investigate *in vivo* the role of extracellular matrix (ECM) ligand-binding to glycosylated sites on DG in the polarized distribution of AQP4, I used the Large^{myd} mouse that presents defective O-glycosylation of DG and found a loss of AQP4 at astrocyte endfeet. Using a mixture of ECM molecules present at the perivascular basal lamina, I found that DG clustering is regulated by laminin in astrocyte cultures. Furthermore, I show that laminin induces a reduction in AQP4-mediated water transport. Subsequently, the analysis of cell surface compartmentalization of AQP4 showed that it depends on both cholesterol and DG. Further experiments revealed an interdependent regulation between laminin binding to DG and lipid raft reorganization. I next investigated the signaling events that may be involved in the coclustering of AQP4 and DG in astrocytes. An increase in tyrosine phosphorylation was observed at 3h in laminin-treated astrocytes and this was concomitant to the maximum laminin-induced clustering of lipid rafts and AQP4. I identified the protein-serine kinase C delta (PKCδ) as one of the main kinases exhibiting an increase in tyrosine phosphorylation upon laminin treatment. The inhibition of PKCδ showed that it is involved not only in the regulation of the laminin-induced clustering of AQP4 but also in AQP4-mediated water transport in astrocytes. Given the crucial role of AQP4 distribution in brain edema, I finally focused on the identification of drugs modulating the laminin-dependent AQP4 clustering which may prevent brain edema. By screening a chemical library, I identified 6 drugs and found that chloranil prevents AQP4 clustering by activating metalloproteinases that cleave DG. These findings revealed the molecular mechanisms regulating the laminin-induced and DG-dependent clustering of AQP4 at astrocyte endfeet and provide a tool to identify modulators of AQP4 clustering that will be tested in models of brain edema.

TABLE OF CONTENTS

LIST OF TABLES

LIST OF FIGURES

LIST OF ABBREVIATIONS

AchR   acetylcholine receptor

ADAMTS   a disintegrin and metalloproteinase with thrombospondin motifs (adamlysins)

AQP   aquaporin

AQP4M1   aquaporin-4 isoform M1

AQP4M23   aquaporin-4 isoform M23

ASIC   activate acid-sensing ion channel

ATP   adenosine-5'-triphosphate

BBB   blood-brain barrier

BMD   Becker muscular dystrophy

BNB   blood-neural barrier

BRB   blood-retina barrier

Ca^{2+} calcium ion

cDNA   complementary deoxyribonucleic acid

Cl^- chloride ion

ClC   chloride channel

CNS   central nervous system

CSF   cerebro-spinal fluid

CtxB   cholera toxin subunit B

DAP   dystroglycan-associated protein

DB   dystrobrevin

DG   dystroglycan

DMD   Duchenne muscular dystrophy

DMEM   Dulbecco's modified Eagle's medium

Dp   dystrophin

DRM   detergent-resistant membrane

DRP   dystrophin-related protein

E   embryonic day

EAAT	excitatory amino acid transporter
ECM	extracellular matrix
ECS	extracellular space
ERGs	electroretinograms
ERK	extracellular signal regulated kinase
FAK	focal adhesion kinase
FCMD	Fukuyama congenital muscular dystrophy
FITC	fluorescein isothiocyanate
FKRP	fukutin-related protein
GD1	IV NeuAc,III 6 NeuAcGg Ose_4-ceramide
GFAP	glial fibrillary acidic protein
GLAST	Na^+-coupled L-glutamate/L-aspartate transporter
GlcNAc	N-acetylglucosamine residue
GLUT	glucose transportert
GLT	glutamate transporter
GM1	monosialotetrahexosylganglioside
H^+	hydrogen ion
HCO_3^-	bicarbonate ion
IL-1β	interleukin-1 beta
ILM	inner limiting membrane
INL	inner nuclear layer
IPL	inner plexiform layer
JNK	c-jun N-terminal kinase
K^+	potassium ion
KCC	potassium chloride cotransporter
Kir	inward-rectifier potassium channel
Kv	voltage-dependent potassium channel
LAT	L-type amino acid transporter
LG	laminin G domain
LGMD	limb-girdle muscular dystrophy

MAPK	mitogen-activated protein kinase
MCA	middle cerebral artery
MCT	monocarboxylate transporter
MD	muscular dystrophy
MDC	congenital muscular dystrophy
MEB	muscle eye brain disease
Mg^{2+}	magnesium ion
mGluR	metabotropic glutamate receptor
MMP	matrix metalloproteinases
MRI	magnetic resonance imaging
MTLE	mesial temporal lobe epilepsy
Na^+	sodium ion
NAPDH	nicotinamide adenine dinucleotide
NCCa-ATP	calcium (Ca^{2+})-activated, $[ATP]_i$-sensitive non-selective cation channel
NMDA	N-methyl-D-aspartic acid
NMJ	neuromuscular junction
NO	nitric oxide
NOS	nitric oxide synthase
NPA	Asparagine-Proline-Alanin
NPPB	5-nitro-(3-phenyl- propylamino) benzoic acid
NR	NMDA receptor subunit
NtA	N-termical agrin domain
OAPs	orthogonal array of particles
ONL	outer nuclear layer
OPL	outer plexiform layer
P2Y	purinergic receptor
PAGE	polyacrylamide gel
PAK	Rac/p21-activated kinase
PBS	phosphate-buffered saline
PDBu	phorbol 12, 13-dibutyrate

PDZ	PSD-95, Dlg and Zo-1
PI3K	phosphoinositide 3-kinase
PKC	protein kinase C
PMA	phorbol 12-myristate-13-acetate
POMGnT	2-N-acetylglucosaminyltransferase
POMT	protein O-mannosyltransferase
PTZ	pentylenetetrazol
Pyk	protein-rich tyrosine kinase
RNS	reactive nitrogen species
RMP	resting membrane potential
ROS	reactive oxygen species
RVD	regulatory volume decrease
S180	serine 180 of AQP4
SAST	syntrophin-associated serine/threonine kinase
SDS	sodium dodecyl sulfate
siCTL	control scrambled siRNA
siRNA	small interference RNA
TfR	transferrin receptor
TNFα	tumour necrosis factor alpha
VDAC	voltage-dependent anion channel
VEGF	vascular endothelial growth factor
VRAC	volume-regulated anion channel
VSOAC	volume-sensitive organic osmolyte-anion channel
VSOR	volume-sensitive outwardly rectifying chloride channel
WWS	Walker-Warburg syndrome

ACKNOWLEDGEMENTS

A thesis is not possible without a rich and favourable professional and personal entourage.

I want to express my gratitude to my supervisor for welcoming me in her laboratory, for her corrections of my papers and for her trust to give me full autonomy in my projects, initiatives and collaborations. Thanks also to my committee members for their questions and critical ideas.

Many thanks to two extraordinary meticulous colleagues, Eric Guadagno and Daniel Tham, who understood my rigour. It was such a pleasure to work with you. I want to extend this acknowledgement to Sarah Stevenson who has been the best co-op student a grad student could ever dream of.

A special thanks for Prof. Wayne Vogl and Dr. Claudia Krebs for not only being the role model that students need but also for the opportunities they offered me to discover the world of medical education. I want to extend this acknowledgement to the anatomy teaching team of both Faculties of Medicine and Dentistry at University of British Columbia for the great working atmosphere that allowed me to fulfill my vocation.

Among the students that shared graduate school with me, I want to thank; Dr. Marcia Graves, Pascal St-Pierre and Spencer Freeman for discussing my ideas; Dr. Kamal Garcha, Dr. Patrick Lajoie, Dr. Martin Williamson and Dr. Charles Lai for their advice in the PhD program; Maxence Le Vasseur, Dr. Cima Cina, Dr. Michael Kozoriz, Dr. Sarah Christine Lidstone, Maria Fairbank, Mytyl Aiga, Annie Aftab, Yu Sun, Christie McShane, Enzo Macri, Sarah Chow, Chris Peters, Steve Bound for making graduate school more friendly and exciting; and finally J'Nelle Young, Hamed Nazzari and Brenda for sharing my passion for teaching.

I want to finally thank Dr. Jacky Goetz and Audrey Zehner for being my family in Canada, Erin Currie and Kathryn Westendorf for all the culture, open-mind and generosity Canada can be proud of.

I am deeply grateful to Natalie Tam for her support and her trust in me. She offered me the healthy balance a man needs to move forward in life in addition to challenging me and opening my mind on the new world.

DEDICATION

"*Les voyages forment la jeunesse*".

Ces mots ont résonné a jamais pendant cette aventure du doctorat.

Ma thèse fût un voyage intellectuel et spirituel. Bien plus que la découverte d'une nouvelle culture, d'un nouveau systeme éducatif ou d'une approche plus réactive de la recherche, elle fût une exploration de moi-même. Ma patience ainsi que ma résistance à l'échec et à la pression ont été fortement malmenées. Mes motivations et mes valeurs ont même été remodelées. Heureusement, mes raciness, à toujours ancrées, m'ont permis de finir cette thèse fortifié et assagi.

Mes parents, mes grand-parents et ma soeur m'ont offert tout l'amour, le soutien, la confiance, l'écoute et les encouragements sans lesquels tout ceci n'aurait pu avoir lieu.

Cette thèse est la continuation de votre éducation.

Pour tata

Pour titi

CO-AUTHORSHIP STATEMENT

The contribution of the different authors involved in the five manuscript chapters included in this thesis can be described as follow:

First manuscript
The immunofluorescence and staining experiments in Figures 2.5, 2.8, 2.9 and 2.10 were carried out by Jennifer Rurak, the primary author of this manuscript.
The immunofluorescence experiments and imaging in Figures 2.3 and 2.7 as well as the immunoblotting experiments in Figure 2.4 were carried out by its secondary author Geoffroy Noël.
The immunofluorescence experiments and imaging in Figures 2.1 and 2.2 were carried out by Leona Lui.
The RT-PCR data in Figures 2.6 were generated by Bharat Joshi.

Second manuscript
All the components of this manuscript were produced by its primary author, Geoffroy Noël, with the exception of the biotinylation experiments in Figure 3.1G carried out by Daniel Tham.

Third manuscript
All the components of this manuscript were produced by its primary author, Geoffroy Noël, with the exception of the fluorescence recovery after photobleaching analyses in Figure 4.3 carried out by Daniel Tham.

Fourth manuscript
All the components of this manuscript were produced by its primary author, Geoffroy Noël, with the exceptions of the Kinex antibody analyses in Figure 5.4 carried out by Kinexus Bioinformatics Corporation and the quantitative analyses in Figure 5.2G carried out by Eric Guadagno.

Fifth manuscript
All the components of this manuscript were produced by its primary author, Geoffroy Noël, with the exception of the screening analyses in Figures 6.1, 6.2, 6.3 and Table 6.1 carried out by Sarah Stevenson.

All the manuscripts were written under the supervision and guidance of Dr. Hakima Moukhles.

1 INTRODUCTION

1.1 Cerebral edema

Excess accumulation of brain water, or cerebral edema, is a potentially lethal complication caused by a variety of pathological conditions that affect the brain. It can result from almost any intracranial insult including trauma, infarction, ischemia, neoplasm, infection or extracranial metabolic perturbations (1-5). It is associated with five separate pathophysiological processes with distinct molecular and physiological antecedents; cytotoxic, vasogenic, interstitial, hyperaemic and osmotic. In 1967, Klatzo I. et al. (6) was the first to describe the cerebral edema with its two main components, cytotoxic and vasogenic, distinct by the integrity of the blood-brain barrier (BBB). In the normal adult brain, water is distributed between the cerebro-spinal fluid (CSF, 75-100 mL), blood (75-100 mL), intracellular content (1,100-1,300 mL) and the interstitial cerebral space (100-150 mL). Under physiological conditions, the osmolarity of extracellular and intracellular fluids is equal. However, pathophysiological variations of extracellular or intracellular osmolarity can generate osmotic gradients that lead to excessive water flow. Between the blood and the brain, the BBB, if intact, behaves like a semi-permeable membrane allowing water transport according to the osmotic laws. The movement of water is driven by differences in the concentration of solute particles (also referred to as osmolytes) on either side of the membrane with water flowing down from the solution with a lower osmolyte concentration into the solution with a higher concentration.

Upon ischemic or hypoxic stress, astrocyte and neuron intracellular content exceeds the osmolyte concentration in the bloodstream, leading to an intracellular accumulation of water, and cytotoxic edema (Fig. 1.1) (7-9). Similarly, when a metabolic disorder such as liver or renal failure lead to a sudden drop in plasma osmolarity, also called acute hyponatremia, an edema described as osmotic edema is triggered. On the other side when the BBB is altered in conjunction to inflammation, neoplastic neovasculature or trauma, a hydrostatic leakage of plasma into the neuropil appears and leads to an extracellular water accumulation, vasogenic edema (Fig. 1.1) (10,11). The other two types of edema are encountered 1) after a surgery or intracerebral haemorrhage by disruption of the BBB and infiltration of plasma into the brain parenchyma; hyperaemic edema, or 2) during an imbalance between CSF production and
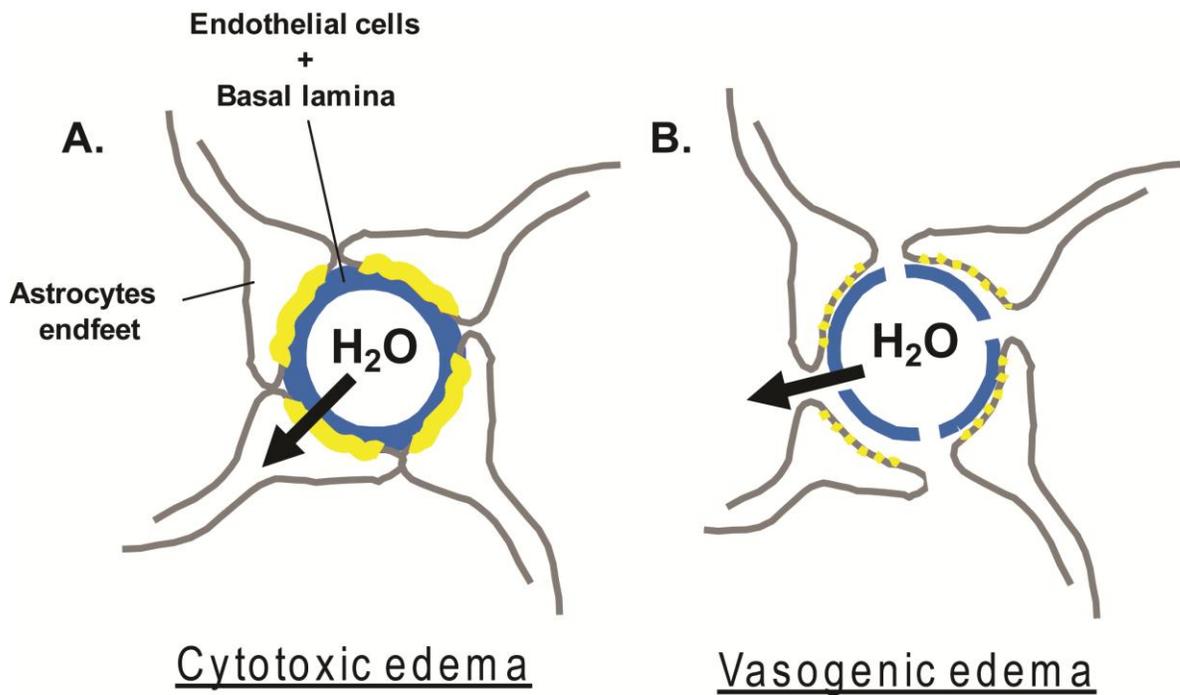
Figure 1.1. Routes of water flow into the brain. A. In cytotoxic edema, water moves from the blood down an osmotic gradient through astrocyte endfeet into the brain. **B.** In vasogenic edema, water moves from the blood down a hydrostatic pressure gradient through a leaky BBB into the brain ECS.

absorption or an obstruction of its drainage which leads to an influx of CSF into the extracellular space of the brain; interstitial edema (12).

1.1.1 Cytotoxic edema

Cytotoxic edema is defined as the premorbid cellular process, otherwise known as cellular edema, oncotic cell swelling, or oncosis, whereby extracellular cations enter into neurons and astrocytes and accumulate intracellularly after an insult to the brain that results in ischemia or hypoxia. These two conditions deprive the cells of energetic molecules such as adenosine triphosphate (ATP) due to abrogation of the mitochondrial oxidative phosphorylation chain (13,14). Cells quickly use up their reserves of ATP and unless normoxia is restored, the deranged cellular machinery loses its ability to extrude sodium (Na^+) via the ATP-dependent Na^+/K^+ ATPase. The lack of Na^+ extrusion by alteration of membrane ionic pump function drives influx of anions, which maintains electrical neutrality and in combination with influx of water results in osmotic expansion of the cell (reviewed by (7,15)). Cellular swelling begins within 5 minutes of middle cerebral artery (MCA) occlusion, particularly around capillaries, and persists for up to 24 hours after reperfusion (16,17). Astrocytes are more prone to pathological swelling than neurons as they are involved in clearance of potassium (K^+) and glutamate, which cause osmotic overload that in turns promotes water inflow. While depletion of ATP induces a reduction in the Na^+/K^+ ATPase activity, it also releases the blockage of calcium (Ca^{2+})-activated, $[ATP]_i$-sensitive non-selective cation (NCCa-ATP) channels and leads to a strong cation inward current. This induced depolarisation leads to the activation of voltage-dependent Ca^{2+} channel which results in an increase in intracellular Ca^{2+} (18), worsening the osmotic overload.

In parallel, ischemia and hypoxia result in a marked reduction in tissue pH due to uncontrolled generation of lactic acid which activate acid-sensing ion channels (ASIC) below pH 7.0 and lead to an influx of Na^+ therefore worsening again cell osmolarity and subsequent swelling (19,20). The same effect is observed when Na^+/H^+ exchangers are activated when pH decreases (21). In addition, ischemia and hypoxia leads to an increase of extracellular glutamate concentration from 0.6 to 320 µM due to the conjunction of an anoxic depolarization with decrease of both glutamate transport, by GLT1 (or EEAT2 in human) and GLAST1 (or EEAT1

3

in human), and glutamate conversion to glutamine, by glutamine synthase, which are all energy demanding processes (22,23). This excess of glutamate results in an unregulated influx of Na^+ and Ca^{2+} in the cytoplasm via the N-methyl-D-aspartate (NMDA) and the metabolic (mGluR) receptor channels (reviewed by (24,25)).

High extracellular glutamate concentration at the expense of decreasing intracellular glutamate in astrocytes limits the available amount of glutamate, which is necessary for the production of glutathione, the most abundant antioxidant in the central nervous system (26). Thus, the protective ability of astrocytes against oxidative stress is reduced under ischemic conditions. This is of primary importance since during ischemia there is a drastic increase in brain levels of free arachidonic acid which leads to mitochondrial free radical production and BBB opening due to its direct effects on endothelial and glial cells (27,28). The effect of free radicals on the disruption of the BBB is accentuated by reperfusion although the restored blood flow is essential for functional recovery (29).

1.1.2 Vasogenic edema

Ischemia initiates early oxidative and inflammatory cascades leading to BBB disruption and vasogenic edema (30). Therefore, vasogenic edema is usually formed later than cytotoxic edema (31). It also occurs in presence of a brain tumour regardless of its cell type of origin or after an intracerebral haemorrhage (reviewed by (32)). In all cases, the antigen level against perivascular extracellular matrix molecules such as collagen, laminin, agrin and fibronectin are attenuated in the ischemic area between 3 and 24 hours after MCA occlusion or in cases of brain tumours and subarachnoid haemorrhage (33-38). The mechanisms of BBB disruption involve endothelial cell alteration and basal lamina degradation by matrix metalloproteinases (MMP) or adamlysins (ADAMTS) which are a family of calcium- and zinc-dependent endopeptidases that digest almost all extracellular matrix (ECM) molecules (39). In cerebral ischemia, MMP-2, -3 and -9 as well as ADAMTS-1 and -4 are increased from 3 to 24 h after MCA occlusion (40-44). MMP9 has been shown to induce the decrease in laminin antigen around the blood vessels after MCA occlusion or subarachnoid haemorrhage, whereas MMP3 has been involved in the degradation of both laminin and agrin (45,46). In parallel, during ischemia, reactive oxygen species (ROS) or nitrogen species (RNS) originate from the activation of the xanthine-xanthine

oxydase and the interruption of the oxidative phosphorylation chain or the nitric oxide (NO) synthase (NOS), respectively (47,48). The increased production of free radical NO during ischemia can directly activate MMP9 by nitrosylation of cysteines in the propeptide (39,49).

Other mechanisms also activate MMP-mediated breakdown of the BBB. Indeed, cerebral ischemia induces the migration of neutrophils from the blood to the ischemic area which peaks at 24-72 h after MCA occlusion (50). The leukocyte adhesion to the endothelium triggers the upregulation of MMP9, MMP3 and ADAMTS-1 and 4 via release of interleukin-1β (IL-1β) and tumour necrosis factor alpha (TNFα), leading to the loss of the thight junctional proteins occludin and zonula occludens-1 that normally ensure the occlusive properties of the BBB (51). This phenomenon is accentuated by the activation of released IL-1β and TNFα by MMPs (52).

In parallel, the profile of BBB leakage is synchronized with the up-regulation of vascular endothelial growth factor (VEGF) expressed by macrophages, astroglia and neurons (53,54). VEGF, which is a major inducer of angiogenesis also upregulated in brain tumours (55,56), has been shown to reduce the expression of zona occludens-1 and occludin (57). In stroke, the increased expression of VEGF plays a dual role; during the acute stage, when edema is fulminating, VEGF may accentuate edema whereas during the subacute stage, it may improve recovery by inducing new vessel formation (58). As a result of the BBB disruption, high molecular weight molecules from the plasma, such as albumin, enter the cerebral interstitial space, or extracellular space (ECS), which creates an osmotic gradient that leads to an influx of water into the brain (59). This phenomenon reaches a peak at 12 h after a permanent MCA occlusion (60) or 1 h after a transient MCA occlusion (43), suggesting that the restoration of blood flow accelerates the evolution of the vasogenic edema.

Advances in translational research now clearly identify cytotoxic edema as the initial, and most important, reversible first step in the sequence that leads to vasogenic edema (61). In addition, the swelling of astrocytes may compromise the microcirculation in the ischemic area as early as 30 minutes after MCA occlusion by narrowing down the capillary lumens (17). In the brain, the protection of cells against swelling is absolutely critical due to the spatial constraints imposed by the skull. Expansion of intracranial tissue can cause compression of small blood vessels, episodes of anoxia, prolonged ischemia, excitotoxicity, cerebral herniation and ultimately mortality (62).

1.2 Regulation of cell swelling

Mammalian cells have flexible but fragile membranes which require osmotic volume regulation to prevent them from oncosis, or cell death by swelling as von Recklinghausen first described it with damaged plasmalemma and other organelle membranes (63). A multitude of internal factors challenge the constancy of cell volume such as alterations in intracellular soluble content by breakdown of macromolecules, accumulation of metabolites and dissipation of ion gradients, all present during an ischemic event. A challenge to cell volume can only be accommodated if osmotic equilibrium across the cell membrane is maintained by cell volume regulatory mechanisms (64). In the case of osmoregulatory mechanisms activated by internal challenges, cells alter the concentration of osmolytes in order to reduce the difference in intracellular versus extracellular concentration, eliminating any change in intracellular water concentration and therefore a concomitant change in cell volume commonly referred to as isosmotic volume changes. Cell swelling triggers Regulatory Volume Decrease (RVD) that is accomplished by fast activation of channels, exchangers and cotransporters (65,66). Indeed when cells are exposed to hypotonic insult, there is an increase in cell volume or hypoosmotic cell swelling that is transient and followed by the release of osmoactive molecules which are either organic (i.e. ideogenic osmoles: amino acids, polyols and methylamines) or non organic (i.e. electrolytes). A concomitant release of cations such as K^+ and anions such as Cl^-, via activation of separate K^+ and Cl^- channels or K-Cl cotransporter, with organic osmolytes such as taurine, glutamate and myo-inositol through a yet unidentified volume organic osmolyte and anion channel (VSOAC) is indeed observed (67,68). As these osmolytes are released from the cell they bring with them obligated water (69). This net flux helps the cell return to its original volume and establish a new osmotic equilibrium within a few minutes (reviewed by (70)).

1.2.1 Inorganic osmolyte release

Swelling activates at least two different types of K^+ channels, calcium-dependent and -independent channels. The calcium-dependent K^+ channels are maxi K+ channels whereas the calcium-independent channels usually involved Kv1.3 or Kv1.5 (reviewed by (71)). Activation of electroneutral K^+/Cl^- (KCC) symport is also known to be involved in RVD. In addition, voltage-dependent anion channel (VDAC) and voltage-dependent Cl^- channel lead to a similar efflux of Cl^-. However, the activation of K^+ channels is effective for RVD only if anion channels are operating in parallel, since prolonged release of K^+ could lead to hyperexcitability of the cells (reviewed by (72,73)).

A robust chloride conductance, which requires ATP, is observed when cells are exposed to hypoosmolar solutions (74). These channels have been referred to as volume-regulated anion channels (VRAC), volume-sensitive outwardly rectifying (VSOR) or VSOAC since a concomitant efflux of taurine, glycine or inositol is observed when Cl^- is released (74-77). Although the VSOAC has been pharmacologically and electrophysiologically characterized, its molecular identity is still unknown. The members of the ClC family or the maxi anion channel are some of the candidates that have been proposed (78,79). Since loss of inorganic osmolytes such as K^+ and Cl^- can be potentially harmful on a long-term basis, the release of organic osmolytes is more sustained.

1.2.2 Organic osmolyte release

Organic osmolytes contribute to 23-29% of total osmolyte content in cells and can be divided into three classes; polyols (glycerol, sorbitol, myo-inositol), amino acids and derivatives (taurine, glutamate, alanine) and methylamines (betaine, glycerophosphorylcholine) (reviewed by (80)). Unlike inorganic ions, most organic osmolytes are neutral and changes in their concentration do not significantly affect membrane potential or enzyme activities (reviewed (81)). They accumulate in the cytoplasm as degradation products or after synthesis and import. Their intracellular concentration drops significantly in response to cell swelling as demonstrated by intracranial microdialysis with taurine concentration being reduced from 53 to 7 mM within

40 minutes (82). The activation of the osmoregulatory release of organic osmolytes has been shown to respond to membrane stretch (reviewed by (83)) or changes in macromolecular crowding and ion strength (reviewed by (84)). In addition to the prompt but passive release of the organic osmolytes in response to cell swelling (reviewed by (85)), a downregulation of their synthesis and uptake is also observed (reviewed by (86)).

The slower the osmotic disorder occurs, the more efficient the osmoregulatory mechanisms are. It explains, for example, why patients with chronic hyponatremia could be asymptomatic whereas severe edema is observed in rapid water intoxication or acute hyponatremia that lead to a too rapid reduction of circulating osmolarity (87,88).

If the cell volume in response to osmotic stress is not corrected, it may cause cell damage and loss of function as reflected by inhibition of glycolysis, glycine oxidation and glutamine breakdown (reviewed by (89,90)). Cell volume regulation is linked to many aspects of cell function, including glucose metabolism, pH regulation and cell excitability. Since during ischemia or hypoxia, intracellular acidosis and lack of ATP potently inhibits RVD, likely due to inhibition of K^+ and VSOAC channels, this contributes to persistent astrocytic swelling (91,92). This process is accentuated by the release of arachidonic acid which has been show to inhibit VSOAC and therefore prevent RVD. The water transport is therefore suggested as a key limiting factor. The osmotic flow of water occurs by passive diffusion across the lipid bilayer; however some cells possess water permeable protein channels called aquaporins to accelerate this water transport (reviewed by (93,94)).

1.3 Aquaporins

Aquaporins (AQPs) are small water channel proteins (MW~30 kDa) that facilitate the transmembrane transport of water, providing cells with a higher water permeability than expected from water diffusion through the lipid bilayer (95,96). The AQPs assemble in cell membranes as tetramers. Each monomer has six membrane-spanning domains surrounding a water pore that can transport water in both directions (97,98). To date, 13 types of AQPs have been identified (95). Mammalian AQPs can be divided into two main classes depending of their strict permeability to water alone or water and glycerol (94). The tissue-specific expression of

mammalian AQPs correlated with the phenotypes of several transgenic mice deficient for specific AQPs suggest roles in renal water reabsorption, CSF dynamics, salivary secretion, airway lubrification and brain edema formation and resorbption (99-102).

AQP4 is the most abundant water channel in the brain, but expression of AQP1 and AQP9 has also been reported. AQP1 is expressed in choroid plexus epithelium and plays a role in CSF formation whereas AQP9 has been detected in specific neuronal populations (103,104). AQP4 is expressed in supporting cells such as astrocytes and ependymal cells where it confers high and mercury-insensitive water permeability (105,106). It is strongly enriched at the borders between the brain parenchyma and major fluid compartments, including blood and CSF (107).

1.3.1 AQP4 structure and localization

AQP4 structure has been revealed recently using crystallography (108-110). The structure unveils that six α-helical transmembrane domains surround the two shorter helices that contain the two NPA motifs (Asparagine-Proline-Alanin) that form the pore (111,112). Because of the absence of cysteine in position 189 like other AQPs, AQP4 is not sensitive to mercury (111). AQP4 structure also reveals that it can oligomerize at the plasma membrane (113).

Several lines of evidence support the hypothesis that AQP4 is the main structural component of the orthogonal arrays of particles (OAPs)(114) as demonstrated by the absence of OAPs in astrocytes of AQP4-deficient mouse (115), the formation of OAPs in oocytes transfected with AQP4 cDNA (116) and labeling of OAPs with AQP4 antibodies using immunogold fracture labeling technique (117).

Recent studies determined that AQP4 has six splice variants, named AQP4a-f (118). Two of these isoforms result from two different mRNAs with translation initiation either at the first methionine residue, M1 (AQP4a), or at the second methionine, M23 (AQP4c, Fig. 1.2) (111,118-121). As a result, AQP4M1 has an N-terminus that is 22 residues longer than AQP4M23, is subject to palmitoylation on cysteine 13 and 17 and can present an interaction between the N-terminal residues and the first NPA motif (117,122-125).
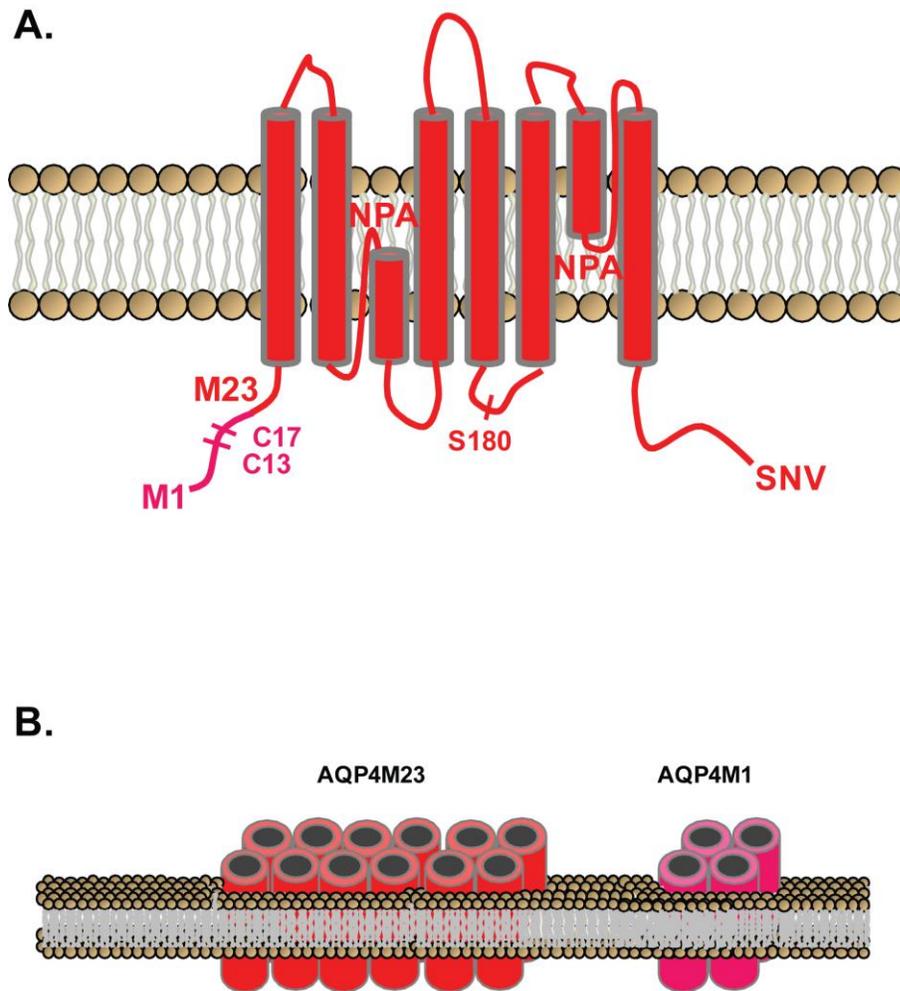
Figure 1.2. Schematic representations of AQP4 structure and M1/M23-dependent formation of OAPs. A. AQP4 monomer consists of six a-helical domains (*cylinders*) around a water pore and two conserved NPA motifs (Asn-Pro-Ala) that allow water but not small solutes or protons to pass across the pore. Amino acids M1 and M23 defining both M1 and M23 isoforms of AQP4 are shown as well as key amino acids C13, C17, S180 and SNV which present palmytoylation, phosphorylation and PDZ-binding motif, respectively. **B.** Orthogonal array of particles formation by either M1 or M23 isoforms.

While the water permeability of these two isoforms present some discrepancy between identical (122), higher in M23 (126,127) or higher in M1 (128), freeze fracture analyses revealed that AQP4M1 and AQP4M23 have different morphological properties. AQP4M23, which is now known to be nearly immobile in membranes (129), promotes the formation of large distinctive OAPs at astrocyte endfeet whereas AQP4M1, which freely diffuse in membranes (130), restricts this, resulting in the formation of much smaller OAPs (131). The relative amount of M1 versus M23 isoforms would therefore determine the size of these arrays, which can contain up to hundreds of tetramers and in brain an approximate 3:1 ratio of M23 to M1 has been reported (122,127,132-134). Consistent with such specific organization into membrane domain, it has been demonstrated recently that AQP4 was segregated into lipid rafts (135,136) and that M1 and M23 differ in their ability to interact with lipids (109). Together, these studies suggest that OAP formation by AQP4M23 is stabilized by hydrophobic intermolecular interaction involving the N-terminal residues (130). Other components of those OAPs have been suggested to relate to the PDZ-binding domain of AQP4 (129). Recently, it has been demonstrated that dystrophyn, a member of the DAP complex, take part of the large OAPs formation (137,138).

Interestingly, it has been shown AQP4 can be a substrate for protein kinase C, G and A or Ca^{2+}/calmodulin-dependent protein kinase II (139-144). The PKC-dependent phosphorylation of AQP4 has been identified to occur on serine 180 (143,145,146). Recently, activators of PKC such as phorbol 12-myristate 13-acetate (PMA) or phorbol 12,13-dibutyrate (PDBu) have been used to decrease the AQP4-mediated water transport (141,143,146,147) and thus treat brain edema 60 min before or 30 min following focal ischemia (148,149). The role of PKC is still unclear as different studies show that it might downregulate AQP4 expression (116,142,150). An activated translocation of AQP4 following phosphorylation could explain some decrease in AQP4 expression at cell surface (128,144) but mutation of S180 show that the OAP formation is not dependent on PKC phosphorylation (151).

The pattern of AQP4 distribution around blood vessels suggests involvement of AQP4 in water movement in and out of the brain. Indeed, in brain, AQP4 is localized to astrocyte processes adjacent to blood vessels as well as at ependymal and pial surfaces in contact to CSF (152). Likewise, in retina and cerebellum, AQP4 is enriched at Müller cell endfeet abutting

blood vessels and the inner limiting membrane (ILM) and at the Bergmann glial cells abutting pial surface.

1.3.2 AQP4 function

Because AQP4 permits bidirectional water transport (69) it has been shown that it plays a role in the early accumulation of water in brain edema but also facilitates the subsequent removal of excess water involved in brain swelling. In human, three studies reported six mutations in AQP4 gene with reduced and increased water transport associated with them (153-155). However, in mouse, there is mounting evidence that AQP4 deficiency is associated with reduced water entry into the brain in cytotoxic edema models of water intoxication or focal cerebral ischemia (Table 1.1) (156) which has been verified in vitro on astrocytes submitted to hypoxia in absence of AQP4 (157). AQP4 deficiency has also been associated to reduced water outflow from brain parenchyma in vasogenic edema models of cortical freeze-injury, hydrocephalus, brain abscess, brain tumor and subarachnoid haemorrhage (Table 1.1) (158-162). On the other side, overexpressing AQP4 accelerates cytotoxic brain swelling demonstrating once more that AQP4 is rate-limiting for brain water accumulation (163). It is worthy to note that the deletion or overexpression of AQP4 confers no abnormalities in brain structure, vascular architecture, in intracranial compliance, pressure or BBB integrity and that their effects are only noticeable when the brain is under stress (99,156,159-161,164,165).

The expression of AQP4 during brain edema has been extensively investigated and the controversial results obtained in different models suggest that compensatory mechanism occurs during brain edema (166-171). After transient focal brain ischemia, two peaks of hemispheric swelling at 30 min and 48 hrs have been shown to coincide with two peaks of AQP4 upregulation (169,172). The reasons of such upregulation of AQP4 in a situation where AQP4 is deleterious are still unclear but studies have shown that interferon-gamma and IL-1β exposure during an ischemic episode lead to the maladaptive AQP4 upregulation (173). Nevertheless, many studies found that from 1 to 24 hrs post ischemia, AQP4 expression decreases (168,171,174,175). On the other side, it has been shown that AQP4 expression increases 24 hrs

Brain edema type	BBB integrity	Animal models	AQP4$^{-/-}$ effects
Cytotoxic	Intact	Water intoxication	Reduced edema (156)
		Focal cerebral ischemia	Reduced edema (156)
Vasogenic	Leaky	Tumor	Increased edema (160)
		Cortical freeze-injury	Increased edema (160)
		Subarachnoid Hemorrhage	Increased edema (162)
		Brain abcess	Increased edema (159)
Interstitial	Intact	Hydrocephalus	Increased edema (160)

Table 1.1. Summary of the effects of AQP4 deficiency on the brain edema types and models.

after traumatic brain injury (160,170,176-179), brain abscess (159,180) or subarachnoid hemorrhage (162,181) with subsequent drop at 48 hrs (166,167). These variations in AQP4 expression in models of vasogenic edema have been correlated with the resolution of edema via use of magnetic resonance imaging (MRI) or apparent diffusion coefficient (182). In addition, it has been shown that the distribution of the upregulated AQP4 is mainly localized at the BBB, the ependyma and the glia limitans which are now considered as cerebral domains where edema fluid clearance occurs (183). Indeed it is commonly accepted that excess of fluid leaves the brain parenchyma along three different routes; across the BBB, across the ependyma into the ventricles and across the glia limiting membrane into the CSF again which represents the main route for vasogenic edema (160,184). The CSF eventually enters the arachnoid granulations and is cleared into the superior sagittal venous sinus. AQP4 localization at those sites is crucial for water efflux as shown in animals with mislocalized AQP4. Together these studies suggest that these upregulations of AQP4 are protective mechanisms (162,165). These processes are similar to the developmental induction of AQP4 during the embryonic stage which is correlated with the reduction of cerebral water (185-188).

Other data in the literature also provide clues as to the role of AQP4 in the propensity for seizures. Relative ECS volume has been demonstrated to play an important role in epileptic seizures. Increases in the ECS volume have been indeed reported in AQP4-deficient mice suggesting that AQP4 might be crucial for the regulation of K^+ concentration gradient (189-191). In absence of volume reduction in AQP4-null mice, the released K^+ is distributed over a large volume leading to an increase threshold for epileptic seizures. However, since AQP4 deletion leads to a slower potassium clearance, these mice show an increased duration and severity of seizure once induced (192-195). Similarly, it has been demonstrated that AQP4 is located at the Müller cell endfeet (196-198) and, by using AQP4 null mouse, that its activity is required for the generation of the b waves in retina (199).

The specific distribution of AQP4 is of major importance because it renders the channel capable of increasing water fluxes crucial for water homeostasis in the brain. The codistribution of AQP4 and potassium channels at the BBB appears to be crucial in such process. Some constituent of the BBB such as agrin and laminin have been identified to play a crucial role on the polarity of AQP4 (126,200,201).

1.4 Blood-brain barrier

The BBB is part of a general blood-neural barrier (BNB) which also includes the blood-retina barrier (BRB). These barriers are specialized structure developed to isolate the central nervous system (CNS), which is a very sensitive system, from blood to maintain a stable and regulated microenvironment for reliable neuronal activity. These barriers ensure appropriate ionic balances, nutrient transport and absolve potentially harmful molecules. The existence of the BBB was first demonstrated in 1885 by Ehrlich (202). As functional entity, the BBB is composed of many types of cells that enclosed an extracellular matrix (203,204). The endothelial cells from the wall of the blood vessels are responsible for the impermeable properties of the barrier thanks to their tight-junctions formed by occludins and claudins, the fact that they are not fenestrated and that the pinocytosis is limited (205). The endothelial cells have transporters, such as glucose transporter isoform-1 (GLUT1), large neutral amino acid transporter (LAT1) and moncaroboxylate transporter isoform-1 (MCT1), to supply neurons with nutrients (206). Another cell type, astroglia, ensheats the endothelial cells by endfoot processes (207). The presence of those processes has been suggested to regulate the properties of the endothelial cells and control the junctional tightening as well as the expression of transporters (208,209). In conjunction with astrocytes, the endothelial cells also produce the basal lamina which constitutes a specialized ECM and is composed of collagen type IV, fibronectin, laminins and proteoglycans (reviewed by (210)). The interactions of those molecules with their receptors at the cell surface of both endothelial cells and astrocytes are believed to be essential for the polarity and maintenance of the BBB.

1.4.1 Basal lamina

The basal laminina present around the blood vessels is critical for the proper function of the endothelial barrier and the polarized distribution of specific protein platform (211). Among the different components of the membrane limitans gliae perivascularis, both structural proteins (laminin, collagen type IV, nidogen and fibronectin) and proteoglycans (perlececan and agrin) play an important role (212,213).

Laminins are composed of three distinct chains referred to as α, β and γ. Currently, five α, four β and three γ chains have been described and give rise, when splice variants are included, to 16 different laminin isoforms (212,214-216). The C-terminal ends of the α-chains contain globular domains composed of five similar modules (LG1-5) which are crucial for binding to cell surface receptors. Around the blood vessels in the CNS, laminin-1 (also referred to as 111) composed of α1 (400 kDa), β1 (200 kDa) and γ1 (200 kDa) chains is the best-characterized laminin (217,218) but laminin-2 (referred to as 211) and -5 (referred to as 332) are also present (217,219-222). The γ3 chain, component of the laminin 12 (referred to as 213), 14 (referred to as 423) and 15 (referred to as 523), has also been reported in brain (223). In the retina, laminin-1 and -2 have been reported at the ILM (224,225). Interestingly these two locations, at astrocytes and Müller cell endfeet, are rich in the dystroglycan-associated protein complex (DAP) immunoreactivity and both LG4 and LG5 of laminin-1 and -2 bind with high affinity to α-dystroglycan (α-DG) (226,227). It is noteworthy that deficiency in laminin α-2 chain has been associated with increase brain edema due to disruption of the blood-brain barrier and a concomitant muscular dystrophy (228-232).

Laminin is essential for the assembly of the basal lamina by interacting with specific cell surface receptors and conversely cell surface receptors are crucial for the polymerization of laminin (233,234). Indeed it has been shown that DG can assemble laminin (235-243) and the absence of DG leads to the disruption of the Reichert membrane, the rodent extra-embryonic matrix responsible for the endoderm growth, with mislocalization of laminin (244). Laminins are also involved in the integrity of the basal lamina by bridging many ECM components together (245,246). In addition to self-polymerize (247), laminins have been shown to interact, via an epidermal-growth-factor like repeat within the laminin γ1 chain, with domain G3 of nidogen which binds to the immunoglobulin-like domain 3 of perlecan (248-252) or with collagen IV (253,254). Interestingly, DG is also crucial in the polymerization of collagen IV (240) which is present at the BBB (255,256).

Agrin is also concentrated at the basal lamina lining the vascular vessels or ILM (257-260). Interestingly, agrin isoforms can bind laminin-1, -2 and -4 and has been suggested to play an important role in the assembly of the basal lamina (261). Agrin plays an important role in the integrity of the BBB as shown in the agrin null mouse (262,263). Agrin can also be spliced at three sites which in rats are called X, Y (or A in chicken) and Z (or B in chicken). Depending on

the splicing events that occur 9 amino acids can be inserted in X, 4 amino acids can be inserted in Y and 8, 11 or 19 amino acids can be inserted in Z (264). The agrin isoform without any insertion, referred as Y0Z0 (A0B0 or C-Agrin0, 0), is secreted by myocytes or found at the BBB whereas the agrin Y4Z8 (A4B8 or C-agrin4, 8) is secreted by neurons (257,260,265-268). The structure of agrin has been characterized and it has been proposed that agrin isoforms can bind α-DG via their 3 LG domains (257,269). In addition, it has been demonstrated that DG is crucial for the clustering of agrin (270,271).

Collagen molecules are trimeric molecules and it exist 27 different collagens (reviewed by (272)). At the basal lamina, collagen IV, XV, XVIII and CXVIII have been reported. Fibronectin is crucial for the polymerization of collagen (273) and is secreted as a dimeric molecule with 2 subunits bound via a sulfure bridge (reviewed by (274)). As receptors, fibronectin interacts mainly with integrins (275). Another ligand of DG found at the BBB is perlecan which present hyaluronic acid residues as well as heparin sulphate glycosaminoglycans capable of binding to collagen.

Both agrin and laminin have been found responsible for the clustering of the AChRs at the motor endplate and the synaptogenesis in the CNS (reviewed by (276)). Now those molecules are proposed to play an important role in the integrity and polarity of the BBB (257,267). Interestingly, the common receptor to laminin and agrin, dystroglycan, is localized at the perivascular astrocyte endfeet (277-279).

1.4.2 Astrocytes endfeet

Astrocytes are the most numerous glial cell type and account for one third of brain mass. They are highly complex and respond to a variety of external stimulations. One of the chief functions of astrocytes is to participate in the tri-partite synapse and modulate synaptic activity. *In vivo* studies have identified the astrocyte endfoot processes enveloping the vessel walls as the center for astrocytic Ca^{2+} signalling that can modulate the local blood flow (280,281). Several lines of evidence expanded the role of astrocytes and it is now clear that astrocytes are active in optimizing the interstitial space for synaptic transmission by tight control of water and ionic homeostasis. Thus, the merging concept of astrocytes includes both active modulation of

neuronal output as well as supportive function. It is accepted that astrocytes are also essential for the maintenance of extracellular K^+ at the level compatible with continued neuronal function (282).

Astrocytes are presenting specific processes at the boundaries between neural and fluid compartments in the brain and retina which contribute to the water balance and the maintenance of a low potassium concentration in the ECS surrounding neurons. It has been demonstrated that the integrity of the perivascular astrocyte endfeet was required to handle excessive amounts of K^+ and clear it into the bloodstream to prevent any epileptic seizure. Neuronal action potentials result in a large release of potassium ions into the extracellular space that would depolarize surrounding neuronal cells. Astrocytes are connected by an extensive network of gap junctions which allows a rapid redistribution of K^+ from areas with high neuronal activity to the astrocyte endfeet with release into the bloodstream (283-285). A similar K^+ buffering, or siphoning, involving Müller cells has been characterized in retina and is responsible for the b waves identified in electroretinograms (ERGs) (286-289).

The inwardly rectifying potassium Kir channels are grouped into seven subfamilies (Kir1.0-7.0) and assemble as homomeric or heteromeric tetramers which further increase their functional diversity. They are characterized by their ability to allow greater influx than efflux of K^+. At resting membrane potentials (RMP) negative to the equilibrium potential for K^+, they carry a K^+ influx, but once the RMP becomes more positive, the current flow mediated by the Kir channels is blocked by intracellular polyamines or magnesium (Mg^{2+}) (290,291). In glia, an increase in extracellular K^+ concentration is equivalent to a drop in RMP which leads to an increase in Kir channel inward currents, thus maintaining the membrane potential near the equilibrium potential of K^+. Around the synapses, astrocytic Kir2.1 and Kir5.1 have been suggested to regulate the K^+ uptake in parallel to the activity of Na^+/K^+ ATPase as well as Na-K-Cl cotransporters (292). The elevated intracellular K^+ is then be rapidly shunted by current flow from a proximal to a distal region of the cell and through the astrocytic syncytium. At the distal region of the syncytium, around blood vessels or vitreous body, the resting potential is more positive than the equilibrium potential for K^+, which allows K^+ to come out to extracellular fluid with a concomitant Cl^- ion efflux. Another Kir channel, the ATP-dependent Kir4.1 (also referred to as BIR10, KAB-2, BIRK1 or Kir1.2), has been reported throughout the CNS with a high concentration at the perivascular astrocyte and Müller cell endfeet (284,293-296).

Several studies suggested that Kir4.1 play a crucial role in the clearance of the excess of K+ into the vascular system or the vitreous body via its weakly rectifying properties (293,297-301). Missense mutations in the Kir4.1 gene have been correlated with seizure susceptibility in humans (302,303). Similarly, in mouse, conditional knock-out of Kir4.1 leads to astrocyte depolarization and enhanced short-term synaptic potentiation in hippocampi (304) and mutations in the Kir4.1 gene have been identified in epileptic mouse model (305). In retina, severe reductions in K^+ currents and depolarization in Müller cells have been reported in Kir4.1 knock-out mouse (306).

Recently, Kir4.1 has been implicated in retinal edema formation (307,308). Like brain edema, retinal edema (or macular edema) is characterized by excessive fluid accumulation in the retina, after BRB leakage due to inflammation (vasogenic component) (reviewed by (309)), and cytotoxic with swelling of Müller cells after ischemia (cytotoxic component). It has been shown that a loss of Kir4.1 during ischemia was associated with the lack of water and K+ extrusion from the Müller cells which led to macular edema (310,311). In the late phase of the macular edema and similarly to the vasogenic brain edema, it has been shown that both Kir4.1 and AQP4 expression increases in association with a corrective egress of water (312).

Spatial buffering of K^+ ions generates osmotic gradients (313) that triggers water movements and changes in extracellular space (Fig. 1.3) (314). AQP4 appears crucial for the clearance of the K^+ ion excess and maintenance of normal neuronal function, and its physiological impact on K^+ buffering has been extensively investigated. In Mesial Temporal Lobe Epilepsy (MTLE) characterized by hyper-excitable hippocampi, AQP4 expression is significantly reduced (194). AQP4 null mice also show increased sensitivity to retinal light damage due to unregulated K^+ buffering (315). In addition several studies have demonstrated the coincident expression pattern of both AQP4 and Kir4.1 at the same glial cell processes (152,316). It has also been shown that the coordinated activity of Kir4.1 and AQP4 in neural tissues is heavily reliant on their proper localization to glial endfeet (117,316-318). Regarding their colocalization at glial endfeet, recent studies have demonstrated that even though they are present in lipid rafts in which close functional interactions between water and potassium channels are suggested to play fundamental roles (135,136,319), their activity is independent of one another (320,321).
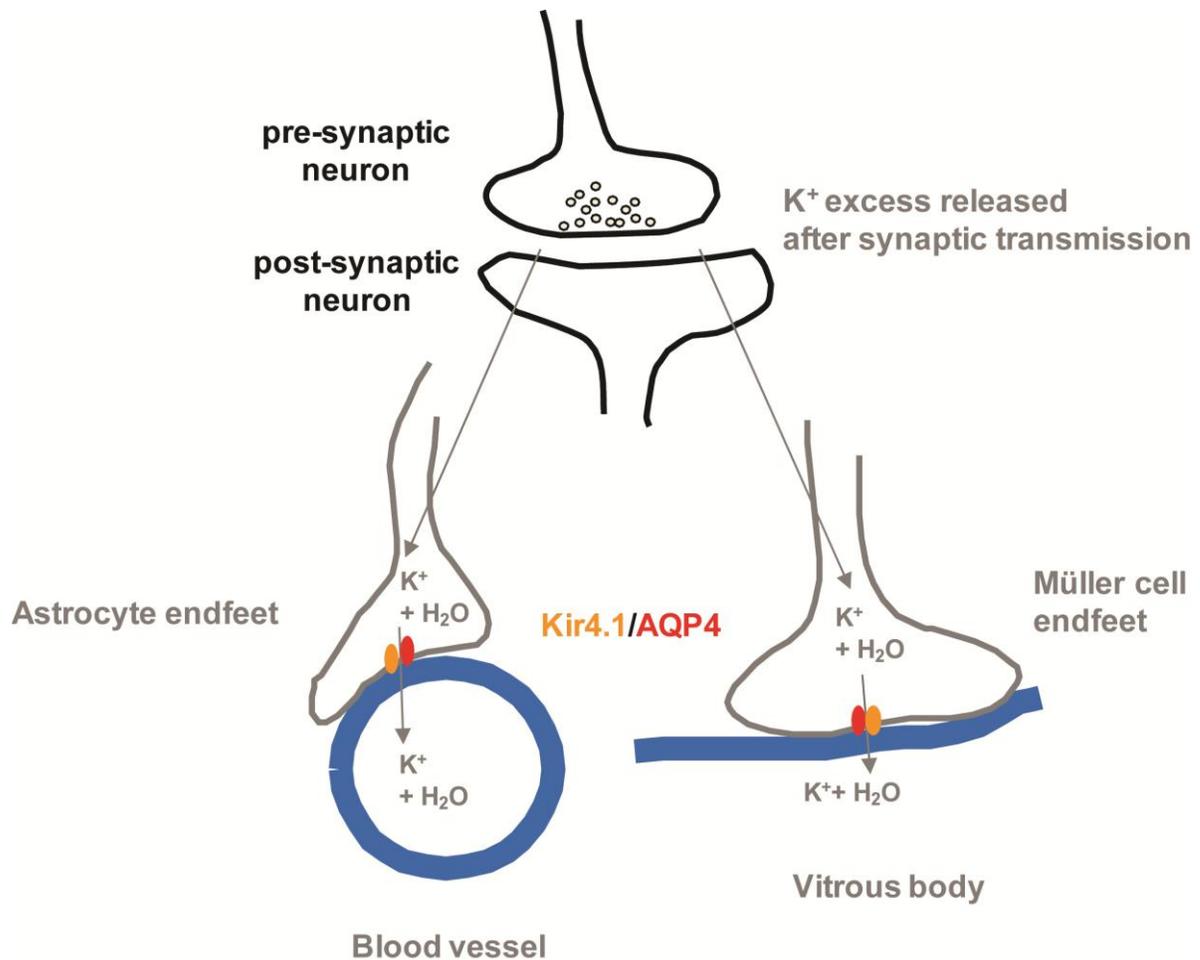
Figure 1.3. Schematic representation of potassium and water homeostasis in the brain and retina. K$^+$ released from synapses is taken up into astrocytes and Müller cells via strongly rectifying Kir2.1 channels. K$^+$ is released from astrocytes and Müller cells via weakly rectifying Kir4.1 channels at endfeet abutting blood vessels and vitreous body, respectively. The fluxes of potassium are followed by water movements.

However, redistribution of the channels away from these cellular domains encumbers the process of spatial K^+ buffering and leads to electrolyte imbalances in regions of high neuronal activity, thus compromising brain and retinal function (192,322). An aberrant accumulation of extracellular K^+ serves to depolarize surrounding neurons giving rise to hyper-excitability which manifests as an increased susceptibility to epileptic seizure (192).

There exists a substantial body of evidence to suggest that the proper patterning of these channels is dependent on the integrity of the dystroglycan-associated protein (DAP) complex (299,323-325). In brain, this complex is highly enriched in astrocyte endfeet abutting blood vessels or lining the subarachnoid space and the cerebral ventricles (326). In the retina, it is present at analogous domains such as both astrocyte endfeet abutting the blood vessels or Müller cells endfeet abutting the ILM apposed to the vitreous body (278,327). This intimates a possible involvement of the improper localization of AQP4 and Kir4.1 in the cognitive and ocular defects that are associated with certain dystrophies.

1.5 Dystroglycan-associated protein complex

Muscular Dystrophy (MD) encompasses a large variety of inheritable diseases characterized by progressive muscle weakness and degeneration. Central to a large number of MDs is a defect in the DAP complex. Mutations involving different components of this subplasmalemmal multiprotein complex, their post-translational modifications and their interactions with the ECM have been shown to cause many forms of MDs (reviewed by (328,329)). At the very least, the composition of the DAP includes numerous intracellular proteins such as syntrophin, dystrobrevin and dystrophin, downstream of dystroglycan, the core protein of the complex (Fig. 1.4). Dystroglycan encodes for a transmembrane protein, β-DG (43 kDa), and an extracellular protein, α-DG (120-156 kDa depending of its level of glycosylation) (330,331). α-DG and β-DG are derived from post-translational cleavage of a single polypeptide (330). α-DG binds the extracellular matrix proteins laminin, agrin and perlecan as well as
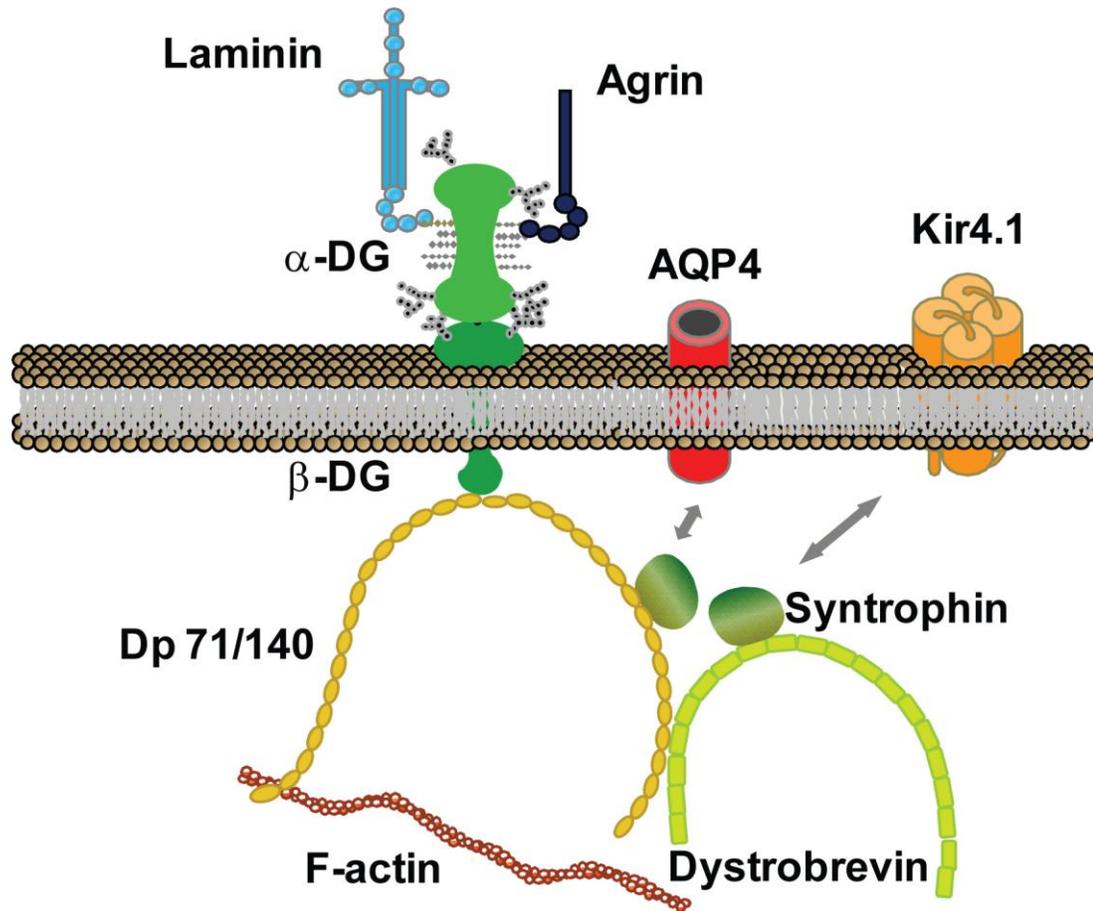
Figure 1.4. Schematic representation of molecular interactions within the DAP complex, the ECM and AQP4/Kir4.1 channels at perivascular astrocyte endfeet. β-DG spans the plasma membrane and interacts with the extracellular α-DG. Extracellularly, α-DG binds to laminin and agrin. Intracellularly the PPXY motif of β-DG binds to the WW domain of dystrophin's C-terminus. Dystrophin binds to syntrophin which interacts with both Kir4.1 and AQP4 via its PDZ domain.

neurexin (240,271,332-337). Intracellularly, β-DG binds directly dystrophin, which in turn binds other cytoskeletal proteins such as syntrophin and actin and thus plays a role in maintaining the structural integrity of muscle fibres during repeating cycles of contraction-relaxation (336,338-341). The DAP complex may also be involved in localizing signalling proteins to specific cell domains since syntrophin can bind signalling molecules such as Grb2, protein Gα, ERK6, MAST or SAST (342-347). Several studies have strongly implicated the laminin binding to DAP in the tyrosine phosphorylation of syntrophin, its binding to Grb2 and, the subsequent activation of Rac1 and PAK1-JNK. The activation of this pathway results in actin remodeling, tyrosine phosphorylation of c-jun and AChRs which regulate their clustering at the neuromuscular junction (239,348-353).

Besides its expression in skeletal muscle, the DAP complex is also present in the CNS where DG is referred to as cranin (337,354). While the DAP complex was found to be fundamental to muscle integrity in MD, the cognitive and ocular defects associated with the disease are currently under investigation. Indeed, several forms of MDs also present a large scope of disabilities, from learning and mental retardation to epilepsy.

1.5.1 Composition and function in the CNS

In the CNS, different compositions of DAP have been characterized depending on the cell type (277) with DG densely localized in both neurons and glial cells (278,327,355-357).

The dystrophin gene encodes for a polypeptide divided into five domains with the amino terminal and rod-like domains binding F-actin (358) and the cystein rich, carboxyl terminal and the WW domains binding the PPPY motif (amino acids 889-893) of β-DG in a phosphorylation-dependent manner (359-361). Three promoters regulate its full length (Dp427) and four internal promoters prompt the expression of different splice variants (362-366). In the CNS, Dp427 is strictly neuronal whereas Dp140 and Dp71 are expressed in glial cells and Dp260 in retina (356,367-370). The dystrophin-related protein (DRP), or utrophin, another member of the DAP, shares an 80% homology with dystrophin and is also expressed in the CNS. Two full-length isoforms and three splice variants have been reported in the literature (371). Its expression pattern in the CNS is similar to the one of dystrophin (372-374) and it has been suggested that

both proteins could complement each other (375). In retina both are expressed around the ILM (376).

Dystrobrevin (DB) is a dystrophin-related protein that participates in the DAP. Two separate genes encode the DBs, α-DB and β-DB (377). Both α-DB and β-DB bind to dystrophin and utrophin (378,379). They are present in both brain and retina with α1- and α2-DB in astrocytes and β-DB in neurons (356,380-384). In retina, DB has been reported at the Müller cell endfeet (376,385). DB binds to dystrophin in a phosphorylation-dependent manner (386) and binds also α-syntrophin which recruits both α2-DB and γ2-syntrophin in astrocyte endfeet (387).

Syntrophins are modular adaptor proteins that bind directly to dystrophin, dystrobrevin and utrophin in the DAP and serve to localize signalling molecules to specific domains. The five different syntrophins, α-, β1-, β2-, γ1- and γ2-syntrophin, contain one PDZ domain as well as two pleckstrin homology domains (PH1 and PH2) which in conjunction with the syntrophin unique domain are required for syntrophin's oligomerization or binding to dystrobrevin, utrophin or dystrophin (388-392). In brain, α-, β1-, β2- and γ2-syntrophins are present at astrocyte endfeet while β1-, γ1- and γ2-syntrophin are found in neurons (344,387,393,394).

Immunolocalization data show that dystrophin, utrophin, dystrobrevin, syntrophin and DG are localized and concentrated postsynaptically in Purkinje cells in cerebellum, pyramidal neurons in hippocampus and cerebral cortex as well as astrocyte and Müller cell endfeet (220,278,367,376). In these locations, growing evidence indicates a role for the DAP complex in the subcellular distribution of various channels. DG has been shown to colocalize with $GABA_A$ receptors at post-synaptic sites of cerebral cortex, hippocampus and cerebellum (368,395-397) where it plays a role in inhibitory transmission of Purkinje cells and long term potentiation at CA3-CA1 synapses (398,399). Gee SH. et al. (400) have shown that syntrophin interacts with NR2, a subtype of glutamate receptors in excitatory synapses. Similarly, α1D adrenergic receptor (401), Kir2.1 and Kir4.1 (402,403), as well as AQP4 (404) have been reported to interact with syntrophins. Most of these interactions involve the PDZ motif (PSD-95, Dlg, ZO-1/Dlg-homologous region) of syntrophin and the consensus domain (S/T)XV contained in the C-terminal domains of these receptors (135,298,404-408).

Despite the central role of DG in the DAP complex, there are no known human mutations in the DG gene (reviewed by (409)). However, 30% of Duchenne Muscular Dystrophy (DMD) and Becker Muscular Dystrophy (BMD) patients with mutations in dystrophin can present detectable cognitive deficits, such as learning, calculation or memory difficulties, as well as severe hydrocephalus, autism and epilepsy (410-418).

The effects of DG deletion have been investigated in mouse models carrying selective deletions of DG or mutations in dystrophin (mdx and mdx^{3cv} mice) which do cause a secondary reduction of DG in the brain. These mouse models show impaired neuronal function and DMD-like malformations in brain, such as in abnormal radial glia and neuroblast migration, profound impairments of long-term potentiation as well as abnormalities in ERGs (397,398,419-423). Similarly, α- and β-DB null mouse exhibits abnormalities in the organization and function of the CNS (382) and utrophin-null mouse shows increase sensitivity to epileptic seizure (424,425). Interestingly, mice models carrying mutations or deletions of glycosyltransferases that impedes the glycosylation-dependent binding of α-DG to ECM also present cerebral and ocular defects similar to the phenotype of Muscle-Eye-Brain disease (MEB), Fukuyama Congenital Muscular Dystrophy (FCMD), Limb-Girdle Muscular Dystrophy (LGMD), Walker-Warburg Syndrome (WWS) and Congenital Muscular Dystrophies type 1C and 1D (MDC1C, MDC1D) (426-429).

1.5.2 Dystroglycan interaction with laminin

Recent studies have shown that the heavy glycosylation of α-DG is crucial for its binding to laminin and varies between tissues (332,338,430,431). α-DG contains three possible N-linked glycosylation sites, one on the N-terminus and two on the C-terminus which are separated by a central mucin-like domain rich in serine/threonine. This region undergoes extensive post-translational O-linked glycosylation that contributes to an apparent molecular weight of 120-156 kDa compared to the predicted 74 kDa (432). The O-glycans expressed by the mucin like domain of α-DG are attached to serine/threonine residues by way of the sugar mannose and are initiated by a peptidic sequence upstream of the mucin domain (433,434). The addition of the first mannose occurs in the endoplasmic reticulum by protein O-mannosyltransferase, POMT1/2 (435,436), and is followed by addition of N-acetylglucosamine residue (GlcNAc) by a protein O-

mannosyl-beta1, 2-N-acetylglucosaminyltransferase, POMGnT1 (437,438). The galactosyl and sialyl transferases involved in the subsequent extension of the chain remain to be identified but fukutin and FKRP are putative candidates (439,440). Another N-acetyl-glucosamine glycosyltransferase, known as Large, has also been demonstrated to play a role in the hyperglycosylated form of α-DG (441-443) and interestingly, it has recently been shown that Large participates in an additional step of O-mannosyl phosphorylation of α-DG which can circumvent any defect in DG binding to laminin (444-446).

The sialylated residues have been shown to confer the interaction of laminin to α-DG (433,447). As the final residues of this sugar chain are crucial for the α-DG binding to laminin, defects in any one of the upstream glycosyltransferases involved in the extension of the chain would disrupt the interaction. This is reflected in the Large[myd], fukutin chimeric or POMGnT1 null mouse models where a reduction of α-DG O-glycosylation on its mucin like domain causes loss of ligand binding which is associated with a progressive myopathy and defects in the CNS (419,448-451). Similarly, in human, FCMD and LGMD patients have been identified with mutations in the fukutin gene (452-454), MEB patients with POMGnT1 mutations (437), WWS patients with POMT1/2, FKRP or Large mutations (455-459), CMD1C and LGMD patients with FKRP or POMT1/2 mutations (460,461) or CMD1D patients with Large mutations (462). All of these human diseases, classified as dystroglycanopathies, are characterized by loss of DG binding to laminin and concomitant brain and ocular defects with increased seizure activity (419,430,449,454,462-467).

1.6 Project outline

The treatment of brain edema remained unchanged for the past 90 years and is very limited, culminating with removal of a large bone flap (decompressive cranioectomy) to allow the brain to swell outside the rigid cranium. The poor therapeutic modalities available for cerebral edema that develops after stroke contributes significantly to the morbidity and mortality of this condition (468). In addition the intravenous injection of hypertonic solutions of mannitol or saline to reduce cellular swelling, which remains the cornerstone of medical therapy for cerebral edema (469,470), can be deleterious as it may lead to seizures because of high cerebral

Gene	Human Dystrophy with CNS disorders	Mouse Model	Brain Edema	AQP4 Perivascular Distribution
Dystrophin	DMD (417) BMD (418)	Mdx (360) Mdx-βgeo (361)	ND Decreased cytotoxic	Absent (323) Reduced (474)
Utrophin	-	Utrophin 0/0 (424)	ND	ND
Dystrobrevin	-	α-DB/β-DB DKO (382)	ND	ND
Syntrophin	-	α-syntrophin null (388)	Decreased cytotoxic	Reduced (404)
Dystroglycan	No (409)	GFAP-Cre/DG null (398)	ND	Absent (398)
POMT1/2	WWS (455)	No (436)	-	-
POMGnT1	MEB (437)	POMGnT1 null (438)	ND	ND
Fukutin	FCMD (453)	Fukutin chimeric (427)	ND	ND
FKRP	LGMD (460)	FKRP deficiency (440)	ND	ND
Large	CMD1D (462)	Large^{myd} (449)	ND	ND
Laminin α2	CMD (230)	Dy (232)	Higher ECS	ND
Agrin	-	Agrin$^{-/-}$ (263)	ND	Reduced (200)

Table 1.2. Summary of dystrophies, mouse models, brain edema presentation and AQP4 distribution for each member of the DAP complex, the enzymes involved in α-DG glycosylation, laminin and agrin (ND:not determined).

ion concentration when sudden egress of water from the interstitial space into the intravascular compartment if proceeded too rapidly (471,472). In case the BBB is compromised, treatment alternatives become even more complicated. The discovery of AQP4 in the brain provided new insights into water routes in and out of the brain and opened avenues into research of novel pharmacologic tools to treat edema formation. On a molecular level, an understanding of the basic physiological processes and mechanisms regulating AQP4 functional distribution is of crucial importance.

Interestingly, it has been shown that deletions or mutations of dystrophin, syntrophin and DG could lead to an improper localization of both AQP4 and Kir4.1 in brain and retina. In α-syntrophin-null as well as dystrophin-null mice, such mislocalization of AQP4 has been correlated with a preventive effect from the formation of brain edema produced by focal cerebral ischemia (Table 1.2) (299,323-325,387,404,407,473-475). In support of its role in the functional distribution of both AQP4 and Kir4.1 in CNS, we have recently shown that DG concentrates and colocalizes with laminin, AQP4 and Kir4.1 in the astrocyte endfeet abutting blood vessels, as well as the Müller cell endfeet apposed to the retinal ILM. In addition we demonstrated that laminin induces the clustering of AQP4 and Kir4.1 through the DAP complex in astrocyte and Müller cell cultures (406,476).

My thesis further investigates the involvement of the DAP complex and its interaction with the different components of the basal lamina in regulating AQP4 polarized distribution and activity. My working hypotheses are **1)** the glycosylation state of α-DG regulates the polarized distribution of AQP4 and Kir4.1 channels in brain and retina, **2)** the ECM molecules cooperate actively in the stability and clustering of AQP4 and this requires signalling cascades, and **3)** impaired signalling will result in AQP4 mistargeting in astrocytes and interfere with the ability of the brain to handle AQP4-mediated water fluxes. So far, only two drugs, tetraethylammonium (TEA) and acetazolamide (AZA) have been identified as potential inhibitors of AQP4 activity and no activators have been found yet (477-481). In my study, I also focused to identify new molecules that could modulate the functional distribution of AQP4 using a highthroughput screen.

1.7 References

1. Saadoun, S., Papadopoulos, M., Bell, B., Krishna, S., and Davies, D. (2002) *J Anat* **200**, 528

2. Marmarou, A., Signoretti, S., Fatouros, P. P., Portella, G., Aygok, G. A., and Bullock, M. R. (2006) *J Neurosurg* **104**, 720-730

3. Ayata, C., and Ropper, A. H. (2002) *J Clin Neurosci* **9**, 113-124

4. Barron, K. D., Dentinger, M. P., Kimelberg, H. K., Nelson, L. R., Bourke, R. S., Keegan, S., Mankes, R., and Cragoe, E. J., Jr. (1988) *Acta Neuropathol* **75**, 295-307

5. Kimelberg, H. K., Feustel, P. J., Jin, Y., Paquette, J., Boulos, A., Keller, R. W., Jr., and Tranmer, B. I. (2000) *Neuroreport* **11**, 2675-2679

6. Klatzo, I. (1967) *J Neuropathol Exp Neurol* **26**, 1-14

7. Kimelberg, H. K. (1995) *J Neurosurg* **83**, 1051-1059

8. Bardutzky, J., and Schwab, S. (2007) *Stroke* **38**, 3084-3094

9. Doerfler, A., Forsting, M., Reith, W., Staff, C., Heiland, S., Schabitz, W. R., von Kummer, R., Hacke, W., and Sartor, K. (1996) *J Neurosurg* **85**, 853-859

10. Fishman, R. A. (1975) *N Engl J Med* **293**, 706-711

11. Liu, H. M., and Sturner, W. Q. (1988) *Forensic Sci Int* **38**, 285-295

12. Chen, H. J., Lee, T. C., and Wei, C. P. (1992) *Stroke* **23**, 957-961

13. Heo, J. H., Han, S. W., and Lee, S. K. (2005) *Free Radic Biol Med* **39**, 51-70

14. Verweij, B. H., Muizelaar, J. P., Vinas, F. C., Peterson, P. L., Xiong, Y., and Lee, C. P. (2000) *J Neurosurg* **93**, 815-820

15. Go, K. G. (1997) *Adv Tech Stand Neurosurg* **23**, 47-142

16. Garcia, J. H., Yoshida, Y., Chen, H., Li, Y., Zhang, Z. G., Lian, J., Chen, S., and Chopp, M. (1993) *Am J Pathol* **142**, 623-635

17. Garcia, J. H., Liu, K. F., Yoshida, Y., Chen, S., and Lian, J. (1994) *Am J Pathol* **145**, 728-740

18. Duffy, S., and MacVicar, B. A. (1996) *J Neurosci* **16**, 71-81

19. Nedergaard, M., Goldman, S. A., Desai, S., and Pulsinelli, W. A. (1991) *J Neurosci* **11**, 2489-2497

20. Immke, D. C., and McCleskey, E. W. (2001) *Nat Neurosci* **4**, 869-870

21. Kempski, O., Staub, F., Jansen, M., Schodel, F., and Baethmann, A. (1988) *Stroke* **19**, 385-392

22. Robinson, M. B., and Dowd, L. A. (1997) *Adv Pharmacol* **37**, 69-115

23. Loo, D. T., Althoen, M. C., and Cotman, C. W. (1995) *J Neurosci Res* **42**, 184-191

24. Rothman, S. M., and Olney, J. W. (1986) *Ann Neurol* **19**, 105-111

25. Szatkowski, M., and Attwell, D. (1994) *Trends Neurosci* **17**, 359-365

26. Rice, M. E., and Russo-Menna, I. (1998) *Neuroscience* **82**, 1213-1223

27. Staub, F., Winkler, A., Peters, J., Kempski, O., Kachel, V., and Baethmann, A. (1994) *J Cereb Blood Flow Metab* **14**, 1030-1039

28. Chan, P. H., and Fishman, R. A. (1984) *Fed Proc* **43**, 210-213

29. Liu, M., Liu, S., Peterson, S. L., Miyake, M., and Liu, K. J. (2002) *Mol Cell Biochem* **234-235**, 379-385

30. Simard, J. M., Kent, T. A., Chen, M., Tarasov, K. V., and Gerzanich, V. (2007) *Lancet Neurol* **6**, 258-268

31. Wu, J. S., Chen, X. C., Chen, H., and Shi, Y. Q. (2006) *Neurol Res* **28**, 50-58

32. Xi, G., Keep, R. F., and Hoff, J. T. (2006) *Lancet Neurol* **5**, 53-63

33. Muellner, A., Benz, M., Kloss, C. U., Mautes, A., Burggraf, D., and Hamann, G. F. (2003) *J Neurotrauma* **20**, 745-754

34. Sellner, J., and Leib, S. L. (2006) *Neurobiol Dis* **21**, 647-656

35. Serena, J., Blanco, M., Castellanos, M., Silva, Y., Vivancos, J., Moro, M. A., Leira, R., Lizasoain, I., Castillo, J., and Davalos, A. (2005) *Stroke* **36**, 1921-1926

36. Scholler, K., Trinkl, A., Klopotowski, M., Thal, S. C., Plesnila, N., Trabold, R., Hamann, G. F., Schmid-Elsaesser, R., and Zausinger, S. (2007) *Brain Res* **1142**, 237-246

37. Rosell, A., Cuadrado, E., Ortega-Aznar, A., Hernandez-Guillamon, M., Lo, E. H., and Montaner, J. (2008) *Stroke* **39**, 1121-1126

38. Hamann, G. F., Okada, Y., Fitridge, R., and del Zoppo, G. J. (1995) *Stroke* **26**, 2120-2126

39. Gasche, Y., Copin, J. C., Sugawara, T., Fujimura, M., and Chan, P. H. (2001) *J Cereb Blood Flow Metab* **21**, 1393-1400

40. Heo, J. H., Lucero, J., Abumiya, T., Koziol, J. A., Copeland, B. R., and del Zoppo, G. J. (1999) *J Cereb Blood Flow Metab* **19**, 624-633

41. Chang, D. I., Hosomi, N., Lucero, J., Heo, J. H., Abumiya, T., Mazar, A. P., and del Zoppo, G. J. (2003) *J Cereb Blood Flow Metab* **23**, 1408-1419

42. Gidday, J. M., Gasche, Y. G., Copin, J. C., Shah, A. R., Perez, R. S., Shapiro, S. D., Chan, P. H., and Park, T. S. (2005) *Am J Physiol Heart Circ Physiol* **289**, H558-568

43. Rosenberg, G. A., Estrada, E. Y., and Dencoff, J. E. (1998) *Stroke* **29**, 2189-2195

44. Yang, Y., Estrada, E. Y., Thompson, J. F., Liu, W., and Rosenberg, G. A. (2007) *J Cereb Blood Flow Metab* **27**, 697-709

45. Sole, S., Petegnief, V., Gorina, R., Chamorro, A., and Planas, A. M. (2004) *J Neuropathol Exp Neurol* **63**, 338-349

46. Gu, Z., Cui, J., Brown, S., Fridman, R., Mobashery, S., Strongin, A. Y., and Lipton, S. A. (2005) *J Neurosci* **25**, 6401-6408

47. Abramov, A. Y., Scorziello, A., and Duchen, M. R. (2007) *J Neurosci* **27**, 1129-1138

48. Mayhan, W. G., and Didion, S. P. (1996) *Stroke* **27**, 965-969; discussion 970

49. Meli, D. N., Christen, S., and Leib, S. L. (2003) *J Infect Dis* **187**, 1411-1415

50. del Zoppo, G. J., Schmid-Schonbein, G. W., Mori, E., Copeland, B. R., and Chang, C. M. (1991) *Stroke* **22**, 1276-1283

51. Cross, A. K., Haddock, G., Stock, C. J., Allan, S., Surr, J., Bunning, R. A., Buttle, D. J., and Woodroofe, M. N. (2006) *Brain Res* **1088**, 19-30

52. Schonbeck, U., Mach, F., and Libby, P. (1998) *J Immunol* **161**, 3340-3346

53. Abumiya, T., Lucero, J., Heo, J. H., Tagaya, M., Koziol, J. A., Copeland, B. R., and del Zoppo, G. J. (1999) *J Cereb Blood Flow Metab* **19**, 1038-1050

54. Weis, S. M., and Cheresh, D. A. (2005) *Nature* **437**, 497-504

55. Lafuente, J. V., Adan, B., Alkiza, K., Garibi, J. M., Rossi, M., and Cruz-Sanchez, F. F. (1999) *J Mol Neurosci* **13**, 177-185

56. Goldman, C. K., Bharara, S., Palmer, C. A., Vitek, J., Tsai, J. C., Weiss, H. L., and Gillespie, G. Y. (1997) *Neurosurgery* **40**, 1269-1277

57. Wang, W., Dentler, W. L., and Borchardt, R. T. (2001) *Am J Physiol Heart Circ Physiol* **280**, H434-440

58. Zhang, Z. G., Zhang, L., Jiang, Q., Zhang, R., Davies, K., Powers, C., Bruggen, N., and Chopp, M. (2000) *J Clin Invest* **106**, 829-838

59. Kuroiwa, T., Cahn, R., Juhler, M., Goping, G., Campbell, G., and Klatzo, I. (1985) *Acta Neuropathol* **66**, 3-11

60. Hatashita, S., and Hoff, J. T. (1990) *Stroke* **21**, 582-588

61. Betz, A. L., Iannotti, F., and Hoff, J. T. (1989) *Cerebrovasc Brain Metab Rev* **1**, 133-154
62. Klatzo, I. (1985) *Br J Anaesth* **57**, 18-22
63. Strange, K. (2004) *Adv Physiol Educ* **28**, 155-159
64. Kimelberg, H. K. (2004) *Adv Exp Med Biol* **559**, 157-167
65. Pasantes-Morales, H., Chacon, E., Murray, R. A., and Moran, J. (1994) *J Neurosci Res* **37**, 720-727
66. Vitarella, D., DiRisio, D. J., Kimelberg, H. K., and Aschner, M. (1994) *J Neurochem* **63**, 1143-1149
67. Yancey, P. H., Clark, M. E., Hand, S. C., Bowlus, R. D., and Somero, G. N. (1982) *Science* **217**, 1214-1222
68. Jackson, P. S., and Strange, K. (1993) *Am J Physiol* **265**, C1489-1500
69. Verkman, A. S., and Mitra, A. K. (2000) *Am J Physiol Renal Physiol* **278**, F13-28
70. Pasantes-Morales, H. (1996) *Metab Brain Dis* **11**, 187-204
71. Moran, J., Morales-Mulia, S., Hernandez-Cruz, A., and Pasantes-Morales, H. (1997) *J Neurosci Res* **47**, 144-154
72. Lang, F., Busch, G. L., Ritter, M., Volkl, H., Waldegger, S., Gulbins, E., and Haussinger, D. (1998) *Physiol Rev* **78**, 247-306
73. Lang, F., Busch, G. L., and Volkl, H. (1998) *Cell Physiol Biochem* **8**, 1-45
74. Jackson, P. S., Morrison, R., and Strange, K. (1994) *Am J Physiol* **267**, C1203-1209
75. Jackson, P. S., and Strange, K. (1995) *J Gen Physiol* **105**, 661-676
76. Jackson, P. S., and Strange, K. (1995) *J Gen Physiol* **105**, 643-660
77. Kimelberg, H. K., Goderie, S. K., Higman, S., Pang, S., and Waniewski, R. A. (1990) *J Neurosci* **10**, 1583-1591
78. Duan, D., Winter, C., Cowley, S., Hume, J. R., and Horowitz, B. (1997) *Nature* **390**, 417-421
79. Wang, L., Chen, L., and Jacob, T. J. (2000) *J Physiol* **524 Pt 1**, 63-75
80. Pasantes-Morales, H., Franco, R., Ordaz, B., and Ochoa, L. D. (2002) *Arch Med Res* **33**, 237-244
81. Hussy, N., Deleuze, C., Bres, V., and Moos, F. C. (2000) *Adv Exp Med Biol* **483**, 227-237
82. Wade, J. V., Olson, J. P., Samson, F. E., Nelson, S. R., and Pazdernik, T. L. (1988) *J Neurochem* **51**, 740-745
83. Okada, Y. (1997) *Am J Physiol* **273**, C755-789
84. Burg, M. B. (2000) *Cell Physiol Biochem* **10**, 251-256
85. Schousboe, A., and Pasantes-Morales, H. (1992) *Can J Physiol Pharmacol* **70 Suppl**, S356-361
86. Lambert, I. H. (2004) *Neurochem Res* **29**, 27-63
87. Verbalis, J. G., and Gullans, S. R. (1991) *Brain Res* **567**, 274-282
88. Lien, Y. H., Shapiro, J. I., and Chan, L. (1991) *J Clin Invest* **88**, 303-309
89. Haussinger, D., and Gerok, W. (1994) *Adv Exp Med Biol* **368**, 33-44
90. Haussinger, D., Lang, F., and Gerok, W. (1994) *Am J Physiol* **267**, E343-355
91. Mongin, A. A., and Kimelberg, H. K. (2005) *Am J Physiol Cell Physiol* **288**, C204-213
92. Strupp, M., Staub, F., and Grafe, P. (1993) *Glia* **9**, 136-145
93. Agre, P., and Kozono, D. (2003) *FEBS Lett* **555**, 72-78
94. King, L. S., Kozono, D., and Agre, P. (2004) *Nat Rev Mol Cell Biol* **5**, 687-698
95. Agre, P., Sasaki, S., and Chrispeels, M. J. (1993) *Am J Physiol* **265**, F461
96. Sidel, V. W., and Solomon, A. K. (1957) *J Gen Physiol* **41**, 243-257

97. Agre, P., King, L. S., Yasui, M., Guggino, W. B., Ottersen, O. P., Fujiyoshi, Y., Engel, A., and Nielsen, S. (2002) *J Physiol* **542**, 3-16

98. Verkman, A. S. (2005) *J Cell Sci* **118**, 3225-3232

99. Ma, T., Yang, B., Gillespie, A., Carlson, E. J., Epstein, C. J., and Verkman, A. S. (1997) *J Clin Invest* **100**, 957-962

100. Ma, T., Fukuda, N., Song, Y., Matthay, M. A., and Verkman, A. S. (2000) *J Clin Invest* **105**, 93-100

101. Ma, T., Song, Y., Gillespie, A., Carlson, E. J., Epstein, C. J., and Verkman, A. S. (1999) *J Biol Chem* **274**, 20071-20074

102. Song, Y., and Verkman, A. S. (2001) *J Biol Chem* **276**, 41288-41292

103. Badaut, J., Petit, J. M., Brunet, J. F., Magistretti, P. J., Charriaut-Marlangue, C., and Regli, L. (2004) *Neuroscience* **128**, 27-38

104. Oshio, K., Watanabe, H., Song, Y., Verkman, A. S., and Manley, G. T. (2005) *FASEB J* **19**, 76-78

105. Nicchia, G. P., Frigeri, A., Liuzzi, G. M., and Svelto, M. (2003) *Faseb J* **17**, 1508-1510

106. Nicchia, G. P., Frigeri, A., Liuzzi, G. M., Santacroce, M. P., Nico, B., Procino, G., Quondamatteo, F., Herken, R., Roncali, L., and Svelto, M. (2000) *Glia* **31**, 29-38

107. Nielsen, S., Nagelhus, E. A., Amiry-Moghaddam, M., Bourque, C., Agre, P., and Ottersen, O. P. (1997) *J Neurosci* **17**, 171-180

108. Ho, J. D., Yeh, R., Sandstrom, A., Chorny, I., Harries, W. E., Robbins, R. A., Miercke, L. J., and Stroud, R. M. (2009) *Proc Natl Acad Sci U S A* **106**, 7437-7442

109. Hiroaki, Y., Tani, K., Kamegawa, A., Gyobu, N., Nishikawa, K., Suzuki, H., Walz, T., Sasaki, S., Mitsuoka, K., Kimura, K., Mizoguchi, A., and Fujiyoshi, Y. (2006) *J Mol Biol* **355**, 628-639

110. Tani, K., Mitsuma, T., Hiroaki, Y., Kamegawa, A., Nishikawa, K., Tanimura, Y., and Fujiyoshi, Y. (2009) *J Mol Biol* **389**, 694-706

111. Jung, J. S., Bhat, R. V., Preston, G. M., Guggino, W. B., Baraban, J. M., and Agre, P. (1994) *Proc Natl Acad Sci U S A* **91**, 13052-13056.

112. King, L. S., Yasui, M., and Agre, P. (2000) *Molecular Medecine Today* **6**, 60-65

113. Yang, B., Verbavatz, J. M., Song, Y., Vetrivel, L., Manley, G., Kao, W. M., Ma, T., and Verkman, A. S. (2000) *Am J Physiol Cell Physiol* **278**, C1108-1115

114. Frigeri, A., Gropper, M. A., Turck, C. W., and Verkman, A. S. (1995) *Proc Natl Acad Sci U S A* **92**, 4328-4331.

115. Verbavatz, J. M., Ma, T., Gobin, R., and Verkman, A. S. (1997) *J Cell Sci* **110 (Pt 22)**, 2855-2860

116. Yang, B., van Hoek, A. N., and Verkman, A. S. (1997) *Biochemistry* **36**, 7625-7632

117. Rash, J. E., Yasumura, T., Hudson, C. S., Agre, P., and Nielsen, S. (1998) *Proc Natl Acad Sci U S A* **95**, 11981-11986

118. Moe, S. E., Sorbo, J. G., Sogaard, R., Zeuthen, T., Petter Ottersen, O., and Holen, T. (2008) *Genomics* **91**, 367-377

119. Lu, M., Lee, M. D., Smith, B. L., Jung, J. S., Agre, P., Verdijk, M. A., Merkx, G., Rijss, J. P., and Deen, P. M. (1996) *Proc Natl Acad Sci U S A* **93**, 10908-10912

120. Umenishi, F., and Verkman, A. S. (1998) *Genomics* **50**, 373-377

121. Hasegawa, H., Ma, T., Skach, W., Matthay, M. A., and Verkman, A. S. (1994) *J Biol Chem* **269**, 5497-5500

122. Neely, J. D., Christensen, B. M., Nielsen, S., and Agre, P. (1999) *Biochemistry* **38**, 11156-11163

123. Suzuki, H., Nishikawa, K., Hiroaki, Y., and Fujiyoshi, Y. (2008) *Biochim Biophys Acta* **1778**, 1181-1189

124. Crane, J. M., Bennett, J. L., and Verkman, A. S. (2009) *J Biol Chem*

125. Guan, X. G., Su, W. H., Yi, F., Zhang, D., Hao, F., Zhang, H. G., Liu, Y. J., Feng, X. C., and Ma, T. H. *IUBMB Life* **62**, 222-226

126. Noell, S., Fallier-Becker, P., Beyer, C., Kroger, S., Mack, A. F., and Wolburg, H. (2007) *Eur J Neurosci* **26**, 2109-2118

127. Silberstein, C., Bouley, R., Huang, Y., Fang, P., Pastor-Soler, N., Brown, D., and Van Hoek, A. N. (2004) *Am J Physiol Renal Physiol* **287**, F501-511

128. Fenton, R. A., Moeller, H. B., Zelenina, M., Snaebjornsson, M. T., Holen, T., and Macaulay, N. (2009) *Cell Mol Life Sci*

129. Crane, J. M., Van Hoek, A. N., Skach, W. R., and Verkman, A. S. (2008) *Mol Biol Cell* **19**, 3369-3378

130. Crane, J. M., and Verkman, A. S. (2009) *J Cell Sci* **122**, 813-821

131. Wolburg, H. (1995) *J Hirnforsch* **36**, 239-258

132. Furman, C. S., Gorelick-Feldman, D. A., Davidson, K. G., Yasumura, T., Neely, J. D., Agre, P., and Rash, J. E. (2003) *Proc Natl Acad Sci U S A* **100**, 13609-13614

133. Rash, J. E., Davidson, K. G., Yasumura, T., and Furman, C. S. (2004) *Neuroscience* **129**, 915-934

134. Sorbo, J. G., Moe, S. E., Ottersen, O. P., and Holen, T. (2008) *Biochemistry* **47**, 2631-2637

135. Fort, P. E., Sene, A., Pannicke, T., Roux, M. J., Forster, V., Mornet, D., Nudel, U., Yaffe, D., Reichenbach, A., Sahel, J. A., and Rendon, A. (2008) *Glia* **56**, 597-610

136. Hibino, H., and Kurachi, Y. (2007) *Eur J Neurosci* **26**, 2539-2555

137. Nicchia, G. P., Cogotzi, L., Rossi, A., Basco, D., Brancaccio, A., Svelto, M., and Frigeri, A. (2008) *J Neurochem*

138. Nicchia, G. P., Rossi, A., Mola, M. G., Pisani, F., Stigliano, C., Basco, D., Mastrototaro, M., Svelto, M., and Frigeri, A. *Neuroscience*

139. Gunnarson, E., Axehult, G., Baturina, G., Zelenin, S., Zelenina, M., and Aperia, A. (2005) *Neuroscience* **136**, 105-114

140. Gunnarson, E., Zelenina, M., and Aperia, A. (2004) *Neuroscience* **129**, 947-955

141. Han, Z., Wax, M. B., and Patil, R. V. (1998) *J Biol Chem* **273**, 6001-6004

142. Yamamoto, N., Sobue, K., Miyachi, T., Inagaki, M., Miura, Y., Katsuya, H., and Asai, K. (2001) *Brain Res Mol Brain Res* **95**, 110-116

143. Zelenina, M., Zelenin, S., Bondar, A. A., Brismar, H., and Aperia, A. (2002) *Am J Physiol Renal Physiol* **283**, F309-318

144. Madrid, R., Le Maout, S., Barrault, M. B., Janvier, K., Benichou, S., and Merot, J. (2001) *EMBO J* **20**, 7008-7021

145. Van Hoek, A. N., Bouley, R., Lu, Y., Silberstein, C., Brown, D., Wax, M. B., and Patil, R. V. (2009) *Am J Physiol Renal Physiol* **296**, F1396-1404

146. McCoy, E. S., Haas, B. R., and Sontheimer, H. (2009) *Neuroscience*

147. Tang, Y., Cai, D., and Chen, Y. (2007) *J Mol Neurosci* **31**, 83-93

148. Fazzina, G., Amorini, A. M., Marmarou, C., Fukui, S., Okuno, K., Glisson, R., Marmarou, A., and Kleindienst, A. (2009) *J Neurotrauma*

149. Kleindienst, A., Fazzina, G., Amorini, A. M., Dunbar, J. G., Glisson, R., and Marmarou, A. (2006) *Acta Neurochir Suppl* **96**, 393-397

150. Nakahama, K., Nagano, M., Fujioka, A., Shinoda, K., and Sasaki, H. (1999) *Glia* **25**, 240-246

151. Strand, L., Moe, S. E., Solbu, T. T., Vaadal, M., and Holen, T. (2009) *Biochemistry* **48**, 5785-5793

152. Nielsen, S., Nagelhus, E. A., Amiry-Moghaddam, M., Bourque, C., Agre, P., and Ottersen, O. P. (1997) *J Neurosci* **17**, 171-180.

153. Romeiro, R. R., Romano-Silva, M. A., De Marco, L., Teixeira, A. L., Jr., and Correa, H. (2007) *Neurosci Lett* **426**, 133-134

154. Sorani, M. D., Zador, Z., Hurowitz, E., Yan, D., Giacomini, K. M., and Manley, G. T. (2008) *Hum Mol Genet* **17**, 2379-2389

155. Kleffner, I., Bungeroth, M., Schiffbauer, H., Schabitz, W. R., Ringelstein, E. B., and Kuhlenbaumer, G. (2008) *Stroke* **39**, 1333-1335

156. Manley, G. T., Fujimura, M., Ma, T., Noshita, N., Filiz, F., Bollen, A. W., Chan, P., and Verkman, A. S. (2000) *Nat Med* **6**, 159-163

157. Fu, X., Li, Q., Feng, Z., and Mu, D. (2007) *Glia* **55**, 935-941

158. Bloch, O., Auguste, K. I., Manley, G. T., and Verkman, A. S. (2006) *J Cereb Blood Flow Metab* **26**, 1527-1537

159. Bloch, O., Papadopoulos, M. C., Manley, G. T., and Verkman, A. S. (2005) *J Neurochem* **95**, 254-262

160. Papadopoulos, M. C., Manley, G. T., Krishna, S., and Verkman, A. S. (2004) *Faseb J* **18**, 1291-1293

161. Feng, X., Papadopoulos, M. C., Liu, J., Li, L., Zhang, D., Zhang, H., Verkman, A. S., and Ma, T. (2009) *J Neurosci Res* **87**, 1150-1155

162. Tait, M. J., Saadoun, S., Bell, B. A., Verkman, A. S., and Papadopoulos, M. C. *Neuroscience* **167**, 60-67

163. Yang, B., Zador, Z., and Verkman, A. S. (2008) *J Biol Chem* **283**, 15280-15286

164. Saadoun, S., Tait, M. J., Reza, A., Davies, D. C., Bell, B. A., Verkman, A. S., and Papadopoulos, M. C. (2009) *Neuroscience* **161**, 764-772

165. Tang, Y., Wu, P., Su, J., Xiang, J., Cai, D., and Dong, Q. *Exp Neurol*

166. Ke, C., Poon, W. S., Ng, H. K., Pang, J. C., and Chan, Y. (2001) *Neurosci Lett* **301**, 21-24

167. Kiening, K. L., van Landeghem, F. K., Schreiber, S., Thomale, U. W., von Deimling, A., Unterberg, A. W., and Stover, J. F. (2002) *Neurosci Lett* **324**, 105-108

168. Meng, S., Qiao, M., Lin, L., Del Bigio, M. R., Tomanek, B., and Tuor, U. I. (2004) *Eur J Neurosci* **19**, 2261-2269

169. Taniguchi, M., Yamashita, T., Kumura, E., Tamatani, M., Kobayashi, A., Yokawa, T., Maruno, M., Kato, A., Ohnishi, T., Kohmura, E., Tohyama, M., and Yoshimine, T. (2000) *Brain Res Mol Brain Res* **78**, 131-137

170. Vizuete, M. L., Venero, J. L., Vargas, C., Ilundain, A. A., Echevarria, M., Machado, A., and Cano, J. (1999) *Neurobiol Dis* **6**, 245-258

171. Sato, S., Umenishi, F., Inamasu, G., Sato, M., Ishikawa, M., Nishizawa, M., and Oizumi, T. (2000) *Acta Neurochir Suppl* **76**, 239-241

172. Ribeiro Mde, C., Hirt, L., Bogousslavsky, J., Regli, L., and Badaut, J. (2006) *J Neurosci Res* **83**, 1231-1240

173. Ito, H., Yamamoto, N., Arima, H., Hirate, H., Morishima, T., Umenishi, F., Tada, T., Asai, K., Katsuya, H., and Sobue, K. (2006) *J Neurochem* **99**, 107-118

174. Frydenlund, D. S., Bhardwaj, A., Otsuka, T., Mylonakou, M. N., Yasumura, T., Davidson, K. G., Zeynalov, E., Skare, O., Laake, P., Haug, F. M., Rash, J. E., Agre, P., Ottersen, O. P., and Amiry-Moghaddam, M. (2006) *Proc Natl Acad Sci U S A* **103**, 13532-13536

175. Friedman, B., Schachtrup, C., Tsai, P. S., Shih, A. Y., Akassoglou, K., Kleinfeld, D., and Lyden, P. D. (2009) *Stroke* **40**, 2182-2190

176. Sun, M. C., Honey, C. R., Berk, C., Wong, N. L., and Tsui, J. K. (2003) *J Neurosurg* **98**, 565-569

177. Hu, H., Yao, H. T., Zhang, W. P., Zhang, L., Ding, W., Zhang, S. H., Chen, Z., and Wei, E. Q. (2005) *J Zhejiang Univ Sci B* **6**, 33-37

178. Ghabriel, M. N., Thomas, A., and Vink, R. (2006) *Acta Neurochir Suppl* **96**, 402-406

179. Neal, C. J., Lee, E. Y., Gyorgy, A., Ecklund, J. M., Agoston, D. V., and Ling, G. S. (2007) *J Neurotrauma* **24**, 1609-1617

180. Saadoun, S., Papadopoulos, M. C., Davies, D. C., Krishna, S., and Bell, B. A. (2002) *J Neurol Neurosurg Psychiatry* **72**, 262-265

181. Badaut, J., Brunet, J. F., Grollimund, L., Hamou, M. F., Magistretti, P. J., Villemure, J. G., and Regli, L. (2003) *Acta Neurochir Suppl* **86**, 495-498

182. Lu, H., and Sun, S. Q. (2003) *Chin Med J (Engl)* **116**, 1063-1069

183. Hirt, L., Ternon, B., Price, M., Mastour, N., Brunet, J. F., and Badaut, J. (2009) *J Cereb Blood Flow Metab* **29**, 423-433

184. Reulen, H. J., Graham, R., Spatz, M., and Klatzo, I. (1977) *J Neurosurg* **46**, 24-35

185. Nicchia, G. P., Nico, B., Camassa, L. M., Mola, M. G., Loh, N., Dermietzel, R., Spray, D. C., Svelto, M., and Frigeri, A. (2004) *Neuroscience* **129**, 935-945

186. Wen, H., Nagelhus, E. A., Amiry-Moghaddam, M., Agre, P., Ottersen, O. P., and Nielsen, S. (1999) *Eur J Neurosci* **11**, 935-945

187. Gomori, E., Pal, J., Abraham, H., Vajda, Z., Sulyok, E., Seress, L., and Doczi, T. (2006) *Int J Dev Neurosci* **24**, 295-305

188. Ferrari, D. C., Nesic, O. B., and Perez-Polo, J. R. *J Neurosci Res*

189. Yao, X., Hrabetova, S., Nicholson, C., and Manley, G. T. (2008) *J Neurosci* **28**, 5460-5464

190. Xiao, F., and Hrabetova, S. (2009) *Neuroscience* **161**, 39-45

191. Zador, Z., Magzoub, M., Jin, S., Manley, G. T., Papadopoulos, M. C., and Verkman, A. S. (2008) *FASEB J* **22**, 870-879

192. Amiry-Moghaddam, M., Williamson, A., Palomba, M., Eid, T., de Lanerolle, N. C., Nagelhus, E. A., Adams, M. E., Froehner, S. C., Agre, P., and Ottersen, O. P. (2003) *Proc Natl Acad Sci U S A* **100**, 13615-13620

193. Binder, D. K., Papadopoulos, M. C., Haggie, P. M., and Verkman, A. S. (2004) *J Neurosci* **24**, 8049-8056

194. Eid, T., Lee, T. S., Thomas, M. J., Amiry-Moghaddam, M., Bjornsen, L. P., Spencer, D. D., Agre, P., Ottersen, O. P., and de Lanerolle, N. C. (2005) *Proc Natl Acad Sci U S A* **102**, 1193-1198

195. Hatton, J. D., and Ellisman, M. H. (1984) *Epilepsia* **25**, 145-151

196. Nagelhus, E. A., Horio, Y., Inanobe, A., Fujita, A., Haug, F. M., Nielsen, S., Kurachi, Y., and Ottersen, O. P. (1999) *Glia* **26**, 47-54.

197. Nagelhus, E. A., Veruki, M. L., Torp, R., Haug, F. M., Laake, J. H., Nielsen, S., Agre, P., and Ottersen, O. P. (1998) *J Neurosci* **18**, 2506-2519

198. Patil, R. V., Han, Z., and Wax, M. B. (1997) *Science* **275**, 1492; author reply 1492

199. Li, J., Patil, R. V., and Verkman, A. S. (2002) *Invest Ophthalmol Vis Sci* **43**, 573-579

200. Noell, S., Fallier-Becker, P., Deutsch, U., Mack, A. F., and Wolburg, H. (2009) *Cell Tissue Res* **337**, 185-195

201. Wolburg, H., Noell, S., Wolburg-Buchholz, K., Mack, A., and Fallier-Becker, P. (2009) *Neuroscientist* **15**, 180-193

202. Ehrlich, P. (1956) *Collected papers : including a complete bibliography*, Pergamon Press, London, New York
203. Risau, W., and Wolburg, H. (1990) *Trends Neurosci* **13**, 174-178
204. Janzer, R. C., and Raff, M. C. (1987) *Nature* **325**, 253-257
205. Reese, T. S., and Karnovsky, M. J. (1967) *J Cell Biol* **34**, 207-217
206. Begley, D. J., and Brightman, M. W. (2003) *Prog Drug Res* **61**, 39-78
207. Kacem, K., Lacombe, P., Seylaz, J., and Bonvento, G. (1998) *Glia* **23**, 1-10
208. Krum, J. M., Kenyon, K. L., and Rosenstein, J. M. (1997) *Exp Neurol* **146**, 33-45
209. Hayashi, Y., Nomura, M., Yamagishi, S., Harada, S., Yamashita, J., and Yamamoto, H. (1997) *Glia* **19**, 13-26
210. Yurchenco, P. D., and Schittny, J. C. (1990) *FASEB J* **4**, 1577-1590
211. Tilling, T., Korte, D., Hoheisel, D., and Galla, H. J. (1998) *J Neurochem* **71**, 1151-1157
212. Hallmann, R., Horn, N., Selg, M., Wendler, O., Pausch, F., and Sorokin, L. M. (2005) *Physiol Rev* **85**, 979-1000
213. Bandtlow, C. E., and Zimmermann, D. R. (2000) *Physiol Rev* **80**, 1267-1290
214. Miner, J. H., and Yurchenco, P. D. (2004) *Annu Rev Cell Dev Biol* **20**, 255-284
215. Aumailley, M., Bruckner-Tuderman, L., Carter, W. G., Deutzmann, R., Edgar, D., Ekblom, P., Engel, J., Engvall, E., Hohenester, E., Jones, J. C., Kleinman, H. K., Marinkovich, M. P., Martin, G. R., Mayer, U., Meneguzzi, G., Miner, J. H., Miyazaki, K., Patarroyo, M., Paulsson, M., Quaranta, V., Sanes, J. R., Sasaki, T., Sekiguchi, K., Sorokin, L. M., Talts, J. F., Tryggvason, K., Uitto, J., Virtanen, I., von der Mark, K., Wewer, U. M., Yamada, Y., and Yurchenco, P. D. (2005) *Matrix Biol* **24**, 326-332
216. Tanzer, M. L. (2006) *J Orthop Sci* **11**, 326-331
217. Hagg, T., Portera-Cailliau, C., Jucker, M., and Engvall, E. (1997) *Brain Res* **764**, 17-27
218. Sievers, J., Pehlemann, F. W., Gude, S., and Berry, M. (1994) *J Neurocytol* **23**, 135-149
219. Wagner, S., and Gardner, H. (2000) *Neurosci Lett* **284**, 105-108
220. Tian, M., Jacobson, C., Gee, S. H., Campbell, K. P., Carbonetto, S., and Jucker, M. (1996) *Eur J Neurosci* **8**, 2739-2747.
221. Villanova, M., Sewry, C., Malandrini, A., Toti, P., Muntoni, F., Merlini, L., Torelli, S., Tosi, P., Maraldi, N. M., and Guazzi, G. C. (1997) *J Submicrosc Cytol Pathol* **29**, 409-413
222. Libby, R. T., Lavallee, C. R., Balkema, G. W., Brunken, W. J., and Hunter, D. D. (1999) *J Neurosci* **19**, 9399-9411
223. Koch, M., Olson, P. F., Albus, A., Jin, W., Hunter, D. D., Brunken, W. J., Burgeson, R. E., and Champliaud, M. F. (1999) *J Cell Biol* **145**, 605-618
224. Toti, P., De Felice, C., Malandrini, A., Megha, T., Cardone, C., and Villanova, M. (1997) *Neuromuscul Disord* **7**, 21-25
225. Morissette, N., and Carbonetto, S. (1995) *J Neurosci* **15**, 8067-8082
226. Hohenester, E., Tisi, D., Talts, J. F., and Timpl, R. (1999) *Mol Cell* **4**, 783-792
227. Wizemann, H., Garbe, J. H., Friedrich, M. V., Timpl, R., Sasaki, T., and Hohenester, E. (2003) *J Mol Biol* **332**, 635-642
228. Villanova, M., Malandrini, A., Sabatelli, P., Sewry, C. A., Toti, P., Torelli, S., Six, J., Scarfo, G., Palma, L., Muntoni, F., Squarzoni, S., Tosi, P., Maraldi, N. M., and Guazzi, G. C. (1997) *Acta Neuropathol* **94**, 567-571
229. Brockmann, K., Dechent, P., Bonnemann, C., Schreiber, G., Frahm, J., and Hanefeld, F. (2007) *Brain Dev* **29**, 357-364
230. Sijens, P. E., Fock, J. M., Meiners, L. C., Potze, J. H., Irwan, R., and Oudkerk, M. (2007) *Brain Dev* **29**, 317-321

231. Alkan, A., Sigirci, A., Kutlu, R., Aslan, M., Doganay, S., and Yakinci, C. (2007) *J Child Neurol* **22**, 655-659

232. Xu, H., Wu, X. R., Wewer, U. M., and Engvall, E. (1994) *Nat Genet* **8**, 297-302

233. Timpl, R., and Brown, J. C. (1996) *BioEssays* **18**, 123-132

234. Colognato, H., and Yurchenco, P. D. (2000) *Dev Dyn* **218**, 213-234

235. Colognato, H., Winkelmann, D. A., and Yurchenco, P. D. (1999) *J Cell Biol* **145**, 619-631

236. Cohen, M. W., Jacobson, C., Yurchenco, P. D., and Morris, G. E. (1997) *The Journal of Cell Biology* **136**, 1047-1058

237. Henry, M. D., Satz, J. S., Brakebusch, C., Costell, M., Gustafsson, E., Fassler, R., and Campbell, K. P. (2001) *J Cell Sci* **114**, 1137-1144

238. Tremblay, M. R., and Carbonetto, S. (2006) *J Biol Chem* **281**, 13365-13373

239. Jacobson, C., Cote, P. D., Rossi, S. G., Rotundo, R. L., and Carbonetto, S. (2001) *J Cell Biol* **152**, 435-450.

240. Henry, M. D., and Campbell, K. P. (1998) *Cell* **95**, 859-870

241. Montanaro, F., Lindenbaum, M., and Carbonetto, S. (1999) *J Cell Biol* **145**, 1325-1340.

242. Weir, M. L., Oppizzi, M. L., Henry, M. D., Onishi, A., Campbell, K. P., Bissell, M. J., and Muschler, J. L. (2006) *J Cell Sci* **119**, 4047-4058

243. Tsiper, M. V., and Yurchenco, P. D. (2002) *J Cell Sci* **115**, 1005-1015.

244. Williamson, R. A., Henry, M. D., Daniels, K. J., Hrstka, R. F., Lee, J. C., Sunada, Y., Ibraghimov-Beskrovnaya, O., and Campbell, K. P. (1997) *Human Molecular Genetics* **6**, 831-841

245. Miner, J. H., and Li, C. (2000) *Dev Biol* **217**, 278-289

246. Noakes, P. G., Gautam, M., Mudd, J., Sanes, J. R., and Merlie, J. P. (1995) *Nature* **374**, 258-262

247. Yurchenco, P. D., Tsilibary, E. C., Charonis, A. S., and Furthmayr, H. (1985) *J Biol Chem* **260**, 7636-7644

248. Kvansakul, M., Hopf, M., Ries, A., Timpl, R., and Hohenester, E. (2001) *EMBO J* **20**, 5342-5346

249. Mayer, U., Nischt, R., Poschl, E., Mann, K., Fukuda, K., Gerl, M., Yamada, Y., and Timpl, R. (1993) *EMBO J* **12**, 1879-1885

250. Ries, A., Gohring, W., Fox, J. W., Timpl, R., and Sasaki, T. (2001) *Eur J Biochem* **268**, 5119-5128

251. Battaglia, C., Mayer, U., Aumailley, M., and Timpl, R. (1992) *Eur J Biochem* **208**, 359-366

252. Hopf, M., Gohring, W., Kohfeldt, E., Yamada, Y., and Timpl, R. (1999) *Eur J Biochem* **259**, 917-925

253. Aumailley, M., Wiedemann, H., Mann, K., and Timpl, R. (1989) *Eur J Biochem* **184**, 241-248

254. Fox, J. W., Mayer, U., Nischt, R., Aumailley, M., Reinhardt, D., Wiedemann, H., Mann, K., Timpl, R., Krieg, T., Engel, J., and et al. (1991) *EMBO J* **10**, 3137-3146

255. Urabe, N., Naito, I., Saito, K., Yonezawa, T., Sado, Y., Yoshioka, H., Kusachi, S., Tsuji, T., Ohtsuka, A., Taguchi, T., Murakami, T., and Ninomiya, Y. (2002) *Arch Histol Cytol* **65**, 133-143

256. Tilling, T., Engelbertz, C., Decker, S., Korte, D., Huwel, S., and Galla, H. J. (2002) *Cell Tissue Res* **310**, 19-29

257. Barber, A. J., and Lieth, E. (1997) *Dev Dyn* **208**, 62-74

258. Halfter, W. (1993) *J. Neurosci.* **13**, 2863-2873

259. Kroger, S. (1997) *Mol Cell Neurosci* **10**, 149-161
260. Stone, D. M., and Nikolics, K. (1995) *J Neurosci* **15**, 6767-6778
261. Kammerer, R. A., Schulthess, T., Landwehr, R., Schumacher, B., Lustig, A., Yurchenco, P. D., Ruegg, M. A., Engel, J., and Denzer, A. J. (1999) *EMBO J* **18**, 6762-6770
262. Serpinskaya, A. S., Feng, G., Sanes, J. R., and Craig, A. M. (1999) *Dev Biol* **205**, 65-78
263. Gautam, M., Noakes, P. G., Moscoso, L., Rupp, F., Scheller, R. H., Merlie, J. P., and Sanes, J. R. (1996) *Cell* **85**, 525-535
264. Ferns, M., Hoch, W., Campanelli, J. T., Rupp, F., Hall, Z. W., and Scheller, R. H. (1992) *Neuron* **8**, 1079-1086
265. Gesemann, M., Brancaccio, A., Schumacher, B., and Ruegg, M. A. (1998) *J Biol Chem* **273**, 600-605
266. Burgess, R. W., Skarnes, W. C., and Sanes, J. R. (2000) *The Journal of Cell Biology* **151**, 41-52
267. Berzin, T. M., Zipser, B. D., Rafii, M. S., Kuo-Leblanc, V., Yancopoulos, G. D., Glass, D. J., Fallon, J. R., and Stopa, E. G. (2000) *Neurobiol Aging* **21**, 349-355
268. Smith, M. A., and Hilgenberg, L. G. (2002) *Neuroreport* **13**, 1485-1495
269. Sugiyama, J., Bowen, D. C., and Hall, Z. W. (1994) *Neuron* **13**, 103-115.
270. Campanelli, J. T., Roberds, S. L., Campbell, K. P., and Scheller, R. H. (1994) *Cell* **77**, 663-674
271. Gee, S. H., Montanaro, F., Lindenbaum, M. H., and Carbonetto, S. (1994) *Cell* **77**, 675-686.
272. Boot-Handford, R. P., and Tuckwell, D. S. (2003) *Bioessays* **25**, 142-151
273. McDonald, J. A., Kelley, D. G., and Broekelmann, T. J. (1982) *J Cell Biol* **92**, 485-492
274. Mao, Y., and Schwarzbauer, J. E. (2005) *Matrix Biol* **24**, 389-399
275. Plow, E. F., Haas, T. A., Zhang, L., Loftus, J., and Smith, J. W. (2000) *J Biol Chem* **275**, 21785-21788
276. Kroger, S., and Schroder, J. E. (2002) *News Physiol Sci* **17**, 207-212
277. Moukhles, H., and Carbonetto, S. (2001) *Journal of Neurochemistry* **78**, 824-834
278. Zaccaria, M. L., Di Tommaso, F., Brancaccio, A., Paggi, P., and Petrucci, T. C. (2001) *Neuroscience* **104**, 311-324
279. Tian, M., Jacobson, C., Gee, S. H., Campbell, K. P., Carbonetto, S., and Jucker, M. (1996) *Eur J Neurosci* **8**, 2739-2747
280. Mulligan, S. J., and MacVicar, B. A. (2004) *Nature* **431**, 195-199
281. Takano, T., Tian, G. F., Peng, W., Lou, N., Libionka, W., Han, X., and Nedergaard, M. (2006) *Nat Neurosci* **9**, 260-267
282. Clausen, T. (1992) *Can J Physiol Pharmacol* **70 Suppl**, S219-222
283. Kofuji, P., and Newman, E. A. (2004) *Neuroscience* **129**, 1045-1056
284. Higashi, K., Fujita, A., Inanobe, A., Tanemoto, M., Doi, K., Kubo, T., and Kurachi, Y. (2001) *American Journal of Physiology. Cell Physiology* **281**, C922-C931
285. Newman, E. A. (1986) *Science* **233**, 453-454
286. Newman, E. A., Frambach, D. A., and Odette, L. L. (1984) *Science* **225**, 1174-1175.
287. Newman, E., and Reichenbach, A. (1996) *Trends Neurosci* **19**, 307-312
288. Newman, E. A. (1986) *Ann N Y Acad Sci* **481**, 273-286
289. Karwoski, C. J., Lu, H. K., and Newman, E. A. (1989) *Science* **244**, 578-580
290. Matsuda, H., Saigusa, A., and Irisawa, H. (1987) *Nature* **325**, 156-159
291. Lopatin, A. N., Makhina, E. N., and Nichols, C. G. (1994) *Nature* **372**, 366-369
292. Ishii, M., Fujita, A., Iwai, K., Kusaka, S., Higashi, K., Inanobe, A., Hibino, H., and Kurachi, Y. (2003) *Am J Physiol Cell Physiol* **285**, C260-267

293. Takumi, T., Ishii, T., Horio, Y., Morishige, K., Takahashi, N., Yamada, M., Yamashita, T., Kiyama, H., Sohmiya, K., Nakanishi, S., and et al. (1995) *J Biol Chem* **270**, 16339-16346.

294. Bredt, D. S., Wang, T. L., Cohen, N. A., Guggino, W. B., and Snyder, S. H. (1995) *Proc Natl Acad Sci U S A* **92**, 6753-6757.

295. Ishii, M., Horio, Y., Tada, Y., Hibino, H., Inanobe, A., Ito, M., Yamada, M., Gotow, T., Uchiyama, Y., and Kurachi, Y. (1997) *J Neurosci* **17**, 7725-7735.

296. Li, L., Head, V., and Timpe, L. C. (2001) *Glia* **33**, 57-71.

297. Kofuji, P., and Connors, N. C. (2003) *Mol Neurobiol* **28**, 195-208

298. Connors, N. C., and Kofuji, P. (2006) *Glia* **53**, 124-131

299. Dalloz, C., Sarig, R., Fort, P., Yaffe, D., Bordais, A., Pannicke, T., Grosche, J., Mornet, D., Reichenbach, A., Sahel, J., Nudel, U., and Rendon, A. (2003) *Hum Mol Genet* **12**, 1543-1554

300. Poopalasundaram, S., Knott, C., Shamotienko, O. G., Foran, P. G., Dolly, J. O., Ghiani, C. A., Gallo, V., and Wilkin, G. P. (2000) *Glia* **30**, 362-372

301. Kucheryavykh, Y. V., Kucheryavykh, L. Y., Nichols, C. G., Maldonado, H. M., Baksi, K., Reichenbach, A., Skatchkov, S. N., and Eaton, M. J. (2007) *Glia* **55**, 274-281

302. Buono, R. J., Lohoff, F. W., Sander, T., Sperling, M. R., O'Connor, M. J., Dlugos, D. J., Ryan, S. G., Golden, G. T., Zhao, H., Scattergood, T. M., Berrettini, W. H., and Ferraro, T. N. (2004) *Epilepsy Res* **58**, 175-183

303. Shang, L., Lucchese, C. J., Haider, S., and Tucker, S. J. (2005) *Brain Res Mol Brain Res* **139**, 178-183

304. Djukic, B., Casper, K. B., Philpot, B. D., Chin, L. S., and McCarthy, K. D. (2007) *J Neurosci* **27**, 11354-11365

305. Ferraro, T. N., Golden, G. T., Smith, G. G., Martin, J. F., Lohoff, F. W., Gieringer, T. A., Zamboni, D., Schwebel, C. L., Press, D. M., Kratzer, S. O., Zhao, H., Berrettini, W. H., and Buono, R. J. (2004) *Mamm Genome* **15**, 239-251

306. Kofuji, P., Ceelen, P., Zahs, K., Surbeck, L. W., Lester, H. A., and Newman, E. A. (2000) *The Journal of Neuroscience* **20**, 5733-5740

307. Wurm, A., Pannicke, T., Iandiev, I., Buhner, E., Pietsch, U. C., Reichenbach, A., Wiedemann, P., Uhlmann, S., and Bringmann, A. (2006) *Am J Pathol* **169**, 1990-1998

308. Kofuji, P., Biedermann, B., Siddharthan, V., Raap, M., Iandiev, I., Milenkovic, I., Thomzig, A., Veh, R. W., Bringmann, A., and Reichenbach, A. (2002) *Glia* **39**, 292-303

309. Vinores, S. A., Derevjanik, N. L., Ozaki, H., Okamoto, N., and Campochiaro, P. A. (1999) *Doc Ophthalmol* **97**, 217-228

310. Pannicke, T., Iandiev, I., Uckermann, O., Biedermann, B., Kutzera, F., Wiedemann, P., Wolburg, H., Reichenbach, A., and Bringmann, A. (2004) *Mol Cell Neurosci* **26**, 493-502

311. Pannicke, T., Uckermann, O., Iandiev, I., Biedermann, B., Wiedemann, P., Perlman, I., Reichenbach, A., and Bringmann, A. (2005) *Glia* **50**, 1-11

312. Iandiev, I., Pannicke, T., Hollborn, M., Wiedemann, P., Reichenbach, A., Grimm, C., Reme, C. E., and Bringmann, A. (2008) *Neurosci Lett* **434**, 317-321

313. Dietzel, I., Heinemann, U., Hofmeier, G., and Lux, H. D. (1980) *Exp Brain Res* **40**, 432-439.

314. Holthoff, K., and Witte, O. W. (1996) *J Neurosci* **16**, 2740-2749

315. Yuan, S., Zhang, W., Ding, J., Yao, J., Jiang, Q., and Hu, G. (2009) *Exp Eye Res* **89**, 119-122

316. Nagelhus, E. A., Horio, Y., Inanobe, A., Fujita, A., Haug, F. M., Nielsen, S., Kurachi, Y., and Ottersen, O. P. (1999) *Glia* **26**, 47-54

317. Nagelhus, E. A., Mathiisen, T. M., and Ottersen, O. P. (2004) *Neuroscience* **129**, 905-913

318. Saadoun, S., Papadopoulos, M. C., and Krishna, S. (2003) *J Clin Pathol* **56**, 972-975

319. Benfenati, V., Nicchia, G. P., Svelto, M., Rapisarda, C., Frigeri, A., and Ferroni, S. (2007) *J Neurochem* **100**, 87-104

320. Zhang, H., and Verkman, A. S. (2008) *J Mol Biol* **382**, 1136-1143

321. Ruiz-Ederra, J., Zhang, H., and Verkman, A. S. (2007) *J Biol Chem* **282**, 21866-21872

322. Holthoff, K., and Witte, O. W. (2000) *Glia* **29**, 288-292

323. Frigeri, A., Nicchia, G. P., Nico, B., Quondamatteo, F., Herken, R., Roncali, L., and Svelto, M. (2001) *FASEB Journal* **15**, 90-98

324. Amiry-Moghaddam, M., Otsuka, T., Hurn, P. D., Traystman, R. J., Haug, F. M., Froehner, S. C., Adams, M. E., Neely, J. D., Agre, P., Ottersen, O. P., and Bhardwaj, A. (2003) *Proc Natl Acad Sci U S A* **100**, 2106-2111

325. Amiry-Moghaddam, M., Xue, R., Haug, F. M., Neely, J. D., Bhardwaj, A., Agre, P., Adams, M. E., Froehner, S. C., Mori, S., and Ottersen, O. P. (2004) *Faseb J* **18**, 542-544

326. Inoue, M., Wakayama, Y., Liu, J. W., Murahashi, M., Shibuya, S., and Oniki, H. (2002) *Tohoku J Exp Med* **197**, 87-93

327. Ueda, H., Gohdo, T., and Ohno, S. (1998) *J Histochem Cytochem* **46**, 185-191

328. Cohn, R. D., and Campbell, K. P. (2000) *Muscle & Nerve* **23**, 1456-1471

329. Kanagawa, M., and Toda, T. (2006) *J Hum Genet* **51**, 915-926

330. Smalheiser, N. R., and Kim, E. (1995) *J Biol Chem* **270**, 15425-15433

331. Holt, K. H., Crosbie, R. H., Venzke, D. P., and Campbell, K. P. (2000) *FEBS Lett* **468**, 79-83

332. Gee, S. H., Blacher, R. W., Douville, P. J., Provost, P. R., Yurchenco, P. D., and Carbonetto, S. (1993) *The Journal of Biological Chemistry* **268**, 14972-14980

333. Sugita, S., Saito, F., Tang, J., Satz, J., Campbell, K., and Südhof, T. C. (2001) *The Journal of Cell Biology* **154**, 435-445

334. Peng, H. B., Xie, H., Rossi, S. G., and Rotundo, R. L. (1999) *The Journal of Cell Biology* **145**, 911-921

335. Campanelli, J. T., Roberds, S. L., Campbell, K. P., and Scheller, R. H. (1994) *Cell* **77**, 663-674

336. Talts, J. F., Andac, Z., Göhring, W., Brancaccio, A., and Timpl, R. (1999) *The EMBO Journal* **18**, 863-870

337. Smalheiser, N. R., and Schwartz, N. B. (1987) *Proc Natl Acad Sci U S A* **84**, 6457-6461.

338. Ervasti, J. M., and Campbell, K. P. (1993) *J Cell Biol* **122**, 809-823

339. Ibraghimov-Beskrovnaya, O., Ervasti, J. M., Leveille, C. J., Slaughter, C. A., Sernett, S., and Campbell, K. P. (1992) *Nature* **355**, 696-702

340. Bowe, M. A., Deyst, K. A., Leszyk, J. D., and Fallon, J. R. (1994) *Neuron* **12**, 1173-1180

341. Petrof, B. J., Shrager, J. B., Stedman, H. H., Kelly, A. M., and Sweeney, H. L. (1993) *Proc Natl Acad Sci U S A* **90**, 3710-3714

342. Brenman, J. E., Chao, D. S., Gee, S. H., McGee, A. W., Craven, S. E., Santillano, D. R., Wu, Z., Huang, F., Xia, H., Peters, M. F., Froehner, S. C., and Bredt, D. S. (1996) *Cell* **84**, 757-767

343. Hasegawa, M., Cuenda, A., Spillantini, M. G., Thomas, G. M., Buee-Scherrer, V., Cohen, P., and Goedert, M. (1999) *J Biol Chem* **274**, 12626-12631.

344. Hogan, A., Shepherd, L., Chabot, J., Quenneville, S., Prescott, S. M., Topham, M. K., and Gee, S. H. (2001) *J Biol Chem* **276**, 26526-26533

345. Lumeng, C., Phelps, S., Crawford, G. E., Walden, P. D., Barald, K., and Chamberlain, J. S. (1999) *Nat Neurosci* **2**, 611-617

346. Oak, S. A., Russo, K., Petrucci, T. C., and Jarrett, H. W. (2001) *Biochemistry* **40**, 11270-11278

347. Okumura, A., Nagai, K., and Okumura, N. (2008) *FEBS J* **275**, 22-33

348. Cote, P. D., Moukhles, H., Lindenbaum, M., and Carbonetto, S. (1999) *Nat Genet* **23**, 338-342.

349. Grady, R. M., Zhou, H., Cunningham, J. M., Henry, M. D., Campbell, K. P., and Sanes, J. R. (2000) *Neuron* **25**, 279-293.

350. Marangi, P. A., Wieland, S. T., and Fuhrer, C. (2002) *J Cell Biol* **157**, 883-895

351. Sadasivam, G., Willmann, R., Lin, S., Erb-Vogtli, S., Kong, X. C., Ruegg, M. A., and Fuhrer, C. (2005) *J Neurosci* **25**, 10479-10493

352. Spence, H. J., Dhillon, A. S., James, M., and Winder, S. J. (2004) *EMBO Rep* **5**, 484-489

353. Weston, C. A., Teressa, G., Weeks, B. S., and Prives, J. (2007) *J Cell Sci* **120**, 868-875

354. Chamberlain, J. S., Pearlman, J. A., Muzny, D. M., Gibbs, R. A., Ranier, J. E., Caskey, C. T., and Reeves, A. A. (1988) *Science* **239**, 1416-1418

355. Moukhles, H., Roque, R., and Carbonetto, S. (2000) *The Journal of Comparative Neurology* **420**, 182-194

356. Blake, D. J., Hawkes, R., Benson, M. A., and Beesley, P. W. (1999) *J Cell Biol* **147**, 645-658

357. Gorecki, D. C., Derry, J. M., and Barnard, E. A. (1994) *Hum Mol Genet* **3**, 1589-1597.

358. Rybakova, I. N., Patel, J. R., and Ervasti, J. M. (2000) *The Journal of Cell Biology* **150**, 1209-1214

359. Ilsley, J. L., Sudol, M., and Winder, S. J. (2001) *Cell Signal* **13**, 625-632

360. Sicinski, P., Geng, Y., Ryder-Cook, A. S., Barnard, E. A., Darlison, M. G., and Barnard, P. J. (1989) *Science* **244**, 1578-1580

361. Wertz, K., and Fuchtbauer, E. M. (1998) *Dev Dyn* **212**, 229-241

362. Gorecki, D. C., and Barnard, E. A. (1995) *Neuroreport* **6**, 893-896.

363. Gorecki, D. C., Monaco, A. P., Derry, J. M., Walker, A. P., Barnard, E. A., and Barnard, P. J. (1992) *Hum Mol Genet* **1**, 505-510.

364. Feener, C. A., Koenig, M., and Kunkel, L. M. (1989) *Nature* **338**, 509-511

365. Nudel, U., Zuk, D., Einat, P., Zeelon, E., Levy, Z., Neuman, S., and Yaffe, D. (1989) *Nature* **337**, 76-78

366. Boyce, F. M., Beggs, A. H., Feener, C., and Kunkel, L. M. (1991) *Proc Natl Acad Sci U S A* **88**, 1276-1280

367. Lidov, H. G., Byers, T. J., and Kunkel, L. M. (1993) *Neuroscience* **54**, 167-187.

368. Lidov, H. G., Byers, T. J., Watkins, S. C., and Kunkel, L. M. (1990) *Nature* **348**, 725-728.

369. Lidov, H. G., Selig, S., and Kunkel, L. M. (1995) *Hum Mol Genet* **4**, 329-335.

370. Chelly, J., Hamard, G., Koulakoff, A., Kaplan, J. C., Kahn, A., and Berwald-Netter, Y. (1990) *Nature* **344**, 64-65

371. Dennis, C. L., Tinsley, J. M., Deconinck, A. E., and Davies, K. E. (1996) *Nucleic Acids Res* **24**, 1646-1652

372. Haenggi, T., Soontornmalai, A., Schaub, M. C., and Fritschy, J. M. (2004) *Neuroscience* **129**, 403-413

373. Uchino, M., Teramoto, H., Naoe, H., Miike, T., Yoshioka, K., and Ando, M. (1994) *Acta Neuropathol* **87**, 129-134

374. Khurana, T. S., Watkins, S. C., and Kunkel, L. M. (1992) *J Cell Biol* **119**, 357-366

375. Culligan, K., Glover, L., Dowling, P., and Ohlendieck, K. (2001) *BMC Cell Biol* **2**, 2

376. Claudepierre, T., Dailoz, C., Mornet, D., Matsumura, K., Sahel, J., and Rendon, A. (2000) *Journal of Cell Sciences* **113**, 3409-3417

377. Peters, M. F., O'Brien, K. F., Sadoulet-Puccio, H. M., Kunkel, L. M., Adams, M. E., and Froehner, S. C. (1997) *J Biol Chem* **272**, 31561-31569

378. Blake, D. J., Hawkes, R., Benson, M. A., and Beesley, P. W. (1999) *The Journal of Cell Biology* **147**, 645-657

379. Sadoulet-Puccio, H. M., Rajala, M., and Kunkel, L. M. (1997) *Proc Natl Acad Sci U S A* **94**, 12413-12418

380. Blank, M., Blake, D. J., and Kroger, S. (2002) *Neuroscience* **111**, 259-273

381. Holzfeind, P. J., Ambrose, H. J., Newey, S. E., Nawrotzki, R. A., Blake, D. J., and Davies, K. E. (1999) *J Biol Chem* **274**, 6250-6258

382. Grady, R. M., Wozniak, D. F., Ohlemiller, K. K., and Sanes, J. R. (2006) *J Neurosci* **26**, 2841-2851

383. Lien, C. F., Hazai, D., Yeung, D., Tan, J., Fuchtbauer, E. M., Jancsik, V., and Gorecki, D. C. (2007) *Cell Tissue Res* **327**, 67-82

384. Ueda, H., Baba, T., Terada, N., Kato, Y., Fujii, Y., Takayama, I., Mei, X., and Ohno, S. (2000) *Neurosci Lett* **283**, 121-124

385. Ueda, H., Baba, T., Kashiwagi, K., Iijima, H., and Ohno, S. (2000) *Invest Ophthalmol Vis Sci* **41**, 3908-3914

386. Balasubramanian, S., Fung, E. T., and Huganir, R. L. (1998) *FEBS Letters* **432**, 133-140

387. Bragg, A. D., Amiry-Moghaddam, M., Ottersen, O. P., Adams, M. E., and Froehner, S. C. (2006) *Glia* **53**, 879-890

388. Adams, M. E., Kramarcy, N., Krall, S. P., Rossi, S. G., Rotundo, R. L., Sealock, R., and Froehner, S. C. (2000) *J Cell Biol* **150**, 1385-1398.

389. Yang, B., Jung, D., Rafael, J. A., Chamberlain, J. S., and Campbell, K. P. (1995) *J Biol Chem* **270**, 4975-4978

390. Piluso, G., Mirabella, M., Ricci, E., Belsito, A., Abbondanza, C., Servidei, S., Puca, A. A., Tonali, P., Puca, G. A., and Nigro, V. (2000) *J Biol Chem* **275**, 15851-15860

391. Ahn, A. H., Freener, C. A., Gussoni, E., Yoshida, M., Ozawa, E., and Kunkel, L. M. (1996) *J Biol Chem* **271**, 2724-2730

392. Oak, S. A., and Jarrett, H. W. (2000) *Biochemistry* **39**, 8870-8877

393. Gorecki, D. C., Abdulrazzak, H., Lukasiuk, K., and Barnard, E. A. (1997) *Eur J Neurosci* **9**, 965-976.

394. Alessi, A., Bragg, A. D., Percival, J. M., Yoo, J., Albrecht, D. E., Froehner, S. C., and Adams, M. E. (2006) *Exp Cell Res* **312**, 3084-3095

395. Levi, S., Grady, R. M., Henry, M. D., Campbell, K. P., Sanes, J. R., and Craig, A. M. (2002) *J Neurosci* **22**, 4274-4285.

396. Brünig, I., Scotti, E., Sidler, C., and Fritschy, J. M. (2002) *The Journal of Comparative Neurology* **443**, 43-55

397. Knuesel, I., Mastrocola, M., Zuellig, R. A., Bornhauser, B., Schaub, M. C., and Fritschy, J. M. (1999) *European Journal of Neuroscience* **11**, 4457-4462

398. Moore, S. A., Saito, F., Chen, J., Michele, D. E., Henry, M. D., Messing, A., Cohn, R. D., Ross-Barta, S. E., Westra, S., Williamson, R. A., Hoshi, T., and Campbell, K. P. (2002) *Nature* **418**, 422-425

399. Anderson, J. L., Head, S. I., and Morley, J. W. (2003) *Brain Res* **982**, 280-283

400. Gee, S. H., Madhavan, R., Levinson, S. R., Caldwell, J. H., Sealock, R., and Froehner, S. C. (1998) *The Journal of Neuroscience* **18**, 128-137

401. Chen, Z., Hague, C., Hall, R. A., and Minneman, K. P. (2006) *J Biol Chem* **281**, 12414-12420

402. Leonoudakis, D., Conti, L. R., Anderson, S., Radeke, C. M., McGuire, L. M., Adams, M. E., Froehner, S. C., Yates, J. R., 3rd, and Vandenberg, C. A. (2004) *J Biol Chem* **279**, 22331-22346

403. Connors, N. C., Adams, M. E., Froehner, S. C., and Kofuji, P. (2004) *J. Biol. Chem.* **279**, 28387-28392

404. Neely, J. D., Amiry-Moghaddam, M., Ottersen, O. P., Froehner, S. C., and Agre, P. (2001) *Proceedings of the National Academy of Sciences of the United States of America* **98**, 14108-14113

405. Connors, N. C., Adams, M. E., Froehner, S. C., and Kofuji, P. (2004) *J Biol Chem* **279**, 28387-28392

406. Noel, G., Belda, M., Guadagno, E., Micoud, J., Klocker, N., and Moukhles, H. (2005) *J Neurochem* **94**, 691-702

407. Puwarawuttipanit, W., Bragg, A. D., Frydenlund, D. S., Mylonakou, M. N., Nagelhus, E. A., Peters, M. F., Kotchabhakdi, N., Adams, M. E., Froehner, S. C., Haug, F. M., Ottersen, O. P., and Amiry-Moghaddam, M. (2006) *Neuroscience* **137**, 165-175

408. Adams, M. E., Mueller, H. A., and Froehner, S. C. (2001) *J Cell Biol* **155**, 113-122

409. Barresi, R., and Campbell, K. P. (2006) *J Cell Sci* **119**, 199-207

410. Blake, D. J., and Kröger, S. (2000) *Trends in Neurosciences* **23**, 92-99

411. Bardoni, A., Sironi, M., Felisari, G., Comi, G. P., and Bresolin, N. (1999) *The Lancet* **353**, 897-898

412. Yoshioka, M., Okuno, T., Honda, Y., and Nakano, Y. (1980) *Archives of Disease in Childhood* **55**, 589-594

413. Dorman, C., DesNoyers Hurley, A., and D'Avignon, J. (1988) *Developmental Medicine & Child Neurology* **30**, 316-327

414. Billard, C., Gillet, P., Barthez, M. A., Hommet, C., and Bertrand, P. (1998) *Developmental Medicine & Child Neurology* **40**, 12-20

415. Anderson, S. W., Routh, D. K., and Ionasescu, V. V. (1988) *Developmental Medicine & Child Neurology* **30**, 328-333

416. Pillers, D. A., Bulman, D. E., Weleber, R. G., Sigesmund, D. A., Musarella, M. A., Powell, B. R., Murphey, W. H., Westall, C., Panton, C., Becker, L. E., and et al. (1993) *Nat Genet* **4**, 82-86

417. Dubowitz, V. (1977) Mental retardation in Duchenne muscular dystrophy. in *Pathogenesis of human muscular dystrophy* (Rowland, L. P. ed.), Excerpta Medica, Amsterdam. pp 688

418. North, K. N., Miller, G., Iannaccone, S. T., Clemens, P. R., Chad, D. A., Bella, I., Smith, T. W., Beggs, A. H., and Specht, L. A. (1996) *Neurology* **46**, 461-465

419. Holzfeind, P. J., Grewal, P. K., Reitsamer, H. A., Kechvar, J., Lassmann, H., Hoeger, H., Hewitt, J. E., and Bittner, R. E. (2002) *Human Molecular Genetics* **11**, 2673-2687

420. Pillers, D. A., Fitzgerald, K. M., Duncan, N. M., Rash, S. M., White, R. A., Dwinnell, S. J., Powell, B. R., Schnur, R. E., Ray, P. N., Cibis, G. W., and Weleber, R. G. (1999) *Hum Genet* **105**, 2-9

421. Kameya, S., Araki, E., Katsuki, M., Mizota, A., Adachi, E., Nakahara, K., Nonaka, I., Sakuragi, S., Takeda, S., and Nabeshima, Y. (1997) *Hum Mol Genet* **6**, 2195-2203

422. Satz, J. S., Philp, A. R., Nguyen, H., Kusano, H., Lee, J., Turk, R., Riker, M. J., Hernandez, J., Weiss, R. M., Anderson, M. G., Mullins, R. F., Moore, S. A., Stone, E. M., and Campbell, K. P. (2009) *J Neurosci* **29**, 13136-13146

423. Vaillend, C., Billard, J. M., Claudepierre, T., Rendon, A., Dutar, P., and Ungerer, A. (1998) *Neuroscience* **86**, 53-66

424. Knuesel, I., Riban, V., Zuellig, R. A., Schaub, M. C., Grady, R. M., Sanes, J. R., and Fritschy, J. M. (2002) *Eur J Neurosci* **15**, 1474-1484

425. Knuesel, I., Zuellig, R. A., Schaub, M. C., and Fritschy, J. M. (2001) *Eur J Neurosci* **13**, 1113-1124

426. Dobyns, W. B., Pagon, R. A., Armstrong, D., Curry, C. J., Greenberg, F., Grix, A., Holmes, L. B., Laxova, R., Michels, V. V., Robinow, M., and et al. (1989) *Am J Med Genet* **32**, 195-210

427. Takeda, S., Kondo, M., Sasaki, J., Kurahashi, H., Kano, H., Arai, K., Misaki, K., Fukui, T., Kobayashi, K., Tachikawa, M., Imamura, M., Nakamura, Y., Shimizu, T., Murakami, T., Sunada, Y., Fujikado, T., Matsumura, K., Terashima, T., and Toda, T. (2003) *Hum Mol Genet* **12**, 1449-1459

428. Santavuori, P., Somer, H., Sainio, K., Rapola, J., Kruus, S., Nikitin, T., Ketonen, L., and Leisti, J. (1989) *Brain Dev* **11**, 147-153

429. Villanova, M., Mercuri, E., Bertini, E., Sabatelli, P., Morandi, L., Mora, M., Sewry, C., Brockington, M., Brown, S. C., Ferreiro, A., Maraldi, N. M., Toda, T., Guicheney, P., Merlini, L., and Muntoni, F. (2000) *Neuromuscul Disord* **10**, 541-547

430. Michele, D. E., Barresi, R., Kanagawa, M., Saito, F., Cohn, R. D., Satz, J. S., Dollar, J., Nishino, I., Kelley, R. I., Somer, H., Straub, V., Mathews, K. D., Moore, S. A., and Campbell, K. P. (2002) *Nature* **418**, 417-421

431. Leschziner, A., Moukhles, H., Lindenbaum, M., Gee, S. H., Butterworth, J., Campbell, K. P., and Carbonetto, S. (2000) *Journal of Neurochemistry* **74**, 70-80

432. Ibraghimov-Beskrovnaya, O., Ervasti, J. M., Leveille, C. J., Slaughter, C. A., Sernett, S. W., and Campbell, K. P. (1992) *Nature* **355**, 696-702

433. Chiba, A., Matsumura, K., Yamada, H., Inazu, T., Shimizu, T., Kusunoki, S., Kanazawa, I., Kobata, A., and Endo, T. (1997) *J Biol Chem* **272**, 2156-2162

434. Breloy, I., Schwientek, T., Gries, B., Razawi, H., Macht, M., Albers, C., and Hanisch, F. G. (2008) *J Biol Chem* **283**, 18832-18840

435. Manya, H., Chiba, A., Yoshida, A., Wang, X., Chiba, Y., Jigami, Y., Margolis, R. U., and Endo, T. (2004) *Proc Natl Acad Sci U S A* **101**, 500-505

436. Willer, T., Prados, B., Falcon-Perez, J. M., Renner-Muller, I., Przemeck, G. K., Lommel, M., Coloma, A., Valero, M. C., de Angelis, M. H., Tanner, W., Wolf, E., Strahl, S., and Cruces, J. (2004) *Proc Natl Acad Sci U S A* **101**, 14126-14131

437. Yoshida, A., Kobayashi, K., Manya, H., Taniguchi, K., Kano, H., Mizuno, M., Inazu, T., Mitsuhashi, H., Takahashi, S., Takeuchi, M., Herrmann, R., Straub, V., Talim, B., Voit, T., Topaloglu, H., Toda, T., and Endo, T. (2001) *Dev Cell* **1**, 717-724

438. Liu, J., Ball, S. L., Yang, Y., Mei, P., Zhang, L., Shi, H., Kaminski, H. J., Lemmon, V. P., and Hu, H. (2006) *Mech Dev* **123**, 228-240

439. Xiong, H., Kobayashi, K., Tachikawa, M., Manya, H., Takeda, S., Chiyonobu, T., Fujikake, N., Wang, F., Nishimoto, A., Morris, G. E., Nagai, Y., Kanagawa, M., Endo, T., and Toda, T. (2006) *Biochem Biophys Res Commun* **350**, 935-941

440. Ackroyd, M. R., Skordis, L., Kaluarachchi, M., Godwin, J., Prior, S., Fidanboylu, M., Piercy, R. J., Muntoni, F., and Brown, S. C. (2009) *Brain* **132**, 439-451

441. Barresi, R., Michele, D. E., Kanagawa, M., Harper, H. A., Dovico, S. A., Satz, J. S., Moore, S. A., Zhang, W., Schachter, H., Dumanski, J. P., Cohn, R. D., Nishino, I., and Campbell, K. P. (2004) **10**, 696-703

442. Kanagawa, M., Saito, F., Kunz, S., Yoshida-Moriguchi, T., Barresi, R., Kobayashi, Y. M., Muschler, J., Dumanski, J. P., Michele, D. E., Oldstone, M. B., and Campbell, K. P. (2004) *Cell* **117**, 953-964

443. Patnaik, S. K., and Stanley, P. (2005) *J Biol Chem* **280**, 20851-20859

444. Barresi, R., Michele, D. E., Kanagawa, M., Harper, H. A., Dovico, S. A., Satz, J. S., Moore, S. A., Zhang, W., Schachter, H., Dumanski, J. P., Cohn, R. D., Nishino, I., and Campbell, K. P. (2004) *Nat Med* **10**, 696-703

445. Yoshida-Moriguchi, T., Yu, L., Stalnaker, S. H., Davis, S., Kunz, S., Madson, M., Oldstone, M. B., Schachter, H., Wells, L., and Campbell, K. P. *Science* **327**, 88-92

446. Saito, Y., Yamamoto, T., Ohtsuka-Tsurumi, E., Oka, A., Mizuguchi, M., Itoh, M., Voit, T., Kato, Y., Kobayashi, M., Saito, K., and Osawa, M. (2004) *Brain Dev* **26**, 469-479

447. Yamada, H., Chiba, A., Endo, T., Kobata, A., Anderson, L. V. B., Hori, H., Fukuta-Ohi, H., Kanazawa, I., Campbell, K. P., Shimizu, T., and Matsumura, K. (1996) *Journal of Neurochemistry* **66**, 1518-1524

448. Lee, Y., Kameya, S., Cox, G. A., Hsu, J., Hicks, W., Maddatu, T. P., Smith, R. S., Naggert, J. K., Peachey, N. S., and Nishina, P. M. (2005) *Mol Cell Neurosci* **30**, 160-172

449. Grewal, P. K., Holzfeind, P. J., Bittner, R. E., and Hewitt, J. E. (2001) *Nat Genet* **28**, 151-154

450. Qu, Q., Crandall, J. E., Luo, T., McCaffery, P. J., and Smith, F. I. (2006) *Eur J Neurosci* **23**, 2877-2886

451. Qu, Q., and Smith, F. I. (2005) *Cerebellum* **4**, 261-270

452. Kondo-Iida, E., Kobayashi, K., Watanabe, M., Sasaki, J., Kumagai, T., Koide, H., Saito, K., Osawa, M., Nakamura, Y., and Toda, T. (1999) *Hum Mol Genet* **8**, 2303-2309

453. Kobayashi, K., Nakahori, Y., Miyake, M., Matsumura, K., Kondo-Iida, E., Nomura, Y., Segawa, M., Yoshioka, M., Saito, K., Osawa, M., Hamano, K., Sakakihara, Y., Nonaka, I., Nakagome, Y., Kanazawa, I., Nakamura, Y., Tokunaga, K., and Toda, T. (1998) *Nature* **394**, 388-392

454. Hayashi, Y. K., Ogawa, M., Tagawa, K., Noguchi, S., Ishihara, T., Nonaka, I., and Arahata, K. (2001) *Neurology* **57**, 115-121

455. Beltràn-Valero de Bernabé, D., Currier, S., Steinbrecher, A., Celli, J., van Beusekom, E., van der Zwaag, B., Kayserili, H., Merlini, L., Chitayat, D., Dobyns, W. B., Cormand, B., Lehesjoki, A.-E., Cruces, J., Voit, T., Walsh, C. A., van Bokhoven, H., and Brunner, H. G. (2002) *American Journal of Human Genetics* **71**, 1033-1043

456. van Reeuwijk, J., Olderode-Berends, M. J., van den Elzen, C., Brouwer, O. F., Roscioli, T., van Pampus, M. G., Scheffer, H., Brunner, H. G., van Bokhoven, H., and Hol, F. A. *Clin Genet*

457. van Reeuwijk, J., Janssen, M., van den Elzen, C., Beltran-Valero de Bernabe, D., Sabatelli, P., Merlini, L., Boon, M., Scheffer, H., Brockington, M., Muntoni, F., Huynen, M. A., Verrips, A., Walsh, C. A., Barth, P. G., Brunner, H. G., and van Bokhoven, H. (2005) *J Med Genet* **42**, 907-912

458. van Reeuwijk, J., Grewal, P. K., Salih, M. A., Beltran-Valero de Bernabe, D., McLaughlan, J. M., Michielse, C. B., Herrmann, R., Hewitt, J. E., Steinbrecher, A., Seidahmed, M. Z., Shaheed, M. M., Abomelha, A., Brunner, H. G., van Bokhoven, H., and Voit, T. (2007) *Hum Genet* **121**, 685-690

459. Prados, B., Pena, A., Cotarelo, R. P., Valero, M. C., and Cruces, J. (2007) *Am J Pathol* **170**, 1659-1668

460. Brockington, M., Yuva, Y., Prandini, P., Brown, S. C., Torelli, S., Benson, M. A., Herrmann, R., Anderson, L. V., Bashir, R., Burgunder, J. M., Fallet, S., Romero, N.,

Fardeau, M., Straub, V., Storey, G., Pollitt, C., Richard, I., Sewry, C. A., Bushby, K., Voit, T., Blake, D. J., and Muntoni, F. (2001) *Hum Mol Genet* **10**, 2851-2859

461. Biancheri, R., Falace, A., Tessa, A., Pedemonte, M., Scapolan, S., Cassandrini, D., Aiello, C., Rossi, A., Broda, P., Zara, F., Santorelli, F. M., Minetti, C., and Bruno, C. (2007) *Biochem Biophys Res Commun* **363**, 1033-1037

462. Longman, C., Brockington, M., Torelli, S., Jimenez-Mallebrera, C., Kennedy, C., Khalil, N., Feng, L., Saran, R. K., Voit, T., Merlini, L., Sewry, C. A., Brown, S. C., and Muntoni, F. (2003) *Hum Mol Genet* **12**, 2853-2861

463. Michele, D. E., and Campbell, K. P. (2003) *J Biol Chem* **278**, 15457-15460

464. Muntoni, F., Brockington, M., DJ, B., Torelli, S., and Brown, S. C. (2002) *The Lancet* **360**

465. Kano, H., Kobayashi, K., Herrmann, R., Tachikawa, M., Manya, H., Nishino, I., Nonaka, I., Straub, V., Talim, B., Voit, T., Topaloglu, H., Endo, T., Yoshikawa, H., and Toda, T. (2002) *Biochemical and Biophysical Research Communications* **291**, 1283-1286

466. Kim, D. S., Hayashi, Y. K., Matsumoto, H., Ogawa, M., Noguchi, S., Murakami, N., Sakuta, R., Mochizuki, M., Michele, D. E., Campbell, K. P., Nonaka, I., and Nishino, I. (2004) *Neurology* **62**, 1009-1011

467. Saito, Y., Yamamoto, T., Mizuguchi, M., Kobayashi, M., Saito, K., Ohno, K., and Osawa, M. (2006) *Brain Res* **1075**, 223-228

468. Hacke, W., Stingele, R., Steiner, T., Schuchardt, V., and Schwab, S. (1995) *Intensive Care Med* **21**, 856-862

469. Wise, B. L., and Chater, N. (1962) *J Neurosurg* **19**, 1038-1043

470. Qureshi, A. I., and Suarez, J. I. (2000) *Crit Care Med* **28**, 3301-3313

471. Kleinschmidt-DeMasters, B. K., and Norenberg, M. D. (1981) *Science* **211**, 1068-1070

472. Ziai, W. C., Toung, T. J., and Bhardwaj, A. (2007) *J Neurol Sci* **261**, 157-166

473. Connors, N. C., and Kofuji, P. (2002) *J Neurosci* **22**, 4321-4327

474. Vajda, Z., Pedersen, M., Fuchtbauer, E. M., Wertz, K., Stodkilde-Jorgensen, H., Sulyok, E., Doczi, T., Neely, J. D., Agre, P., Frokiaer, J., and Nielsen, S. (2002) *Proc Natl Acad Sci U S A* **99**, 13131-13136

475. Wakayama, Y., Jimi, T., Inoue, M., Kojima, H., Murahashi, M., Kumagai, T., Yamashita, S., Hara, H., and Shibuya, S. (2002) *Arch Neurol* **59**, 431-437

476. Guadagno, E., and Moukhles, H. (2004) *Glia* **47**, 138-149

477. Detmers, F. J., de Groot, B. L., Muller, E. M., Hinton, A., Konings, I. B., Sze, M., Flitsch, S. L., Grubmuller, H., and Deen, P. M. (2006) *J Biol Chem* **281**, 14207-14214

478. Huber, V. J. (2009) *Bioorg Med Chem* **17**, 425-426

479. Huber, V. J., Tsujita, M., Kwee, I. L., and Nakada, T. (2008) *Bioorg Med Chem*

480. Huber, V. J., Tsujita, M., and Nakada, T. (2008) *Bioorg Med Chem*

481. Huber, V. J., Tsujita, M., Yamazaki, M., Sakimura, K., and Nakada, T. (2007) *Bioorg Med Chem Lett* **17**, 1270-1273

2 DISTRIBUTION OF POTASSIUM ION AND WATER PERMEABLE CHANNELS AT PERIVASCULAR GLIA IN BRAIN AND RETINA OF LARGE[myd] MOUSE[1]

2.1 Introduction

The dystroglycan-associated protein (DAP) complex is a group of interacting proteins that link the cytoskeleton to the extracellular matrix (ECM). In muscle, where the complex has been most thoroughly examined, it is believed to maintain the structural integrity of muscle fibres by protecting myotubes from the shear stress arising from repeated cycles of contraction and relaxation (1,2). The axis of the complex is composed of the transmembrane protein β-dystroglycan (β-DG) whose cytoplasmic domain interacts with the subplasmalemmal dystrophin (3) while its extracellular domain interacts with α-dystroglycan (α-DG) (4). Dystrophin in turn binds to F-actin of the cytoskeleton (5) while α-DG binds to laminin (4) and other ligands including agrin, perlecan and neurexin (6-8). Several other proteins also comprise the DAP and their expression varies depending on cell or tissue type. In muscle, these include at least 6 transmembrane proteins (α-, β-, δ-, γ-, ε- sarcoglycan and sarcospan) and numerous cytoplasmic proteins including syntrophin, dystrobrevin, syncoilin, Grb2 and nNOS (9). Mutations of various members of the DAP complex underlie the pathogenesis of many muscular dystrophies, a class of congenital disorders characterized primarily by progressive muscle weakness and degeneration (10).

The ability of α-DG to bind ECM ligands such as laminin is dependent on a dense region of O-linked glycosylation in its mucin like domain (11). Several forms of muscular dystrophy, including Fukuyama congenital muscular dystrophy (FCMD), Muscle-Eye Brain disease (MEB), Walker-Warburg Syndrome (WWS) and congenital muscular dystrophies type 1C (MDC1C) and type 1D (MDC1D), have all been associated with a reduction in α-DG glycosylation and a concomitant loss of laminin binding (12-15). Each of these disorders has been linked to a mutation in a single gene encoding a putative glycosyltransferase that may be involved in the O-linked glycosylation of α-DG (14,16-18). Interestingly, in addition to their

muscle phenotypes, these diseases have defects in brain and ocular development, the etiologies of which are poorly understood (12,14,17,19,20).

Dystroglycan and many members of the DAP complex are expressed in the CNS where they form complexes in both neuronal and glial cells including astrocytes and retinal Muller cells (21-23). Of particular interest, DG is enriched at boundaries between neural tissues and fluid compartments, namely at glial cell endfeet abutting blood vessels of the brain and retina and at those facing the pia mater of the brain as well as at the inner limiting membrane of the retina apposed to the vitreous body (24,25). These domains are also enriched for both the inwardly rectifying potassium channel, Kir4.1, and the water permeable channel aquaporin 4, AQP4 (26-28). Based on the highly polarized distribution of the Kir4.1 channel and studies using Kir4.1 knock out mice (29), this channel is critical for the regulation of extracellular K^+ ions in neural tissues (28,30). This process, called potassium buffering, consists of funneling excess extracellular K^+ ions from regions of high neuronal activity to blood vessels via glial cells (31) and generates osmotic gradients (32). In addition, neuronal activation leads to a decrease in adjacent extracellular space suggesting water movement (33). These data together with the co-distribution of Kir4.1 and AQP4 channels to the same subcellular domains led to the suggestion that Kir4.1-mediated K^+ ions buffering is coupled to water transport through AQP4 (27). Recently, further evidence substantiating this showed that a redistribution of AQP4 away from perivascular glial endfeet was accompanied by a delayed potassium clearance in α-syntrophin null mice (34).

Multiple lines of evidence suggest that the integrity of the DAP complex is essential for the proper localization and function of Kir4.1 and AQP4. Indeed, mutations in the dystrophin gene result in a dramatic reduction of the expression of AQP4 and Kir4.1 at perivascular astrocytic endfeet (35-38). Furthermore, the deletion of α-syntrophin also results in a reduction of perivascular AQP4 expression (39). Together, these data indicate that the polarized distribution of both Kir4.1 and AQP4 is dependent on the DAP complex. In addition, in cultured astrocytes and retinal Müller cells, laminin induces the coclustering of Kir4.1 and AQP4 along with the DAP complex (40,41), suggesting that the ability of the DAP to bind ECM ligands is essential for the localization and stability of these channels.

In the present study, we set out to characterize the polarized distribution of Kir4.1, AQP4 and components of the DAP complex in brain and retina of the Large[myd] mouse. This

mouse model of glycosylation-deficient muscular dystrophy carries a spontaneous mutation of the LARGE 1 gene and presents with a progressive myopathy (42). Consistent with FCMD, MEB, WWS and MDC1D patients, this mouse also displays cerebral abnormalities characterized by aberrant neuronal migration throughout the brain and a severe hypoglycosylation of α-DG with a concomitant loss of laminin binding (13). In this study, we used immunofluorescence and immunoblot analyses to examine the alterations in the polarized distribution and expression of Kir4.1, AQP4 and other components of the DAP complex in brain and retina of the Large^{myd} mouse. We hypothesized that the reduction of O-linked glycosylation in α-DG and resultant loss of laminin binding will compromise the polarized distribution pattern of Kir4.1 and AQP4. In brain, our data show a loss of Kir4.1 and AQP4 channels as well as α- and β1-syntrophin isoforms from perivascular astrocytic endfeet. This loss reflects a mislocalization of the channels, since immunoblot data reveal that their total expression levels remain unchanged in the Large^{myd} compared to control mice. However, in retina the perivascular distribution of Kir4.1, AQP4, β-DG and β1-syntrophin is retained. These data reveal that the mechanisms involved in the polarized distribution of these channels at glial cell endfeet differ between brain and retina.

2.2 Materials and methods

2.2.1 Tissues

Homozygous (n=3) and heterozygous Large^{myd} mice (n=2) as well as wild-type littermate mice (n=2) used in this study were genotyped using PCR tail DNA following the protocol described by (43). Once the genotype was determined the mice were deeply anesthetized and tissues of interest were dissected on ice. Brains and eyes embedded in Tissue-Tek (O.C.T. compound; Pelco International, Redding, CA, USA) and fresh frozen in liquid nitrogen-cooled isopentane (-80°C) were generously provided by Dr. S. Carbonetto (McGill University, Montreal, QC, Canada). Upon receipt, the tissues were immediately transferred to -80°C where they were maintained for later analysis. 12-15 μm horizontal brain and sagittal eye cryostat sections were mounted on Superfrost/Plus glass slides (Fisher, Ottawa, ON, Canada) and processed for subsequent immunofluorescence.

2.2.2 Antibodies

The following antibodies were used: rabbit anti-Kir4.1 and AQP4 against residues 356–375 of rat Kir4.1 and against rat GST AQP4 corresponding to residues 249–323, respectively (Alomone Laboratories, Jerusalem, Israel), rabbit anti-laminin against purified mouse Engelbreth-Holm-Swarm Sarcoma laminin that recognizes laminin α1, β1 and γ1 chains and rabbit anti-β-DG against the 15 of the last 16 amino acids of the C terminus of β-DG (a generous gift from Dr S. Carbonetto, McGill University, Montreal), rabbit anti-GFAP against the glial fibrillary acidic protein (GFAP) isolated from cow spinal cord (Dako, Mississauga, ON, Canada), rabbit anti-agrin against purified agrin (a generous gift from Dr M. Ferns, University of California, Davis, CA, USA), rabbit anti-α-syntrophin (SYN17) against residues 191-206 of α-syntrophin and rabbit anti-β1-syntrophin (SYN37) against residues 220-240 of mouse β1-syntrophin, plus an NH_2-terminal cysteine (a generous gift from Dr. S. Froehner, University of Washington, Seattle, WA, USA); mouse monoclonal antibody (mAb) to α-DG against rabbit skeletal muscle membrane (IIH6C4, Upstate Cell Signaling Solutions, Lake Placid, NY, USA), mouse anti-β-DG against the 15 of the last 16 amino acids at the C-terminus of the human dystroglycan sequence (43DAG1/8D5, Novocastra Laboratories, Newcastle-upon-tyne, UK), mouse anti-β-actin against a synthetic β-actin N-terminal peptide (Sigma-Aldrich, St. Louis, MO, USA); rat mAb to heparan sulfate proteoglycan perlecan against heparan sulfate proteoglycan from mouse Engelbreth-Holm-Swarm Sarcoma tumor that reacts with perlecan domain 4 (A7L6, Chemicon International, CA, USA).

2.2.3 Immunofluorescence

Brain and retina sections were fixed by immersion in 4% (w/v) paraformaldehyde in 0.1 mol/L phosphate buffer for 20 min followed by rinsing in phosphate-buffered saline (PBS) 3 x 15 min. Sections were then incubated for 1 h at room temperature (20–22°C) in a solution containing 3% bovine serum albumin (Sigma-Aldrich) and 0.2% Triton X-100. Double immunolabeling was performed by incubating the sections at 22°C for 1 h in the presence of primary antibodies against agrin (1/700) or laminin (1/1500) and perlecan (1/50); GFAP (1/500), Kir4.1 (1:100), AQP4 (1:200), α-syntrophin (1:500), β1-syntrophin (1:100), or α-DG (1/50) and perlecan (1/50). Subsequently, they were rinsed with PBS (3 x 15 min) and incubated with

Alexa Fluor 568 goat anti-rabbit IgG and Alexa Fluor 488 goat anti-rat or Alexa Fluor 488 goat anti-rabbit IgG and Alexa Fluor 568 goat anti-rat or Alexa Fluor 488 goat anti-mouse IgM and Alexa Fluor 568 goat anti-rat for 1 h (1/200; Molecular Probes, Eugene, ON, USA). Finally the sections were thoroughly rinsed with PBS and mounted on glass coverslips using Prolong Gold Antifade Reagent with or without 4',6-diamidino-2-phenylindole (Invitrogen, Burlington, ON, Canada). To confirm the specificity of the labeling, control sections were treated equivalently in the absence of primary antibodies.

2.2.4 Immunoblotting

Brain regions from Large^{myd} mice and littermate wild-type controls containing frontal cerebral cortex and hippocampus were homogenized using a Dounce homogenizer in cold PBS containing 1x complete protease inhibitor cocktail (Boehringer Mannheim, Mannheim, Germany). The homogenates were centrifuged at 200 g for 5 min and the pellet was solubilized in extraction buffer (25 mmol/l Tris pH 7.4, 25 mmol/l glycine and 150 mmol/l NaCl) containing 1% Triton X-100, 1x complete protease inhibitor cocktail and 5 mmol/l EDTA. The samples were left on ice for 15 min with occasional vortexing followed by a 10 min centrifugation at 16 000 g. Extracted proteins were denatured by boiling the samples for 9 min in reducing sample buffer and then loaded on a 10% sodium dodecyl sulfate–polyacrylamide electrophoresis gels. The gels were electrotransferred to nitrocellulose membranes (Bio-Rad, Mississauga, ON, Canada) and the blots were probed with rabbit antisera to Kir4.1 (1/1000) or AQP4 (1/1000) or with mouse mAbs to β-DG (1/200) or β-actin (1/25000). Bound antibodies were detected using horseradish peroxidase-conjugated goat anti-rabbit IgG or goat anti-mouse IgG (1/2000; Jackson ImmunoResearch, West Grove, PA, USA). To control for the specificity of the Kir4.1 antibody, extracts of wild-type and Large^{myd} brain were incubated in the presence of 2 μg of anti-Kir4.1 that had been preincubated with 2 μg of the immunizing peptide for 1 h. Signals were visualized on Bioflex econo films (Interscience, Markham, ON, Canada) using chemiluminescence (Amersham Biosciences, Buckinghamshire, UK).

2.2.5 RNA extraction and RT-PCR

Total RNA was extracted from 50 μg of previously snap-frozen mouse tissues in liquid nitrogen using micro-homogenizing device (VWR, Mississauga, ON, Canada) and TRIZOL® reagent (Invitrogen) following the supplied protocol. The quality and integrity of RNA was assessed on formaldehyde agarose gel and concentration was determined using NanoDrop® ND-1000 spectrophotometer (NanoDrop Technologies, Wilmington, DE, USA). Total cDNA was prepared using Oligo dT$_{(25)}$ (custom made, Invitrogen), 1 μg of total RNA from each sample and SuperScript™ III Reverse Transcriptase (RT; Invitrogen) following the supplied protocol. The presence of *Large1*, *Large2* and *Large2* alternative spliced transcripts was assessed on 2 μl of synthesized total cDNA of each tissue by PCR using the set of primers described by (44) and Platinum®-Taq DNA polymerase (Invitrogen). A set of β-actin primers (Forward: 5'TCT ACG AGG GCT ATG CTC TCC3', Reserse: 5'GGA TGC CAC AGG ATT CCA TAC3'), no-RNA and no-RT were used as controls.

2.3 Results

2.3.1 Abnormalities in the localization of basement membrane proteins in the Large[myd] brain

Previous data reported a disruption of the glia limitans which leads to abnormal neuronal migration in the Large[myd] brain (13). This disruption is reflected in a reduction of laminin (Fig. 2.1B) and perlecan (Fig. 2.1G) (13,45) as well as agrin labeling (Fig. 2.1F) in the basement membrane surrounding the surface of the brain. However, no apparent changes in laminin (Fig. 2.1B), agrin (Fig. 2.1F), or perlecan (Fig. 2.1G) immunolabeling were seen at the vascular basement membrane in the Large[myd] mouse compared to the wild-type control (Fig. 2.1A, I and J). Interestingly, scattered puncta labeled for laminin and perlecan (Fig. 2.1M) have been reported in the neuropil of the Large[myd] brain (45). Here we show that these puncta also label for

Figure 2.1 Disruption of the glia limitans and accumulation of agrin and perlecan puncta in the Large^{myd} brain. Horizontal brain sections containing cerebral cortex and cerebellum from wild-type **(A)** and Large^{myd} mice **(B)** were immunolabeled for laminin. Compared to the wild-type brain (arrows), the glia limitans of the Large^{myd} brain shows reduced laminin immunolabeling (arrows). Horizontal brain sections containing cortex from wild-type **(C-E**; **I-K)** and Large^{myd} mice **(F-H**; **L-O)** double immunolabeled for agrin **(C, F, I, L)** and perlecan **(D, G, J, M)** show reduced immunolabeling at the glia limitans (arrows in **F** and **G**) and presence of scattered puncta positive for both these proteins in the parenchyma of the cerebral cortex of the Large^{myd} mouse **(L-O)**. Note that the perivascular basement membrane from both wild-type **(A, I,** and **J)** and Large^{myd} mice **(B, F,** and **G)** is equally immunolabeled for laminin, agrin and perlecan. The merged images show the co-distribution between agrin and perlecan **(E, H, K, and N).** A high magnification of the boxed area in **L** is illustrated in **O.** Scale bar, 1 mm for **A** and **B,** 30 μm for **C-K** and 10 μm for **L-N.**
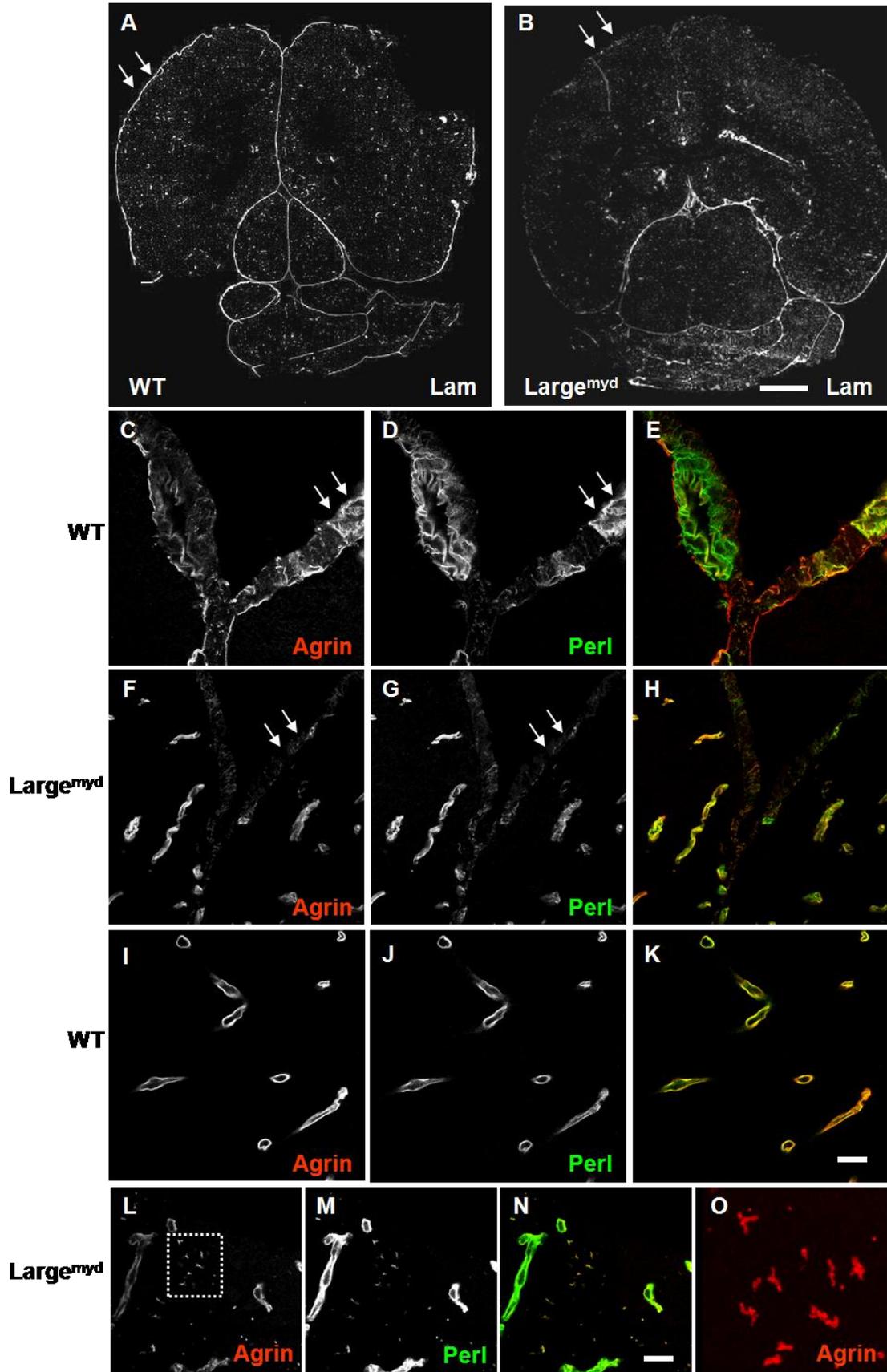
agrin (Fig. 2.1L) and that they are particularly abundant in the frontal cerebral cortex where a large number of them appears as complex geometrical structures when examined at high magnification (Fig. 2.1O). These data indicate that despite a hypoglycosylation of α-DG in all regions and sites within the Large[myd] brain (46), the disruption of basement membrane proteins localization is restricted to the glia limitans. This suggests that mechanisms implicating other receptors such as integrins may be involved in the assembly of the vascular basement membrane.

2.3.2 Loss of perivascular localization of AQP4 and Kir4.1 in the Large[myd] brain

Previous studies have shown that Kir4.1 and AQP4 are concentrated in astrocytic endfeet around blood vessels both in brain and retina (26-28,34,39,47,48) where they are codistributed with α-DG and β-DG (40,41). Laminin, a ligand that binds glycosylated moieties of α-DG, is highly expressed in vascular basement membrane (49) and recent studies by (50) showed that its binding to α-DG occurs within the first half of the mucin-like domain and relies on the O-glycosylation of this domain by the glycosyltransferase Large1. A disruption of α-DG binding to basement membrane ligands such as laminin and agrin has been reported both in brain and muscle of the Large[myd] mouse (13,42). Similar results have been reported in patients with MEB, FCMD and MCD1C (13,14). In addition, the targeting of the α-DG core protein, β-DG, α- syntrophin and dystrophin to astrocytic endfeet around blood vessels is impaired in the Large[myd] brain indicating that α-DG targets proteins to functional sites through its interaction with basement membrane proteins (13). In previous studies we have shown that the coclustering of Kir4.1 and AQP4 with α-DG in astrocytes and Müller cells is induced by laminin (40,41). In light of these data, we asked whether the perivacular targeting of these channels is impaired in the Large[myd] brain and assessed their mistargeting by immunofluorescence. We used perlecan as a marker for vascular basement membrane and found that while perlecan-positive blood vessels (Fig. 2.2B and H) were immunolabeled for AQP4 (Fig. 2.2A) and Kir4.1 in the wild-type brain (Fig. 2.2G) and heterozygous brain (data not shown), they were devoid of labeling for both types of channels in the Large[myd] brain (Fig. 2.2D-F and J-L). This is in agreement with previous findings by Michele et al (2002) (46) showing that AQP4 expression was lost at perivascular astrocytes of Large[myd] brain. To verify that astrocyte endfeet were still present at perivascular sites, we used GFAP as a marker for astrocytes and perlecan as a marker for
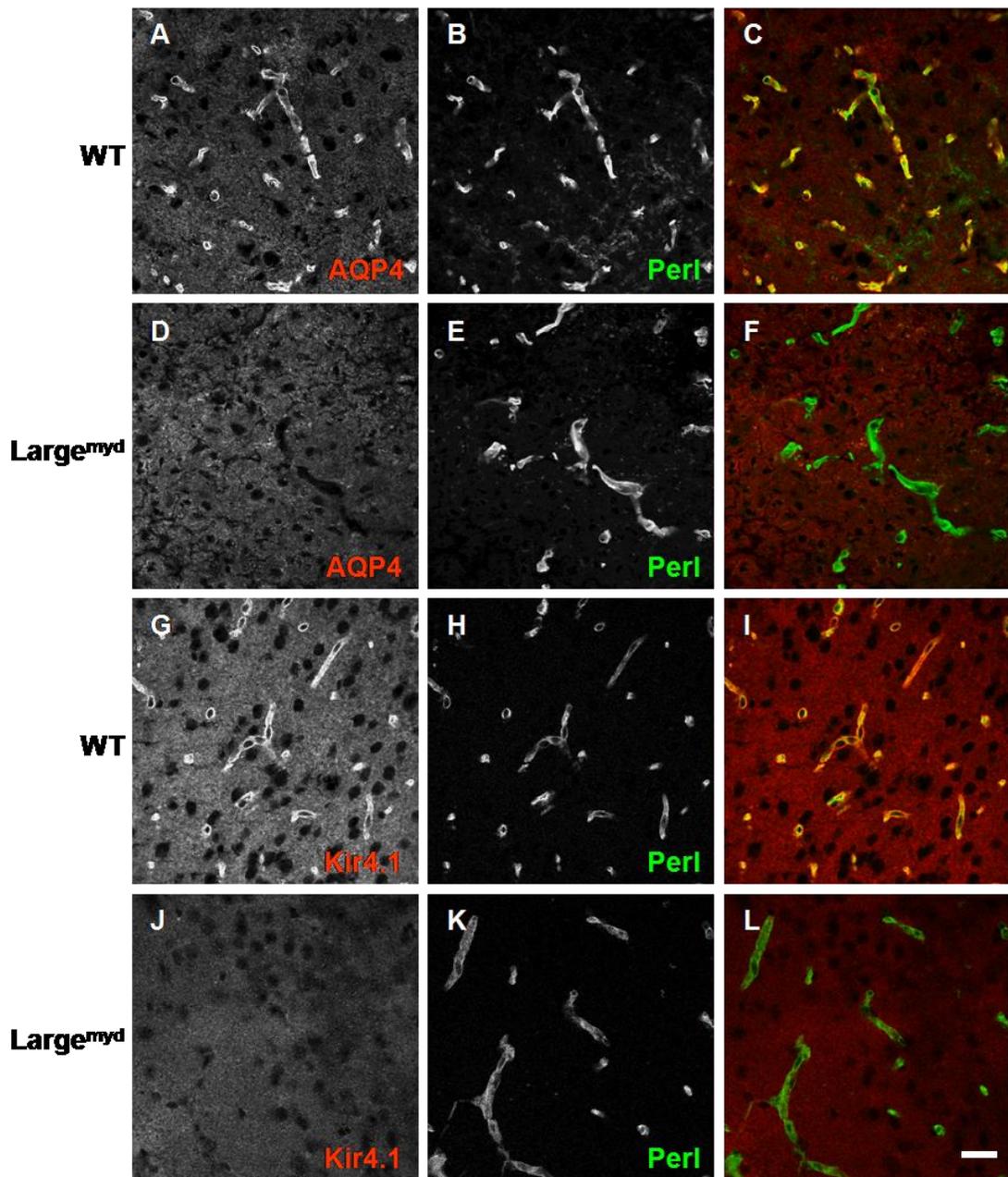
Figure 2.2 AQP4 and Kir4.1 fail to localize to perivascular astrocyte endfeet in the Large^myd brain. Horizontal brain sections containing cerebral cortex from wild-type (**A-C**; **G-I**) and Large^myd mice (**D-F**; **J-L**) were double immunolabeled for AQP4 (**A**, **D**) and perlecan (**B**, **E**) or Kir4.1 (**G**, **J**) and perlecan (**H**, **K**). The perivascular labeling for AQP4 (**D**) and Kir4.1 (**J**) is undetectable in the Large^myd compared to the wild-type control brain (**A**, **G**). The merged images show the co-distribution between AQP4 and perlecan (**C**) and Kir4.1 and perlecan (**I**). Scale bar, 30 μm.

vascular basement membrane and found that similarly to wild-type brain (Fig. 2.3A-C) most perlecan-positive blood vessels were surrounded by GFAP-positive astrocyte endfeet in the Large^{myd} brain (Fig. 2.3D-F). This together with the comparable number of blood vessels in the Large^{myd} brain (Fig. 2.2E and K) and the wild-type control (Fig. 2.2B and H), as reflected by perlecan immunoabelling, indicates that the loss of labeling for the channels is indeed because of their mistargeting within perivascular astrocyte endfeet. At the glia limitans, a significant reduction in the labeling for both AQP4 and Kir4.1 was seen (data not shown). Immunoblot analysis shows that total expression levels of both Kir4.1 and AQP4 channels are similar in the Large^{myd} and wild-type brains (Fig. 2.4), supporting the hypothesis that α-DG hypoglycosylation and the consequent loss of ligand binding lead to Kir4.1 and AQP4 mistargeting to perivascular astrocytic endfeet.

2.3.3 Loss of perivascular localization of α- and β1-syntrophins in the Large^{myd} brain

We have previously shown that α-DG-ligand binding is involved in syntrophin clustering in Muller glial cell cultures (41). Other studies have demonstrated that a PSD-95, Dlg and ZO-1 (PDZ)-mediated interaction with α-syntrophin is important in localizing and stabilizing AQP4 in specific membrane domains of perivascular glia (39). Recent biochemical studies have shown that in brain astrocytes, Kir4.1 co-purifies with DG and members of the DG-containing complex through a direct interaction of its PDZ ligand domain (-SNV) with the PDZ domain of α-syntrophin (51,52). Furthermore, we have shown that a deletion of the -SNV C-terminal sequence in Kir4.1 prevents its laminin-induced coclustering with α-DG in Müller glia, indicating that the PDZ-domain-mediated interaction is crucial for Kir4.1 clustering (41). To investigate the importance of α-DG glycosylation in targeting cytoplasmic components of the complex as well as their possible implication in the proper targeting of Kir4.1 and AQP4 to perivascular astrocytes, we examined the expression pattern of both α- and β1-syntrophins in the Large^{myd} brain. As previously described by Michele et al (2002) (46), we found that α-syntrophin is no longer concentrated at perivascular astrocytic endfeet in the Large^{myd} brain (Fig. 2.5D) compared to the wild-type brain (Fig. 2.5A) and heterozygous brain (data not shown). In addition, we found that β1-syntrophin is also lost from perivascular astrocytes in the Large^{myd}
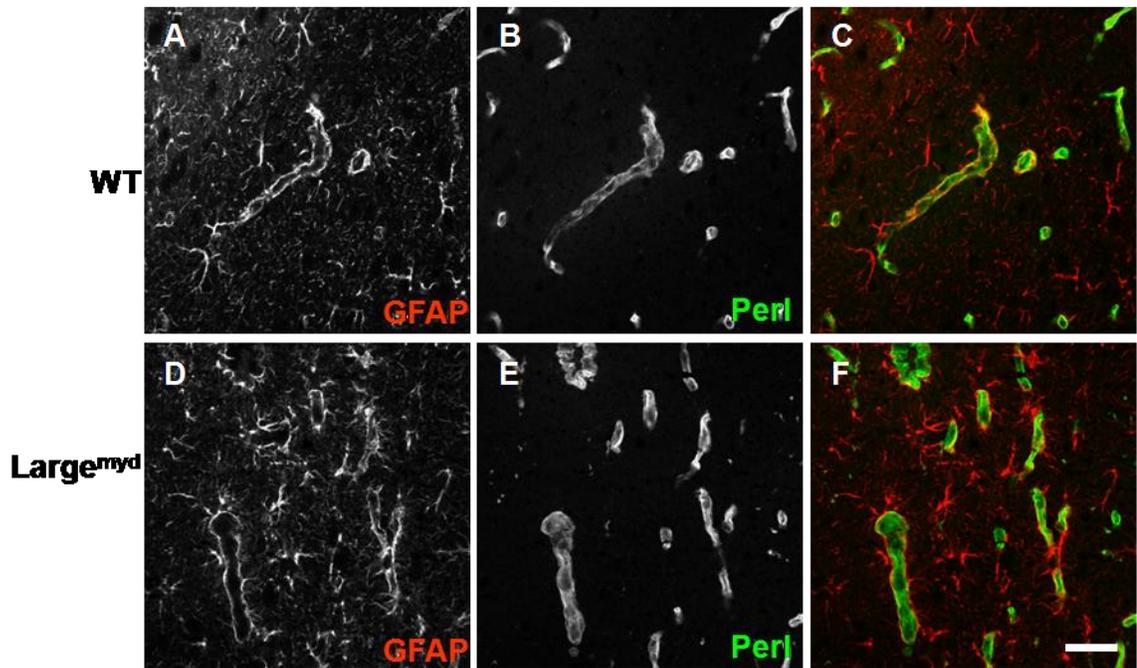
Figure 2.3 GFAP positive astrocyte endfeet are present around blood vessels in the Large^{myd} brain. Horizontal brain sections containing cerebral cortex from wild-type (**A-C**) and Large^{myd} mice (**D-F**) were double immunolabeled for GFAP (**A** and **D**) and perlecan (**B** and **E**). The merged images show the co-distribution between GFAP and perlecan around blood vessels both in wild-type (**C**) and Large^{myd} brains (**F**). Scale bar, 35 µm
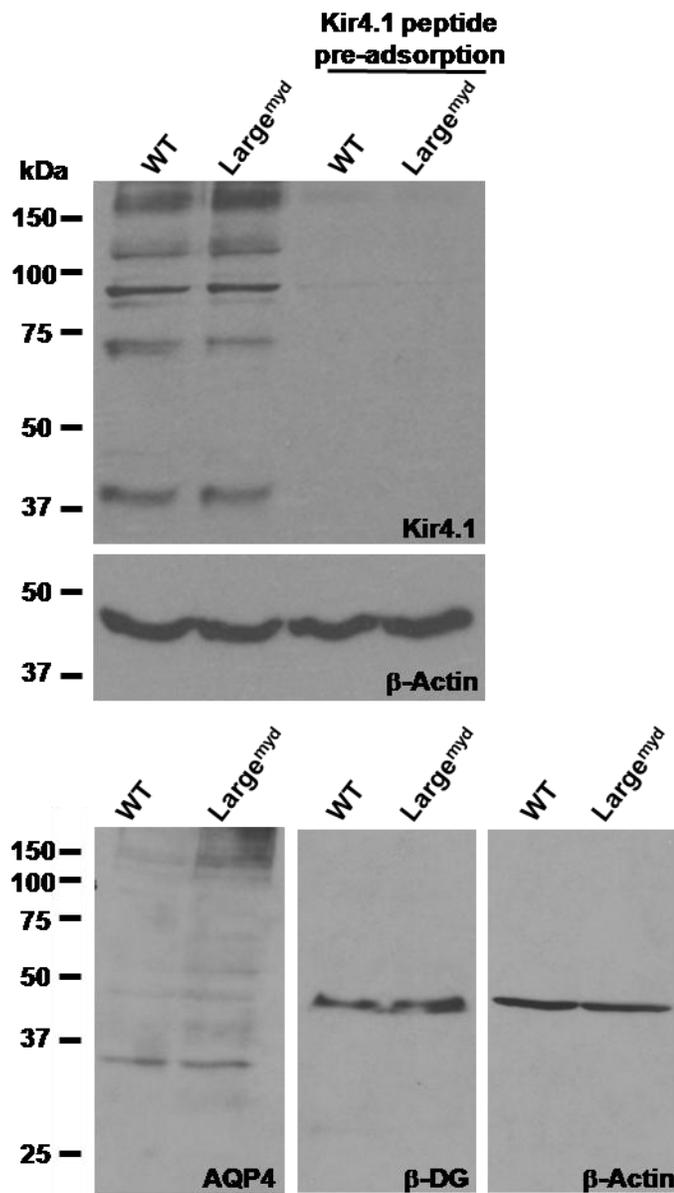
Figure 2.4 Total Kir4.1 and AQP4 expression levels are unchanged in the Large^myd brain. Homogenates from Large^myd and wild-type brain were immunoblotted for Kir4.1, AQP4, β-DG and β-actin. To control for the specificity of the Kir4.1 antibody, brain extracts from both Large^myd and wild-type mice were incubated in the presence of anti-Kir4.1 that had been preincubated with the peptide used for the immunization. β-actin labeling shows equal protein loading between Large^myd and wild-type brain extracts.
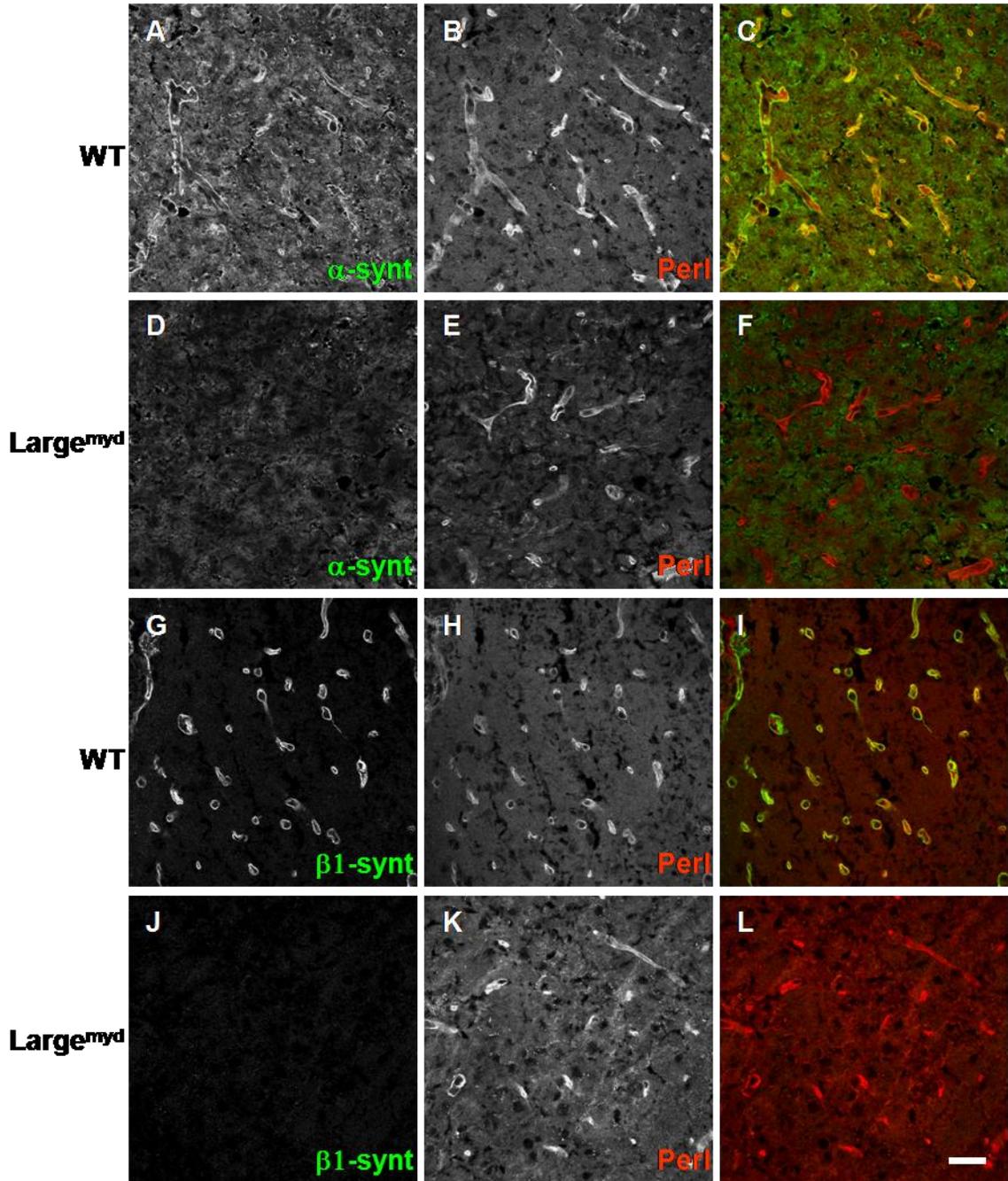
Figure 2.5 α- and β1-syntrophins fail to localize to perivascular astrocyte endfeet in the Large^{myd} brain. Horizontal brain sections from wild-type (**A-C**; **G-I**) and Large^{myd} mice (**D-F**; **J-L**) were double immunolabeled for α-syntrophin (**A, D**) and perlecan (**B, E**) or β$_1$-syntrophin (**G, J**) and perlecan (**H, K**). The merged images show the co-distribution between α-syntrophin and perlecan (**C**) or β$_1$-syntrophin and perlecan (**I**). Scale bar, 30 μm.

brain (Fig. 2.5J). Given that syntrophin interacts with Kir4.1 and AQP4 (51,52), these data suggest that the mistargeting of the channels may be a consequence of syntrophin mistargeting.

2.3.4 Expression of Large1 and Large2 mRNAs in retina and impact of Large1 mutation on Kir4.1 and AQP4 localization in the Large[myd] retina

In retina, Kir4.1 and AQP4 are concentrated both in perivascular glia and Müller cell endfeet where they play a crucial role in K^+ ion buffering and therefore participate in the retinal electrical activity. In previous studies we have shown that Kir4.1 and AQP4 undergo clustering upon laminin treatment suggesting that their polarized distribution is mediated through α-DG interaction with laminin (40,41). To investigate, in vivo, the role of α-DG glycosylation in this process we assessed the distribution of these channels in the Large[myd] retina by immunofluorescence. We first determined, by RT-PCR, the expression of Large1, Large 2 and Large2 alternative splice variants in wild-type mouse retina in parallel with brain regions and other non neural tissues where the expression of these transcripts has already been established (44). Here we show that retina not only expresses Large1 but also Large2 and its alternative transcripts (Fig. 2.6). Interestingly, unlike cortex and hippocampus that express only Large1, the cerebellum expresses the same transcripts of large as in the retina (Fig. 2.6). Despite the expression of Large2 and Large2 transcripts in retina, α-DG is hypoglycosylated, as reflected by lack of perivascular immunofluorescence when using the IIH6 antibody directed against O-linked glycosylated moieties of the protein (Fig. 2.7D). In contrast with the Large[myd] brain ((46) and data not shown), perivascular β-DG immunolabeling is maintained in the Large[myd] retina (Fig. 2.7J). Furthermore, the majority of the laminin labeling is lost at the inner limiting membrane of the Large[myd] retina (Fig. 2.8I), suggesting that Large1-associated glycosylation of α-DG plays a critical role in the proper assembly of the laminin-rich basement membrane at this site. However, laminin labeling associated with the vascular basement membrane is maintained in the Large[myd] retina (Fig. 2.8F).

In parallel, we performed histological studies on eyes from 3 (Fig. 2.8D and E) and 10 months old Large[myd] mice (Fig. 2.8G and H). Consistent with data previously described by (53), a profound disruption in the layering of retinas from both age groups of was found (Fig. 8E and H). In addition, many fibrous bundles and rosette-like structures were present throughout the

62
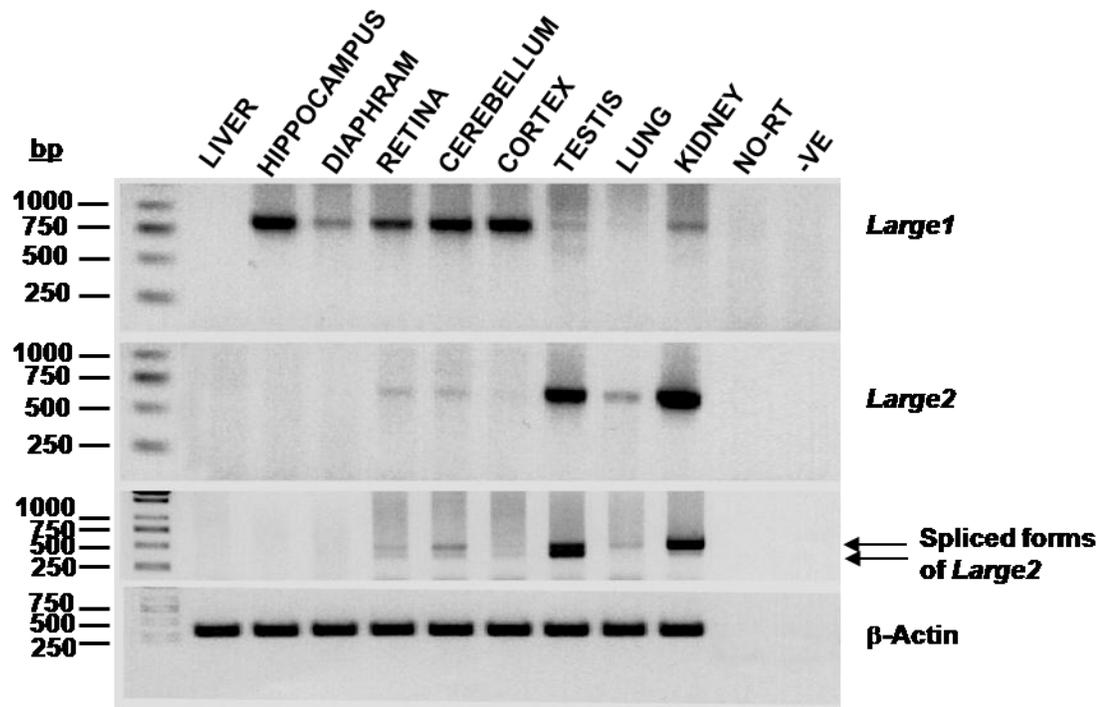
Figure 2.6 Expression profile of Large1 and Large2 in wild-type retina. RT–PCR of mouse *Large1* and *Large2* mRNAs from retina, various brain regions, diaphragm, liver, kidney, lung, testis and liver. Note that like in the kidney and testis, retina as well as cerebellum express not only *Large1* but also *Large2* and the *Large2* spliced forms.
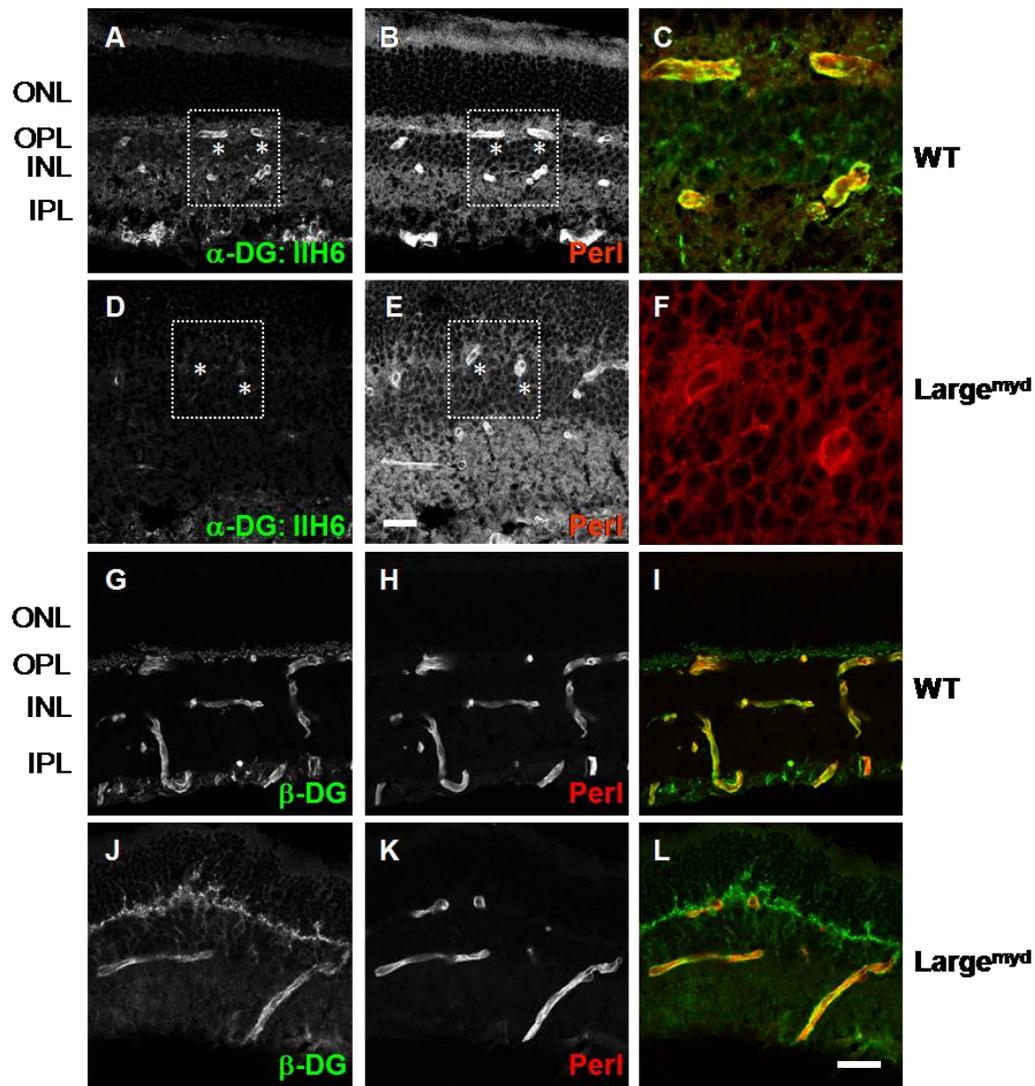
Figure 2.7 Loss of perivascular IIH6-associated immunolabeling of α-dystroglycan and maintenance of β-dystroglycan in the Large^myd retina. Retina sections from wild-type (**A-C**; **G-I**) and Large^myd (**D-F**; **J-L**) mice were double immunolabeled for α-DG using the IIH6 antibody against carbohydrate moieties (**A, D**) and perlecan (**B, E**) or for β-DG (**G, J**) and perlecan (**H, K**). Perlecan positive blood vessels are devoid of IIH6 labeling in the Large^myd (asterisks in **D** and **E**) compared to the wild-type control (asterisks in **A** and **B**). High magnifications of the boxed areas in **A, B** and **D, E** are illustrated as merged images in **C** and **F.** The merged images in **I** and **L** show the co-distribution between β-DG and perlecan around blood vessels both in wild-type and Large^myd retina. ONL, outer nuclear layer; OPL, outer plexiform layer; INL, inner nuclear layer; IPL, inner plexiform layer. Scale bar, 25 μm.
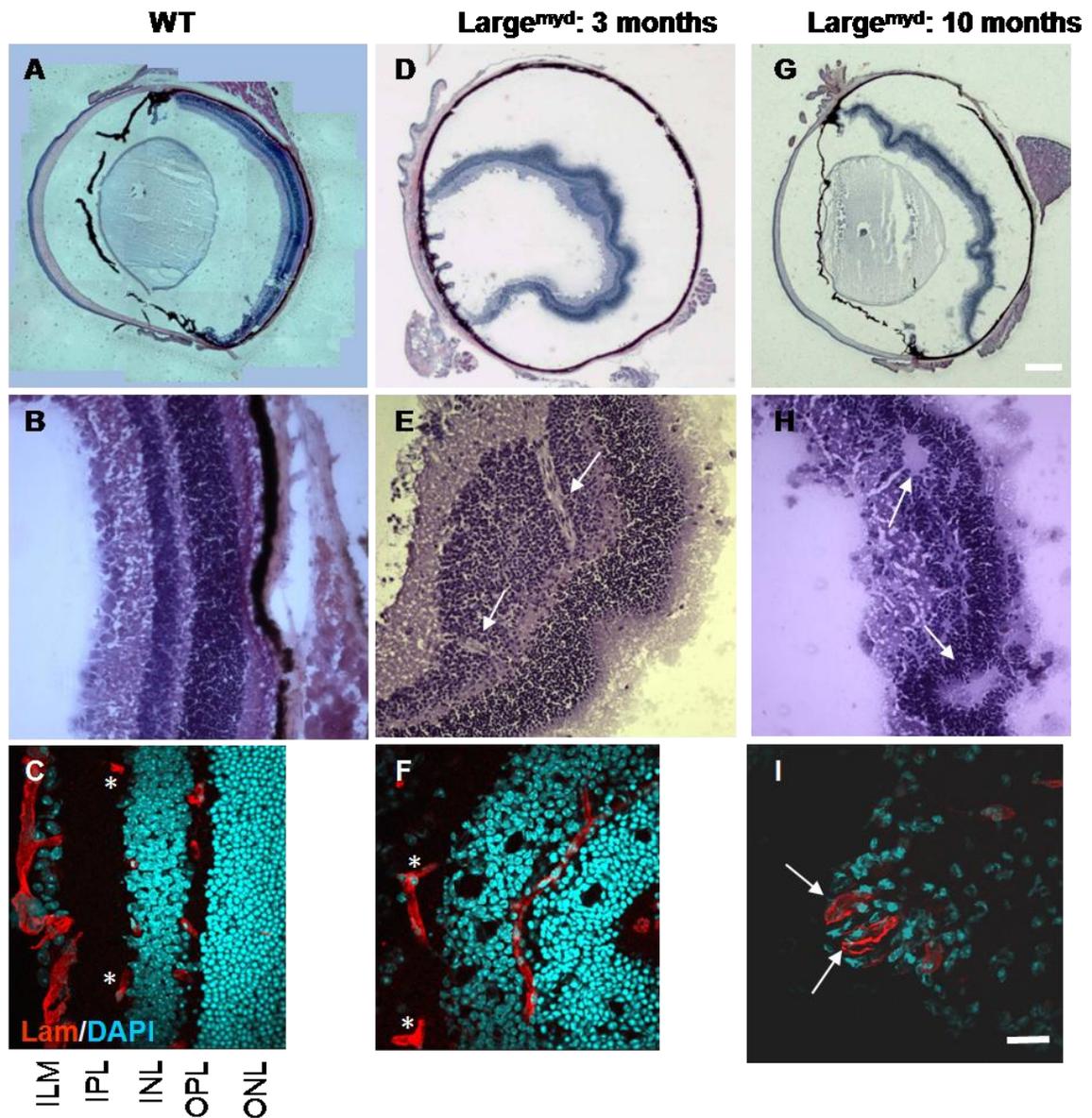
Figure 2.8 Disruption of the lamination and the inner limiting membrane in the Large^myd retina. Cryostat sections from wild-type **(A-C)** and Large^myd eyes **(D-I)** were stained with hematoxylin and eosin. The lamination of retinas from both 3 months **(D, E)** and 10 months old mice **(G, H)** was severely disrupted. In addition, fibrous bundles (arrows in **E**) and rosette-like structures (arrows in **H**) were seen. Laminin immunolabeling shows a profound disruption of the ILM (arrows in **I**) and no apparent changes in the perivascular basement membrane in the Large^myd (asterisks in **F**) compared to wild-type retina (asterisks in **C**). ONL, outer nuclear layer; OPL, outer plexiform layer; INL, inner nuclear layer; IPL, inner plexiform layer; ILM, inner limiting membrane. Scale bar, 250 μm for A, D and G and 25 μm for B, E, H, C, F and I.

retina (Fig. 2.8E and H). Radial Müller cell processes spanning the ganglion cell- and inner plexiform layers in wild-type control retina appear discontinuous and tortuous in Large^{myd} retina as reflected by vimentin immunolabeling (data not shown). These phenotypes were as severe in 3 months as in 10 months old mutant mice arguing against their progressive nature.

Subsequently, we analyzed Kir4.1 and AQP4 localization by immunofluorescence and found that although there is a reduction in the labeling for these channels around blood vessels in the Large^{myd} compared to wild-type and heterozygous retina, they remain substantially expressed at these sites (Fig. 2.9C and D). These data are in contrast with those in the Large^{myd} brain where no detectable labeling for either Kir4.1 or AQP4 was found (Fig. 2.2D and J), showing that the molecular mechanisms underlying the polarized distribution of these channels in retina may be different from those in brain.

2.3.5 Loss of perivascular localization of α-syntrophin but not β$_1$-syntrophin in the Large^{myd} retina

Data from (54) show that Kir4.1 and AQP4 bind to α-syntrophin in retina. However while this association is critical for AQP4 localization in brain, it is not in retina where AQP4 localization was only marginally decreased in perivascular astrocytes and Muller cell endfeet as assessed by immunoelectron microscopy in the α-syntrophin null mouse (55). Interestingly, Kir4.1 localization was unaffected both in brain and retina of these mice (34,55). In the present study, we show that Kir4.1 and AQP4 polarized distribution to astrocyte endfeet was profoundly disrupted in brain but not in retina of the Large^{myd} mouse. In brain, this was accompanied by loss of perivascular labeling of both α- and β1-syntrophins. To see whether a similar response is found in the retina, we investigated the localization of both these syntrophins in the Large^{myd} and wild-type control mice. Similarly to brain (Fig. 2.5D), α-syntrophin labeling in retina was no longer detected at perivascular glia (Fig. 2.10E) whereas β1-syntrophin labeling was still readily detected at these sites (Fig. 2.10M). These data together with the lack of IIH6 mAb immunolabeling (Fig. 2.7D), show that while α-syntrophin targeting to perivascular domains depends on the interaction between the α-DG glycans detected by IIH6 and the extracellular matrix proteins, the same may not be true for of β1-syntrophin.
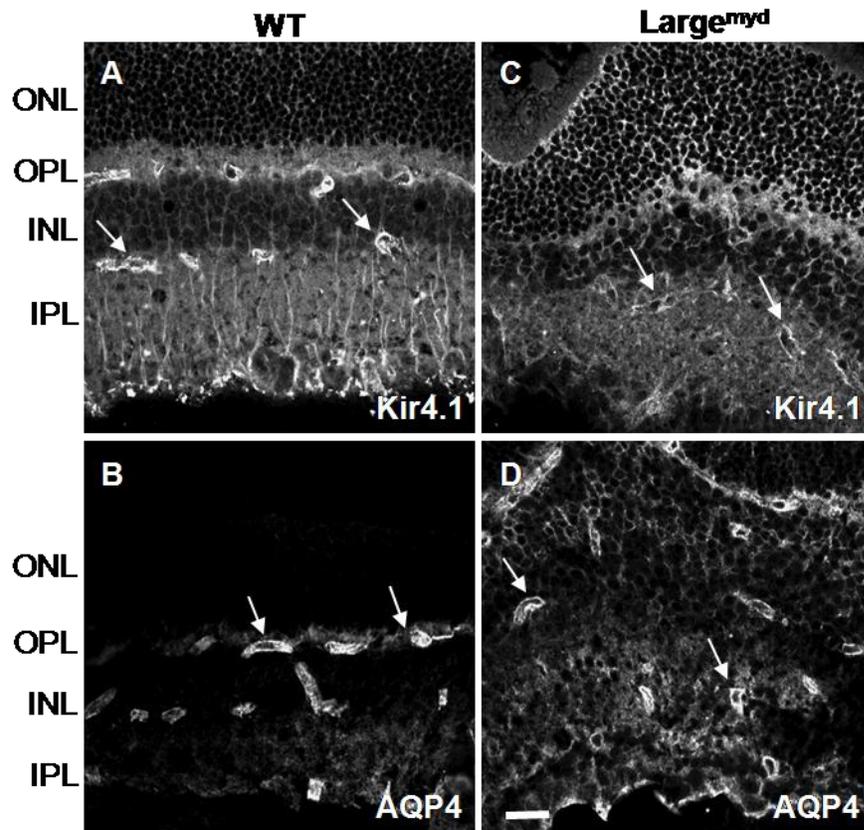
Figure 2.9 Perivascular Kir4.1 and AQP4 are maintained in the Large^{myd} retina. Retina sections from wild-type (**A** and **B**) and Large^{myd} mice (**C** and **D**) were immunolabeld for Kir4.1 (**A** and **C**) or for AQP4 (**B** and **D**). Note that a significant labeling for Kir4.1 (arrows, **C**) and AQP4 (arrows, **D**) is maintained at perivascular glial endfeet of the Large^{myd} retina. ONL, outer nuclear layer; OPL, outer plexiform layer; INL, inner nuclear layer; IPL, inner plexiform layer. Scale bar, 25 μm.
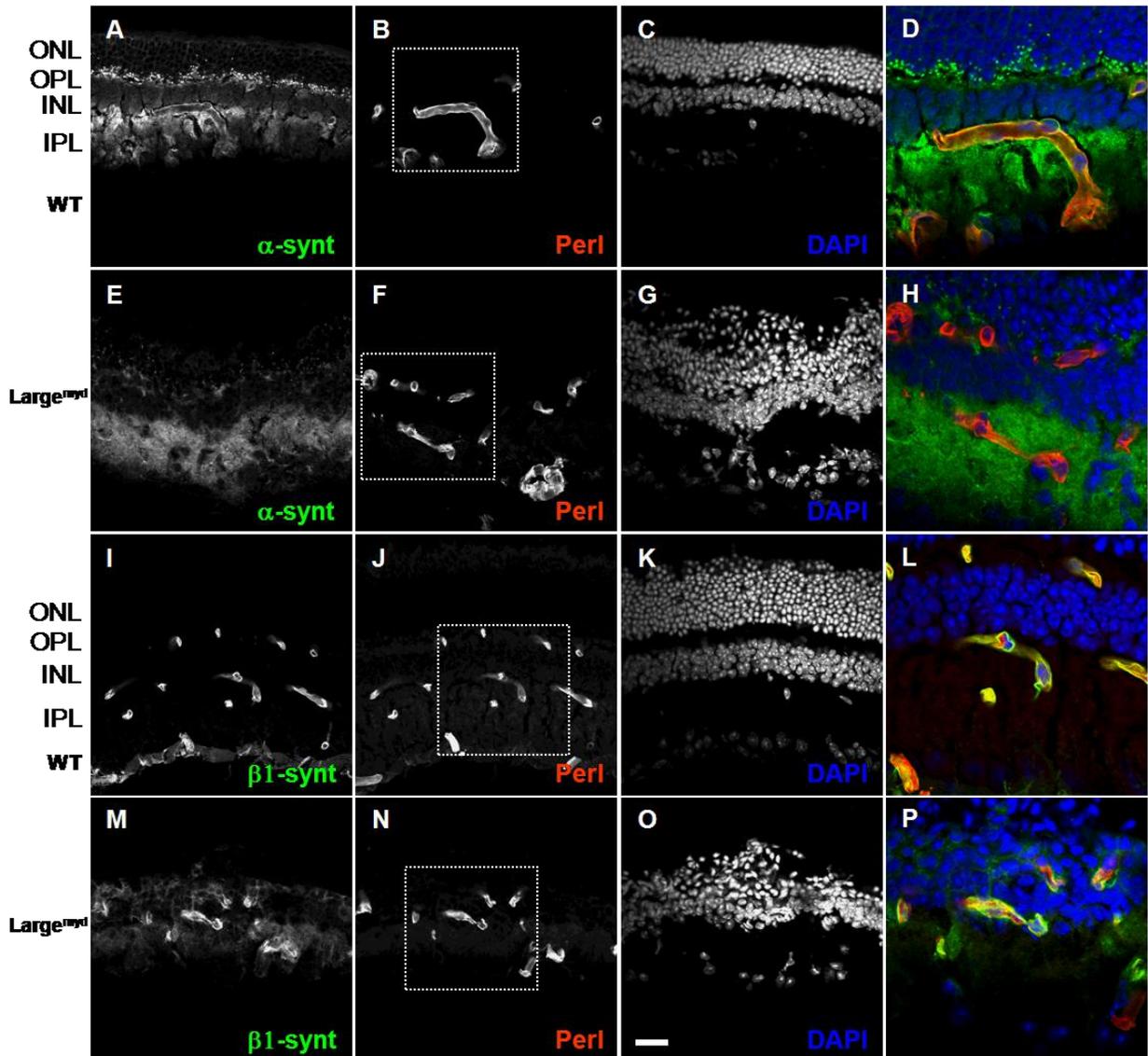
Figure 2.10 Perivascular β1-syntrophin but not α-syntrophin is still expressed in the Large^myd retina. Retina sections from wild-type (**A-D**; **I-L**) and Large^myd mice (**E-H**; **M-P**) were double immunolabeled for α-syntrophin (**A**, **E**) and perlecan (**B**, **F**) or β1-syntrophin (**I**, **M**) and perlecan (**J**, **N**). Unlike a-syntrophin (**E**), β1-syntrophin (**M**) is still localized around blood vessels in the Large^myd retina. High magnifications of the boxed areas in **B, F, J**, and **N** are illustrated as merged images in **D**, **H**, **L**, and **P**. These confirm the co-distribution between α-syntrophin and perlecan (**D**) and β1-syntrophin and perlecan (**L**, **P**). ONL, outer nuclear layer; OPL, outer plexiform layer; INL, inner nuclear layer; IPL, inner plexiform layer. Scale bar, 25 μm.

2.4 Discussion

2.4.1 AQP4 and Kir4.1 redistribution in brain

The proper localization and coordinated activity of glial Kir4.1 and AQP4 is essential to normal neuronal function and is believed to underlie potassium ion homeostasis and water flux in brain (56,57). Several studies suggest that the DAP complex is involved in the stability of Kir4.1 and AQP4 channels at astrocytic domains active in electrolyte balance and fluid movement (36,39,40,58,59). In this study, we have used immunofluorescence to investigate the distribution pattern of these channels in the brain of the Large[myd] mouse, a model of glycosylation-deficient forms of muscular dystrophy (46). It is noteworthy that selective deletion of brain (60) or muscle DG (61) result in pathologies like those seen in the Large[myd] mouse (46,62). This supports the idea that hypoglycosylation of α-DG and subsequent loss of ligand-binding underlies these pathologies in the Large[myd] mouse, although defects in the glycosylation of other proteins and their contribution to some of the phenotypes cannot be excluded. In agreement with previous findings, we show that in the brain of this mouse AQP4 fails to localize at perivascular domains (46). Furthermore, Kir4.1 is also lost from these sites supporting our hypothesis that the inability of the complex to bind extracellular ligands because of α-DG hypoglycosylation compromises the distribution of both AQP4 and Kir4.1 channels. These findings are consistent with previous studies using animal models characterized by disruptions of members of the DAP complex other than DG. In fact, dystrophin mutant mice exhibit a dramatic reduction in perivascular expression of both Kir4.1 and AQP4 with no apparent disruption in the formation or density of the blood vessels themselves (35-37,63,64). The mislocalization of channels caused by mutations of members of the DAP complex is not unique to Kir4.1 and AQP4 in the CNS. In fact, muscles of dystrophic mice and patients present an abnormal aggregation of acetylcholine receptors at the neuromuscular junction (65). Similarly, a selective deletion of Schwann cells DG results in reduced voltage-gated sodium channels aggregation at the nodes of Ranvier (66). These findings, together with our data, provide compelling evidence that an unbreached continuity between the DAP complex and the ECM is essential to the localization and stability of both Kir4.1 and AQP4 to perivascular domains of astrocytic endfeet and that any compromise, be it cytoplasmic or extracellular, causes their mislocalization.

There exists evidence that both Kir4.1 and AQP4 associate with the DAP complex via the intracellular protein α-syntrophin. Both channels contain a consensus C-terminal SXV motif that binds to the PDZ domain of α-syntrophin (39,67) and the α-syntrophin null mouse shows loss of AQP4 from perivascular astrocytic membranes in brain (58). Interestingly, in accordance with Michele et al (2002) (46) we report here that AQP4 and α-syntrophin (Fig. 2.2D and 2.5D) are no longer localized to perivascular astrocytic endfeet in the brain of the Large^{myd} mouse. These data not only substantiate the hypothesis that α-syntrophin provides a link between the DAP complex and this channel but they also show that severance of the link between the complex and the ECM adversely affects the stability of α-syntrophin at perivascular sites. In contrast with muscle, where most members of the DAP complex remain localized at the sarcolemma, dystrophin, β-DG as well as α-syntrophin fail to localize at astrocytic endfeet in the brain of the Large^{myd} mouse. This difference between brain and muscle is surprising especially that the interaction between α-DG and the ECM is impaired in both tissues. Nevertheless, it reveals that the functional implications of such an interaction are distinct depending on the tissue.

While the immunofluorescence data show lack of Kir4.1 and AQP4 labeling at perivascular astrocytes in the Large^{myd} brain, immunoblot analyses show no reduction in their total expression levels (Fig. 2.4) revealing a redistribution of these channels to other astrocytic domains. This is in agreement with data reported for Kir4.1 in the retina of mdx^{3cv} and Dp71 null mice (35,36,63) and for AQP4 in the brain of α-syntrophin null mouse (39). Interestingly, other components of the DAP complex including β-DG and dystrophin fail to localize at perivacular astrocytes despite normal total expression levels (Fig. 2.4;(46)). These data combined with our current findings provide evidence that the distribution of Kir4.1, AQP4 and components of the DAP complex to specialized membrane domains, such as astrocyte endfeet relies on a coordinated interaction between all these proteins.

The physiological impact of the redistribution of AQP4 in α-syntrophin null mice has been correlated with delayed K^{+} ion clearance in brain indicating that water flux through perivascular AQP4 is required for efficient removal of K^{+} after neuronal activation (34). Likewise, the Kir4.1 knock out mouse exhibits reduced potassium currents and potassium buffering capacity (68). In models of pathogenic brain edema induced by acute water intoxication and focal ischemic stroke, AQP4 deletion has been shown to reduce significantly

70

the progression of cytotoxic edema (69). In light of these data and our findings showing a redistribution of Kir4.1 and AQP4, it is reasonable to speculate that the Large^{myd} mouse may present with similar physiological effects under specific experimental conditions.

2.4.2 AQP4 and Kir4.1 distribution in retina

Similarly to brain, retinal glial cells express Kir4.1, AQP4 and the DAP complex in a highly polarized fashion so as to facilitate potassium buffering (56). In fact most of what is known about the involvement of these channels in potassium siphoning has come to light from studies using retinal Müller glia (70). At least two glycoforms of α-DG are expressed in retina (71), however the expression of the Large glycosyltransferase isoforms that may be associated with α-DG glycosylation has not been documented. We therefore determined the expression of isoforms of Large by RT-PCR and found that in addition to Large1, Large2 and its alternative transcripts are also expressed in retina. Immunolabeling with the IIH6 mAb showed that the α-DG carbohydrate epitopes normally recognized by this antibody are lacking at perivascular glia in the Large^{myd} retina. Assuming that both Large1 and Large2 are expressed within the same retinal glial cells, these data suggest that there is no functional redundancy between these two putative glycosyltransferases and that Large1 is the primary glycosyltransferase associated with the biosynthesis of glycans detected by the IIH6 antibody. It is possible that Large2 is also involved in the biosynthesis of glycans of α-DG which cannot be detected by the IIH6 antibody. However, it remains to be determined whether these would be sufficient for ligand interaction.

Subsequently, we investigated the distribution of Kir4.1 and AQP4 in retina by immunofluorescence. In contrast with our findings in brain, our data revealed a significant labeling for these channels at perivascular glia in the Large^{myd} retina. Furthermore, while β-DG and α-syntrophin ((46) and data not shown) as well as β1-syntrophin fail to localize at astrocyte endfeet in the Large^{myd} brain, perivascular staining for β-DG and β1-syntrophin comparable to that in wild-type retina is found in the Large^{myd} retina. Interestingly, a normal expression of β-DG and other components of the complex has been reported at the sarcolemmal membrane of MEB, FCMD and Large^{myd} skeletal muscles (46). These also presented a normal localization of α-DG core protein (46). It is therefore possible that α-DG core protein is still expressed perivascularly in the Large^{myd} retina.

71

The differential effects of the Large^{myd} mutation on the distribution of Kir4.1 and AQP4 channels between brain and retina provides compelling evidence that the underlying mechanisms involved in their targeting are different between these tissues. The presence of perivascular β1-syntrophin in the Large^{myd} retina raises the possibility that it may compensate for α-syntrophin loss at perivascular glia and therefore target the channels appropriately at these sites. This is in accordance with the data of (55) showing that the entire pool of perivascular Kir4.1 and 30% of AQP4 are still expressed in the retina of the α-syntrophin null mouse. This indicates that the localization of most of AQP4 but not Kir4.1 depends on α-syntrophin (55). Of particular interest, β1-syntrophin is still expressed in retina of the α-syntrophin null mouse, suggesting that it may be involved in localizing Kir4.1 as well as a pool of AQP4 (55).

The primary objective of this study was to determine the impact of the Large^{myd} mutation on the perivascular localization of Kir4.1 and AQP4 in brain and retina. In brain, we show that the hypoglycosylation of α-DG secondary to mutation of Large1 is associated with loss of both AQP4 and Kir4.1 as well as α- and β_1-syntrophins from perivascular domains. In retina however, significant labeling for both channel types as well as β1-syntrophin and β-DG is present at perivascular glia. These data show that in retina Kir4.1 and AQP4 may be anchored and stabilized at glial cell endfeet via a mechanism that is dependent on β1-syntrophin but independent on the interaction of the ECM with α-DG glycans involving Large1. Our findings point to a spatial variability in the role of Large1-associated α-DG glycosylation in the polarized distribution of the channels. This indicates that there are distinct functional implications for the Large1-associated glycosylation in brain and retina.

2.5. References

1.	Petrof, B. J., Shrager, J. B., Stedman, H. H., Kelly, A. M., and Sweeney, H. L. (1993) *Proc Natl Acad Sci U S A* **90**, 3710-3714
2.	Sunada, Y., and Campbell, K. P. (1995) *Curr Opin Neurol* **8**, 379-384
3.	Jung, D., Yang, B., Meyer, J., Chamberlain, J. S., and Campbell, K. P. (1995) *J Biol Chem* **270**, 27305-27310
4.	Ibraghimov-Beskrovnaya, O., Ervasti, J. M., Leveille, C. J., Slaughter, C. A., Sernett, S. W., and Campbell, K. P. (1992) *Nature* **355**, 696-702
5.	Way, M., Pope, B., Cross, R. A., Kendrick-Jones, J., and Weeds, A. G. (1992) *FEBS Lett* **301**, 243-245
6.	Bowe, M. A., Deyst, K. A., Leszyk, J. D., and Fallon, J. R. (1994) *Neuron* **12**, 1173-1180
7.	Talts, J. F., Andac, Z., Gohring, W., Brancaccio, A., and Timpl, R. (1999) *Embo J* **18**, 863-870
8.	Sugita, S., Saito, F., Tang, J., Satz, J., Campbell, K., and Sudhof, T. C. (2001) *J Cell Biol* **154**, 435-445
9.	Ehmsen, J., Poon, E., and Davies, K. (2002) *J Cell Sci* **115**, 2801-2803
10.	Cohn, R. D., and Campbell, K. P. (2000) *Muscle Nerve* **23**, 1456-1471
11.	Chiba, A., Matsumura, K., Yamada, H., Inazu, T., Shimizu, T., Kusunoki, S., Kanazawa, I., Kobata, A., and Endo, T. (1997) *J Biol Chem* **272**, 2156-2162
12.	Kim, D. S., Hayashi, Y. K., Matsumoto, H., Ogawa, M., Noguchi, S., Murakami, N., Sakuta, R., Mochizuki, M., Michele, D. E., Campbell, K. P., Nonaka, I., and Nishino, I. (2004) *Neurology* **62**, 1009-1011
13.	Michele, D. E., Barresi, R., Kanagawa, M., Saito, F., Cohn, R. D., Satz, J. S., Dollar, J., Nishino, I., Kelley, R. I., Somer, H., Straub, V., Mathews, K. D., Moore, S. A., and Campbell, K. P. (2002) *Nature* **418**, 417-422
14.	Longman, C., Brockington, M., Torelli, S., Jimenez-Mallebrera, C., Kennedy, C., Khalil, N., Feng, L., Saran, R. K., Voit, T., Merlini, L., Sewry, C. A., Brown, S. C., and Muntoni, F. (2003) *Hum Mol Genet* **12**, 2853-2861
15.	Brockington, M., Yuva, Y., Prandini, P., Brown, S. C., Torelli, S., Benson, M. A., Herrmann, R., Anderson, L. V., Bashir, R., Burgunder, J. M., Fallet, S., Romero, N., Fardeau, M., Straub, V., Storey, G., Pollitt, C., Richard, I., Sewry, C. A., Bushby, K., Voit, T., Blake, D. J., and Muntoni, F. (2001) *Hum Mol Genet* **10**, 2851-2859
16.	Kobayashi, K., Nakahori, Y., Miyake, M., Matsumura, K., Kondo-Iida, E., Nomura, Y., Segawa, M., Yoshioka, M., Saito, K., Osawa, M., Hamano, K., Sakakihara, Y., Nonaka, I., Nakagome, Y., Kanazawa, I., Nakamura, Y., Tokunaga, K., and Toda, T. (1998) *Nature* **394**, 388-392
17.	Beltran-Valero de Bernabe, D., Currier, S., Steinbrecher, A., Celli, J., van Beusekom, E., van der Zwaag, B., Kayserili, H., Merlini, L., Chitayat, D., Dobyns, W. B., Cormand, B., Lehesjoki, A. E., Cruces, J., Voit, T., Walsh, C. A., van Bokhoven, H., and Brunner, H. G. (2002) *Am J Hum Genet* **71**, 1033-1043
18.	Yoshida, A., Kobayashi, K., Manya, H., Taniguchi, K., Kano, H., Mizuno, M., Inazu, T., Mitsuhashi, H., Takahashi, S., Takeuchi, M., Herrmann, R., Straub, V., Talim, B., Voit, T., Topaloglu, H., Toda, T., and Endo, T. (2001) *Dev Cell* **1**, 717-724
19.	Hayashi, Y. K., Ogawa, M., Tagawa, K., Noguchi, S., Ishihara, T., Nonaka, I., and Arahata, K. (2001) *Neurology* **57**, 115-121

20. Kano, H., Kobayashi, K., Herrmann, R., Tachikawa, M., Manya, H., Nishino, I., Nonaka, I., Straub, V., Talim, B., Voit, T., Topaloglu, H., Endo, T., Yoshikawa, H., and Toda, T. (2002) *Biochem Biophys Res Commun* **291**, 1283-1286

21. Blake, D. J., Hawkes, R., Benson, M. A., and Beesley, P. W. (1999) *J Cell Biol* **147**, 645-658

22. Moukhles, H., and Carbonetto, S. (2001) *J Neurochem* **78**, 824-834

23. Moukhles, H., Roque, R., and Carbonetto, S. (2000) *J Comp Neurol* **420**, 182-194

24. Ueda, H., Gohdo, T., and Ohno, S. (1998) *J Histochem Cytochem* **46**, 185-191

25. Zaccaria, M. L., Di Tommaso, F., Brancaccio, A., Paggi, P., and Petrucci, T. C. (2001) *Neuroscience* **104**, 311-324

26. Nielsen, S., Nagelhus, E. A., Amiry-Moghaddam, M., Bourque, C., Agre, P., and Ottersen, O. P. (1997) *J Neurosci* **17**, 171-180

27. Nagelhus, E. A., Horio, Y., Inanobe, A., Fujita, A., Haug, F. M., Nielsen, S., Kurachi, Y., and Ottersen, O. P. (1999) *Glia* **26**, 47-54

28. Higashi, K., Fujita, A., Inanobe, A., Tanemoto, M., Doi, K., Kubo, T., and Kurachi, Y. (2001) *Am J Physiol Cell Physiol* **281**, C922-931

29. Kofuji, P., Ceelen, P., Zahs, K. R., Surbeck, L. W., Lester, H. A., and Newman, E. A. (2000) *J Neurosci* **20**, 5733-5740

30. Brew, H., Gray, P. T., Mobbs, P., and Attwell, D. (1986) *Nature* **324**, 466-468

31. Newman, E., and Reichenbach, A. (1996) *Trends Neurosci* **19**, 307-312

32. Dietzel, I., Heinemann, U., Hofmeier, G., and Lux, H. D. (1980) *Exp Brain Res* **40**, 432-439

33. Holthoff, K., and Witte, O. W. (1996) *J Neurosci* **16**, 2740-2749

34. Amiry-Moghaddam, M., Williamson, A., Palomba, M., Eid, T., de Lanerolle, N. C., Nagelhus, E. A., Adams, M. E., Froehner, S. C., Agre, P., and Ottersen, O. P. (2003) *Proc Natl Acad Sci U S A* **100**, 13615-13620

35. Dalloz, C., Sarig, R., Fort, P., Yaffe, D., Bordais, A., Pannicke, T., Grosche, J., Mornet, D., Reichenbach, A., Sahel, J., Nudel, U., and Rendon, A. (2003) *Hum Mol Genet* **12**, 1543-1554

36. Connors, N. C., and Kofuji, P. (2002) *J Neurosci* **22**, 4321-4327

37. Nicchia, G. P., Nico, B., Camassa, L. M., Mola, M. G., Loh, N., Dermietzel, R., Spray, D. C., Svelto, M., and Frigeri, A. (2004) *Neuroscience* **129**, 935-945

38. Nico, B., Frigeri, A., Nicchia, G. P., Corsi, P., Ribatti, D., Quondamatteo, F., Herken, R., Girolamo, F., Marzullo, A., Svelto, M., and Roncali, L. (2003) *Glia* **42**, 235-251

39. Neely, J. D., Amiry-Moghaddam, M., Ottersen, O. P., Froehner, S. C., Agre, P., and Adams, M. E. (2001) *Proc Natl Acad Sci U S A* **98**, 14108-14113

40. Guadagno, E., and Moukhles, H. (2004) *Glia* **47**, 138-149

41. Noel, G., Belda, M., Guadagno, E., Micoud, J., Klocker, N., and Moukhles, H. (2005) *J Neurochem* **94**, 691-702

42. Grewal, P. K., Holzfeind, P. J., Bittner, R. E., and Hewitt, J. E. (2001) *Nat Genet* **28**, 151-154

43. Browning, C. A., Grewal, P. K., Moore, C. J., and Hewitt, J. E. (2005) *Neuromuscul Disord* **15**, 331-335

44. Grewal, P. K., McLaughlan, J. M., Moore, C. J., Browning, C. A., and Hewitt, J. E. (2005) *Glycobiology* **15**, 912-923

45. Kanagawa, M., Michele, D. E., Satz, J. S., Barresi, R., Kusano, H., Sasaki, T., Timpl, R., Henry, M. D., and Campbell, K. P. (2005) *FEBS Lett* **579**, 4792-4796

46. Michele, D. E., Barresi, R., Kanagawa, M., Saito, F., Cohn, R. D., Satz, J. S., Dollar, J., Nishino, I., Kelley, R. I., Somer, H., Straub, V., Mathews, K. D., Moore, S. A., and Campbell, K. P. (2002) *Nature* **418**, 417-421

47. Nagelhus, E. A., Veruki, M. L., Torp, R., Haug, F. M., Laake, J. H., Nielsen, S., Agre, P., and Ottersen, O. P. (1998) *J Neurosci* **18**, 2506-2519

48. Poopalasundaram, S., Knott, C., Shamotienko, O. G., Foran, P. G., Dolly, J. O., Ghiani, C. A., Gallo, V., and Wilkin, G. P. (2000) *Glia* **30**, 362-372

49. Tian, M., Jacobson, C., Gee, S. H., Campbell, K. P., Carbonetto, S., and Jucker, M. (1996) *Eur J Neurosci* **8**, 2739-2747

50. Kanagawa, M., Saito, F., Kunz, S., Yoshida-Moriguchi, T., Barresi, R., Kobayashi, Y. M., Muschler, J., Dumanski, J. P., Michele, D. E., Oldstone, M. B., and Campbell, K. P. (2004) *Cell* **117**, 953-964

51. Leonoudakis, D., Conti, L. R., Anderson, S., Radeke, C. M., McGuire, L. M., Adams, M. E., Froehner, S. C., Yates, J. R., 3rd, and Vandenberg, C. A. (2004) *J Biol Chem* **279**, 22331-22346

52. Connors, N. C., Adams, M. E., Froehner, S. C., and Kofuji, P. (2004) *J. Biol. Chem.* **279**, 28387-28392

53. Lee, Y., Kameya, S., Cox, G. A., Hsu, J., Hicks, W., Maddatu, T. P., Smith, R. S., Naggert, J. K., Peachey, N. S., and Nishina, P. M. (2005) *Mol Cell Neurosci* **30**, 160-172

54. Connors, N. C., and Kofuji, P. (2006) *Glia* **53**, 124-131

55. Puwarawuttipanit, W., Bragg, A. D., Frydenlund, D. S., Mylonakou, M. N., Nagelhus, E. A., Peters, M. F., Kotchabhakdi, N., Adams, M. E., Froehner, S. C., Haug, F. M., Ottersen, O. P., and Amiry-Moghaddam, M. (2006) *Neuroscience* **137**, 165-175

56. Nagelhus, E. A., Mathiisen, T. M., and Ottersen, O. P. (2004) *Neuroscience* **129**, 905-913

57. Amiry-Moghaddam, M., Frydenlund, D. S., and Ottersen, O. P. (2004) *Neuroscience* **129**, 999-1010

58. Amiry-Moghaddam, M., Otsuka, T., Hurn, P. D., Traystman, R. J., Haug, F. M., Froehner, S. C., Adams, M. E., Neely, J. D., Agre, P., Ottersen, O. P., and Bhardwaj, A. (2003) *Proc Natl Acad Sci U S A* **100**, 2106-2111

59. Vajda, Z., Nielsen, S., Sulyok, E., and Doczi, T. (2001) *Orv Hetil* **142**, 223-225

60. Moore, S. A., Saito, F., Chen, J., Michele, D. E., Henry, M. D., Messing, A., Cohn, R. D., Ross-Barta, S. E., Westra, S., Williamson, R. A., Hoshi, T., and Campbell, K. P. (2002) *Nature* **418**, 422-425

61. Cohn, R. D., Henry, M. D., Michele, D. E., Barresi, R., Saito, F., Moore, S. A., Flanagan, J. D., Skwarchuk, M. W., Robbins, M. E., Mendell, J. R., Williamson, R. A., and Campbell, K. P. (2002) *Cell* **110**, 639-648

62. Holzfeind, P. J., Grewal, P. K., Reitsamer, H. A., Kechvar, J., Lassmann, H., Hoeger, H., Hewitt, J. E., and Bittner, R. E. (2002) *Human Molecular Genetics* **11**, 2673-2687

63. Frigeri, A., Nicchia, G. P., Nico, B., Quondamatteo, F., Herken, R., Roncali, L., and Svelto, M. (2001) *Faseb J* **15**, 90-98

64. Vajda, Z., Pedersen, M., Fuchtbauer, E. M., Wertz, K., Stodkilde-Jorgensen, H., Sulyok, E., Doczi, T., Neely, J. D., Agre, P., Frokiaer, J., and Nielsen, S. (2002) *Proc Natl Acad Sci U S A* **99**, 13131-13136

65. Levedakou, E. N., Chen, X. J., Soliven, B., and Popko, B. (2005) *Mol Cell Neurosci* **28**, 757-769

66. Saito, F., Moore, S. A., Barresi, R., Henry, M. D., Messing, A., Ross-Barta, S. E., Cohn, R. D., Williamson, R. A., Sluka, K. A., Sherman, D. L., Brophy, P. J., Schmelzer, J. D., Low, P. A., Wrabetz, L., Feltri, M. L., and Campbell, K. P. (2003) *Neuron* **38**, 747-758

67.   Connors, N. C., Adams, M. E., Froehner, S. C., and Kofuji, P. (2004) *J Biol Chem* **279**, 28387-28392

68.   Kofuji, P., Ceelen, P., Zahs, K., Surbeck, L. W., Lester, H. A., and Newman, E. A. (2000) *The Journal of Neuroscience* **20**, 5733-5740

69.   Manley, G. T., Fujimura, M., Ma, T., Noshita, N., Filiz, F., Bollen, A. W., Chan, P., and Verkman, A. S. (2000) *Nat Med* **6**, 159-163

70.   Kofuji, P., and Newman, E. A. (2004) *Neuroscience* **129**, 1045-1056

71.   Moukhles, H., Roque, R., and Carbonetto, S. (2000) *The Journal of Comparative Neurology* **420**, 182-194

3 AGRIN PLAYS A MAJOR ROLE IN THE COALESCENCE OF THE AQP4 CLUSTERS FORMED BY GAMMA-1-CONTAINING LAMININ[2]

3.1 Introduction

Astrocytes represent the main glial cell population in the central nervous system that contributes to the cerebral water balance. Aquaporin-4 (AQP4) constitutes the principal water channel in the brain and is mainly concentrated in the perivascular astrocyte endfeet. The specific distribution of AQP4 is of major importance because it renders the channel capable of increasing water fluxes between the brain and the bloodstream and therefore plays a role in the water homeostasis. Indeed, recent studies in AQP4 over-expressing or knockout mice suggested a role of AQP4 in the pathophysiology of brain edema (1-3).

Dystroglycan (DG), a central element of the dystroglycan-associated protein (DAP) complex, is involved in the pathogenesis of brain dysfunctions associated with many forms of muscular dystrophies (4). DG is a receptor for several extracellular matrix (ECM) molecules, such as laminin, agrin and perlecan, and links the ECM to the actin cytoskeleton (5). Multiple lines of evidence suggest that the integrity of the DAP complex is essential for the proper localization and function of AQP4. Indeed, mutations in the dystrophin gene and the deletion of the syntrophin gene, two members of the DAP complex, result in a dramatic reduction of the expression of AQP4 at perivascular astrocytes (6,7). However, while it is well-understood that AQP4 has an important impact on the homeostasis in the brain parenchyma, and that its polarized distribution is known to depend on the presence of DG, the role that the basal lamina is playing in this polarized distribution of AQP4 remains unclear.

The perivascular basal lamina, also known as membrane limitans gliae perivascularis, is made of ECM molecules secreted by both astrocytes and endothelial cells (8,9). Among the different components of the membrane limitans gliae perivascularis, laminin, agrin, collagen type IV, fibronectin and perlecan play an important physiological role.

Laminins are composed of three distinct chains referred to as α, β and γ. Currently, five α, four β and three γ chains have been described and give rise, when splice variants are included,

to 16 different laminin isoforms (10,11). The C-terminal ends of the α-chains contain globular domains composed of five similar modules (LG1-5). Around the blood vessels in the CNS, laminin-1 (also referred as 111) composed of α1 (400 kDa), β1 (200 kDa) and γ1 (200 kDa) chains is the best-characterized laminin (12-16) but laminin-2 (211) and -5 (332) are also present (12,14,16-18). The γ3 chain, component of the laminin 12 (213), 14 (423) and 15 (523), has also been reported to be expressed in brain (19).

Laminin is essential for the assembly of the basal lamina by interacting with specific cell surface receptors and conversely cell surface receptors are crucial for the polymerization of laminin (20). Indeed, it has been shown that DG can assemble laminin (21-29) and the absence of DG leads to the disruption of the Reichert membrane, the extra-embryonic matrix in mouse, with mislocalization of laminin (29-31). Laminins are also involved in the integrity of the basal lamina by bridging many ECM components together (32). In addition to self polymerization (33), laminins have been shown to interact, via an epidermal-growth-factor like repeat within the laminin γ1 chain, with domain G3 of nidogen which binds to the immunoglobulin-like domain 3 of perlecan (34-38) or with collagen IV(39,40). Interestingly, DG is also crucial in the polymerization of collagen IV (41) which is present at the blood-brain barrier (BBB) (42).

Agrin is also concentrated at the basal lamina lining the vascular vessels (43-47). Interestingly, agrin isoforms can bind laminin-1, -2 and -4 and has been suggested to play an important role in the assembly of the basal lamina (48,49). Agrin plays an important role in the integrity of the BBB as shown in the agrin null mouse (50). Agrin can also be spliced at three sites which in rats are called X, Y (or A in chicken) and Z (or B in chicken). Depending on the splicing events that occur 9 amino acids can be inserted in X, 4 amino acids can be inserted in Y and 8, 11 or 19 amino acids can be inserted in Z (51). The agrin isoform without any insertion, referred as Y0Z0 (A0B0 or C-Agrin0, 0), is secreted by myocytes or found at the BBB whereas the agrin Y4Z8 (A4B8 or C-agrin4, 8) is secreted by neurons (43,52-54). The structure of agrin has been characterized and it has been proposed that agrin isoforms can bind α-DG via their 3 LG domains (16,43,55). Recently, it has been shown that DG is crucial for the clustering of agrin (56,57).

Recently, several studies have suggested that AQP4 participates in highly organized membrane domains in association with the DAP complex in brain where two of its isoforms, M1 and M23, play different roles (58,59). Interestingly, a recent study also reported a selective increase in mRNA expression of AQP4M23 but not AQP4M1 upon exogenous agrin treatment and this was associated with an increase in the AQP4-mediated water permeability (60,61). Similarly, agrin has been proposed to play a major role in the distribution of AQP4 around the cerebral blood vessels (62,63). We recently found that laminin but not exogenous agrin, nor fibronectin, induces the coclustering of AQP4 and lipid rafts in astrocytes (23,64). Therefore, this raises the question of whether the agrin-mediated modulation of AQP4M1 and AQP4M23 expression is crucial for their laminin-induced clustering and if laminin has an effect on water permeability. Here, we investigate the effect of different ECM components on both AQP4 distribution in astrocytes but also its isoform specific expression. We also focused on the role of laminin together with agrin in the expression of the M1 and M23 expression and their respective contribution in AQP4 cluster formation. Since both laminin and fibronectin have recently been proposed to influence cell volume on myocytes (65), we finally assessed the functional significance of laminin-mediated AQP4 clustering on water transport, using a model of hypo-osmotic shock where a decrease in the calcein-loaded fluorescence has been correlated with cytoplasmic volume increase and AQP4 activity (66-71).

3.2 Materials and methods

3.2.1 Antibodies

The following antibodies were used in the present study: rabbit anti-AQP4 against rat GST AQP4 corresponding to residues 249–323 (Alomone Laboratories, Jerusalem, Israel), mouse anti-β-DG, 43DAG1/8D5, against the 15 of the last 16 amino acids at the C-terminus of the human dystroglycan sequence (Novocastra Laboratories, Newcastle, UK), rabbit anti-agrin against purified agrin (generous gift from Dr M. Ferns, University of California, Davis, CA, USA) and mouse anti-mitochondrial heat shock protein 70 against a synthetic peptide corresponding to residues 615-633 (Affinity BioReagents, USA). The laminin-γ1 blocking antibodies were a generous gift from Dr. T. O'Connor (University of British Columbia, BC, Canada).

3.2.2 Astrocyte primary cultures

Primary hippocampal astrocyte cultures were prepared from post-natal day 1 (P1) rats (Sprague-Dawley, Charles River) or mouse (C57BL/6, Charles River). Cortices were dissected, and meninges and choroid plexus were removed. They were then cut into small pieces and incubated for 25 min with trypsin (3.0 mg/ml; Gibco, Burlington, Canada). Dissociated cortices were then plated in culture flasks and grown in Dulbecco's modified Eagle's medium (DMEM) supplemented with 10% fetal bovine serum, 1% penicillin-streptomycin and 1 mM L-glutamine (Gibco) for 2-3 weeks. The culture medium was changed every 3 days. To remove microglia and oligodendrocyte progenitors, the flasks were shaken the day following the plating. After trypsinization, the cells were plated on glass coverslips coated with poly-D-lysine (0.1 mg/ml; Sigma) in 24-well plates at a density of 200-250 x10^3 cells/ml. Two days after plating, the cells were treated for 1 to 8 hours with 20 nM Engelbreth-Holm-Swarm Sarcoma laminin-1, 30 nM Engelbreth-Holm-Swarm Sarcoma collagen IV Miller (Sigma-Aldrich, St. Louis, MO, USA) or 40 μg/ml Matrigel^{TM} (BD Biosciences, USA).

3.2.3 siRNA transfections

Mouse astrocytes were transfected in suspension before plating with 100 nmol/l Agrin siRNAs (ON-TARGETplus SMARTpool siRNA reagents; Dharmacon, USA) and control siRNA (ON-TARGETplus siCONTROL nontargeting siRNA; Dharmacon) using Lipofectamine-2000 (Invitrogen, USA), following the manufacturer's protocol. One day and a half after plating, astrocytes were treated or not for 8 hours with 20 nM of laminin and subsequently analyzed by immunofluorescence or RT-PCR.

3.2.4 Immunofluorescence

Cells were rinsed with warm PBS and fixed by immersion in 4% (w/v) paraformaldehyde in 0.1 M phosphate buffer for 20 min followed by rinsing in PBS, 3 x 15 min. The cells were incubated for 1 h at room temperature (20–22°C) in a solution containing 2% bovine serum

albumin (Sigma) and 0.25% Triton X-100. Double immunolabelling was performed by incubating the cells at room temperature for 1 h in the presence of primary antibodies against β-DG (1/25) and AQP4 (1:200) or β-DG (1/25) and agrin (1/500). Subsequently, they were rinsed with PBS (3 x 15 min) and incubated with Alexa Fluor 568 goat anti-mouse IgG and Alexa Fluor 647 goat anti-rabbit or Alexa Fluor 488 goat anti-mouse IgG and Alexa Fluor 568 goat anti-rabbit IgG for 1 h (1/200; Molecular Probes, USA). After several washes with PBS, coverslips were mounted on glass slides using Prolong Gold Antifade Reagent with or without 4', 6-diamidino-2-phenylindole (Invitrogen, Burlington, ON, Canada). To confirm the specificity of the labeling, control cells were treated equivalently in the absence of primary antibodies. Fluorescent labeling of cultured cells was visualized using a confocal microscope (Fluoview 1000; Olympus) and an Uplan Apochromat 1.35 NA 60x objective (Olympus).

3.2.5 Cell surface biotinylation

Primary astrocyte cultures grown in 25 cm^2 flasks were placed on ice and washed with cold PBS containing 1.0 mM CaCl$_2$ and 0.5 mM MgCl$_2$ (DPBS) three times for 5 min each before being incubated with 0.5 mg/ml EZ-Link Sulfo-NHS-LC-Biotin (Pierce Biotechnology, Rockford, IL, USA) for 30 min at 4°C. The biotin solution was removed, and the reaction was quenched with 50 mM NH$_4$Cl in DPBS for 10 min. The cells were extensively washed and incubated for 20 min with extraction buffer (25 mM Tris pH 7.4, 25 mM glycine, 150 mM NaCl and 5 mM EDTA) containing 1% Triton X-100 and 1 x complete protease inhibitor cocktail (Roche, Laval, QC, Canada). The biotinylated proteins were precipitated using streptavidin covalently attached to agarose beads (Pierce Biotechnology, Rockford, USA).

3.2.6 Immunoblotting

Astrocyte cultures were harvested and lysed on ice for 20 min in extraction buffer (25 mM Tris pH 7.4, 25 mM glycine and 150 mM NaCl) containing 1% Triton X-100, 1 x complete protease inhibitor cocktail and 5 mM EDTA. Nuclei and cellular debris were removed from the suspension by centrifugation at 16,000 g for 10 min. Extracted proteins were denatured by boiling for 9 min in reducing sample buffer and then loaded on a 10% sodium dodecyl sulfate-polyacrylamide electrophoresis gels. The gels were electrotransferred to nitrocellulose

membranes (Bio-Rad, Mississauga, ON, Canada) and the blots were probed with antibodies to β-DG (1/300), AQP4 (1/1000) and HSP-70 (1/1000). Bound antibodies were detected using horseradish peroxidase-conjugated goat anti-rabbit IgG or goat anti-mouse IgG (1/2000; Jackson ImmunoResearch, USA). Signals were visualized on Bioflex econo films (Interscience, Markham, ON, Canada) using chemiluminescence (Amersham Biosciences, Buckinghamshire, UK).

3.2.7 Water permeability measurements

For water permeability measurements, cells were grown on round coverglasses and loaded with calcein by incubation for 45 min with 6 μM calcein-acetoxymethyl (calcein-AM, Molecular Probes) at 37°C. Loading of calcein was similar in all the conditions tested. After being rinsed in PBS (pH 7.4), the coverglasses were mounted in a perfusion chamber on the stage of a two-photon laser-scanning microscope Zeiss LSM510-Axioskop-2 fitted with a 40X-W/0.80 numerical aperture objective lens directly coupled to a Mira Ti:sapphire laser ($\sim$ 100-fs pulses, 76 MHz, pumped by a 5 W Verdi laser; Coherent) which continuously measured calcein fluorescence. The cells were perfused with isotonic CSF 330 mOsm (120 mM NaCl, 3.3 mM KCl, 26 mM $NaHCO_3$, 1.3 mM $MgSO_4$, 1.2 mM NaH_2PO_4, 1.8 mM $CaCl_2$ and 11 mM D-Glucose) and scanned every 3.4 s with excitation at 835 nm. An in-line heater/cooler was constructed in which perfusate passed through 80 cm of tubing enclosed by a water jacket with circulating fluid. Effluent temperature was monitored via an in-line thermistor. The fluorescent signal which has large two-photon absorption cross-sections, were excited at 835–840 nm and epifluorescence was detected at 560 nm from the optical slice within the cell body. The cells were then subjected to an osmotic shock by switching the perfusate to a hypoosmotic, 250 mOsm, CSF, obtained by omission of 40 mM NaCl from the isotonic solution. Solution osmolarities were measured using a freezing point-depression osmometer and perfusion solutions were gravity pumped with a flow rate approximately 4ml/min as used in water transport measurements. The swelling of the cells was monitored as a decrease of calcein fluorescence, which occurred to the dilution of the fluorophore (66-69,72).

3.2.8 RNA extraction and RT-PCR

Total RNA extraction was performed on mouse confluent primary astrocyte cultures transfected with siCTL or siAgrin and treated with 20 nM laminin or 40 μg/ml Matrigel^{TM}, and on mouse brains dissected out immediately after sacrificing mice by exposure to CO_2, using a micro-homogenizing device (VWR, Mississauga, ON, Canada) and TRIZOL® reagent (Invitrogen) following the supplied protocol. The quality and integrity of RNA was assessed on formaldehyde agarose gel and concentration was determined using NanoDrop® ND-1000 spectrophotometer (NanoDrop Technologies, USA).

Total cDNA was prepared using Oligo dT $_{(18)}$ (Invitrogen), 1 μg of total RNA from each sample and SuperScript™ III Reverse Transcriptase (RT; Invitrogen) following the supplied protocol. The presence of M1 and M23 isofroms of AQP4 was assessed on 2 μl of synthesized total cDNA of condition by PCR using the set of primers described by (60) and Platinum®-Taq DNA polymerase (Invitrogen). A set of GAPDH primers (Forward: 5'ACC ACA GTC CAT GCC ATC AC3', Reverse: 5'TCC ACC ACC CTG TTG CTG TA3') was used as control. To verify that the amplified signal was not the product of genomic DNA, RNA samples that were not reverse transcribed (- RT) were used.

3.2.9 Quantitative analyses

The number of clusters and surface area of the DG, AQP4 and laminin clusters were determined on images subjected to a threshold using ImagePro Plus software (Media Cybernetics, Inc.). Pictures from the same experiment were captured using identical acquisition parameters and subjected to the same threshold. Statistical analyses were performed using GraphPad Prism 3.00 software and unpaired Student's *t*-test.

3.3 Results

3.3.1 Endogenous agrin is recruited at the laminin-induced clusters of β-DG and is crucial for their stabilization

In previous studies, our laboratory showed that neither exogenous C-agrin 4, 8 nor C-agrin 0, 0 could induce β-DG clustering on their own or potentiate cluster formation in the presence of laminin (23,73). The splice variant C-agrin 0,0 (also known as A0B0) has since been reported to be restricted to the subendothelial basal lamina of CNS capillaries and meningeal cells (47) whereas C-agrin 4,8 is secreted by both neurons and astrocytes (74). We therefore studied the distribution of endogenous agrin in the presence or absence of laminin. Figure 3.1 illustrates primary astrocyte cultures stained with an antibody against agrin recognizing the different splice variants. The results show that the immunoreactivity is mainly perinuclear without any specific plasma membrane labeling in absence of laminin (Fig. 3.1C). In contrast, when the astrocytes were treated for 12 hours with laminin-1 and immunolabeled for agrin, agrin is found to be coclustered with β-DG clusters (Fig. 3.1D). We therefore investigated the cell surface expression of endogenous agrin using a biotinylation assay followed by immunoblot. Figure 3.1G shows that the cell surface expression was significantly increased upon laminin treatment suggesting that exogenous laminin influences the cell surface expression of endogenous agrin as well as its clustering.

We then asked whether endogenous agrin plays a role in the laminin-induced clustering of β-DG. Astocyte cultures were transfected with Agrin siRNA to silence endogenous agrin and the laminin-induced clustering was assessed by immunofluorescence. In control astrocytes transfected with scramble siCTL showed a band at 250 kDa by western blot using an antibody against agrin whereas siAgrin transfected cells did not present such a band confirming the high efficiency of agrin silencing (Fig. 3.2G). When these cultures were assessed for β-DG clustering upon laminin treatment, we observed a decrease in immunoreactivity for agrin in the siAgrin transfected astrocytes as well as a reduction in the fluorescence intensity of the β-DG clusters (Fig. 3.2B). A quantitative analysis comparing the β-DG clusters between the control and siAgrin transfected astrocytes reveals that the number of β-DG clusters remains constant whereas the total area covered by these clusters shows a significant decrease upon agrin

Figure 3.1 Laminin treatment results in an increase in the cell-surface expression of endogenous agrin in β-DG-containing clusters. (A-I) Rat hippocampal astrocytes incubated with (**B, D and F**) or without (**A, C and E**) 20 nM laminin were double immunolabeled for β-DG **(A-B)** and agrin **(C-D)**. Scale bar, 30 μm. **G.** Astrocytes were incubated with 20 nM laminin (+**LAM**) or left untreated (-**LAM**) and proteins were harvested in extraction buffer. Immunoblots were probed for agrin.

-LAM   +LAM

A β-DG   B β-DG

C Agrin   D Agrin

E Merge   F Merge

G.

-LAM +LAM   -LAM +LAM

Agrin

β-Actin

Biotinylated
Proteins

Membrane
Extract

Cell
Surface

Figure 3.2 Silencing of endogenous agrin expression prevents the extension of β-DG clustering upon laminin treatment. (A-I) Rat hippocampal astrocytes transfected with siCTL or siAgrin and incubated with 20 nM laminin (+**LAM**) were double immunolabeled for β-DG **(A-B)** and agrin **(C-D)**. Scale bar, 30 μm. **G.** Astrocytes were transfected with siCTL or siAgrin for a duration of 2 days. Proteins were harvested in extraction buffer. Immunoblots were probed for HSP70 and agrin. Representative blots from three independent experiments are shown. **H.** Quantitative analysis of the laminin-induced clustering of β-DG. The histograms represent the mean number of clusters ±SE and surface area of clusters ±SE in astrocyte cultures treated with laminin for 8 hours after transfection with siCTL or siAgrin from three experiments. All quantifications were performed on 15 fields acquired randomly from each experiment.

siCTL+LAM   siAgrin+LAM
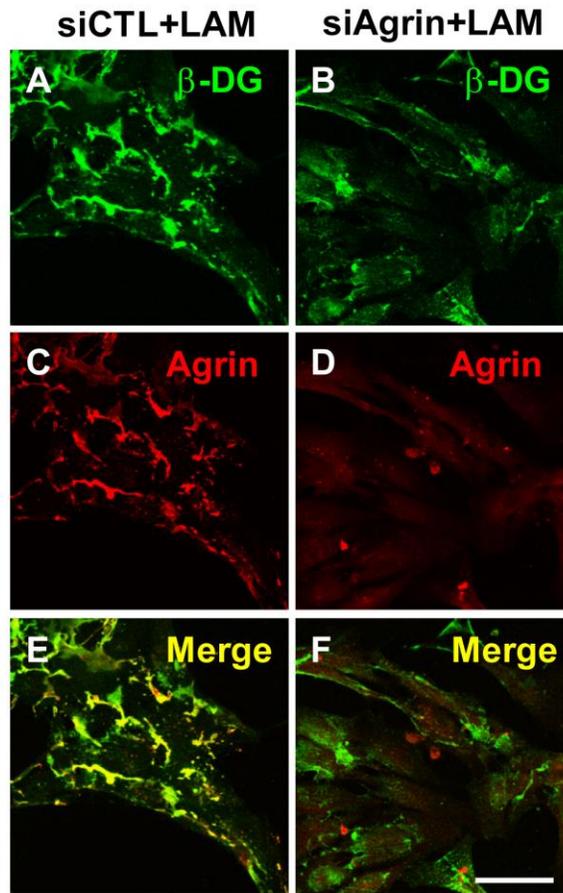
G.
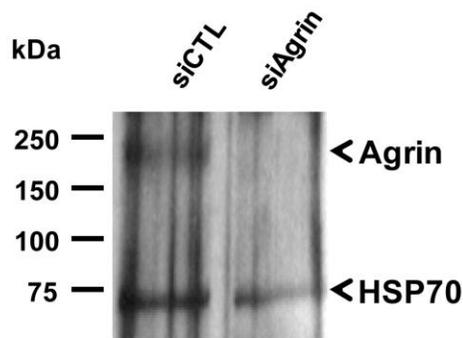
H.
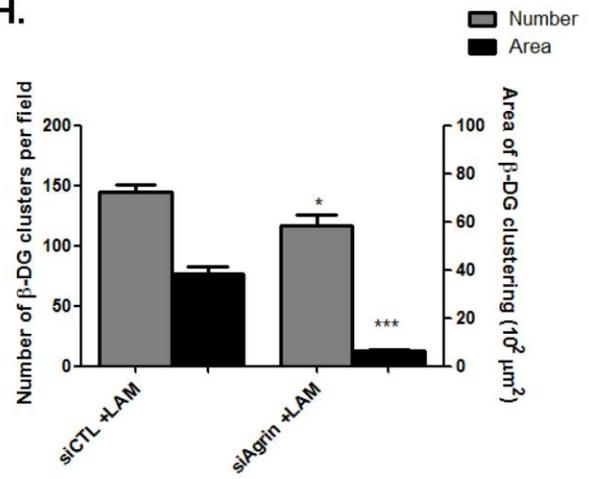
silencing (Fig. 3.2D). Together these results suggest a crucial role for endogenous agrin in the consolidation of the laminin-induced β-DG clusters. Laminin clustering might be a dynamic process whereby small dot-like structures are consolidated first into linear arrays and second into complex plaque-like clusters.

3.3.2 Matrigel^{TM} induces a laminin-like effect on β-DG and AQP4 clustering which can be prevented by laminin-γ1 antibody or DG silencing

We previously established that exogenous laminin-1 was able to induce β-DG and AQP4 clustering after 12 hours treatment. Interestingly, we found that neither exogenous C-agrin 0,0, C-agrin 4,8 nor fibronectin could induce a similar clustering (23,73). Astrocyte cultures were therefore incubated with other ECM molecules, such as collagen IV and Matrigel^{TM} to determine their effects on β-DG and AQP4 distribution. We observed that the immunoreactivity of both β-DG and AQP4 was diffusively distributed within both control (-LAM) and collagen IV treated astrocytes (Fig. 3.3A, C, F, H). In contrast, when astrocytes were cultured in presence of Matrigel^{TM} we observed a laminin-like clustering of β-DG and AQP4 (Fig. 3.3B, G, E, and J). When quantified, the clustering of both β-DG and AQP4 was higher in astrocytes treated with Matrigel^{TM} compared to astrocytes treated with laminin alone (Fig. 3.3P and O). These results suggest that Matrigel^{TM} is more efficient in the induction of β-DG and AQP4 clustering compared to laminin-1. Since Matrigel^{TM} is an artificial basal lamina mixture composed of 50% laminin and 30% collagen, we decided to test whether collagen IV, which is the most abundant collagen present around blood vessels, could explain the greater Matrigel^{TM}-induced clustering compared to laminin-1. Astrocytes were cotreated with laminin-1 and collagen IV and the distribution of β-DG and AQP4 was assessed by immunofluorescence. Interestingly, no difference was observed compared to laminin alone suggesting that collagen IV is not one of the Matrigel^{TM} components participating to the laminin-induced clustering of β-DG and AQP4.

To investigate further the molecular mechanisms determining the effect of Matrigel^{TM} compared to laminin, we decided to incubate astrocytes with an antibody directed against LE1 domain of laminin-γ1 and purified as previously described (75). This domain of laminin γ1 has been identified as a nidogen-binding site that is crucial for ECM morphogenesis (35,76-79).
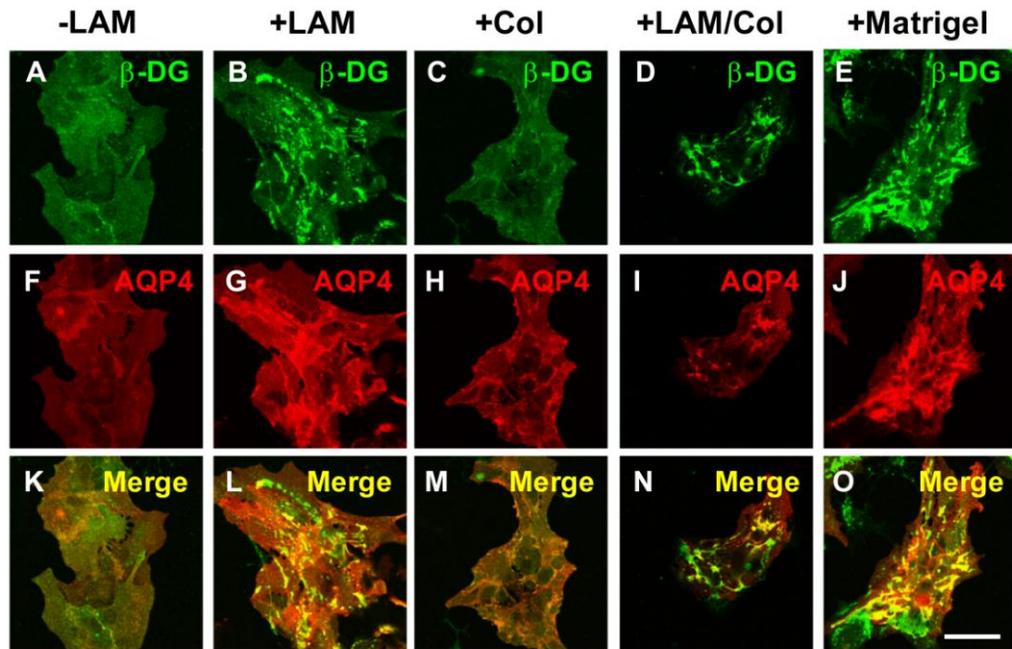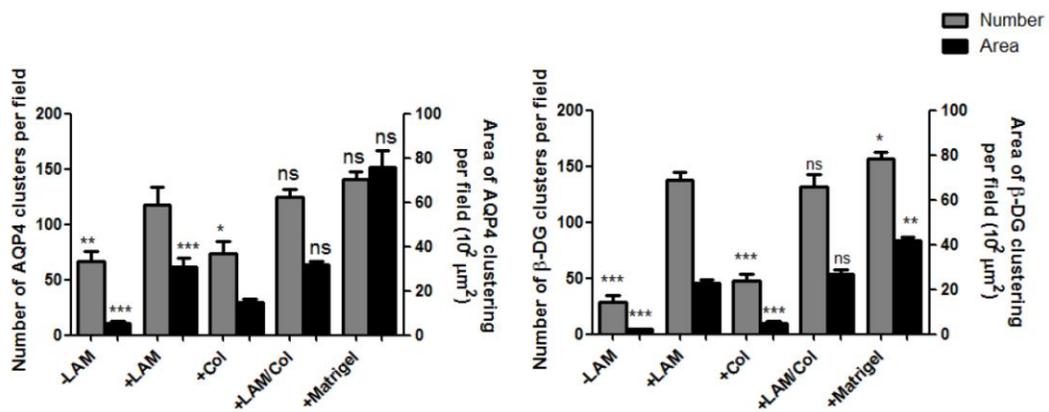
Figure 3.3 Laminin and Matrigel^{TM} treatments induce the clustering of β-DG and AQP4.
(A-O) Rat hippocampal astrocytes incubated in the absence (**A, F and K**) or the presence of 20 nM laminin (**B, G and L**), 30 nM collagen IV (**C, H and M**), 20 nM laminin and 30 nM collagen IV (**D, I and N**) or 40 μg/ml Matrigel^{TM} (**E, J and O**) were double immunolabeled for β-DG **(A-E)** and AQP4 **(F-J)**. Scale bar, 30 μm. **P and Q.** Quantitative analysis of AQP4 (**P**) and β-DG (**Q**) clustering upon laminin, laminin/collagen IV or Matrigel^{TM} treatment. The histograms represent the mean number of clusters ±SE and surface area of clusters ±SE in astrocyte cultures treated with laminin, laminin/collagen IV or Matrigel^{TM} for 8 hours from three experiments. All quantifications were performed on 15 fields acquired randomly from each experiment.

Figure 3.4 shows that coincubation of astrocytes with laminin-γ1 antibodies completely block the laminin-induced clustering of β-DG and AQP4 (Fig. 3.4B and E). However, we observed that astrocytes coincubated with Matrigel^{TM} and laminin-γ1 antibodies were still expressing residual β-DG and AQP4 clustering (Fig. 3.4C and F). Together these results suggest that Matrigel^{TM} effect on β-DG and AQP4 is mainly mediated by laminin-γ1 containing laminins present in the mixture but that other molecular determinants are present in Matrigel^{TM} and are responsible of the remaining β-DG and AQP4 clustering.

Finally, to investigate the role of laminin-binding to DG in Matrigel^{TM} effect, astrocyte cultures were transfected with siDAG1 which leads to an efficient silencing of DG (Fig. 3.5J). The distribution of β-DG and AQP4 was assessed by immunofluorescence following the addition of laminin-1 or Matrigel^{TM} in the culture medium. Figure 3.5 shows that DG silencing prevented both laminin- and Matrigel^{TM} -induced clustering of β-DG and AQP4 (Fig. 3.5B, E, C, F and K). These results confirm our previous observation that DG silencing prevented laminin-induced β-DG and AQP4 clustering (23) and suggest here that the Matrigel^{TM} effect on β-DG and AQP4 is mediated by DG.

The different properties of AQP4 isoforms M1 and M23 to form orthogonal array of particles (OAPs) have been extensively studied in the last few years. Current consensus implicates M23 as being the principal isoform triggering OAPs formation and M1 being a more mobile isoform (80-89). It also has been proposed that the ratio of M23/M1 would determine the extent of OAPs density and that exogenous agrin could play a role in this ratio. Indeed Noell at al.(60) have shown that C-agrin 4,8 induces an increase of M23 expression compared to M1 and leads to a high OAPs density in cultured astrocytes. We therefore investigated the expression of the AQP4 isoforms M1 and M23 in astrocytes treated with laminin-1 and Matrigel^{TM} using RT-PCR. The expression of the two AQP4 isoforms did not differ between the different treatments. Figure 3.6 shows that the treatments with laminin, Matrigel^{TM} or the agrin siRNA did not induce any change in either M1 or M23 mRNA (Fig. 3.6A) and protein expression (Fig. 3.6B). The laminin treated, Matrigel^{TM}-treated and the agrin knock-down astrocytes with or without laminin treatment displayed the same expression of the AQP4 isoforms as the control untreated astrocytes. Only, the brain presented a higher expression of M23 compared to M1 confirming previous results (60). These findings demonstrate that none of the ECM molecules tested here were able to change the M1/M23 expression ratio in astrocytes.

Figure 3.4 Laminin γ1 antibody prevents the laminin- and Matrigel^{TM} -induced clustering of β-DG and AQP4. (A-I) Rat hippocampal astrocytes incubated with 20 nM laminin (**A, B, D, E, G** and **H**) or 40 µg/ml Matrigel^{TM} (**C, F** and **I**) in the absence (**A, D** and **G**) or the presence of laminin g1 antibodies (**B, C, E, F, H** and **I**) were double immunolabeled for β-DG (**A-C**) and AQP4 (**D-F**). Scale bar, 30 µm. **J and K.** Quantitative analysis of the laminin- and Matrigel^{TM} -induced clustering of AQP4 (**J**) and β-DG (**K**) in the absence (**Preimmune**) or the presence of laminin γ1 antibodies (**Laminin γ1 IgG**). The histograms represent the mean number of clusters ±SE and surface area of clusters ±SE in astrocyte cultures treated with laminin or Matrigel^{TM} for 8 hours in absence or presence laminin g1 antibodies from three experiments. All quantifications were performed on 15 fields selected at random from each experiment.
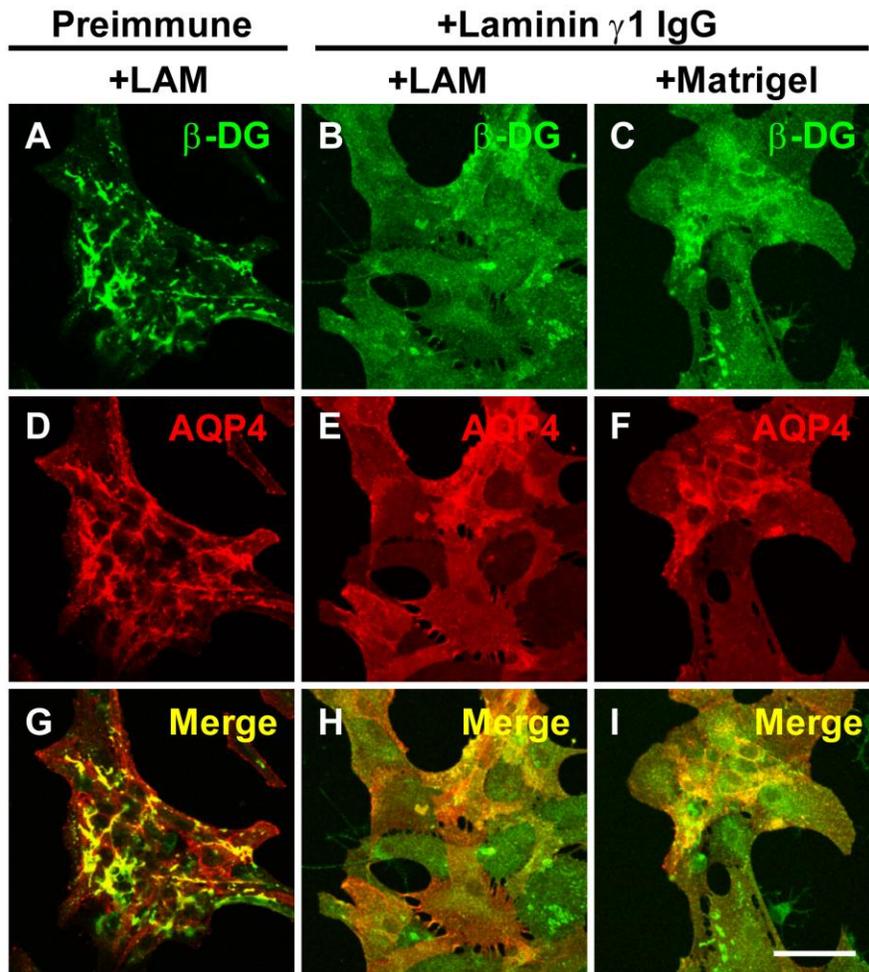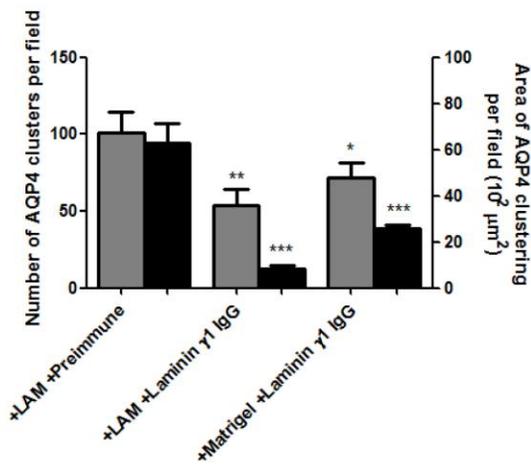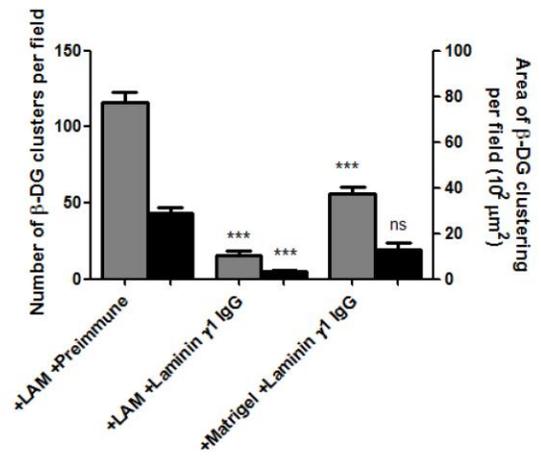
Figure 3.5 Dystroglycan silencing prevents the laminin- and Matrigel^{TM} -induced clustering of β-DG and AQP4. (A-I) Rat hippocampal astrocytes transfected with siCTL **(A, D** and **G)** or siDAG1 transfected **(B, C, E, F, H** and **I)** and incubated with 20 nM laminin **(A, B, D, E, G** and **H)** or 40 μg/ml Matrigel^{TM} **(C, F** and **I)** were double immunolabeled for β-DG **(A-C)** and AQP4 **(D-F)**. Scale bar, 30 μm. **J**. Astrocytes were transfected with siCTL or siDAG1 for a duration of 2 days. Proteins were harvested in extraction buffer. Immunoblots were probed for HSP70, β-DG and AQP4. Representative blots from three independent experiments are shown. **K**. Quantitative analysis of the laminin- and Matrigel^{TM} -induced clustering of AQP4. The histograms represent the mean number of clusters ±SEM and surface area of clusters ±SEM in astrocyte cultures treated with laminin or Matrigel^{TM} for 8 hours after transfection with siCTL or siDAG1 from three experiments. All quantifications were performed on 15 fields acquired randomly from each experiment.

95
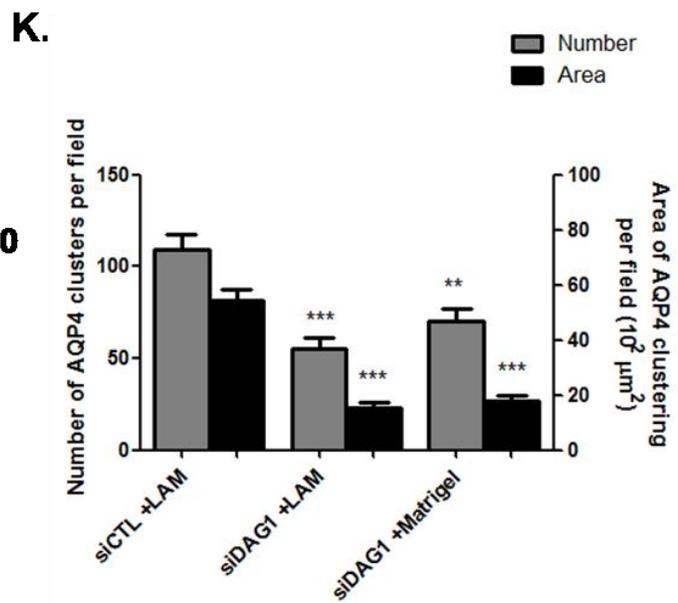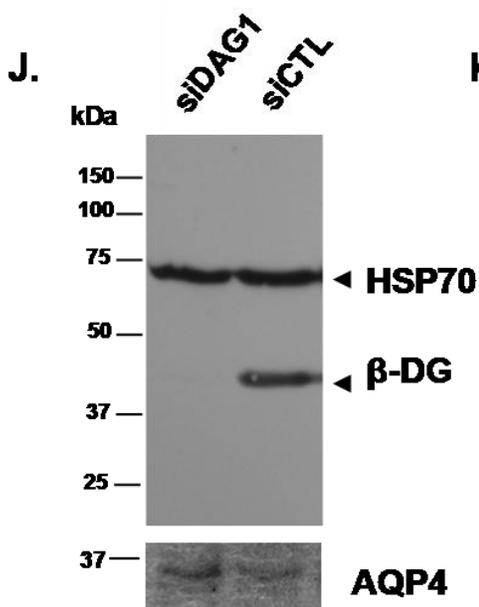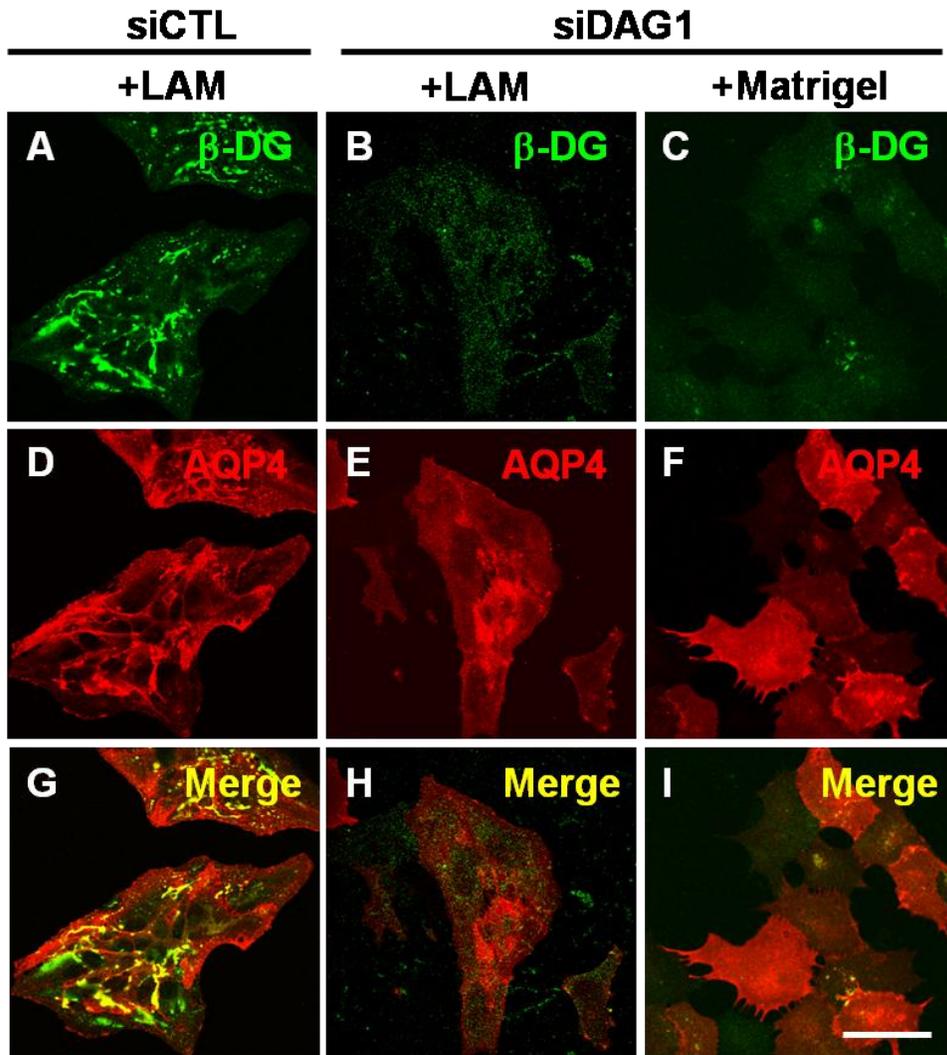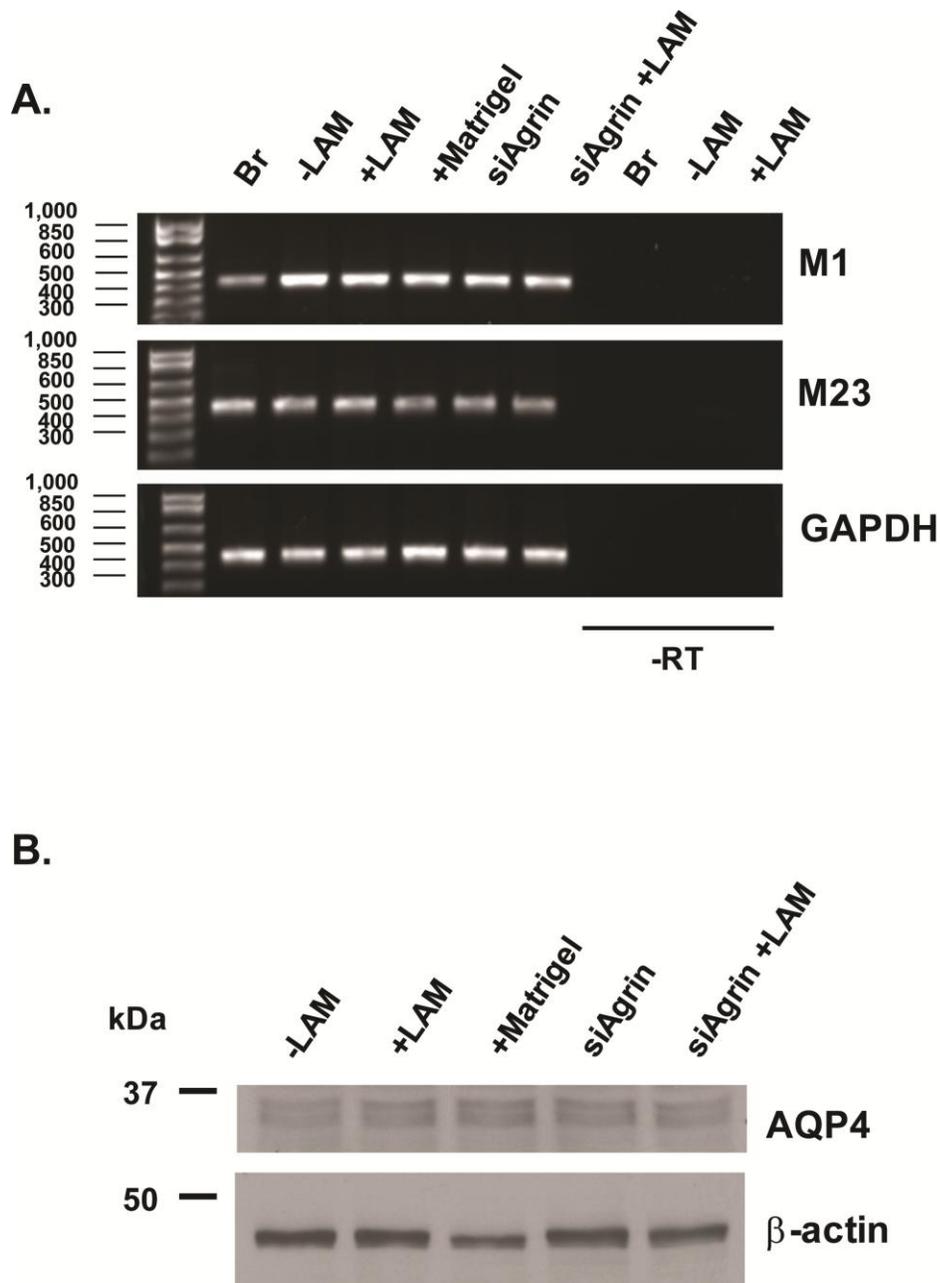
Figure 3.6 Expression of M1 and M23 isoforms of AQP4 in mouse brain and mouse astrocytes transfected with siCTL or siAgrin and treated with laminin or Matrigel^{TM} A. RT-PCR of M1 and M23 isoforms of AQP4 shows that the 2 transcripts are expressed in similar amount in the different conditions tested in mouse astrocytes. However, in mouse brain, M23 isoform is expressed at an higher level compare to M1. **B.** Astrocytes were transfected with siCTL or siAgrin for a duration of 2 days. Cells were treated or not with laminin or Matrigel Proteins were harvested in extraction buffer. Immunoblots were probed for β-DG and AQP4. Representative blots from three independent experiments are shown.

3.3.3 Laminin induces a decrease in cell swelling upon hypoosmotic shock

Noell et al. (60) showed that exogenous C-agrin 4,8 was able to induce an increase in water permeability in astrocytes. Here, we asked whether ECM molecules, specifically laminin and collagen, have an effect on AQP4-mediated water transport in astrocytes. Cultured astrocytes were loaded with calcein and brought into a flow through chamber for few minutes at constant flow in isotonic CSF (330 mOsm) to allow equilibration. After 120 s of acquisition by 2-photon microscopy, the solution was switched to hypotonic CSF (220 mOsm) for another 120 s before returning to isotonic CSF again. Under normal growth conditions without any ECM molecule, the calcein fluorescence intensity decreased by 20-25% (Fig. 3.7B), indicating a volume increase in the imaged cell (Fig. 3.7A), and then returned to the initial intensity when cells returned to isotonic conditions. However, laminin-treated astrocytes subjected to the same experimental paradigm, presented a decrease in cell swelling upon hypoosmotic shock. The decrease in calcein fluorescence in hypotonic condition is approximately 10-15% under laminin treatment (Fig. 3.7C). The clustering of AQP4 was assessed after the water transport measurement by immunofluorescence (Appendix A). To determine whether laminin could influence the initial cell volume before any hypoosomotic shock, we decided to acquire z-scans of the calcein signal in both control and laminin-treated astrocytes. Appendix B shows that the cell volume was similar in both condition confirming our precedent observation that laminin has minimal effect on the morphology/volume of the cells (23). Interestingly, the collagen IV treatment did not show any effect on the swelling of astrocytes in comparison to control astrocytes suggesting that the effect observed with laminin was specific to a laminin receptor and not due to non specific alterations associated to the ECM molecules used (Fig. 3.7D).

When we coated the coverslips with laminin-1 prior to plating the astrocytes (data not shown), we obtained similar results as the laminin treatment on top of the cells confirming again the specific implication of laminin binding to a receptor. We have previously shown that DG is the laminin receptor involved in the regulation of the laminin-induced clustering of DG and AQP4. We therefore silenced DG in astrocytes and assessed the water transport of these cells after treatment with laminin. Figure 3.7E shows that the silencing of DG rescues the decrease in cell swelling induced by laminin upon hypoosmotic shock supporting a role for the binding of

Figure 3.7 Laminin treatment induces a decrease cell swelling upon hypoosmotic shock. (A) Calcein-loaded astrocytes in the x-y plane were recorded from 0 to 300s after incubation with (**+LAM**) or without (**-LAM**) 20 nM laminin. **B and C.** Mean trace of recordings from a time series of 30 calcein-loaded astrocytes treated with (**+LAM**) or without (**-LAM**) 20 nM laminin. The buffer solution was changed from isotonic to hypotonic and from hypotonic to isotonic at 120 and 240s, respectively (dotted line). **D and E.** Mean trace of recordings from a time series of 30 calcein-loaded astrocytes treated with (**+LAM**) or without (**-LAM**) 20 nM laminin, 30 nM collagen IV (**+Col**) or 20 nM laminin after silencing of DG (**siDAG1+LAM**). The buffer solution was changed from isotonic to hypotonic and from hypotonic to isotonic at 120 and 240s, respectively (dotted line).

A.

cal | cal | cal — **-LAM**
0s | 150s | 300s

cal | cal | cal — **+LAM**
0s | 150s | 300s

t

B.

300 mOsm | 250 mOsm | 300 mOsm

Normalized intensity

● -LAM

Time (s)

C.

300 mOsm | 250 mOsm | 300 mOsm

Normalized intensity

○ +LAM

Time (s)

D.

● -LAM
● +Col

Normalized intensity

Time (s)

E.

○ +LAM
▲ siDAG1 +LAM

Normalized intensity

Time (s)
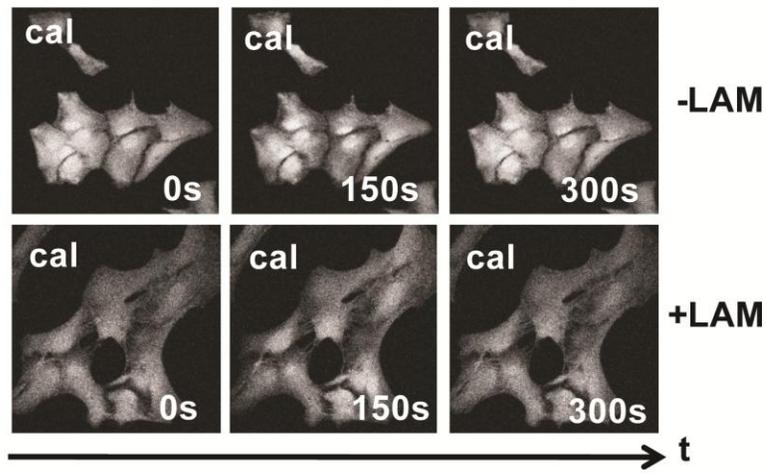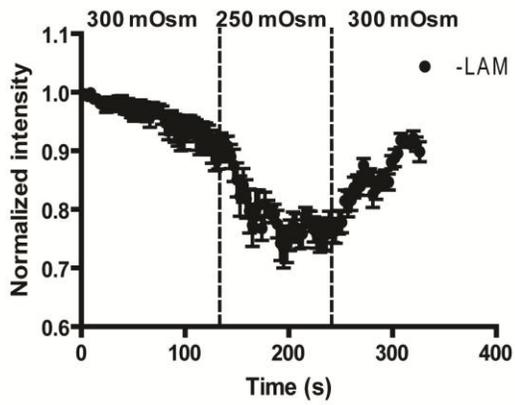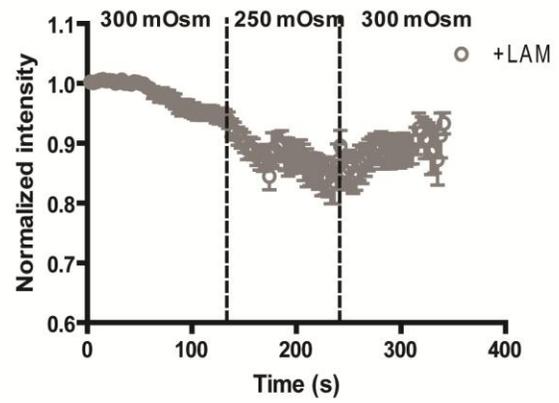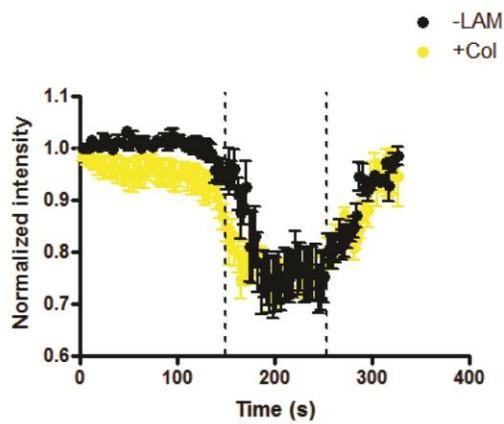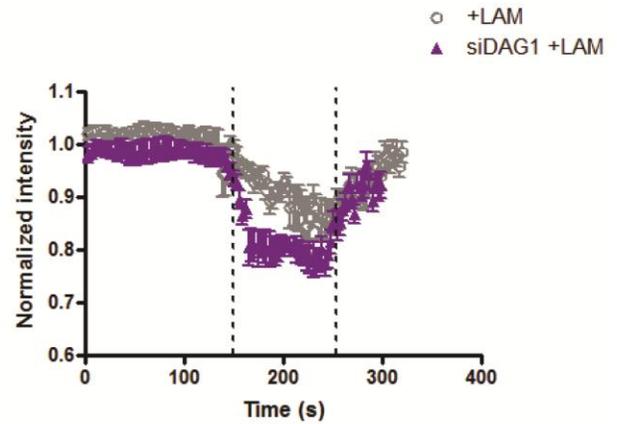
laminin to DG in this process. In addition to the volume changes observed, the exchange rate of water was faster in laminin-treated DG knock-down astrocytes compare to the laminin-treated controls. This is reflected by the steeper slope of the swelling curve for cells deficient for DG (Fig. 3.7E). These results show that laminin binding to DG regulates the rate of water transport across the membrane of cultured astrocytes.

3.4 Discussion

The present study has provided three main findings: first, that endogenous agrin is recruited in the laminin-induced clusters of β-DG, where it plays an important role in the morphogenesis of the clusters. Second that the artificial ECM mixture, Matrigel^{TM}, induces a clustering of β-DG and AQP4 in the same manner as laminin. The effect is stronger and involves more than laminin-γ1-containing laminins as antibodies against this chain do not totally prevent the Matrigel^{TM}-induced clustering. However this effect was revealed to be DG-dependent since silencing of DG expression prevents the Matrigel^{TM}-induced clustering of AQP4. Together, this suggests that another laminin containing LG4/5 but not LE1 domain is present in Matrigel^{TM} and is responsible for DG clustering. Laminins 5, 12, 14 and 15 could be such potentiators (90). Considering the higher affinity that α-DG has for the α2 chain, present in laminin 12, as well as the lack of self-polymerization of α3 and α4 chains also present in laminin 12, laminin 12 might be the best possibility (91-95). Finally, this study shows that exogenous laminin-1 treatment decreased the swelling capacity of cultured astrocytes under hypotonic conditions.

Studies conducted previously by other groups have described agrin as being important within CNS for the integrity of the blood-brain barrier (43,96,97) and our results confirm these findings. It has also been suggested that agrin plays a pivotal role in the assembly of OAPs in the endfoot membranes of astrocytes (61). The agrin A0B0 variant has been shown to lack any effect on AQP4 expression levels or water transport activity (60) even though it is able to induce increased insertion of AQP4 in to the plasma membrane. The agrin A4B8 variant has been shown to increase the level of M23 isoform of AQP4 compared to M1 isoform and that led to an increased swelling capacity of astrocytes. In our laboratory, we have shown that exogenous agrins A0B0 and A4B8 are both unable to potentiate the effect of laminin on the clustering of

AQP4. Here, our study investigated further the role of exogenous and endogenous agrin in AQP4 expression and distribution and showed that endogenous agrin is crucial in the stabilization of DG and therefore AQP4 clustering without playing a role in M1 or M23 isoforms expression.

The role of agrin in the laminin-induced clustering of DG might be similar in nature to that of perlecan, which has been suggested to act as a linker between DG and laminin (24,29). In addition, these results correlate well with those of previous studies suggesting that DG mediates the assembly of laminin at agrin clusters (25) and that agrin facilitates the laminin polymerization (98). Alternatively, agrin could play the role of linker between the sulfatides present at the cell surface and laminin (98-100). These findings that in absence of agrin AQP4 immunoreactivity is randomly distributed across the surface of the cell (62) support the above results. In addition, our data could explain why agrin-null mouse and wild-type mice differ neither in AQP4 immunoreactivity at the astrocyte endfeet nor M1/M23 expression ratio but differ in the OAPs density (47,61).

Several studies presented evidences suggesting that AQP4 is mainly responsible for rapid water movement into and out of the brain (101). AQP4 knockdown in cultured astrocytes significantly contributed to protection against water influx during hypoxia, suggesting a dominant role of AQP4 in edema formation (102,103). Here, we showed that the presence of laminin-1 in the culture medium of astrocytes induced a slower and smaller volume increase after hypotonic stimulation. This effect was specific to laminin binding to DG since DG silencing rescued this effect. In addition, the plating of astrocytes on laminin-1 or the treatment of laminin on top of astrocytes led to similar results suggesting that the effect was not due to an ECM "encaging" of the cells. Collagen VI treatment did not induce any change in the swelling capacity of the astrocytes confirming again the specificity of laminin. It is difficult to determine with certainty if this effect is strictly dependent on AQP4 activity since astrocytes with no expression of AQP4 do not present a swelling comparable to the control cells (data not shown).

According to Neveux I. et al., (65), laminin and fibronectin treatment on myocytes triggered an earlier onset of a larger hypotonic-induced Volume-Sensitive Osmolyte Anion Channels (VSOACs) current which lead to an earlier Regulatory Volume Decrease (RVD). Similarly, it could be hypothesized that laminin treatment triggers an earlier RVD in astrocytes which could explain the observed reduction in water swelling. Interestingly, Noell et al. (60) have shown that exogenous agrin A4B8 was able to induce a reverse effect by increasing the

volume increase of astrocytes following hypoosmotic shock. They suggested that this effect was a result of the upregulation of M23 expression compared to M1 and that M23 isoform was therefore the more conductive water channel. However, some controversy exists regarding whether the two AQP4 isoforms differ in their activities. It has been proposed that M23 might be more efficient than M1 but also that both isoforms have the same water transport capacity (82,86,104,105).

From the well-known distribution of AQP4 *in vivo* and the precedent studies, it could be hypothesized that endogenous and exogenous agrin have a role in the insertion and expression of AQP4 which leads to stabilized clusters in the presence of laminin. However, it is laminin that localizes AQP4 into specific membrane domains. The enrichment of AQP4 at the perivascular endfeet of astrocytes that is observed in the brain may therefore be the result of the combined effects of both agrin and laminin. In what appears to be a paradox, our results also indicate that the localization of AQP4 to astrocyte endfeet may be accompanied by concomitant suppression of channel conductivity. We propose that this may represent a protective mechanism that serves *in vivo* to insulate the brain from osmotic variations in the bloodstream under normal circumstances. However, this suppression may be released in response to stress cues resulting from the occurrence of pathological states, thereby allowing for rapid rectification of osmotic imbalances via the perivascular population of AQP4 channels. Alternatively, this result may indicate that our chosen model inadequately reflects the complexities of the regulatory interactions that may take place in the intact brain, which may vary on a domain-by-domain basis. Whereas astrocytes come into contact with laminin at their endfoot regions only *in vivo*, the entire dorsal surfaces of the cells were available to laminin in this study, which may have resulted in there having been an initial overabundance of AQP4 at the cell surface. As excessive AQP4 accumulation may be deleterious to cell survival, as has been demonstrated to be the case in cytotoxic edema; the cells may have subsequently down-regulated AQP4 amounts, leading to a reduction in overall permeability.

3.5 References

1. Manley, G. T., Fujimura, M., Ma, T., Noshita, N., Filiz, F., Bollen, A. W., Chan, P., and Verkman, A. S. (2000) *Nat Med* **6**, 159-163
2. Papadopoulos, M. C., and Verkman, A. S. (2005) *J Biol Chem* **280**, 13906-13912
3. Yang, B., Zador, Z., and Verkman, A. S. (2008) *J Biol Chem* **283**, 15280-15286
4. Moore, S. A., Saito, F., Chen, J., Michele, D. E., Henry, M. D., Messing, A., Cohn, R. D., Ross-Barta, S. E., Westra, S., Williamson, R. A., Hoshi, T., and Campbell, K. P. (2002) *Nature* **418**, 422-425
5. Ibraghimov-Beskrovnaya, O., Ervasti, J. M., Leveille, C. J., Slaughter, C. A., Sernett, S. W., and Campbell, K. P. (1992) *Nature* **355**, 696-702
6. Amiry-Moghaddam, M., Otsuka, T., Hurn, P. D., Traystman, R. J., Haug, F. M., Froehner, S. C., Adams, M. E., Neely, J. D., Agre, P., Ottersen, O. P., and Bhardwaj, A. (2003) *Proc Natl Acad Sci U S A* **100**, 2106-2111
7. Vajda, Z., Pedersen, M., Fuchtbauer, E. M., Wertz, K., Stodkilde-Jorgensen, H., Sulyok, E., Doczi, T., Neely, J. D., Agre, P., Frokiaer, J., and Nielsen, S. (2002) *Proc Natl Acad Sci U S A* **99**, 13131-13136
8. Bandtlow, C. E., and Zimmermann, D. R. (2000) *Physiol Rev* **80**, 1267-1290
9. Hallmann, R., Horn, N., Selg, M., Wendler, O., Pausch, F., and Sorokin, L. M. (2005) *Physiol Rev* **85**, 979-1000
10. Aumailley, M., Bruckner-Tuderman, L., Carter, W. G., Deutzmann, R., Edgar, D., Ekblom, P., Engel, J., Engvall, E., Hohenester, E., Jones, J. C., Kleinman, H. K., Marinkovich, M. P., Martin, G. R., Mayer, U., Meneguzzi, G., Miner, J. H., Miyazaki, K., Patarroyo, M., Paulsson, M., Quaranta, V., Sanes, J. R., Sasaki, T., Sekiguchi, K., Sorokin, L. M., Talts, J. F., Tryggvason, K., Uitto, J., Virtanen, I., von der Mark, K., Wewer, U. M., Yamada, Y., and Yurchenco, P. D. (2005) *Matrix Biol* **24**, 326-332
11. Miner, J. H., and Yurchenco, P. D. (2004) *Annu Rev Cell Dev Biol* **20**, 255-284
12. Hagg, T., Portera-Cailliau, C., Jucker, M., and Engvall, E. (1997) *Brain Res* **764**, 17-27
13. Lom, B., and Hockberger, P. E. (1997) *J Neurobiol* **33**, 72-84
14. Wagner, S., and Gardner, H. (2000) *Neurosci Lett* **284**, 105-108
15. Jucker, M., Tian, M., Norton, D. D., Sherman, C., and Kusiak, J. W. (1996) *Neuroscience* **71**, 1153-1161
16. Tian, M., Jacobson, C., Gee, S. H., Campbell, K. P., Carbonetto, S., and Jucker, M. (1996) *Eur J Neurosci* **8**, 2739-2747
17. Villanova, M., Malandrini, A., Sabatelli, P., Sewry, C. A., Toti, P., Torelli, S., Six, J., Scarfo, G., Palma, L., Muntoni, F., Squarzoni, S., Tosi, P., Maraldi, N. M., and Guazzi, G. C. (1997) *Acta Neuropathol* **94**, 567-571
18. Villanova, M., Sewry, C., Malandrini, A., Toti, P., Muntoni, F., Merlini, L., Torelli, S., Tosi, P., Maraldi, N. M., and Guazzi, G. C. (1997) *J Submicrosc Cytol Pathol* **29**, 409-413
19. Koch, M., Olson, P. F., Albus, A., Jin, W., Hunter, D. D., Brunken, W. J., Burgeson, R. E., and Champliaud, M. F. (1999) *J Cell Biol* **145**, 605-618
20. Colognato, H., and Yurchenco, P. D. (2000) *Dev Dyn* **218**, 213-234
21. Colognato, H., Winkelmann, D. A., and Yurchenco, P. D. (1999) *J Cell Biol* **145**, 619-631
22. Cohen, M. W., Jacobson, C., Yurchenco, P. D., Morris, G. E., and Carbonetto, S. (1997) *J Cell Biol* **136**, 1047-1058

23. Noel, G., Tham, D. K., and Moukhles, H. (2009) *J Biol Chem* **284**, 19694-19704
24. Henry, M. D., Satz, J. S., Brakebusch, C., Costell, M., Gustafsson, E., Fassler, R., and Campbell, K. P. (2001) *J Cell Sci* **114**, 1137-1144
25. Tremblay, M. R., and Carbonetto, S. (2006) *J Biol Chem* **281**, 13365-13373
26. Montanaro, F., Lindenbaum, M., and Carbonetto, S. (1999) *J Cell Biol* **145**, 1325-1340
27. Tsiper, M. V., and Yurchenco, P. D. (2002) *J Cell Sci* **115**, 1005-1015
28. Weir, M. L., Oppizzi, M. L., Henry, M. D., Onishi, A., Campbell, K. P., Bissell, M. J., and Muschler, J. L. (2006) *J Cell Sci* **119**, 4047-4058
29. Kanagawa, M., Michele, D. E., Satz, J. S., Barresi, R., Kusano, H., Sasaki, T., Timpl, R., Henry, M. D., and Campbell, K. P. (2005) *FEBS Lett* **579**, 4792-4796
30. Williamson, R. A., Henry, M. D., Daniels, K. J., Hrstka, R. F., Lee, J. C., Sunada, Y., Ibraghimov-Beskrovnaya, O., and Campbell, K. P. (1997) *Hum Mol Genet* **6**, 831-841
31. Barresi, R., Michele, D. E., Kanagawa, M., Harper, H. A., Dovico, S. A., Satz, J. S., Moore, S. A., Zhang, W., Schachter, H., Dumanski, J. P., Cohn, R. D., Nishino, I., and Campbell, K. P. (2004) *Nat Med* **10**, 696-703
32. Miner, J. H., and Li, C. (2000) *Dev Biol* **217**, 278-289
33. Yurchenco, P. D., Tsilibary, E. C., Charonis, A. S., and Furthmayr, H. (1985) *J Biol Chem* **260**, 7636-7644
34. Kvansakul, M., Hopf, M., Ries, A., Timpl, R., and Hohenester, E. (2001) *EMBO J* **20**, 5342-5346
35. Mayer, U., Nischt, R., Poschl, E., Mann, K., Fukuda, K., Gerl, M., Yamada, Y., and Timpl, R. (1993) *EMBO J* **12**, 1879-1885
36. Ries, A., Gohring, W., Fox, J. W., Timpl, R., and Sasaki, T. (2001) *Eur J Biochem* **268**, 5119-5128
37. Battaglia, C., Mayer, U., Aumailley, M., and Timpl, R. (1992) *Eur J Biochem* **208**, 359-366
38. Hopf, M., Gohring, W., Kohfeldt, E., Yamada, Y., and Timpl, R. (1999) *Eur J Biochem* **259**, 917-925
39. Aumailley, M., Wiedemann, H., Mann, K., and Timpl, R. (1989) *Eur J Biochem* **184**, 241-248
40. Fox, J. W., Mayer, U., Nischt, R., Aumailley, M., Reinhardt, D., Wiedemann, H., Mann, K., Timpl, R., Krieg, T., Engel, J., and et al. (1991) *EMBO J* **10**, 3137-3146
41. Henry, M. D., and Campbell, K. P. (1998) *Cell* **95**, 859-870
42. Urabe, N., Naito, I., Saito, K., Yonezawa, T., Sado, Y., Yoshioka, H., Kusachi, S., Tsuji, T., Ohtsuka, A., Taguchi, T., Murakami, T., and Ninomiya, Y. (2002) *Arch Histol Cytol* **65**, 133-143
43. Barber, A. J., and Lieth, E. (1997) *Dev Dyn* **208**, 62-74
44. Kroger, S. (1997) *Mol Cell Neurosci* **10**, 149-161
45. Hering, H., and Kroger, S. (1999) *Dev Biol* **214**, 412-428
46. Koulen, P., Honig, L. S., Fletcher, E. L., and Kroger, S. (1999) *Eur J Neurosci* **11**, 4188-4196
47. Stone, D. M., and Nikolics, K. (1995) *J Neurosci* **15**, 6767-6778
48. Denzer, A. J., Schulthess, T., Fauser, C., Schumacher, B., Kammerer, R. A., Engel, J., and Ruegg, M. A. (1998) *EMBO J* **17**, 335-343
49. Bose, C. M., Qiu, D., Bergamaschi, A., Gravante, B., Bossi, M., Villa, A., Rupp, F., and Malgaroli, A. (2000) *J Neurosci* **20**, 9086-9095
50. Serpinskaya, A. S., Feng, G., Sanes, J. R., and Craig, A. M. (1999) *Dev Biol* **205**, 65-78

51. Ferns, M., Hoch, W., Campanelli, J. T., Rupp, F., Hall, Z. W., and Scheller, R. H. (1992) *Neuron* **8**, 1079-1086
52. Gesemann, M., Brancaccio, A., Schumacher, B., and Ruegg, M. A. (1998) *J Biol Chem* **273**, 600-605
53. Denzer, A. J., Gesemann, M., Schumacher, B., and Ruegg, M. A. (1995) *J Cell Biol* **131**, 1547-1560
54. Burgess, R. W., Skarnes, W. C., and Sanes, J. R. (2000) *J Cell Biol* **151**, 41-52
55. Sugiyama, J., Bowen, D. C., and Hall, Z. W. (1994) *Neuron* **13**, 103-115
56. Campanelli, J. T., Roberds, S. L., Campbell, K. P., and Scheller, R. H. (1994) *Cell* **77**, 663-674
57. Gee, S. H., Montanaro, F., Lindenbaum, M. H., and Carbonetto, S. (1994) *Cell* **77**, 675-686
58. Nicchia, G. P., Cogotzi, L., Rossi, A., Basco, D., Brancaccio, A., Svelto, M., and Frigeri, A. (2008) *J Neurochem*
59. Nicchia, G. P., Rossi, A., Nudel, U., Svelto, M., and Frigeri, A. (2008) *Glia* **56**, 869-876
60. Noell, S., Fallier-Becker, P., Beyer, C., Kroger, S., Mack, A. F., and Wolburg, H. (2007) *Eur J Neurosci* **26**, 2109-2118
61. Noell, S., Fallier-Becker, P., Deutsch, U., Mack, A. F., and Wolburg, H. (2009) *Cell Tissue Res* **337**, 185-195
62. Warth, A., Kroger, S., and Wolburg, H. (2004) *Acta Neuropathol* **107**, 311-318
63. Wolburg, H., Noell, S., Wolburg-Buchholz, K., Mack, A., and Fallier-Becker, P. (2009) *Neuroscientist* **15**, 180-193
64. Guadagno, E., and Moukhles, H. (2004) *Glia* **47**, 138-149
65. Neveux, I., Doe, J., Leblanc, N., and Valencik, M. L. *Am J Physiol Cell Physiol*
66. Benfenati, V., Nicchia, G. P., Svelto, M., Rapisarda, C., Frigeri, A., and Ferroni, S. (2007) *J Neurochem* **100**, 87-104
67. Han, Z., Wax, M. B., and Patil, R. V. (1998) *J Biol Chem* **273**, 6001-6004
68. Hibino, H., and Kurachi, Y. (2007) *Eur J Neurosci* **26**, 2539-2555
69. Huber, V. J., Tsujita, M., Yamazaki, M., Sakimura, K., and Nakada, T. (2007) *Bioorg Med Chem Lett* **17**, 1270-1273
70. Huber, V. J., Tsujita, M., Kwee, I. L., and Nakada, T. (2009) *Bioorg Med Chem* **17**, 418-424
71. Huber, V. J., Tsujita, M., and Nakada, T. (2009) *Bioorg Med Chem* **17**, 411-417
72. Huber, V. J., Tsujita, M., and Nakada, T. (2008) *Bioorg Med Chem*
73. Noel, G., Belda, M., Guadagno, E., Micoud, J., Klocker, N., and Moukhles, H. (2005) *J Neurochem* **94**, 691-702
74. Tournell, C. E., Bergstrom, R. A., and Ferreira, A. (2006) *Neuroscience* **141**, 1327-1338
75. Bonner, J., and O'Connor, T. P. (2001) *J Neurosci* **21**, 9782-9791
76. Gerl, M., Mann, K., Aumailley, M., and Timpl, R. (1991) *Eur J Biochem* **202**, 167-174
77. Ekblom, P., Ekblom, M., Fecker, L., Klein, G., Zhang, H. Y., Kadoya, Y., Chu, M. L., Mayer, U., and Timpl, R. (1994) *Development* **120**, 2003-2014
78. Poschl, E., Mayer, U., Stetefeld, J., Baumgartner, R., Holak, T. A., Huber, R., and Timpl, R. (1996) *EMBO J* **15**, 5154-5159
79. Kadoya, Y., Salmivirta, K., Talts, J. F., Kadoya, K., Mayer, U., Timpl, R., and Ekblom, P. (1997) *Development* **124**, 683-691
80. Crane, J. M., Bennett, J. L., and Verkman, A. S. (2009) *J Biol Chem*
81. Crane, J. M., and Verkman, A. S. (2009) *J Cell Sci* **122**, 813-821

82. Fenton, R. A., Moeller, H. B., Zelenina, M., Snaebjornsson, M. T., Holen, T., and Macaulay, N. (2009) *Cell Mol Life Sci*

83. Furman, C. S., Gorelick-Feldman, D. A., Davidson, K. G., Yasumura, T., Neely, J. D., Agre, P., and Rash, J. E. (2003) *Proc Natl Acad Sci U S A* **100**, 13609-13614

84. Nicchia, G. P., Mastrototaro, M., Rossi, A., Pisani, F., Tortorella, C., Ruggieri, M., Lia, A., Trojano, M., Frigeri, A., and Svelto, M. (2009) *Glia* **57**, 1363-1373

85. Rash, J. E., Davidson, K. G., Yasumura, T., and Furman, C. S. (2004) *Neuroscience* **129**, 915-934

86. Silberstein, C., Bouley, R., Huang, Y., Fang, P., Pastor-Soler, N., Brown, D., and Van Hoek, A. N. (2004) *Am J Physiol Renal Physiol* **287**, F501-511

87. Sorbo, J. G., Moe, S. E., Ottersen, O. P., and Holen, T. (2008) *Biochemistry* **47**, 2631-2637

88. Strand, L., Moe, S. E., Solbu, T. T., Vaadal, M., and Holen, T. (2009) *Biochemistry* **48**, 5785-5793

89. Suzuki, H., Nishikawa, K., Hiroaki, Y., and Fujiyoshi, Y. (2007) *Biochim Biophys Acta*

90. Hamill, K. J., Kligys, K., Hopkinson, S. B., and Jones, J. C. (2009) *J Cell Sci* **122**, 4409-4417

91. Talts, J. F., Sasaki, T., Miosge, N., Gohring, W., Mann, K., Mayne, R., and Timpl, R. (2000) *J Biol Chem* **275**, 35192-35199

92. Yu, H., and Talts, J. F. (2003) *Biochem J* **371**, 289-299

93. Wizemann, H., Garbe, J. H., Friedrich, M. V., Timpl, R., Sasaki, T., and Hohenester, E. (2003) *J Mol Biol* **332**, 635-642

94. McKee, K. K., Harrison, D., Capizzi, S., and Yurchenco, P. D. (2007) *J Biol Chem* **282**, 21437-21447

95. Cheng, Y. S., Champliaud, M. F., Burgeson, R. E., Marinkovich, M. P., and Yurchenco, P. D. (1997) *J Biol Chem* **272**, 31525-31532

96. Berzin, T. M., Zipser, B. D., Rafii, M. S., Kuo-Leblanc, V., Yancopoulos, G. D., Glass, D. J., Fallon, J. R., and Stopa, E. G. (2000) *Neurobiol Aging* **21**, 349-355

97. Smith, M. A., and Hilgenberg, L. G. (2002) *Neuroreport* **13**, 1485-1495

98. McKee, K. K., Capizzi, S., and Yurchenco, P. D. (2009) *J Biol Chem* **284**, 8984-8994

99. McFarlane, A. A., and Stetefeld, J. (2009) *Protein Sci* **18**, 2421-2428

100. Nitkin, R. M., and Rothschild, T. C. (1990) *J Cell Biol* **111**, 1161-1170

101. Nicchia, G. P., Frigeri, A., Liuzzi, G. M., Santacroce, M. P., Nico, B., Procino, G., Quondamatteo, F., Herken, R., Roncali, L., and Svelto, M. (2000) *Glia* **31**, 29-38

102. Fu, X. M., Yao, Y. J., Yang, Z., Xiang, L., and Gao, J. (2005) *Sichuan Da Xue Xue Bao Yi Xue Ban* **36**, 641-644

103. Fu, X., Li, Q., Feng, Z., and Mu, D. (2007) *Glia* **55**, 935-941

104. Jung, J. S., Bhat, R. V., Preston, G. M., Guggino, W. B., Baraban, J. M., and Agre, P. (1994) *Proc Natl Acad Sci U S A* **91**, 13052-13056

105. Neely, J. D., Christensen, B. M., Nielsen, S., and Agre, P. (1999) *Biochemistry* **38**, 11156-11163

4 INTERDEPENDENCE OF LAMININ-MEDIATED CLUSTERING OF LIPID RAFTS AND THE DYSTROGLYCAN COMPLEX IN ASTROCYTES[3]

4.1 Introduction

The basement membrane is a specialized extracellular matrix (ECM) composed of collagen, fibronectin, perlecan, agrin, and laminin. Several studies have focused on the involvement of these ECM molecules in the formation and maturation of neuromuscular junctions (1-4) and interneuronal synapses (5). More recently, much effort has been made by our group and others to understand the role of these molecules at the interface of astroglia and blood vessels (6-8). Laminin is highly expressed at the perivascular ECM and the laminin receptor, dystroglycan (α-DG), together with many other components of the dystroglycan-associated protein (DAP) complex, is particularly enriched at astrocyte endfeet abutting the blood vessels (9-11). The binding of laminin to α-DG at these specialized astrocyte domains in brain plays a key role in the polarized distribution of components of the DAP complex (6,12).

Multiple lines of evidence indicate that the DAP complex is crucial for the functional distribution both of the water-permeable channel, AQP4, and the inwardly rectifying potassium channel, Kir4.1, at astrocyte endfeet. Indeed, mutations in the dystrophin gene, deletion of α-syntrophin or loss of laminin binding to α-DG caused by a mutation in the Large1 glycosyltransferase result in a dramatic reduction of the expression of AQP4 and Kir4.1 at perivascular astrocyte endfeet (6,7,12-15). The mislocalization of AQP4 in the dystrophin mutant and α-syntrophin null mice results in delayed onset of brain edema and K^+ clearance (16-18). Collectively, these studies highlight a cooperative role between the ECM and both the extracellular and cytoplasmic components of the DAP complex in the proper targeting of proteins to functional domains of astrocytes leading to the regulation of electrolyte balance and fluid movement.

Although the role of DG in targeting other members of the DAP complex (6) as well as AQP4 and Kir4.1 to astrocyte endfeet has been well established (12), the mechanisms underlying this highly organized distribution remain poorly understood. In C2C12 myotubes, agrin triggers AChR clustering, a DG-dependent process, through the coalescence of lipid rafts which is necessary for proper AChR gating functions (19-21). In oligodendrocytes, laminin induces the relocalization of α6β1 integrin to lipid rafts containing PDGFαR, thereby providing a potential mechanism for the incorporation of cell survival signals (22). Lipid rafts are defined as small (10–200 nm), heterogeneous, highly dynamic, sterol- and sphingolipid-enriched domains that compartmentalize cellular processes. These small rafts can sometimes be stabilized to form larger platforms through protein-protein and protein-lipid interactions (23). Indeed, the immunological synapse is a good example where rafts are brought together to form large functional membrane domains (24). At the immunological synapse, agrin induces the clustering of lipid rafts and their colocalization with CD3 and CD28 complex surface antigens as well as with Lck tyrosine kinase leading to T cell activation (24). Together, these studies provide evidence for a functional role of ligand-induced clustering of lipid rafts.

We have previously shown that laminin induces the coclustering of the DAP complex with Kir4.1 and AQP4 in glial cell cultures (8,25). Moreover, *in vivo* studies have shown that the perivascular localization of these channels and several components of the DAP complex at astrocyte endfeet require the interaction of laminin with α-DG (6,12). In light of these data we asked whether lipid rafts contribute to the laminin-DG-dependent compartmentalization of the DAP complex and AQP4 to key active domains of astrocytes. We show here using fluorescently labeled cholera toxin subunit B (CtxB), a common marker for GM1-containing lipid rafts, that laminin induces a dramatic reorganization of GM1 into large clusters or macrodomains that colocalize extensively with components of the DAP complex in cortical astrocyte cultures. Laminin-mediated clustering of AQP4 is dependent both on cholesterol-sensitive lipid rafts and the DAP complex bringing novel insight into ECM-dependent membrane domain organization and the mechanisms underlying the polarized distribution of these proteins in astrocytes.

4.2 Materials and methods

4.2.1 Antibodies

The following antibodies were used in the present study: rabbit anti-AQP4 against rat glutathione S-transferase AQP4 corresponding to residues 249–323 (Alomone Laboratories, Jerusalem, Israel), rabbit anti-laminin against purified mouse Engelbreth-Holm-Swarm Sarcoma laminin which recognizes laminin $\alpha1$, $\beta1$ and $\gamma1$ chains, rabbit polyclonal antibody to dystrophin (a generous gift from Dr. S. Carbonetto, McGill University, Montreal, Quebec, Canada), rabbit anti-caveolin-1 against the N terminus of human caveolin-1 (Santa Cruz Biotechnology, Santa Cruz, CA), rabbit anti-GFAP against the glial fibrillary acidic protein isolated from cow spinal cord (Dako, Mississauga, Ontario, Canada), mouse anti-β-DG, 43DAG1/8D5, against the 15 of the last 16 amino acids at the C terminus of the human dystroglycan sequence (Novocastra Laboratories, Newcastle-upon-tyne, UK), mouse anti- syntrophin, SYN1351, against *Torpedo* syntrophin (Affinity Bioreagents), mouse anti-flotillin-1 (BD Biosciences), mouse anti-α–tubulin against residues 426-450 (Abcam), mouse anti-TfR against the transferrin receptor (TfR) against residues 3-28 of the human TfR tail (Zymed Laboratories Inc.) and mouse anti-utrophin (8A4, Dvelopmental Studies Hybridoma Bank, University of Iowa).

4.2.2 Astrocyte primary cultures

Primary cortical astrocyte cultures were prepared from embryonic day 18 rats (E18) (Sprague-Dawley, Charles River). Cortices were dissected, and meninges and choroid plexus were removed. They were then cut into small pieces and incubated for 25 min with trypsin (3.0 mg/ml; Invitrogen). Dissociated cortices were then plated in culture flasks and grown in Dulbecco's modified Eagle's medium supplemented with 10% fetal bovine serum, 1% penicillin-streptomycin and 1 mM L-glutamine (Invitrogen) for 2-3 weeks. The culture medium was changed every 3 days. To remove microglia and oligodendrocyte progenitors, the flasks were shaken the day following the plating. After trypsinization, the cells were plated on glass coverslips coated with poly-D-lysine (0.1 mg/ml; Sigma) in 24-well plates at a density of 200-250 x10^3 cells/ml. Two days after plating, the cells were treated for 8 h with either 30 nM Engelbreth-Holm-Swarm Sarcoma laminin-1 (Sigma-Aldrich), C-agrin 4,8 (10 nM), C-agrin 0,0

(10 nM, generous gift from Dr M Ferns, University of California, Davis) or with 100 nM fibronectin (Sigma).

4.2.3 siRNA transfections and cholesterol depletion and repletion

Astrocytes were transfected in suspension before plating with 100 nM *Dag*1 and *Aqp4* siRNAs (siGENOME and ON-TARGETplus SMARTpool siRNA reagents; Dharmacon) and control siRNA (ON-TARGETplus siCONTROL nontargeting siRNA; Dharmacon) using Lipofectamine 2000 (Invitrogen), following the manufacturer's protocol. One day and a half after plating, astrocytes were treated for 8 h with 30 nM of laminin-1 (Sigma-Aldrich) and subsequently analyzed by immunofluorescence. The efficiency of transfection was assessed by immunoblot analysis of proteins extracted on ice using an extraction buffer (25 mM Tris pH 7.4, 25 mM glycine and 150 mM NaCl) containing 1% Triton X-100, 1 x Complete protease inhibitor mixture, and 5 mM EDTA.

For the cholesterol depletion experiments, the cells were incubated in the presence of 10 μM mevastatin or 0.5 µg/ml filipin for 8 h or with 20 mM methyl β-cyclodextrin (Sigma) for 1 h at 37°C. For the cholesterol repletion experiments, the cells were incubated in the presence of 10 μM mevastatin and 50 µg/ml cholesterol (Sigma) for 8 h at 37°C.

4.2.4 Immunofluorescence

Cells were washed and incubated for 25 minutes at 4°C with chilled phosphate-buffered saline (PBS) containing 10 µg/ml FITC-conjugated CtxB (Sigma). Then, they were rinsed with warm PBS and fixed by immersion in 4% (w/v) paraformaldehyde in 0.1 M phosphate buffer for 20 min followed by rinsing in PBS, 3 x 15 min. The cells were incubated for 1 h at room temperature (20–22°C) in a solution containing 2% bovine serum albumin (Sigma) and 0.25% Triton X-100. Double immunolabeling was performed by incubating the cells at room temperature for 1 h in the presence of primary antibodies against β-DG (1/25) and laminin (1/1500) or AQP4 (1:200), syntrophin (1:100) and laminin (1/1500), utrophin (1/10) and dystrophin (1/100), flotillin-1 (1/25) and AQP4 (1/100), β-DG (1/25) and caveolin-1 (1/100). Subsequently, they were rinsed with PBS (3 x 15 min) and incubated with Alexa Fluor 568 goat

anti-mouse IgG and Alexa Fluor 647 goat anti-rabbit or Alexa Fluor 568 goat anti-mouse IgG and Alexa Fluor 488 goat anti-rabbit IgG for 1 h (1/200; Molecular Probes). After several washes with PBS, coverslips were mounted on glass slides using Prolong Gold Antifade Reagent with or without 4', 6-diamidino-2-phenylindole (Invitrogen). To confirm the specificity of the labeling, control cells were treated equivalently in the absence of primary antibodies. Fluorescent labeling of cultured cells was visualized using a confocal microscope (Fluoview 1000; Olympus) and an Uplan Apochromat 1.35 numerical aperture 60x objective (Olympus).

4.2.5 Fluorescence recovery after photobleaching analysis

Cortical astrocytes plated in 8-well μ-slides (Ibidi, Munich, Germany) were incubated with 10 μg/ml FITC-CtxB for 20 min. Images were acquired on a confocal microscope (FV1000; Olympus) with an Uplan Apochromat 1.35 numerical aperture 60x objective and fully opened pinhole. Photobleaching of FITC-CtxB was performed for 50 ms using a 405 simultaneous scanner set at 60% power within a circular area of 15 pixels diameter. Fluorescence recovery data were collected every second for over 120 s from 8 cells per experiment and analyzed with Prism software (GraphPad) using non-linear regression.

4.2.6 Subcellular fractionation of proteins from astrocyte cultures

To separate detergent-soluble from -insoluble fractions, the cultured astrocytes were harvested and suspended in 0.5 ml of ice-cold TNE buffer (25 mM Tris-HCl, pH 7.5, 150 mM NaCl, 5 mM EDTA) supplemented with 0.5% Triton X-100 and 1 x Complete protease inhibitor mixture. After 20 min incubation on ice, the lysates were centrifuged at 800 g for 10 min. The supernatant was further centrifuged at 100,000 g for 1 h at 4°C to obtain detergent-resistant membranes (DRMs) and non-detergent resistant membranes (non-DRMs).

For the flotation assay, astrocyte cultures were harvested and lysed on ice for 30 min in TNE buffer supplemented with 1% Triton X-100 and 1 x Complete protease inhibitor mixture. Nuclei and cellular debris were removed from the suspension by centrifugation at 1000 g for 10 min. Other astrocyte cultures were harvested and lysed in a detergent-free buffer using 500 mM sodium carbonate, pH 11.0, as previously described (26). The protein extracts were collected and

subjected to a flotation assay using a discontinuous sucrose gradient. To prepare the latter, 1 ml of supernatant was mixed with 3 ml of 85% sucrose in TNE and transferred to the bottom of a Beckman centrifuge tube. The diluted cell lysate was overlaid with 2 ml of 50% sucrose, 3 ml of 35% sucrose, 1 ml of 15% sucrose and finally with 200 μL of TNE buffer. The samples were centrifuged in an SW41 rotor at 200,000 g for 20 h at 4°C. Fractions numbered 1-8 were collected from the top of the gradient and analyzed by western and dot blots.

4.2.7 Immunoblotting and dot blotting

The samples obtained from siRNA-tranfected astrocytes as well as from the subcellular fractionation of astrocyte cultures were denatured by boiling for 9 min in reducing sample buffer and then loaded on a 10% SDS-PAGE gels. The gels were electrotransferred to nitrocellulose membranes (Bio-Rad, Mississauga, Ontario, Canada) and the blots were probed with antibodies to AQP4 (1/1000), caveolin-1 (1/500), flotillin-1 (1/500), β-DG (1/300), α–tubulin (1/1000) and TfR (1/1000). Bound antibodies were detected using horseradish peroxidase-conjugated goat anti-rabbit IgG or goat anti-mouse IgG (1/2000; Jackson ImmunoResearch). To detect the GM1 ganglioside, 1μL of each fraction was dotted onto a nitrocellulose membrane and probed with horseradish peroxidase-coupled CtxB (10 ng/ml horseradish peroxidase-CtxB; Sigma). Signals were visualized on Bioflex econo films (Interscience, Markham, Ontario, Canada) using chemiluminescence (Amersham Biosciences).

4.2.8 Quantitative analyses

The number of clusters, surface area of the clusters and the colocalization between clusters containing GM1 and β-DG, β-DG and laminin, β-DG and AQP4, laminin and GM1 as well as AQP4 and GM1 were determined on images subjected to a threshold using ImagePro Plus software (Media Cybernetics, Inc.). Signals were considered as clusters when their intensity was above background and above surrounding diffuse immunofluorescence and when their size was at least 1.5 μm^2. Clusters were counted in an average of 15 random fields per treatment, and experiments were repeated at least three times. Images from the same experiment were captured using identical acquisition parameters and subjected to the same threshold. Statistical analyses were performed using GraphPad Prism 3.00 software and unpaired Student's *t* test.

4.3 Results

4.3.1 Cholesterol regulates AQP4 distribution to detergent-resistant membrane domains in astrocytes

To determine the distribution pattern of β-DG and AQP4 in lipid raft-containing fractions, Triton X-100 extracts from primary astrocyte cultures were subjected to a flotation assay. The distribution of these proteins was also evaluated in lipid raft fractions obtained using detergent-free astrocytes extracts. The efficiency of the subcellular fractionation was confirmed by probing the obtained fractions with antibodies to the TfR, α-tubulin, flotillin-1, caveolin-1, as well as with horseradish peroxidase -CtxB to detect GM1 (Fig. 4.1A). Fractions 1-4 obtained from Triton X-100 and detergent free extracts were both enriched for the lipid raft markers flotillin-1, caveolin-1 and GM1 (Fig. 4.1A). As previously described (27), AQP4 was enriched in low density lipid raft-containing fractions 1 to 4 and was not detected in non-lipid raft fractions 5-8 (Fig. 4.1A). However, β-DG co-distributed with the TfR and α-tubulin to fractions 5-8 (Fig. 4.1A). This is in agreement with previous findings showing that β-DG was not found in the GM1-containing lipid raft fractions isolated from embryonic stem cell cultures (28).

We then determined whether the disruption of lipid rafts using mevastatin, filipin or methyl β-cyclodextrin to deplete membrane cholesterol resulted in alteration of AQP4 distribution in astrocyte cultures. In control astrocytes, we found that the DRM fraction was enriched for flotillin-1 and caveolin-1 as well as GM1 and contained AQP4 but virtually no β-DG (+DMSO, Fig. 4.1B). However, high amounts of β-DG were found in the non-DRM fraction (+DMSO, Fig. 4.1B), confirming the results obtained using the flotation assay (Fig. 4.1A). In astrocyte cultures treated with either mevastatin (+Mevastatin, Fig. 4.1B), filipin (Appendix C) or methyl β-cyclodextrin (Appendix C), a decrease in the amounts of flotillin-1 and caveolin-1 was observed in the DRM compared with control untreated cells
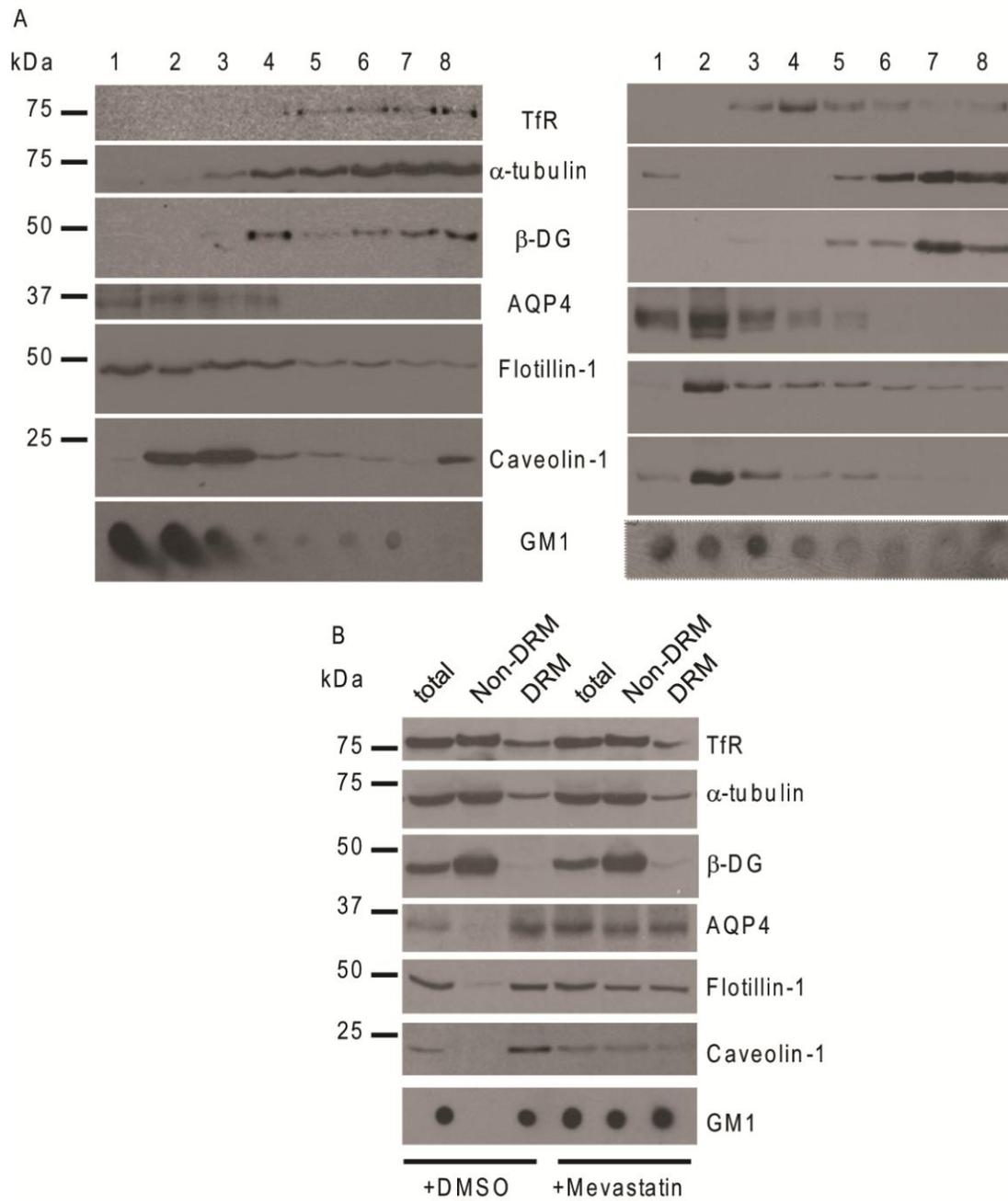
Figure 4.1 The association of AQP4 with the DRMs is dependent on cholesterol in astrocytes. (**A**) Rat cortical astrocytes were solubilized either in 1% Triton X-100 (left panel) or detergent-free buffer (right panel) and fractionated through a discontinuous sucrose gradient. (**B**) Astrocytes were incubated with 10 μM mevastatin for 8h, and proteins were harvested in DRMs and non-DRMs. Immunoblots were probed for the TfR, α-tubulin, β-DG, AQP4, flotillin-1, caveolin-1 and the dot blot was labeled for GM1. Representative blots from three independent experiments are shown.

(+DMSO, Fig. 4.1B). Moreover, a pool of flotillin-1, caveolin-1 and GM1 translocated to non-DRM confirming that mevastatin (Fig. 4.1B), filipin and methyl β-cyclodextrin (Appendix C) efficiently depleted membrane cholesterol. Most interestingly, AQP4 also partially translocated to non-DRM fractions indicative of the cholesterol-dependent association of a pool of AQP4 with DRM (Fig. 4.1B; Appendix C).

4.3.2 Laminin induces the reorganization and stabilization of GM1 in astrocytes

To investigate the effect of laminin on the organization of lipid rafts containing the ganglioside GM1, we used FITC-CtxB. In laminin-treated astrocytes, GM1 presented a robust clustering (Fig. 4.2E) compared with control untreated astrocytes where the distribution of GM1 was diffuse (Fig. 4.2A). These clusters presented a high degree of colocalization with the laminin clusters (Fig. 4.2E-H). Furthermore, laminin did not induce a detectable change in the morphology of astrocytes, because laminin-treated astrocytes presented a flat and polygonal shape similar to that of control untreated astrocytes as assessed by wheat germ agglutinin labeling (Appendix D). Together these data show that the laminin-induced reorganization of the raft component GM1 is not associated with a change in astrocyte morphology.

To determine whether laminin-induced clustering of GM1 affected its diffusion in the membrane (29,30), we performed fluorescence recovery after photobleaching of FITC-CtxB in untreated and laminin-treated astrocytes (Fig. 4.3). Laminin treatment resulted in a dramatic reduction in the rate of FITC-CtxB recovery, but only for FITC-CtxB localized within the laminin-induced clusters (Fig. 4.3A-C). This shows that laminin stabilizes GM1-bound FITC-CtxB within the clusters and reduces the exchange rate of FITC-CtxB within the bleached region with FITC-CtxB outside the bleached region. Therefore, the colocalization of CtxB and laminin clusters not only reflects a laminin-induced redistribution of GM1 but also reveals a role for laminin in the stabilization of this raft component in astrocyte membrane domains.
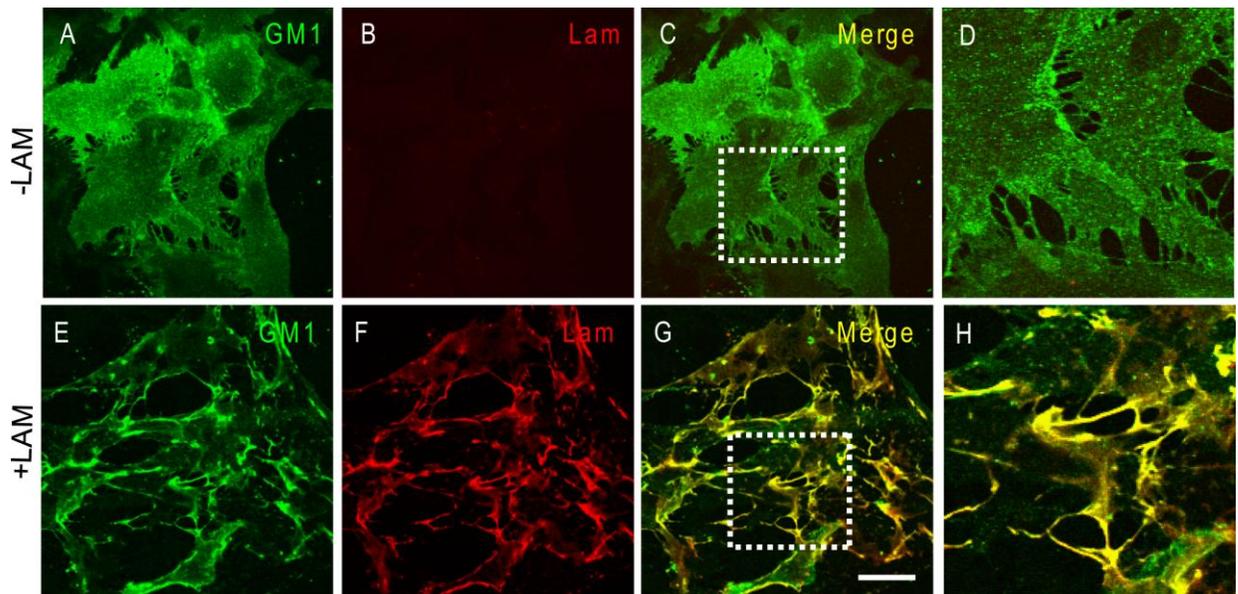
Figure 4.2 Laminin organizes GM1-containing lipid rafts into clusters in astrocytes. (**A-D**) Rat cortical astrocytes incubated in the absence or the presence (**E-H**) of 30 nM laminin were labeled for GM1 using FITC-CtxB (**A** and **E**) and for laminin (**B** and **F**). High magnifications of the areas boxed in **C** and **G** are shown in **D** and **H**, respectively. Scale bar, 45 μm.
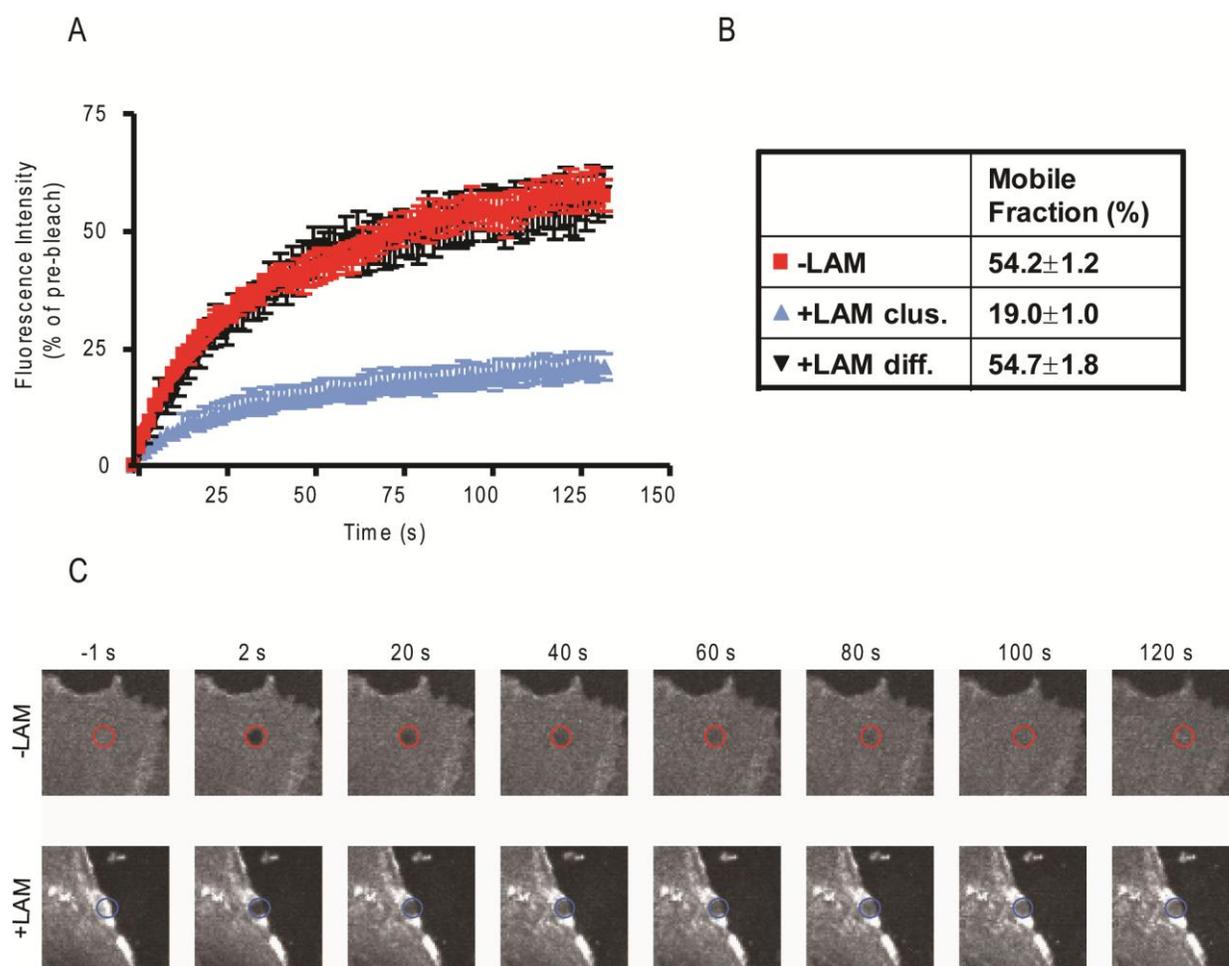
Figure 4.3 Laminin regulates the membrane diffusion of GM1-containing lipid rafts labeled with FITC-CtxB. (**A**) Rat cortical astrocytes treated with 30 nM laminin were incubated with 10µg/ml FITC-CtxB at room temperature and areas within CtxB clusters were bleached and imaged for fluorescence recovery. Areas with diffuse FITC-CtxB labeling in both astrocytes treated with laminin and untreated astrocytes were also bleached and imaged for over 120 s. Percent fluorescence intensity ±S.E. in the bleached area during recovery is shown for one representative experiment out of three (n=8 cells/experiment). (**B**) Percent mobile fraction of FITC-CtxB in areas of untreated astrocytes (-LAM), diffuse areas (+LAM diff.) and clustered areas of laminin-treated astrocytes (+LAM clus.). (**C**) Representative images of FITC-CtxB labeled astrocytes are shown before bleaching (-1 s), shortly after bleaching (2 s), and at various time points during fluorescence recovery.

4.3.3 Laminin induces the coclustering of the DAP complex, AQP4 and GM1

Given that laminin induces the coclustering of the DAP complex with both Kir4.1 and AQP4 (8), we asked whether this coincided with the laminin-induced clustering of GM1. In the absence of laminin, GM1 labeled with FITC-CtxB was homogeneously distributed throughout the cell (Fig. 4.4A, E and I). Utrophin (Fig. 4.4B), dystrophin (Fig. 4.4C), syntrophin (Fig. 4.4F), β-DG (Fig. 4.4J) and AQP4 (Fig. 4.4K) also exhibited a homogeneous distribution. Upon laminin treatment, CtxB-labeled GM1 coclustered with utrophin and dystrophin (Fig. 4.4M-P), syntrophin and laminin (Fig. 4.4Q-T) as well as with β-DG and AQP4 clusters (Fig. 4.4U-X). This laminin-induced clustering of these DAP complex components was not accompanied by a change in their expression levels as determined by western blot analysis (data not shown).

Quantitative analysis revealed over 2-fold increase in the number of GM1 clusters in the laminin-treated compared with the untreated astrocytes that parallels the increase in the number of β-DG, laminin and AQP4 clusters, as previously reported (Fig. 4.5A; 8,25). The surface area of GM1-containing clusters increased significantly by >6-fold in the laminin-treated compared with untreated astrocytes, as did the surface area of β-DG and AQP4 (Fig. 4.5B). The higher laminin concentration used in the present study (30 nM instead of 15 nM) may account for the increase in the surface area of these AQP4 clusters relative to a previous study (8). A significant degree of colocalization was found between β-DG, GM1 and AQP4 upon laminin treatment (Fig. 4.5C). These results demonstrate an important role for the ECM and more specifically for laminin in the coclustering of the DAP complex and GM1-containing lipid rafts in astrocytes. In addition, the fluorescence data in Fig. 4.6 show that flotillin-1, another marker of lipid rafts, underwent clustering upon laminin treatment (Fig. 4.6G compared with Fig. 4.6A) and that these clusters colocalized extensively with AQP4 clusters (Fig. 4.6G-I). In contrast, the distribution of the lipid raft marker, caveolin-1, did not change upon laminin treatment (Fig. 4.6, compare J to D) and remained distinct from β-DG clusters (Fig. 4.6J-L).

Figure 4.4 Laminin-induced clustering of the dystrophin complex and AQP4 is associated with the organization of GM1-containing lipid rafts. Rat cortical astrocytes incubated in the absence (**A**-**L**) or the presence (**M**-**X**) of 30 nM laminin were first labeled for GM1 using FITC-CtxB and then double immunolabeled for utrophin (**B** and **N**) and dystrophin (**C** and **O**), syntrophin (**F** and **R**) and laminin (**G** and **S**) as well as for β-DG (**J** and **V**) and AQP4 (**K** and **W**). Scale bar, 50 μm.

A

Number of clusters per field

B

Area of clustering per field (10^3 mm^2)

C

	GM1 /β-DG	β-DG /Lam	β-DG /AQP4	Lam /GM1	AQP4 / GM1
+LAM	0.74 ± 0.010***	0.83 ± 0.008***	0.62 ± 0.013***	0.80 ± 0.012***	0.53 ± 0.015***
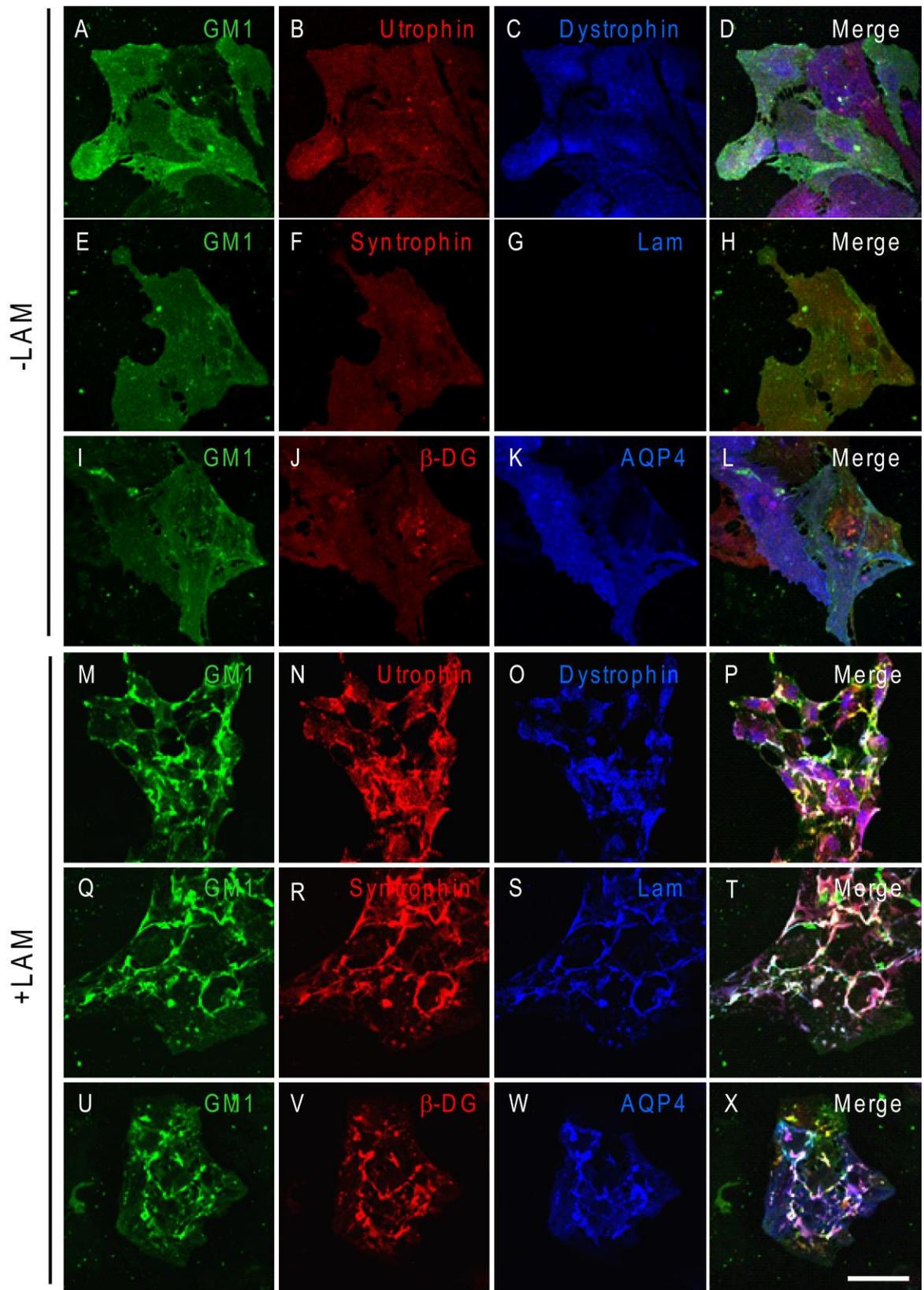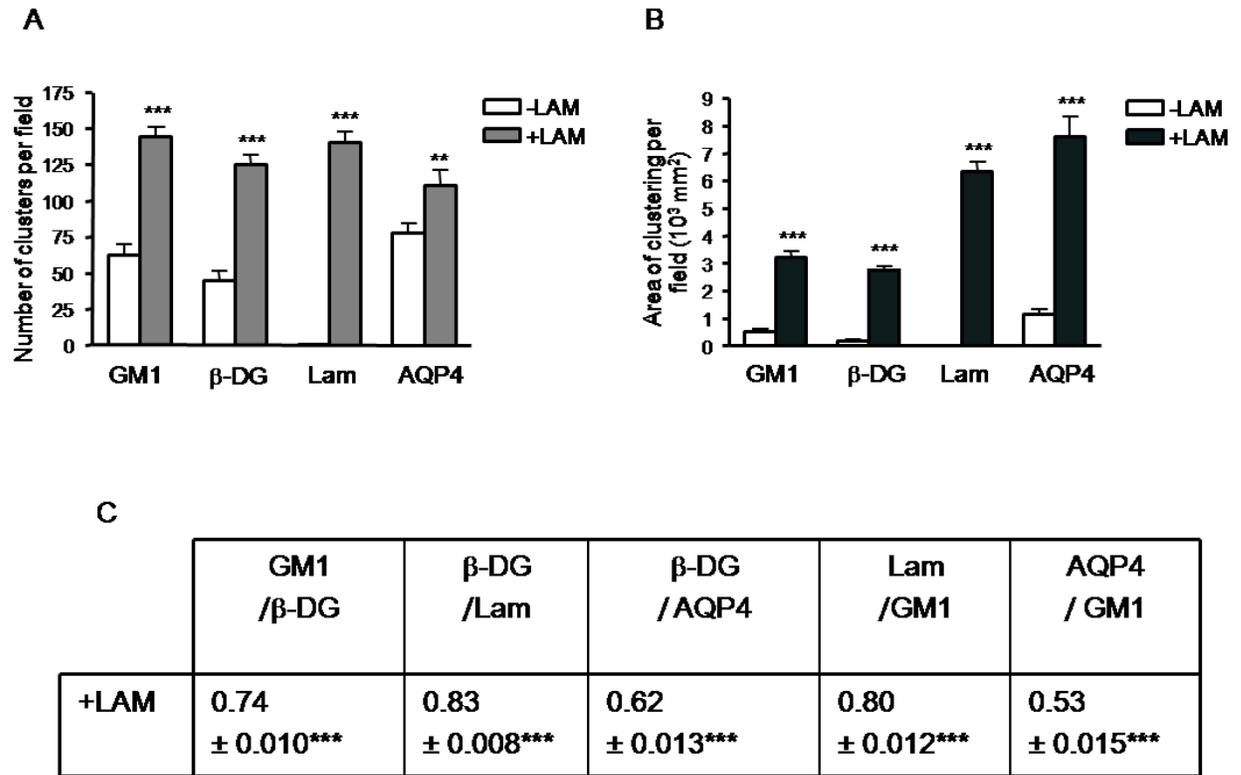
Figure 4.5 Quantitative analysis of the laminin-induced clustering of GM1-containing lipid rafts, β-DG, laminin and AQP4. (**A** and **B**) The histograms represent the mean number of clusters ±S.E. and surface area of clusters ±S.E. in astrocyte cultures treated with laminin (+LAM) and control untreated cultures (-LAM) from three experiments. The asterisks represent statistically significant differences from control (-LAM) as assessed by Student's t test (***$p<0.0001$; **$p<0.001$). (**C**) The table represents the mean Pearson's colocalization coefficient ±S.E. from three experiments. The asterisks represent statistically significant differences from control untreated cells as assessed by Student's t test (***$p<0.0001$). All quantifications were performed on 15 fields acquired randomly from each experiment.
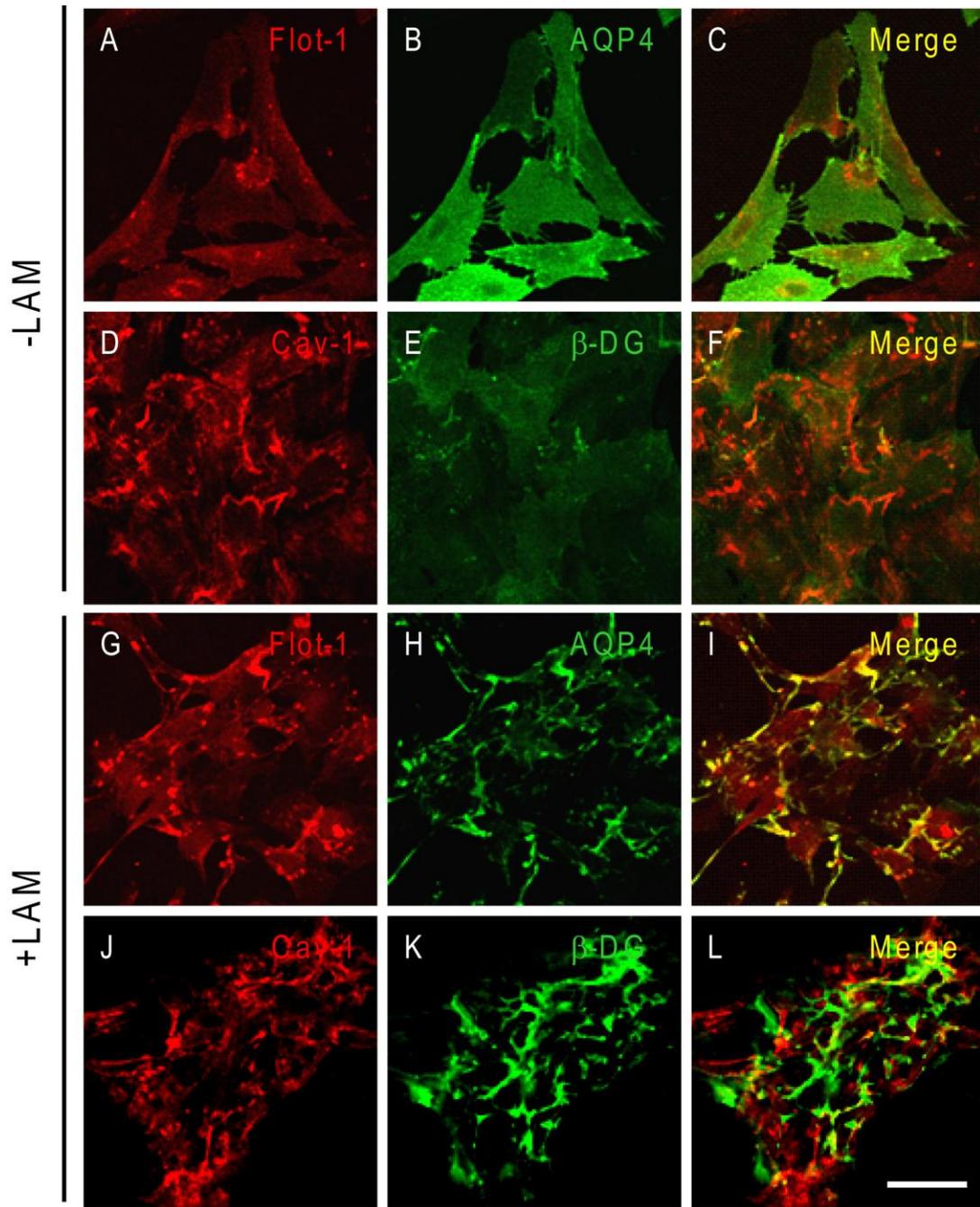
Figure 4.6 Laminin induces the coclustering of the lipid raft marker flotillin-1 with AQP4 but not of caveolin-1 with β-DG. Astrocytes incubated with in the absence (**A**-**F**) or the presence (**G**-**L**) of 30 nM laminin were double immunolabeled for flotillin-1 (**A** and **G**) and AQP4 (**B** and **H**) or caveolin-1 (**D** and **J**) and β-DG (**E** and **K**). Scale bar, 50 μm.

We also observed that laminin induces the coclustering of GM1-containing lipid rafts with β-DG and AChR in C2C12 myotubes (Appendix E) as has been previously described for the ECM protein agrin (21,24,31,32). However, this is not the case for GM1 in astrocytes treated with either soluble recombinant C-agrin 4,8 (Appendix F) or C-agrin 0,0 (data not shown). Similarly, fibronectin did not induce GM1 clustering (Appendix F). These data argue that, in the astrocytes examined in the present study, laminin plays a primary role in GM1 reorganization.

4.3.4 Cholesterol is required for the laminin-induced coclustering of β-DG, AQP4 and GM1-containing lipid rafts

Based on the laminin-induced colocalization of GM1-containing lipid raft clusters with the DAP complex and AQP4 clusters (Figs. 4.4M-X; and 4.5C), we examined qualitatively and quantitatively whether lipid raft integrity is crucial for the DAP/AQP4 clustering. To disrupt lipid rafts, we used the cholesterol-depleting and -sequestering agents mevastatin and filipin, respectively. Astrocytes treated both with laminin and mevastatin (Fig. 4.7I-P) or laminin and filipin (Appendix G) were fluorescently labeled for GM1, β-DG, laminin and AQP4. We found that GM1 (Fig. 4.7, compare I and M to A and E), β-DG (Fig. 4.7, compare J and N to B and F) and AQP4 (Fig. 4.7, compare O to G) had a uniform distribution and virtually no clustering throughout the cells similar to untreated astrocytes (Fig. 4.4I-L). Likewise, laminin did not cluster (Fig. 4.7, compare K to C) and presented a diffuse immunolabeling pattern. The diffuse immunolabeling is indicative of binding of exogenous laminin that is, however ineffective in terms of assembling at the cell surface and clustering the DAP complex and AQP4.

When astrocytes were incubated in the presence of laminin, mevastatin, and cholesterol, clustering of GM1, β-DG, laminin and AQP4 was significantly rescued (Fig. 4.7Q-Z). These data show that the laminin-induced cluster formation requires membrane cholesterol.

Figure 4.7 The laminin-induced clustering of GM1, β-DG and AQP4 is dependent on cholesterol. Astrocytes incubated in the presence of 30 nM laminin and DMSO (**A**-**H**), 30 nM laminin and 10 μM mevastatin diluted in DMSO (**I-P**), or 30 nM laminin, 10 μM mevastatin and 50 μg/ml cholesterol (**Q-X**) were labeled for GM1 (**A**, **I**, and **Q**), β-DG (**B**, **J**, and **R**) and laminin (**C**, **K**, and **S**) or GM1 (**E**, **M**, and **U**), β-DG (**F**, **N**, and **V**) and AQP4 (**G**, **O**, and **W**). Scale bar, 50 μm. (**Y**, **Z**) The histograms represent the mean number of clusters as well as their mean surface area ±S.E. from three different experiments. The quantifications were performed on 15 fields acquired randomly from each experiment. The asterisks and number signs represent statistically significant differences from laminin and laminin plus mevastatin-treated astrocytes, respectively, as assessed by Student's t test (***$p<0.0001$; **$p<0.001$; #$p<0.03$; # #$p<0.005$; ###$p\leq0.0001$).
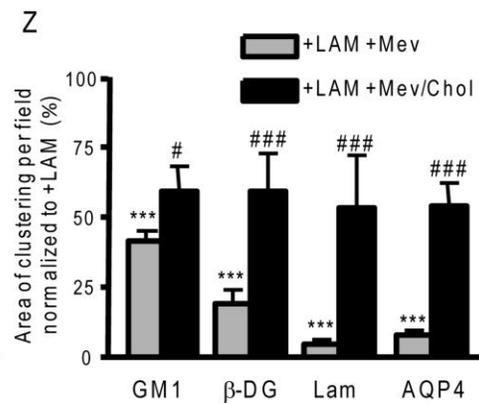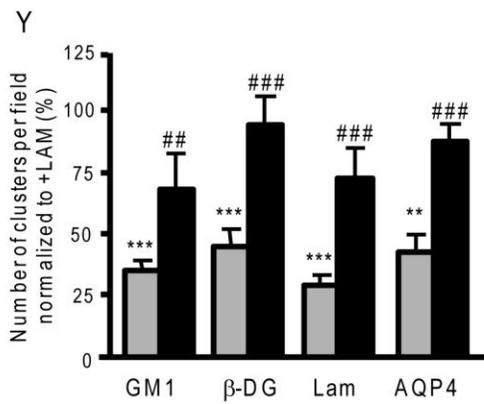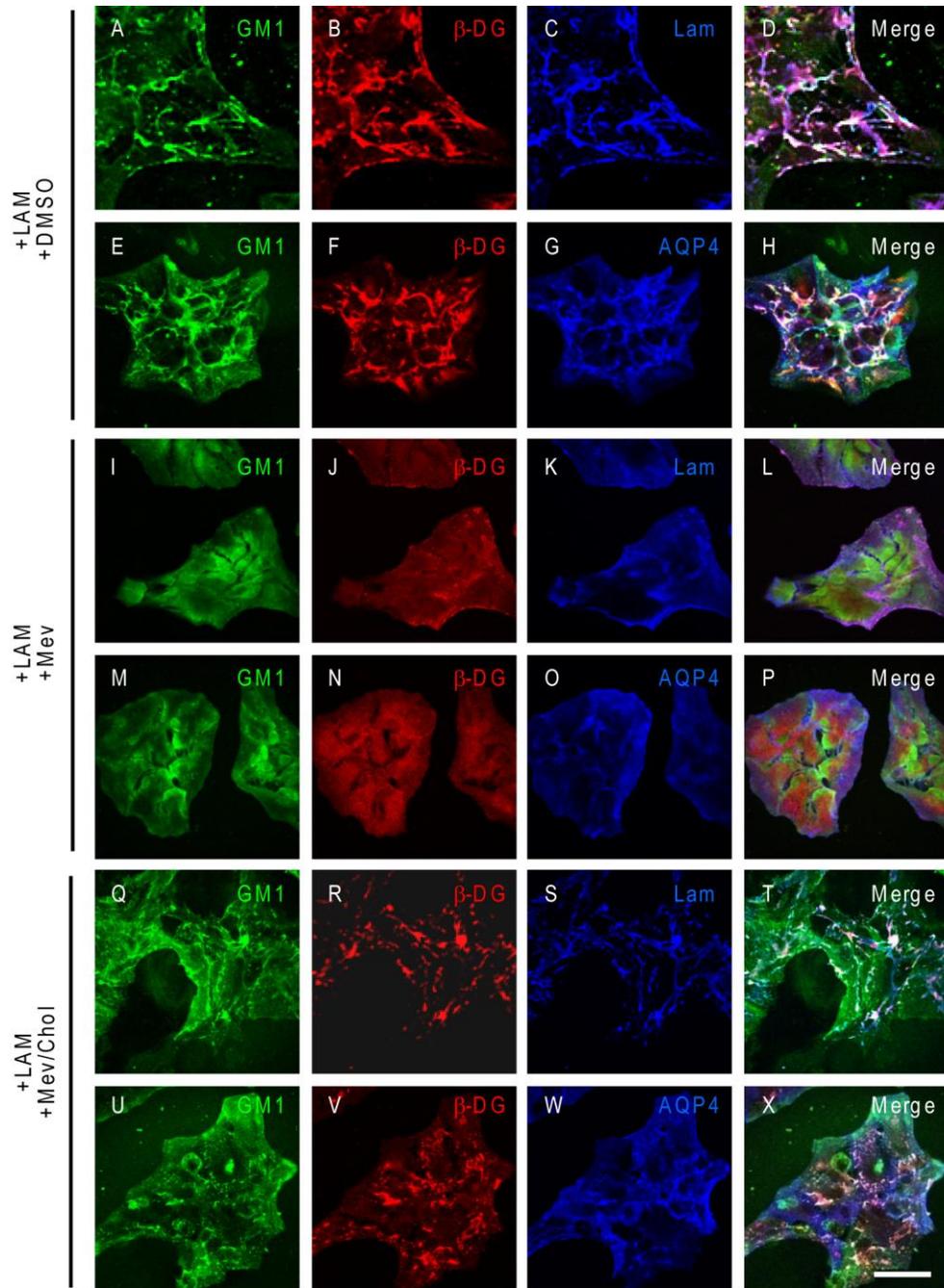
To assess the effect of cholesterol depletion on the expression levels of α-DG, β-DG, and AQP4, we compared by western blot the amounts of these proteins in mevastatin-treated astrocytes *versus* untreated astrocytes (Appendix H). We found that the expression levels of these proteins are similar in treated and untreated astrocytes, indicating that the decrease in the clustering of DG and AQP4 in mevastatin-treated astrocytes is not a consequence of a reduction in their expression levels. These data demonstrate the cholesterol dependence of laminin-induced cell surface organization and DG and AQP4 clustering.

4.3.5 Dystroglycan is required for the laminin-induced clustering of GM1

We have previously shown both in astrocytes and Müller glia that the laminin binding receptor α-DG, but not β1-integrin, clusters extensively upon laminin treatment (8,25). We therefore asked whether DG had a role in the laminin-mediated clustering of GM1. To address this question, we used siRNA to silence DG expression (si*Dag1*) and determined whether this altered the laminin-mediated clustering of GM1 by quantitative fluorescence analysis. As previous evidence demonstrated a dramatic alteration of the morphology of si*Aqp4*-transfected rat astrocytes that occurs between 2 and 6 days after transfection, we carried out our analysis at 2 days following transfection (33,34). First, we assessed by western blot the efficiency of the si*Dag1* transfection and found that β-DG could not be detected in the si*Dag1*-transfected cells when compared with the control scrambled siRNA- transfected astrocytes (siCTL; Fig. 4.8A) and untransfected astrocytes (data not shown). As an additional control, we used siRNA to silence AQP4 expression (si*Aqp4*) and found that, although this inhibited AQP4 expression, it had no impact on β-DG expression (Fig. 4.8A). Second, we verified that the morphology and the GFAP immunolabeling of the si*Dag1*- and si*Aqp4*- transfected astrocytes were comparable to that of siCTL-transfected cells (Appendix I). The data obtained here show a high efficiency of si*Dag1* gene silencing and no detectable effect of either si*Dag1* or si*Aqp4* on astrocyte morphology when compared with siCTL-transfected (Appendix I) or to untransfected astrocytes at 2 days post-transfection (data not shown).
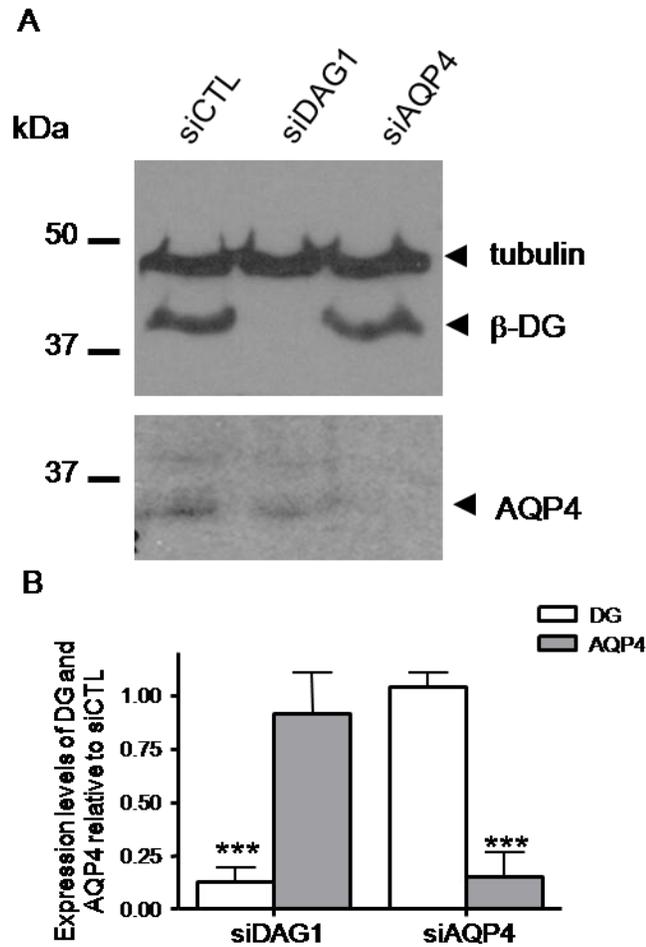
Figure 4.8 Dystroglycan and AQP4 siRNAs mediate gene silencing in astrocytes. (**A**) Western blot analysis of β-DG and AQP4 was performed 2 days following the transfection of astrocytes with si*Dag1*, si*Aqp4* and siCTL (scrambled siRNA). (**B**) The histograms represent the mean expression levels of β-DG and AQP4 ±S.E. from three experiments normalized to tubulin and compared with siCTL. The asterisks represent statistically significant differences from control as assessed by Student's t test (***p<0.0001).

The immunofluorescence analysis corroborates the western blot data (Fig. 4.8) and shows virtually no immunolabeling for β-DG in the si*Dag1*-transfected astrocytes (Fig. 4.9J and N). However, some small clusters of laminin (Fig. 4.9O) were detected even in the absence of any signal for β-DG (Fig. 4.9N). Of particular interest, the laminin-induced GM1 clustering in the siCTL-transfected astrocytes (Fig. 4.9A and E) was significantly reduced in the si*Dag1*-transfected astrocytes (Fig. 4.9I and M). In addition, the astrocytes deficient for DG exhibited reduced clustering of AQP4 compared with the siCTL astrocytes (Fig. 4.9, compare K to C). The si*Aqp4*-transfected astrocytes presented a decrease in AQP4 imunolabeling (Fig. 4.9, compare S to C) and no change in β-DG (Fig. 4.9R and V) and laminin immunolabeling and clustering (Fig. 4.9W) compared with control cells (Fig. 4.9B, F and G). In addition, the laminin-induced clustering of GM1 was not affected by AQP4 silencing (Fig. 4.9Q and U). It is noteworthy that the effect of si*Dag1* was more pronounced on the surface area of the GM1, β-DG, laminin and AQP4 clusters than on their number (Fig. 4.10, compare B to A). This suggests that, despite the fact that a small proportion of these clusters can form, their size is dramatically reduced in astrocytes deficient for DG.

4.4. Discussion

4.4.1 Laminin coclusters GM1 with the DAP complex and AQP4 in astrocytes

In brain, astrocytes are polarized and present an asymmetrical distribution of proteins such as DG and AQP4 that are diffusely distributed along the astrocyte processes in the parenchyma but highly concentrated at astrocyte endfeet abutting blood vessels. Astrocyte endfeet interact with the perivascular ECM and previous studies have shown both *in vivo* and *in vitro* that astrocyte interaction with laminin via DG is essential for the concentration of several members of the DAP complex as well as Kir4.1 and AQP4 at specialized astrocyte membrane domains (6,8,12). Although such a distribution is functionally important in potassium ion and water homeostasis, the mechanisms regulating the formation of these Kir4.1- and AQP4-enriched domains remain to be elucidated. AQP4 is associated with lipid raft-containing

Figure 4.9 Dystroglycan is essential for the laminin-induced GM1-containing lipid raft, β-DG and AQP4 coclustering. Astrocytes were transfected with siCTL (**A**-**H**), si*Dag1* (**I**-**P**) or si*Aqp4* (**Q**-**X**) and incubated with 30 nM laminin. They were then incubated with FITC-CtxB to label GM1 (**A**, **E**, **I**, **M**, **Q**, and **U**) and double immunolabeled for β-DG (**B**, **J**, and **R**) and AQP4 (**C**, **K**, and **S**) or β-DG (**F**, **N**, and **V**) and laminin (**G**, **O**, and **W**). Scale bar, 50 μm.
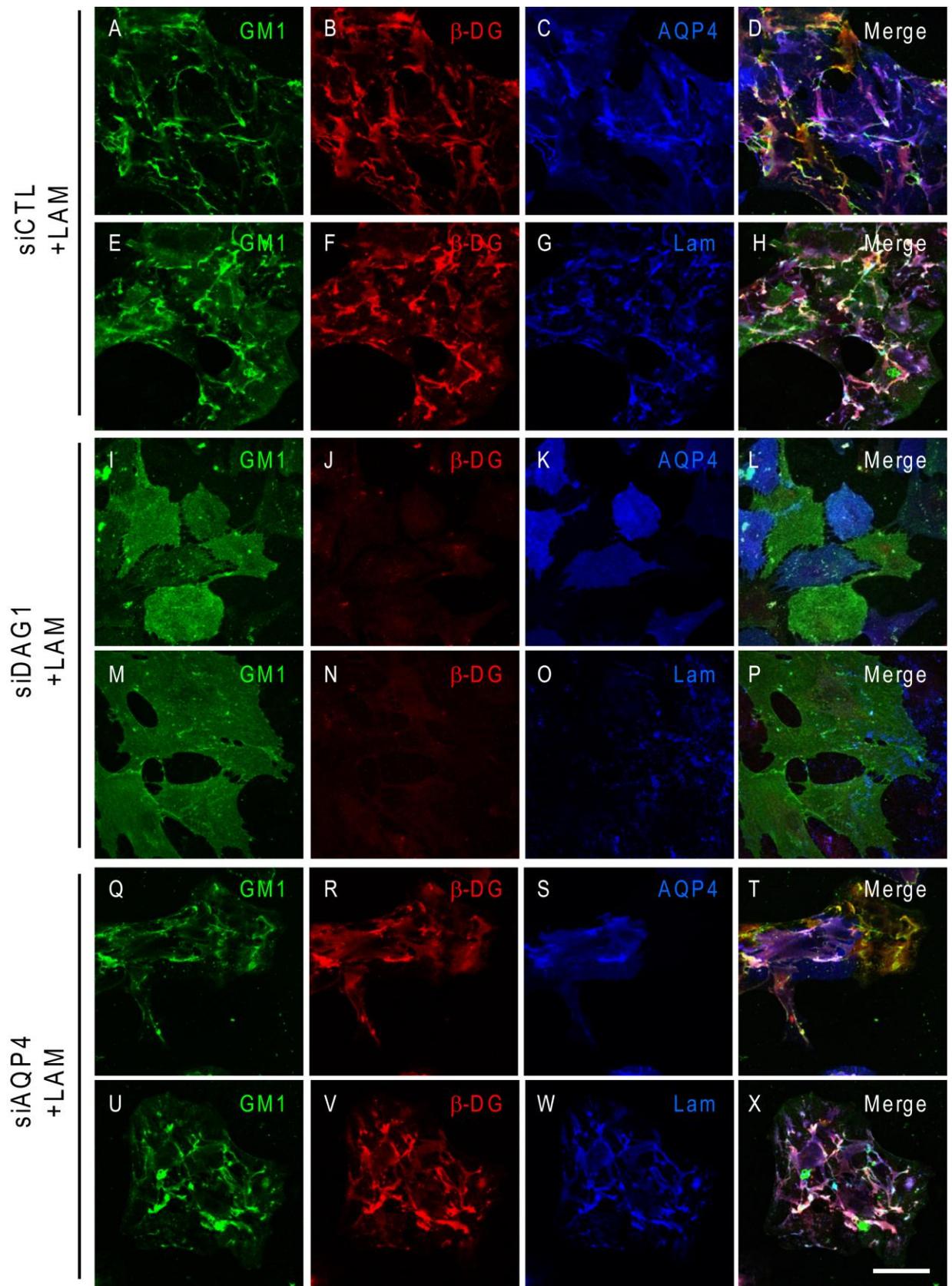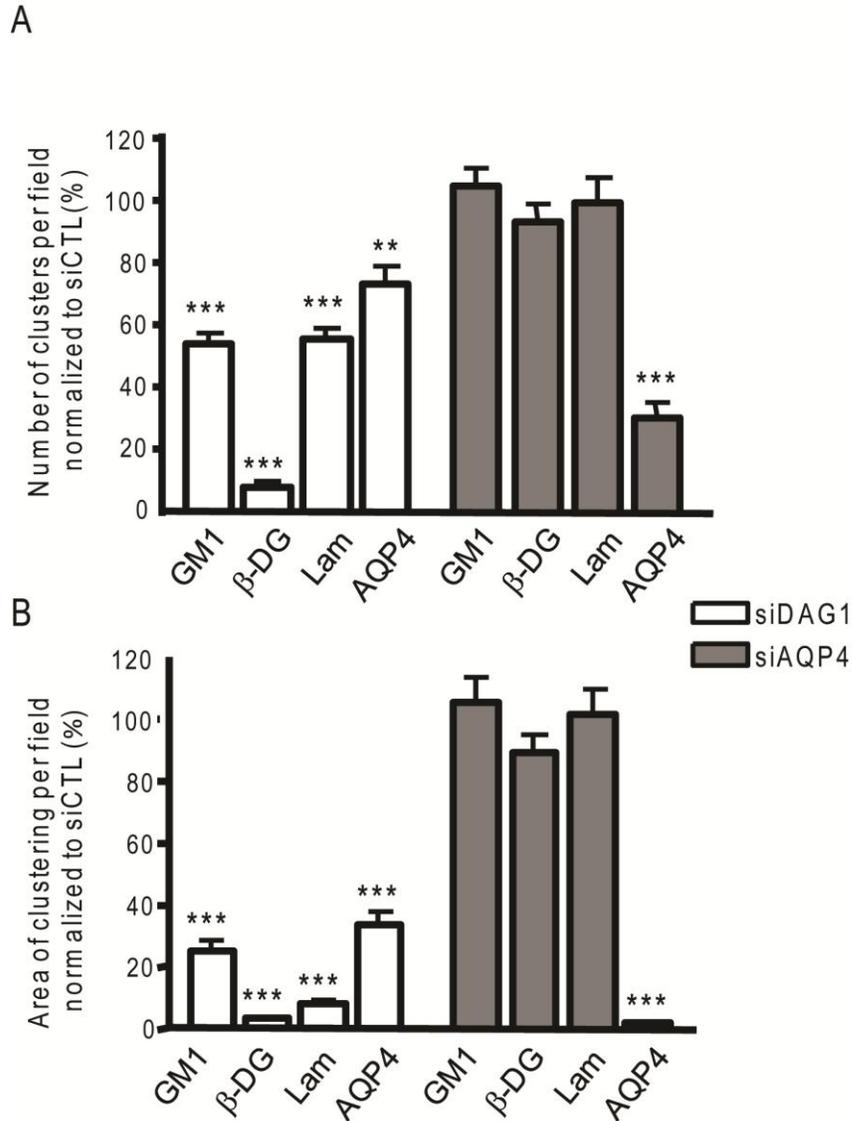
Figure 4.10 Quantitative analysis of the effect of the dystroglycan silencing on the laminin-induced clustering of GM1-containing lipid rafts, β-DG and AQP4. (**A** and **B**) The histograms represent the mean number of clusters ±S.E. and surface area of clusters ±S.E. in astrocyte cultures from three experiments. The asterisks represent statistically significant differences from control siCTL-transfected cells as assessed by Student's t test (***p<0.0001). All quantifications were performed on 15 fields acquired randomly from each experiment.

fractions in both brain and retina (27,35) as is another aquaporin, AQP5, that participates in fluid secretion in parotid gland cells (36). We therefore undertook a study to evaluate the role of lipid rafts in laminin-DG-dependent AQP4 clustering, and our data show that laminin induced a dramatic redistribution of GM1 into large cell surface clusters or macrodomains that colocalized extensively with β-DG and AQP4. The recruitment of AQP4 to laminin-rich clusters is therefore interdependent on both DG and cholesterol-rich lipid raft domains.

The DAP complex and AQP4 associate in a subset of rafts containing GM1 and flotillin-1 distinct from caveolin-1-containing caveolae. Indeed, flotillin has been reported to be localized to lipid raft domains distinct from caveolin-1 (37). Laminin therefore promotes coclustering of the DAP complex and AQP4 with a select population of lipid rafts in astrocyte membrane domains. How these coclusters of the DAP complex and AQP4/GM1/flotillin-containing lipid rafts are organized remains uncertain. In fact, laminin-induced clustering does not result in the recruitment of β-DG to DRMs (Appendix J). Raft-dependent laminin remodeling may induce spatial reorganization in the membrane such that the DAP complex and lipid rafts coexist and interact within the same polarized macrodomain. Indeed, the fact that GM1-bound CtxB exhibits reduced exchange in laminin-induced clusters shows that lipid raft dynamics and behavior are altered within these large membrane domains.

4.4.2 Laminin-induced coclustering of GM1, the DAP complex and AQP4 depends on the integrity of lipid rafts and dystroglycan

Cholesterol depletion experiments show that the integrity of lipid rafts is essential not only for the recruitment of AQP4 to DRMs (27) but also for the laminin-dependent assembly of the AQP4, β-DG and GM1-enriched domains. Conversely, DG silencing resulted in the disruption of laminin assembly and a significant decrease of clustering of not only AQP4 and β-DG at the cell surface but also the raft marker GM1. Coordinate plasma membrane domain organization by both lipid rafts and laminin binding to the DG complex may therefore restrict lateral diffusion of AQP4 within the plasma membrane shedding new light on the mechanisms involved in the polarized distribution of AQP4, and the DAP complex, at perivascular astrocyte endfeet.

Interestingly, the coclustering of GM1 and β-DG with AQP4 and AChRs in astrocytes and C2C12 myotubes (Appendix E), respectively, is consistent with a role for laminin in orchestrating the distribution of both lipids and a specific set of proteins to establish functional membrane domains. In C2C12 myotubes, laminin-induced coclustering of components of the DAP complex with AChRs requires Src- and Fyn-dependent tyrosine phosphorylation that enhance the association of postsynaptic proteins with cholesterol-rich membrane domains leading to the stabilization of AChR-containing synapses in muscle (32). Laminin-mediated clustering of α6β1-integrin within the platelet-derived growth factor receptor-containing lipid rafts in oligodendrocytes creates a signaling environment that promotes survival of these cells (22). Furthermore, integrin-mediated adhesion to the ECM regulates Rac1 signaling by preventing internalization of lipid raft-containing membrane domains (38). More recently, the laminin-mediated clustering of GM1 and the agrin association with lipid rafts have both been involved in promoting neurite outgrowth by activating Lyn/Akt/MAPK and Fyn/MAPK signaling pathways, respectively (39,40). These data define a role for the ECM in regulating raft-associated signaling. It is therefore likely that the laminin-mediated reorganization of GM1-containing lipid rafts and coclustering with the DAP complex provides a signaling environment that promotes the formation of AQP4-rich membrane domains in astrocytes.

4.4.3 Potential role of laminin and lipid raft-dependent clustering of AQP4 on its activity

AQP4 is the main structural component of intramembrane particles called orthogonal arrays of particles (41-43). Recently, an increase of the density of orthogonal arrays of particles as well as an increase in AQP4 expression accompanied by a more efficient water transport has been reported in astrocytes treated with the ECM molecule, agrin (44). This substantiates further the role of the ECM in the formation of assemblies of orthogonal arrays of particles rich in AQP4 at astrocyte endfeet. Mislocalization of AQP4 at perivascular astrocyte endfeet in the Large^{myd} mouse (6,12) and loss of its clustering in astrocytes deficient in DG may cause the dispersion or a decrease in the density of orthogonal arrays of particles at these specialized domains that will ultimately alter water transport.

Recent studies have reported that lack of the lipid raft gangliosides GM1 and GD1 (45) or depletion of cholesterol resulted in abnormal paranodal sodium channel clusters in the peripheral nervous system and prevented the agrin-induced clustering of AChRs in C2C12

133

myotubes, respectively (31,45,46). Moreover, cholesterol depletion in neuronal cultures decreases the number of synapses and α-amino-3-hydroxy-5-methyl-4-isoazolpropionic acid receptor stability (47). In some instances, it has been demonstrated that cholesterol can influence the activity of ion channels (19,48). These data raise the interesting hypothesis that lipid rafts may participate in the regulation of the AQP4 channel properties that define its role in water transport.

The present study demonstrates that loss of interaction between laminin and DG mimics the effect of membrane cholesterol depletion on AQP4 clustering and points to a concerted action between lipid rafts and ligand binding to DG that leads to the formation of membrane specializations at specific astrocytic sites. These findings therefore implicate lipid rafts in the polarization of the DAP complex and AQP4 in astrocyte endfeet and potentially in AQP4-mediated water transport.

4.5. References

1.	Arikawa-Hirasawa, E., Rossi, S. G., Rotundo, R. L., and Yamada, Y. (2002) *Nat Neurosci* **5**, 119-123
2.	Marangi, P. A., Wieland, S. T., and Fuhrer, C. (2002) *J Cell Biol* **157**, 883-895
3.	Nishimune, H., Valdez, G., Jarad, G., Moulson, C. L., Muller, U., Miner, J. H., and Sanes, J. R. (2008) *J Cell Biol* **182**, 1201-1215
4.	Ruegg, M. A., and Bixby, J. L. (1998) *Trends Neurosci* **21**, 22-27
5.	Huh, K. H., and Fuhrer, C. (2002) *Mol Neurobiol* **25**, 79-112
6.	Michele, D. E., Barresi, R., Kanagawa, M., Saito, F., Cohn, R. D., Satz, J. S., Dollar, J., Nishino, I., Kelley, R. I., Somer, H., Straub, V., Mathews, K. D., Moore, S. A., and Campbell, K. P. (2002) *Nature* **418**, 417-422
7.	Amiry-Moghaddam, M., Otsuka, T., Hurn, P. D., Traystman, R. J., Haug, F. M., Froehner, S. C., Adams, M. E., Neely, J. D., Agre, P., Ottersen, O. P., and Bhardwaj, A. (2003) *Proc Natl Acad Sci U S A* **100**, 2106-2111
8.	Guadagno, E., and Moukhles, H. (2004) *Glia* **47**, 138-149
9.	Zaccaria, M. L., Di Tommaso, F., Brancaccio, A., Paggi, P., and Petrucci, T. C. (2001) *Neuroscience* **104**, 311-324
10.	Blake, D. J., Hawkes, R., Benson, M. A., and Beesley, P. W. (1999) *The Journal of Cell Biology* **147**, 645-657
11.	Moukhles, H., and Carbonetto, S. (2001) *Journal of Neurochemistry* **78**, 824-834
12.	Rurak, J., Noel, G., Lui, L., Joshi, B., and Moukhles, H. (2007) *J Neurochem* **103**, 1940-1953
13.	Dalloz, C., Sarig, R., Fort, P., Yaffe, D., Bordais, A., Pannicke, T., Grosche, J., Mornet, D., Reichenbach, A., Sahel, J., Nudel, U., and Rendon, A. (2003) *Hum Mol Genet* **12**, 1543-1554
14.	Nico, B., Frigeri, A., Nicchia, G. P., Corsi, P., Ribatti, D., Quondamatteo, F., Herken, R., Girolamo, F., Marzullo, A., Svelto, M., and Roncali, L. (2003) *Glia* **42**, 235-251
15.	Frigeri, A., Nicchia, G. P., Nico, B., Quondamatteo, F., Herken, R., Roncali, L., and Svelto, M. (2001) *Faseb J* **15**, 90-98
16.	Amiry-Moghaddam, M., Williamson, A., Palomba, M., Eid, T., de Lanerolle, N. C., Nagelhus, E. A., Adams, M. E., Froehner, S. C., Agre, P., and Ottersen, O. P. (2003) *Proc Natl Acad Sci U S A* **100**, 13615-13620
17.	Amiry-Moghaddam, M., Xue, R., Haug, F. M., Neely, J. D., Bhardwaj, A., Agre, P., Adams, M. E., Froehner, S. C., Mori, S., and Ottersen, O. P. (2004) *Faseb J* **18**, 542-544
18.	Vajda, Z., Pedersen, M., Fuchtbauer, E. M., Wertz, K., Stodkilde-Jorgensen, H., Sulyok, E., Doczi, T., Neely, J. D., Agre, P., Frokiaer, J., and Nielsen, S. (2002) *Proc Natl Acad Sci U S A* **99**, 13131-13136
19.	Barrantes, F. J. (1993) *Braz J Med Biol Res* **26**, 553-571
20.	Gee, S. H., Montanaro, F., Lindenbaum, M. H., and Carbonetto, S. (1994) *Cell* **77**, 675-686
21.	Stetzkowski-Marden, F., Gaus, K., Recouvreur, M., Cartaud, A., and Cartaud, J. (2006) *J Lipid Res* **47**, 2121-2133
22.	Baron, W., Decker, L., Colognato, H., and ffrench-Constant, C. (2003) *Curr Biol* **13**, 151-155
23.	Pike, L. J. (2006) *J Lipid Res* **47**, 1597-1598

24. Khan, A. A., Bose, C., Yam, L. S., Soloski, M. J., and Rupp, F. (2001) *Science* **292**, 1681-1686

25. Noel, G., Belda, M., Guadagno, E., Micoud, J., Klocker, N., and Moukhles, H. (2005) *J Neurochem* **94**, 691-702

26. Song, K. S., Li, S., Okamoto, T., Quilliam, L. A., Sargiacomo, M., and Lisanti, M. P. (1996) *J Biol Chem* **271**, 9690-9697

27. Hibino, H., and Kurachi, Y. (2007) *Eur J Neurosci* **26**, 2539-2555

28. Shah, W. A., Peng, H., and Carbonetto, S. (2006) *J Gen Virol* **87**, 673-678

29. Kenworthy, A. K. (2007) *Methods Mol Biol* **398**, 179-192

30. Lajoie, P., Partridge, E. A., Guay, G., Goetz, J. G., Pawling, J., Lagana, A., Joshi, B., Dennis, J. W., and Nabi, I. R. (2007) *J Cell Biol* **179**, 341-356

31. Stetzkowski-Marden, F., Recouvreur, M., Camus, G., Cartaud, A., Marchand, S., and Cartaud, J. (2006) *J Mol Neurosci* **30**, 37-38

32. Willmann, R., Pun, S., Stallmach, L., Sadasivam, G., Santos, A. F., Caroni, P., and Fuhrer, C. (2006) *EMBO J* **25**, 4050-4060

33. Nicchia, G. P., Frigeri, A., Liuzzi, G. M., and Svelto, M. (2003) *Faseb J* **17**, 1508-1510

34. Benfenati, V., Nicchia, G. P., Svelto, M., Rapisarda, C., Frigeri, A., and Ferroni, S. (2007) *J Neurochem* **100**, 87-104

35. Fort, P. E., Sene, A., Pannicke, T., Roux, M. J., Forster, V., Mornet, D., Nudel, U., Yaffe, D., Reichenbach, A., Sahel, J. A., and Rendon, A. (2008) *Glia* **56**, 597-610

36. Ishikawa, Y., Cho, G., Yuan, Z., Inoue, N., and Nakae, Y. (2006) *Biochim Biophys Acta* **1758**, 1053-1060

37. Glebov, O. O., Bright, N. A., and Nichols, B. J. (2006) *Nat Cell Biol* **8**, 46-54

38. del Pozo, M. A., Alderson, N. B., Kiosses, W. B., Chiang, H. H., Anderson, R. G., and Schwartz, M. A. (2004) *Science* **303**, 839-842

39. Ichikawa, N., Iwabuchi, K., Kurihara, H., Ishii, K., Kobayashi, T., Sasaki, T., Hattori, N., Mizuno, Y., Hozumi, K., Yamada, Y., and Arikawa-Hirasawa, E. (2009) *J Cell Sci* **122**, 289-299

40. Ramseger, R., White, R., and Kroger, S. (2009) *J Biol Chem*

41. Sasaki, H., Kishiye, T., Fujioka, A., Shinoda, K., and Nagano, M. (1996) *Cell Struct Funct* **21**, 133-141

42. Verbavatz, J. M., Ma, T., Gobin, R., and Verkman, A. S. (1997) *J Cell Sci* **110** (**Pt 22**), 2855-2860

43. Rash, J. E., Davidson, K. G., Yasumura, T., and Furman, C. S. (2004) *Neuroscience* **129**, 915-934

44. Noell, S., Fallier-Becker, P., Beyer, C., Kroger, S., Mack, A. F., and Wolburg, H. (2007) *Eur J Neurosci* **26**, 2109-2118

45. Susuki, K., Baba, H., Tohyama, K., Kanai, K., Kuwabara, S., Hirata, K., Furukawa, K., Rasband, M. N., and Yuki, N. (2007) *Glia* **55**, 746-757

46. Campagna, J. A., and Fallon, J. (2006) *Neuroscience* **138**, 123-132

47. Hering, H., Lin, C. C., and Sheng, M. (2003) *J Neurosci* **23**, 3262-3271

48. Romanenko, V. G., Rothblat, G. H., and Levitan, I. (2002) *Biophys J* **83**, 3211-3222

5 LAMININ-INDUCED REDISTRIBUTION OF AQUAPORIN-4 IS MEDIATED BY THE PHOSPHORYLATION OF THE PROTEIN-SERINE KINASE C δ IN ASTROCYTES[4]

5.1 Introduction

The dystroglycan-associated protein (DAP) complex is a group of interacting proteins that link the cytoskeleton to the extracellular matrix (ECM). In muscle, where the complex has been most thoroughly examined, it is believed to maintain the structural integrity of muscle fibers by protecting myotubes from the shear stress arising from repeated cycles of contraction and relaxation (1). The axis of the complex is composed of the two subunits of dystroglycan (DG), α-DG and β-DG, which form a bridge between the extracellular matrix and the intracellular cytoskeleton (2,3). Both are derived from post-translational cleavage of a single polypeptide. Extracellular α-DG binds the ECM proteins laminin, agrin, perlecan and neurexin (4-7), whereas transmembrane β-DG interacts directly with α-DG and intracellular dystrophin, which in turn binds syntrophin, dystrobrevin and cytoskeletal actin (2,8-10).

Mutations of various members of the DAP complex underlie the pathogenesis of many muscular dystrophies, a class of congenital disorders characterized primarily by progressive muscle weakness and degeneration and secondarily by defects in brain and ocular development, the etiologies of which are poorly understood (11-14).

Dystroglycan and many members of the DAP complex are expressed in the central nervous system where they form complexes in both neurons and astrocytes (15,16). Of particular interest, DG is enriched at boundaries between neural tissues and fluid compartments, namely at glial cell endfeet abutting blood vessels of the brain (17). These specialized membrane domains are enriched for the water permeable channel aquaporin-4, AQP4 (18).

Multiple lines of evidence suggest that the integrity of the DAP complex is essential for the proper localization and function of AQP4. Indeed, mutations in the dystrophin gene or deletion of α-syntrophin result in a dramatic reduction of the expression of AQP4 at

perivascular astrocyte endfeet (19-21). In addition, in cultured astrocytes, laminin induces the coclustering of AQP4 with the DAP complex (22,23), suggesting that the ability of the DAP to bind ECM ligands is essential for the localization and stability of this channel.

The DAP complex may be involved in localizing signalling proteins to specific cell domains. Several studies have strongly implicated the DAP complex in enzymatic cascades that regulate the clustering of acetylcholine receptors (AChRs) at the neuromuscular junction (NMJ) (24-27). It is interesting to note that laminin binding to DG induces the tyrosine phosphorylation of DG and syntrophin, which increases its binding to Grb2 and, via Grb2-Sos1, activates Rac1 and PAK1-JNK. The activation of this pathway results in actin remodelling, PI3K/AKT pathway activation and tyrosine phosphorylation of c-jun and AChR via the activation of c-Src (28-35).

In several respects, the clustering of AQP4 in astrocytes apposed to the laminin-rich basal lamina is similar to the clustering of AChR at NMJs. In previous results, we have shown that laminin induces the coclustering of lipid rafts with the DAP complex and AQP4, and that lipid rafts integrity is crucial for their clustering (23). Recent studies in muscle have shown that agrin and laminin induce a similar lipid raft-dependent coclustering of AChR with the DAP complex at the NMJ (36-39).

Since lipid rafts have been associated with the recruitment of signalling proteins and syntrophin can bind signaling molecules such as nNOS, Grb2, guanine nucleotide-binding protein alpha subunit (protein Gα), stress-activated protein kinase-3 (ERK6), microtubule-associated serine/threonine kinase, syntrophin-associated serine/threonine kinase, ARMS and diacylglycerol kinase-zeta (40-49), we hypothesize that the laminin-mediated coclustering of DG, AQP4 and lipid rafts is associated with the recruitment of signalling molecules and their level of phosphorylation at these clusters.

In the present study, we set out to characterize the signalling events involved in the coclustering of DG and AQP4 upon laminin treatment. Here we used immunofluorescence and immunoblot analyses to examine the dynamic and alterations of DG and AQP4 clustering in astrocytes treated with laminin after using selective kinase inhibitors. We hypothesized that the coclustering of lipid rafts with the laminin-induced clusters of DG and AQP4 as we previously reported (23) may be associated with the activation of signaling cascades. Indeed, our data show an increase in tyrosine phosphorylation approximately at 3 hours following laminin treatment coinciding with the time where laminin-induced clustering of DG, AQP4 and GM1, reaches a

"plateau". In addition, we show that laminin induces the formation of phosphotyrosine-rich clusters that are reminiscent of laminin clusters. Incubation with the tyrosine kinase inhibitor, genistein, induces a significant decrease in DG and AQP4 clustering. Furthermore, we used antibody-based microarrays which allowed us to identify both the proline-rich/Ca^{2+}-activated tyrosine kinase 2 (Pyk2) and the protein-serine kinase C delta (PKCδ) as two of the main kinases exhibiting a high increase in tyrosine phosphorylation upon laminin treatment. Using specific inhibitors, we also demonstrated that PKCδ is the only enzyme involved in the laminin-induced clustering of AQP4. Signalling through PKC was found to be a regulator of not only the coalescence of the laminin-induced clusters of AQP4 and DG but also AQP4-mediated water transport in astrocytes treated with laminin.

5.2 Materials and methods

5.2.1 Antibodies

The following antibodies were used in the present study: rabbit anti-AQP4 against rat GST AQP4 corresponding to residues 249–323 (Alomone Laboratories, Jerusalem, Israel), rabbit anti-laminin against purified mouse Engelbreth-Holm-Swarm (EHS) Sarcoma laminin that recognizes laminin α1, β1 and γ1 chains, mouse anti-β-DG, 43DAG1/8D5, against the 15 of the last 16 amino acids at the C-terminus of the human dystroglycan sequence (Novocastra Laboratories, Newcastle, UK), rabbit anti-PKCδ against synthetic peptide corresponding to residues 662-673 (Abcam), anti-phospho-PKCδ against synthetic phospho-peptide from residues surrounding Y311 (Abcam), rabbit anti-Pyk2 against human GST Pyk2 corresponding to residues 726-863 (Upstate), rabbit anti-phospho-Pyk2 against the phosphorylated isoform Y579 (Upstate), anti-FAK, mouse anti-phosphotyrosine, 4G10, against phosphotyramine-KLH (Upstate) and mouse anti-β-actin against a synthetic β-actin N-terminal peptide (Sigma-Aldrich, St. Louis, MO, USA).

5.2.2 Astrocyte primary cultures

Primary hippocampal astrocyte cultures were prepared from postnatal day 1 Sprague-Dawley rats (Charles River). Hippocampi were dissected, and meninges and choroid plexus were removed. They were then cut into small pieces and incubated for 25 min with trypsin (3.0 mg/ml; Gibco, Burlington, Canada). Dissociated cortices were then plated in culture flasks and grown in Dulbecco's modified Eagle's medium (DMEM) supplemented with 10% fetal bovine serum, 1% penicillin-streptomycin and 1 mM L-glutamine (Gibco) for 2-3 weeks. The culture medium was changed every 3 days. To remove microglia and oligodendrocyte progenitors, the flasks were shaken the day following the plating. After trypsinization, the cells were plated on glass coverslips coated with poly-D-lysine (0.1 mg/ml; Sigma) in 24-well plates at a density of 200-250x10^3 cells/ml. Two days after plating, the cells were treated for every hour up to 8 hours with 15 nM Engelbreth-Holm-Swarm Sarcoma laminin-1 (Sigma-Aldrich, St. Louis, MO, USA) in the absence of serum.

5.2.3 siRNA transfections

Astrocytes were transfected in suspension before plating with 100 nmol/l Pyk2 siRNAs (ON-TARGETplus SMARTpool siRNA reagents; Dharmacon, USA) and control siRNA (ON-TARGETplus siCONTROL nontargeting siRNA; Dharmacon) using Lipofectamine-2000 (Invitrogen, USA), following the manufacturer's protocol. One day and a half after plating, astrocytes were treated for 4 hours with 15 nM of laminin-1 and subsequently analyzed by immunofluorescence.

5.2.4 Drug treatments

For the tyrosine kinase inhibition experiments, the cells were incubated in the presence of 50 µM genistein (Calbiochem), 0.5 µg/ml herbimycin (Calbiochem) or with 5 nM staurosporin (Calbiochem) for 4 hours at 37°C in the presence of laminin. For the specific inhibition of Pyk2 or PKCδ, the cells were incubated in the presence of 50 µM dantrolene (Calbiochem), and 0.15-0.30 µg/ml Ro 31-8220 (Sigma) or 1.5-3 µg/ml GF-109203 (Sigma), respectively.

5.2.5 Kinex antibody microarray preparation

Primary hippocampal astrocytes were treated or not with 15 nM laminin for 3 hours. The cells were washed twice in ice-cold PBS and then sonicated in Kinex lysis buffer (20 mM MOPS, 1% Triton X-100, 2 mM EGTA, 5 mM EDTA, 30 mM NaF, 1 mM Na_3VO_4, 1 mM phenylmethylsulfonyl fluoride, 5 μM pepstatin A, 1x complete protease inhibitor mixture (Roche Applied Science), 1 mM DTT). 100 μg of cleared lysate protein from control and laminin-treated astrocytes were shipped to Kinexus Bioinformatics Corporation (Vancouver, Canada) for Kinex antibody microarray services.

5.2.6 Immunofluorescence

Cells were washed and incubated for 25 minutes at 4°C with chilled phosphate-buffered saline (PBS) containing 10 μg/ml FITC-conjugated cholera toxin subunit B (CtxB, Sigma). Then, they were rinsed with warm PBS and fixed by immersion in 4% (w/v) paraformaldehyde in 0.1 M phosphate buffer for 20 min followed by rinsing in PBS, 3 x 15 min. The cells were incubated for 1 h at room temperature (20–22°C) in a solution containing 2% bovine serum albumin (Sigma) and 0.25% Triton X-100. Double immunolabelling was performed by incubating the cells at room temperature for 1 h in the presence of primary antibodies against β-DG (1/25) and laminin (1/1500) or AQP4 (1:200), phosphotyrosine 4G10 (1:400) and laminin (1/1500), β-DG (1/25) and phospho-PKCδ (1/100). Subsequently, they were rinsed with PBS (3 x 15 min) and incubated with Alexa Fluor 568 goat anti-mouse IgG and Alexa Fluor 647 goat anti-rabbit, Alexa Fluor 488 goat anti-mouse IgG and Alexa Fluor 568 goat anti-rabbit IgG or Alexa Fluor 568 goat anti-mouse IgG and Alexa Fluor 488 goat anti-rabbit IgG for 1 h (1/200; Molecular Probes, USA). After several washes with PBS, coverslips were mounted on glass slides using Prolong Gold Antifade Reagent with or without 4', 6-diamidino-2-phenylindole (Invitrogen, Burlington, ON, Canada). To confirm the specificity of the labeling, control cells were treated equivalently in the absence of primary antibodies. Fluorescent labeling of cultured cells was visualized using a confocal microscope (Fluoview 1000; Olympus) and an Uplan Apochromat 1.35 NA 60× objective (Olympus).

5.2.7 Immunoblotting

Astrocyte cultures were harvested and lysed on ice for 20 min in extraction buffer (25 mM Tris pH 7.4, 25 mM glycine and 150 mM NaCl) containing 1% Triton X-100, 1 x complete protease inhibitor cocktail, 1 mM phenylmethylsulfonylfluoride, 1 mM sodium orthovanadate, 30 mM sodium fluoride, 20 mM sodium pyrophosphate and 5 mM EDTA. Nuclei and cellular debris were removed from the suspension by centrifugation at 16,000 g for 10 min. Extracted proteins were denatured by boiling for 9 min in reducing sample buffer and then loaded on a 10% sodium dodecyl sulfate-polyacrylamide electrophoresis gels. The gels were electrotransferred to nitrocellulose membranes (Bio-Rad, Mississauga, ON, Canada) and the blots were probed with antibodies to phosphotyrosine (1/1000), PKCδ (1/500), phospho-PKCδ (1/500), β-DG (1/300), AQP4 (1/1000), Pyk2 (1/1000), phospho-Pyk2 (1/1000), FAK (1/1500) and β-actin (1/20000). Bound antibodies were detected using horseradish peroxidase-conjugated goat anti-rabbit IgG or goat anti-mouse IgG (1/2000; Jackson ImmunoResearch, USA). Signals were visualized on Bioflex econo films (Interscience, Markham, ON, Canada) using chemiluminescence (Amersham Biosciences, Buckinghamshire, UK).

5.2.8 Water permeability measurements

For water permeability measurements, cells were grown on round coverglasses and loaded with calcein by incubation for 45 min with 6 μM calcein-AM (Molecular Probes) at 37°C. Loading of calcein was similar in all the conditions tested. After being rinsed in PBS (pH 7.4), the coverglasses were mounted in a perfusion chamber on the stage of a two-photon laser-scanning microscope Zeiss LSM510-Axioskop-2 fitted with a 40X-W/0.80 numerical aperture objective lens directly coupled to a Mira Ti:sapphire laser (∼100-fs pulses, 76 MHz, pumped by a 5 W Verdi laser; Coherent) which continuously measured calcein fluorescence. The cells were perfused with isotonic CSF 330 mOsm (120 mM NaCl, 3.3 mM KCl, 26 mM NaHCO$_3$, 1.3 mM MgSO$_4$, 1.2 mM NaH$_2$PO$_4$, 1.8 mM CaCl$_2$ and 11 mM D-Glucose) and scanned every 3.4 s with excitation at 835 nm. An in-line heater/cooler was constructed in which perfusate passed through 80 cm of tubing enclosed by a water jacket with circulating fluid. Effluent temperature was monitored via an in-line thermistor. The fluorescent signal which has large two-photon absorption cross-sections, were excited at 835–840 nm and epifluorescence was detected with

external detectors with 560 nm from the optical slice within the cell body. The cells were then subjected to an osmotic shock by switching the perfusate to a hypoosmotic, 250 mOsm, CSF, obtained by omission of 40 mM NaCl from the isotonic solution. Solution osmolarities were measured using a freezing point-depression osmometer and perfusion solutions were gravity pumped with a flow rate of approximately 4ml/min as used in water transport measurements. The swelling of the cells was monitored as a decrease of calcein fluorescence, which occurs as a result of the dilution of the fluorophore and a reduction of self-quenching (50-54).

5.2.9 Quantitative analyses

The number of clusters and surface area of the DG, AQP4 and laminin clusters were determined on images subjected to a threshold using ImagePro Plus software (Media Cybernetics, Inc.). Pictures from the same experiment were captured using identical acquisition parameters and subjected to the same threshold. Statistical analyses were performed using GraphPad Prism 3.00 software and unpaired Student's t-test.

On receiving the Kinex protein microarray data, we created a corrected fold change to account for error in the replicates and stringently selected candidate proteins with a true increase that was outside the error limits of replicates. Using the data provided by Kinexus, we calculated our corrected fold change = [(average intensity of treated samples - % error of replicates) / (average intensity of control samples + % error of replicates)]. This corrected fold change was used to rank the candidate proteins, and those with a corrected fold change of >1.5 was selected for further investigation.

5.3 Results

We previously described the formation of large clusters containing lipid rafts, AQP4 and DG following astrocyte treatment with extracellular laminin-1. Several lines of evidence point to a role of ECM in regulating raft-associated signalling (55-58). We hypothesize that the laminin-induced redistribution of lipid rafts and coclustering with the DAP complex in astrocytes provides a signalling platform that promotes the formation of AQP4-rich clusters in astrocytes.

In the present study, we focused on the identification of candidate signalling molecules that may regulate this process.

5.3.1 Modulation of protein phosphorylation by laminin and implication in DG and AQP4 cluster formation

We carried out a time-dependent study of the laminin-induced clustering of GM1, β-DG and AQP4 every hour following the laminin treatment from 1 to 8h. We found that the maximum clustering of GM1 and AQP4 reaches a "plateau" at 3h following laminin treatment and that this was preceded by the clustering of β-DG and laminin that occurs 1h earlier (Fig. 5.1 and Appendix K). However, the maximum area of the clusters of GM1, AQP4, β-DG and laminin reaches a "plateau" at 5h after laminin treatment (Fig. 5.1V). Together these results indicate a primary assembly of DG and laminin into clusters followed by AQP4 and GM1 clustering.

The immunoblot analysis of the tyrosine phosphorylation revealed an increase between 3-4h in laminin-treated compared to untreated astrocytes (Fig. 5.3A). In addition, astrocytes were coincubated with laminin and either genistein or herbimycin, two commonly used tyrosine kinase inhibitors. We found that while herbimycin did not alter the level of tyrosine phosphorylation, genistein decreased it significantly (Fig. 5.3A), suggesting that the laminin-induced increase in tyrosine phosphorylation is tyrosine kinase dependent. We subsequently studied the effect of tyrosine kinase inhibition on the formation of DG and AQP4 clusters. These inhibitors were coincubated with laminin and the clustering was assessed after 4 hours by immunofluorescence. Figure 5.3C and E shows that the degree of DG and AQP4 clustering was greatly altered upon genistein treatment. These results suggest the requirement of tyrosine kinase activity in the laminin-induced coclustering of DG with AQP4.

Figure 5.1 Laminin-induced clustering of GM1, β-DG, and AQP4 is time-dependent. Rat hippocampal astrocytes incubated in the absence (**A**-**D**) or the presence (**E**-**T**) of 15 nM laminin were first labeled for GM1 using FITC-CtxB (**A, E, I, M** and **Q**) and then double immunolabeled for β-DG (**B, F, J, N** and **R**) and AQP4 (**C, G, K, O** and **S**). Scale bar, 30 μm. Quantitative analysis of the laminin-induced GM1, β-DG, laminin and AQP4 clusters (**U** and **V**). The histograms represent the mean number of clusters ±SE (**U**) and surface area of clusters ±SE (**V**) in astrocyte cultures treated with laminin for 0 to 8 hours from three different experiments. All quantifications were performed on 15 fields acquired randomly from each experiment.
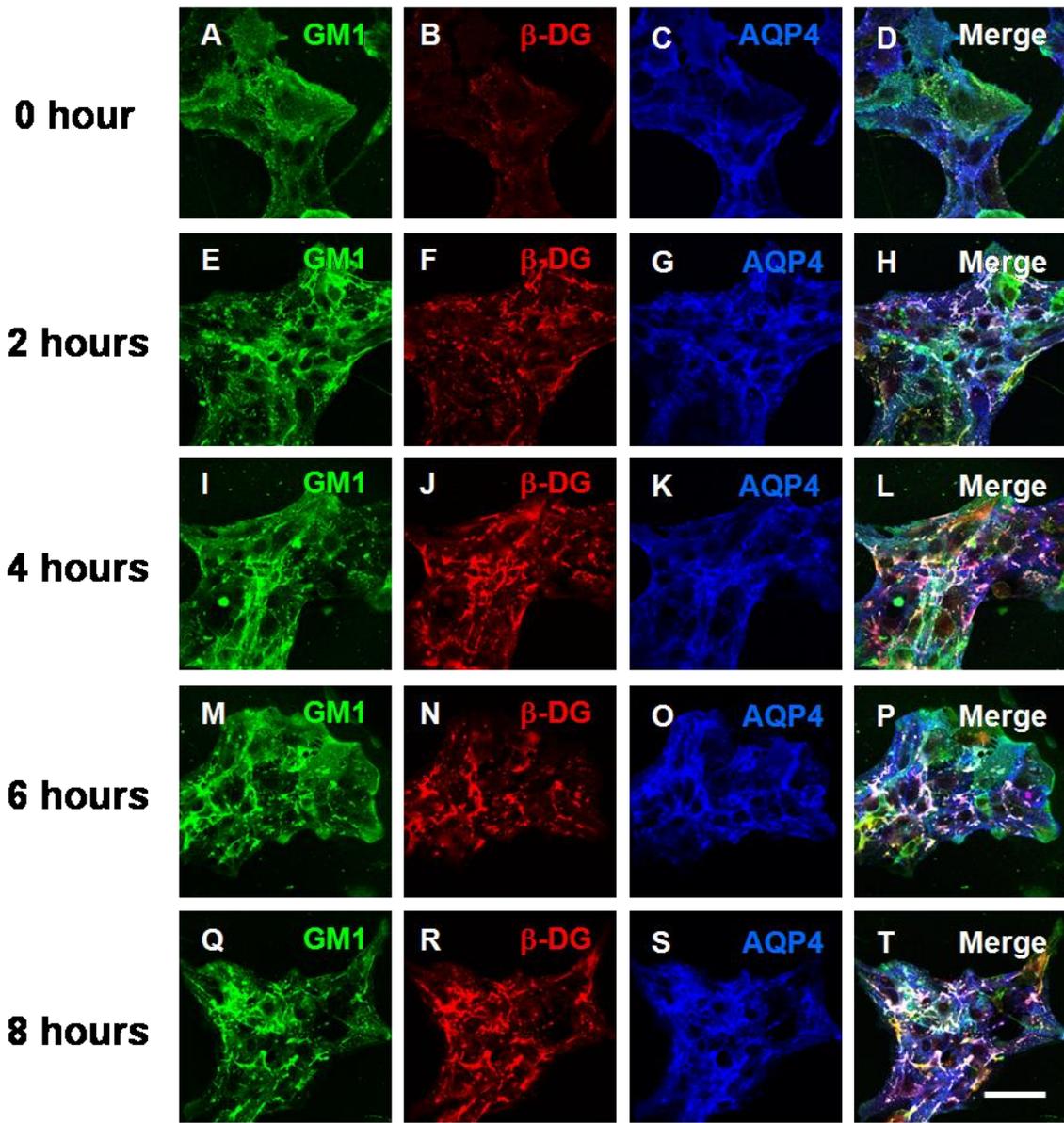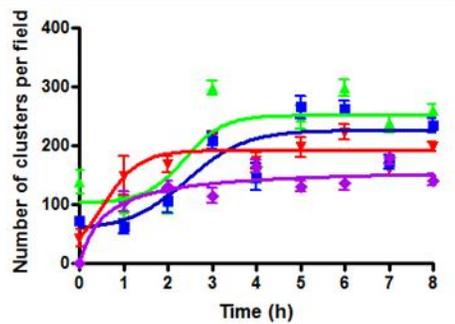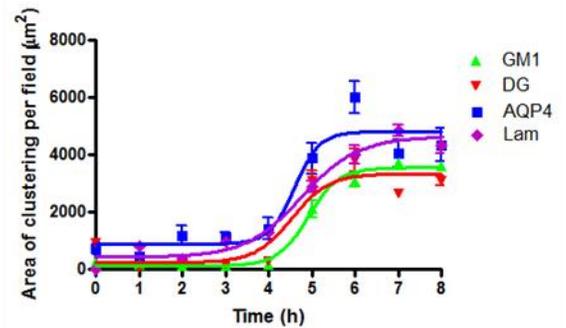
Figure 5.2 The laminin-induced increase in tyrosine phosphorylation and clustering of β-DG and AQP4 are prevented by the tyrosine kinase inhibitor, genistein. Astrocytes were incubated in the presence (**+LAM**) or the absence (**-LAM**) of 15 nM laminin for 3 hours either alone or with 0.5 µg/ml herbimycin (+**LAM** +**Herb**) or 50 mM genistein (+**LAM** +**Gen**). Protein extracts were immunoblotted for phosphotyrosine (**PY**). A representative blots from three independent experiments is shown (**A**). Rat hippocampal astrocytes incubated in the presence of 15 nM laminin alone (+**LAM, B, D** and **F**) or with 50 µM genistein (+**LAM** +**Genistein, C, E** an**d G**) were double immunolabeled for β-DG (**B** and **C**) and AQP4 (**D** and **E**). Scale bar, 30 µm.

A.

Blot: PY

+LAM   +Genistein +LAM

B β-DG   C β-DG

D AQP4   E AQP4

F Merge   G Merge
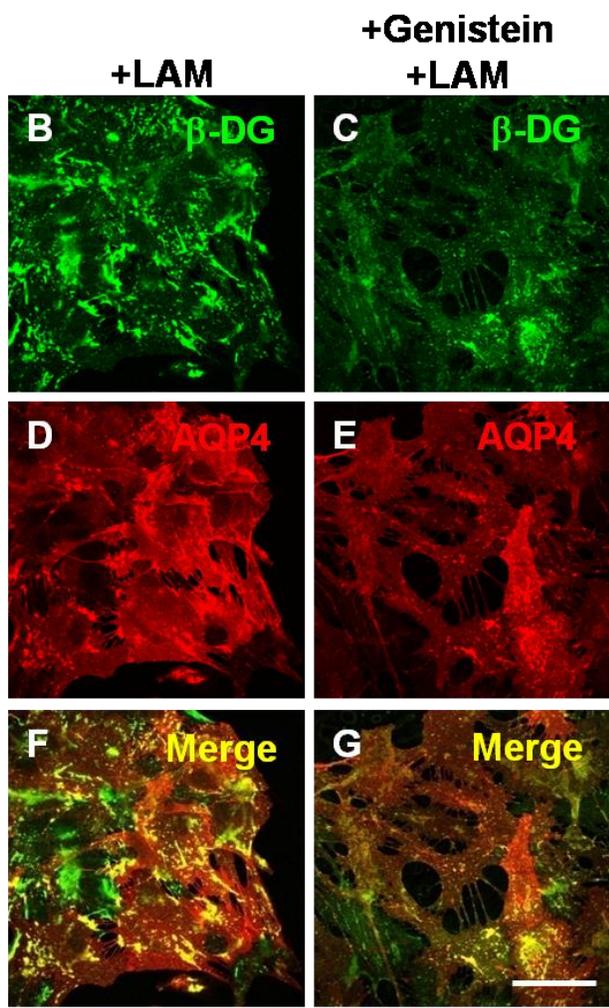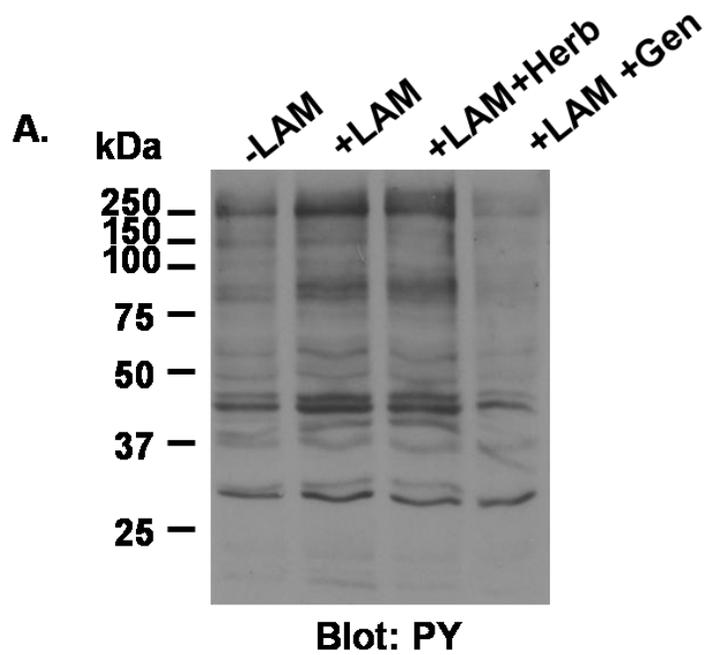
5.3.2 Reorganization of the tyrosine phosphorylation labeling upon laminin treatment and identification of Pyk2 and PKC as the main targets of tyrosine phosphorylation

To investigate the effect of laminin on the organization of tyrosine phosphorylated proteins, we labeled laminin-treated astrocytes for tyrosine phosphorylated proteins and quantified their clustering. We show that laminin enhanced tyrosine phosphorylation labeling, induced clustering of tyrosine phosphorylated proteins, and that some of these clusters codistributed with laminin clusters (Fig. 5.3).

Quantitative analysis revealed over 1.6-fold increase in the number of phosphotyrosine clusters in the laminin-treated compared to the untreated astrocytes reminiscent of the increase in the number of β-DG, laminin, GM1 and AQP4 clusters, as previously reported (Fig. 5.3G). It is important to note here that we previously demonstrated that laminin does not induce a detectable change in the morphology of astrocytes as laminin-treated astrocytes presented a flat and polygonal shape similar to that of control untreated astrocytes as assessed by WGA labeling (23). Together these data show that the laminin treatment of astrocytes induces an increase in protein tyrosine phosphorylation and that reorganization into clusters of these phosphotyrosine proteins is associated with their increase.

In parallel experiments, we screened for signalling molecules to identify those that exhibit increased phosphorylation upon laminin treatment using the Kinexus antibody KAM-1.1 microarray. Such an approach allowed us to identify both the proline-rich/Ca^{2+}-activated tyrosine kinase 2 (Pyk2) and the protein-serine kinase C delta (PKCδ) as two of the main proteins for which tyrosine phosphorylation increases upon laminin treatment (Fig. 5.4). Figure 5.4 shows that Pyk2 phosphorylation on tyrosine 579 and PKCδ on tyrosine 313 (or 311 in human compared to rats) are enhanced by which reach 1.51 and 2.21, respectively. Together these results identify Pyk2 and PKCδ as two different kinases which phosphorylation is activated by laminin.
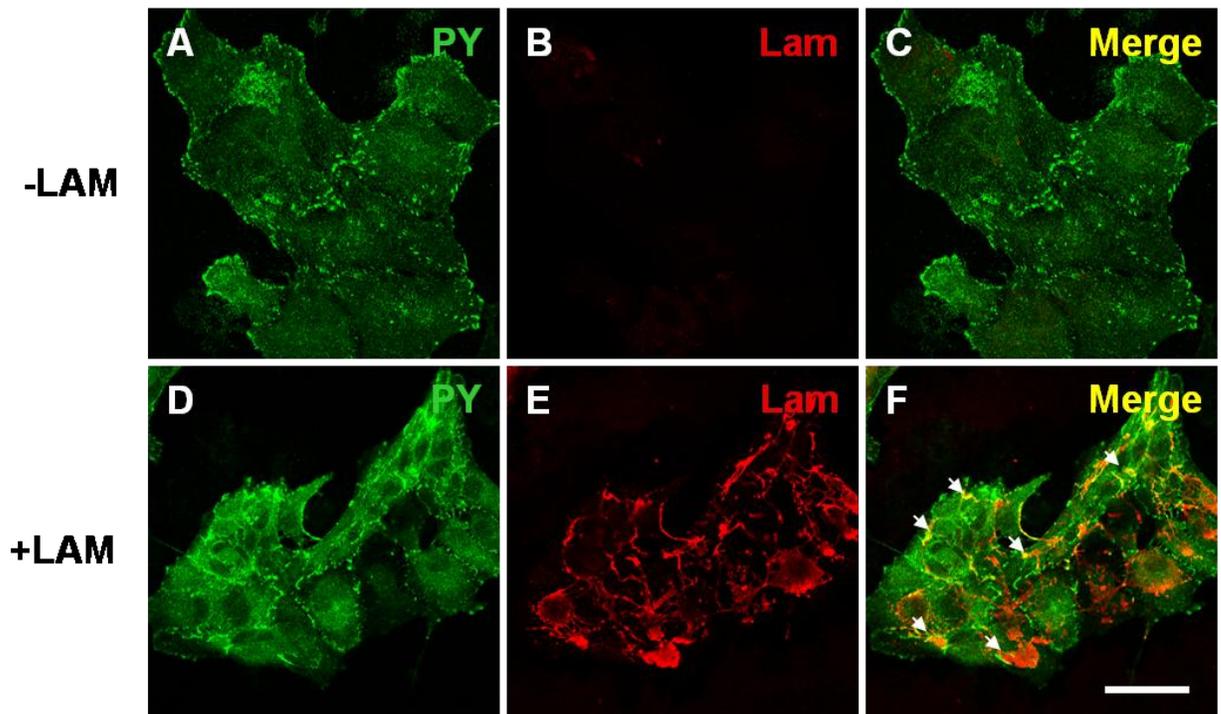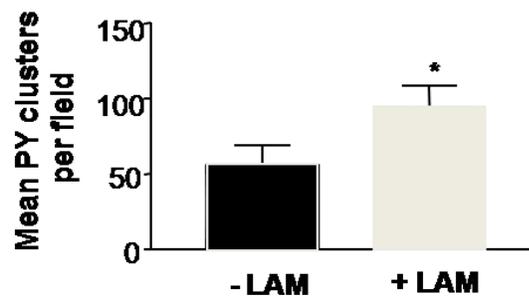
Figure 5.3 Laminin organizes phosphotyrosine protein distribution into clusters in astrocytes. Rat hippocampal astrocytes incubated in the absence (**-LAM, A**-**C**) or the presence of 15 nM laminin (+**LAM, D**-**F**) were labeled for phosphotyrosine (**PY; A** and **D**) and laminin (**B** and **E**). Scale bar, 30 μm. Quantitative analysis of the laminin-induced clustering of phosphotyrosine (**G**). The histograms represent the mean number of clusters ±SE in astrocyte cultures treated with laminin for 3 hours from three different experiments. All quantifications were performed on 15 fields acquired randomly from each experiment.
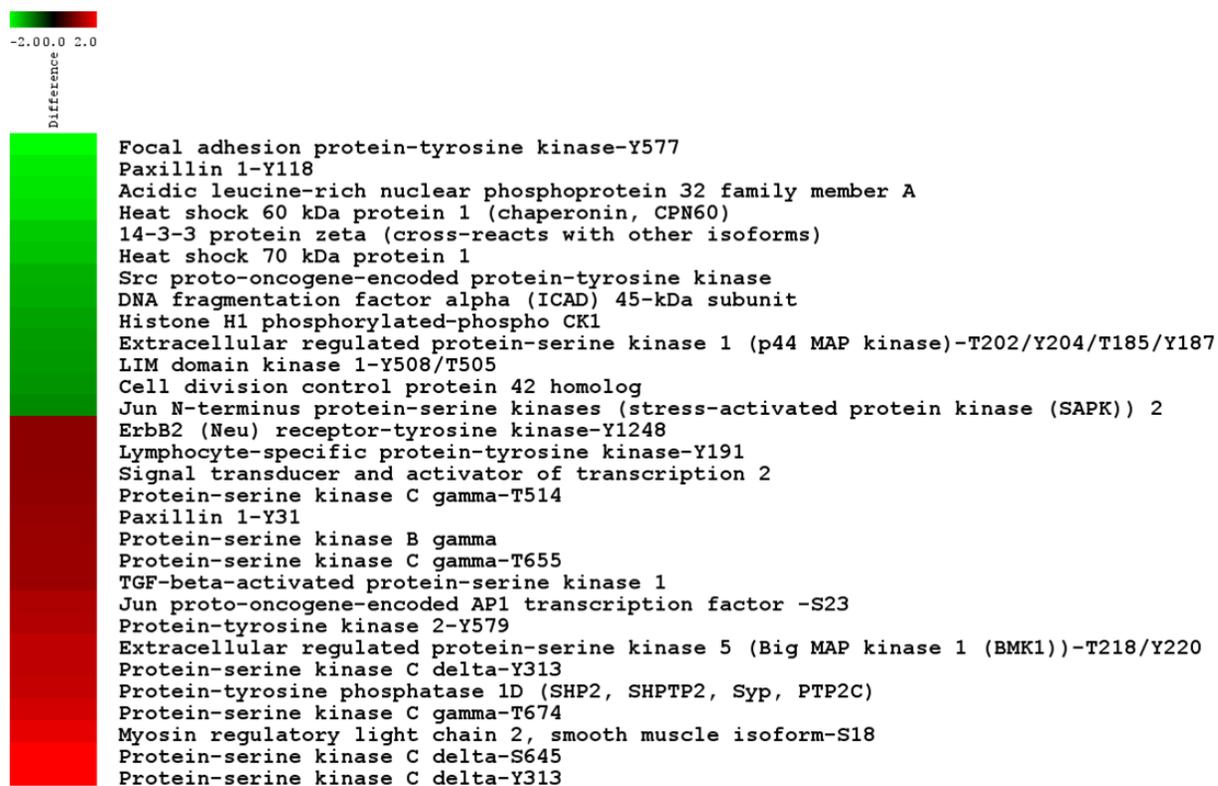
Figure 5.4 Laminin induces changes in the expression of signaling molecules as identified by the Kinexus antibody KAM-1.1 microarray chip. Equal amounts of protein extracts from laminin-treated astrocytes labeled with Cy5 and untreated astrocytes labeled with Cy3 were applied to separate antibody chips. Red and green represent the ratios of proteins from laminin-treated astrocytes over untreated astrocytes which expression increases and decreases, respectively. Note that the protein-serine kinase C δ undergoes a high level of tyrosine phosphorylation on residue Y313.

5.3.3 Involvement of PKC but not Pyk2 in the laminin-induced coclustering of DG and AQP4

Implication of Pyk2 and PKCδ in the laminin-induced clustering of the DAP complex with AQP4 was first investigated by confirming the increase signal by western blot of the two phosphoisoforms of these kinases and second by their localization by immunofluorescence in astrocytes treated with laminin. Appendix L shows that the phosphorylation of Pyk2 on tyrosine 579 is clearly increased in the presence of laminin and that the level of total Pyk2 remains unchanged. We therefore asked whether Pyk2 had a role in the laminin-mediated clustering of DG and AQP4. To address this question, we used the general inhibitors of tyrosine phosphorylation, staurosporin, herbimycin and genistein. Appendix L shows that both staurosporine and genistein prevented the increased tyrosine phosphorylation of Pyk2 in laminin-treated astrocytes. These results indicate a similar effect of genistein on the tyrosine phosphorylation, the laminin-induced clusters of DG (Fig. 5.2) and the phosphorylated form of Pyk2.

Alternatively, siRNA to silence the Pyk2 gene (siPyk2) was used and we determined whether this knock-down altered the laminin-mediated clustering of DG and AQP4 by quantitative fluorescence analysis. First, we assessed by western blot the efficiency of the siPyk2 transfection and found that Pyk2 expression was significantly decreased (Appendix L). Pyk2 could not be detected in the siPyk2 transfected cells when compared to the control scrambled siRNA transfected astrocytes (siCTL; Appendix L) and untransfected astrocytes (data not shown). The data obtained here show a high efficiency of siPyk2 gene silencing at 2 days post-transfection but this silencing did not show any effect on AQP4 clustering (Appendix L) and similar results were obtained using dantrolene, a selective Pyk2-specific inhibitor (data not shown). Previous studies have suggested a compensation of Pyk2 loss by the focal adhesion kinase (FAK) in different *in vitro* system and that FAK could interact with DG (59). Since these two kinases have been shown to be involved in polarization of cellular compartment, we therefore assessed the level of FAK in siPyk2 in astrocytes. Appendix L shows that the level of FAK does not increase in the siPyk2-transfected astrocytes and suggests that FAK does not compensate for the loss of Pyk2 in astrocyte cultures.

We then investigated the role of PKCδ in the laminin-induced clustering of DG and AQP4. Western blot analyses confirm the data obtained from the microarray analysis showing a high level of phosphorylation on tyrosine 311 of PKCδ (Fig. 5.5A). We also examined the localization of the phosphorylated form of PKCδ in astrocytes and found that PKC-δ-Y311 distribution is altered in laminin-treated astrocytes (Fig. 5.5E) and that PKC-δ-Y311 presented some colocalization with β-DG (Fig. 5.5 C-G). Based on this laminin-induced colocalization of PKC-δ-Y311 with the β-DG clusters, we examined quantitatively whether the PKC activity is involved in the DG/AQP4 clustering. To disrupt PKC activity, we used two commonly used selective PKC inhibitors, GF-109203 and Ro 31-8220 (Fig. 5.6). Astrocytes treated both with laminin and GF-109203 or laminin and Ro 31-8220 were fluorescently labeled for β-DG and AQP4. We found that the number of β-DG clusters increased upon the incubation with these inhibitors but that the total area occupied by these clusters decreased, suggesting a break-down of DG clusters (Fig. 5.6A, D, G and K). However, Figure 5.6 B, E, H and J show that both the number and area of AQP4 clusters decreased. Together these results suggest that GF-109203 and Ro 31-8220 prevent the coalescence of β-DG clusters upon laminin treatment with a concomitant block of AQP4 clustering confirming the dynamic of DG and AQP4 clustering.

5.3.4 Modulation of AQP4 function by PKC

It has been previously shown that the phosphorylation of AQP4 by PKC modulates the water permeability of this water permeable channel (51,60-66). This raises the question of whether laminin regulates AQP4 phosphorylation and whether this phosphorylation is implicated in its functional properties.

We previously showed that laminin treatment of astrocytes leads to a decrease in cell swelling upon hypoosmotic shock (data presented in chapter 3). We therefore used a similar assay to test whether inhibition of PKC in presence of laminin could alter the hypoosmotic-induced cell swelling. Astrocytes were thus loaded with calcein and subjected to a hypoosmotic chock for 60 seconds by dropping the osmolarily of the CSF from 300 mOsm to 250 mOsm. Figure 5.7A-I shows a time lapse representation of the calcein signal during 360 seconds

Figure 5.5 Laminin induces an increase and redistribution in phospho-PKCδ in astrocytes. Astrocytes were incubated in the presence (**+LAM**) or absence (**-LAM**) of 15 nM laminin-1 for 3 hours. Protein extracts were immunobloted for phospho-PKCδ, PKCδ and β-actin. A representative blot from three independent experiments is shown (**A**). Rat hippocampal astrocytes incubated in the absence (**-LAM**, **B, D** and **F**) or presence of 15 nM laminin (**+LAM, C, E** and **G**) were double immunolabeled for β-DG (**B** and **C**) and phospho-PKCδ (**D** and **E**). Scale bar, 30 μm.
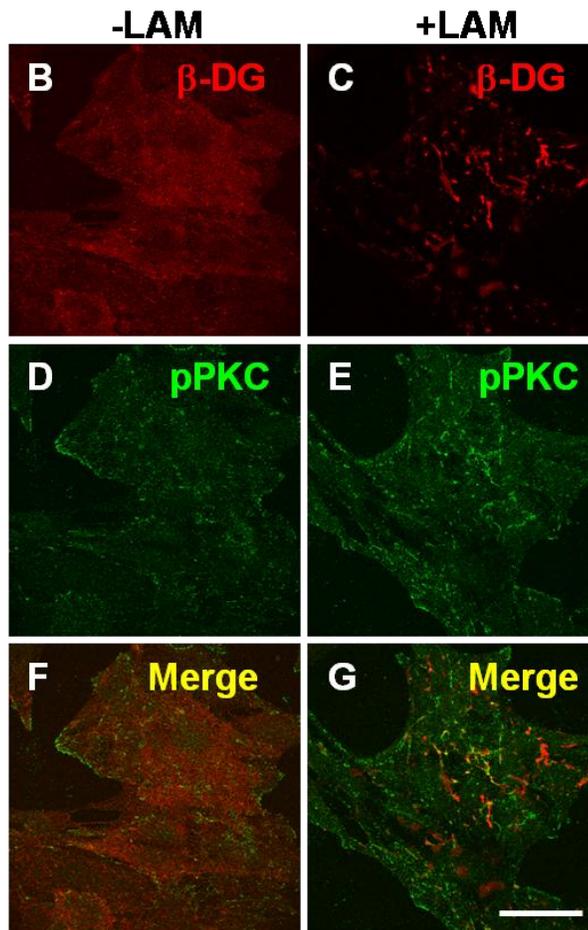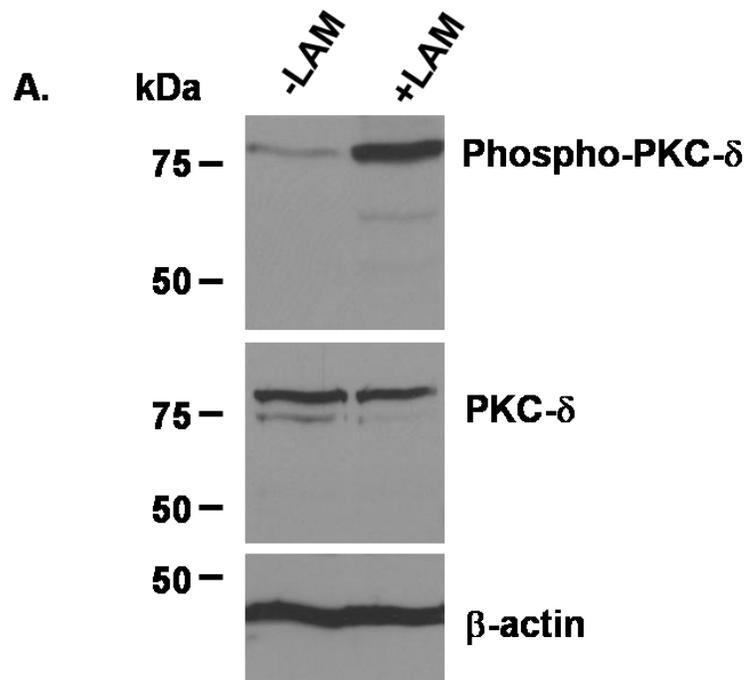
Figure 5.6 PKC inhibitors, Ro 31-8220 and GF-109203, prevent the laminin-induced clustering of β-DG, and AQP4. Rat hippocampal astrocytes incubated in the presence of 15 nM laminin alone (+**LAM**) or with 3 μg/ml GF-109203 (+**LAM** +**GF**) or 0.30 μg/ml Ro 31-8220 (+**LAM** +**Ro**) were double immunolabeled for β-DG (**A, D** and **G)** and AQP4 (**B, E** and **H)**. Scale bar, 30 μm. **J** and **K.** Quantitative analysis of the laminin-induced clustering of β-DG and AQP4. The histograms represent the mean number of clusters ±SE and surface area of clusters ±SE of AQP4 (**J**) and β-DG (**K**) clusters in astrocyte cultures treated with laminin and 1.5-3 μg/ml GF-109203 or 0.15-0.30 μg/ml Ro 31-8220 for 3 hours from three different experiments. All quantifications were performed on 15 fields acquired randomly from each experiment.

157
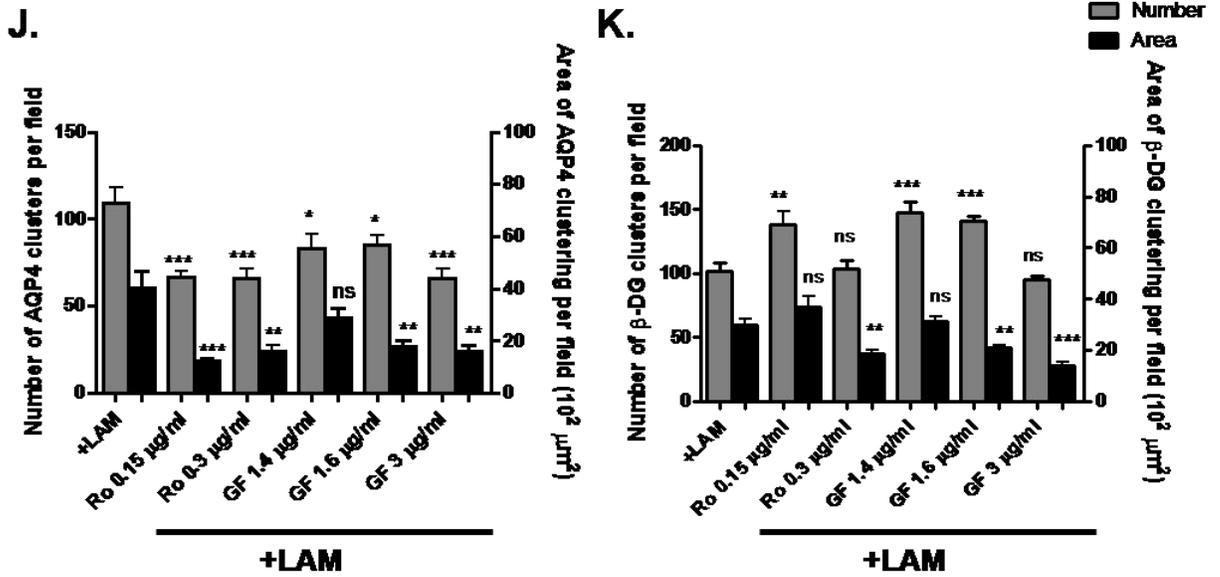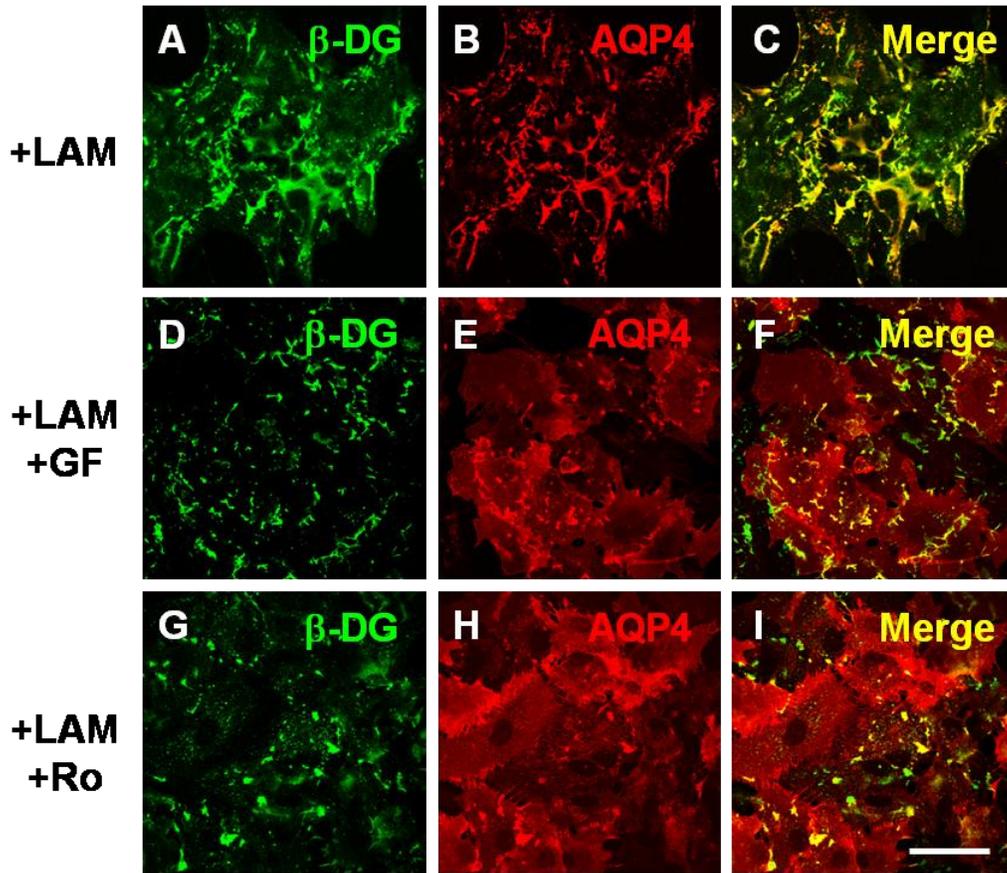
Figure 5.7 Cell volume measurements in cultured astrocytes. Calcein-loaded astrocytes in the x-y plane were recorded from 0 to 300 seconds after incubation with (+**LAM; D, E** and **F**) or without (-**LAM; A, B** and **C**) 15 nM laminin alone or in the presence of 0.3 µg/ml Ro 31-8220 (+**LAM +Ro; G, H and I**). Mean trace of recordings from a time series of 30 calcein-loaded astrocytes treated with (+**LAM; K**) or without (-**LAM; J**) 15 nM laminin alone or with 0.3 µg/ml Ro 31-8220 (+**LAM +Ro; K**). The buffer solution was changed from isotonic to hypotonic and from hypotonic to isotonic at 160 and 240 seconds, respectively (dotted line).
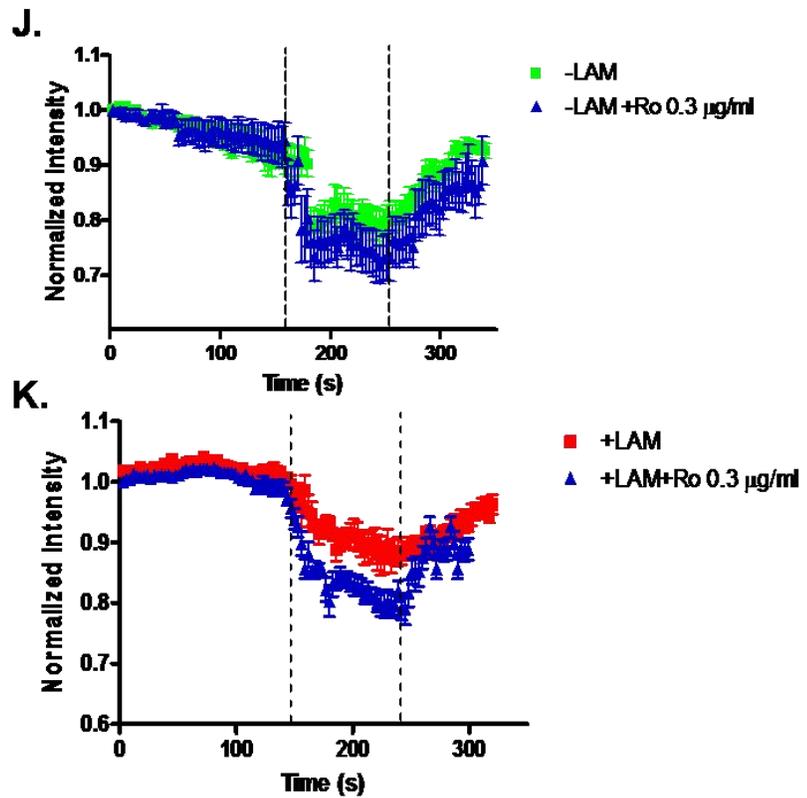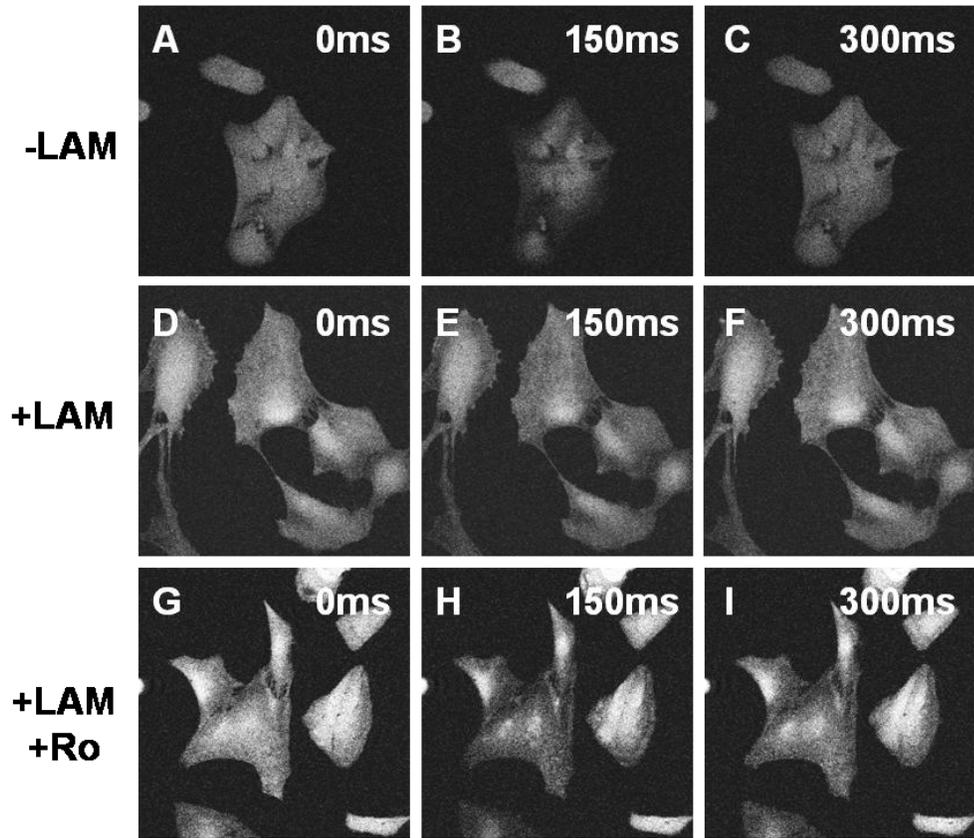
between untreated, laminin-treated and laminin and Ro 31-8220 co-treated astrocytes. We found that laminin treatment reduced the cell swelling reflected by a lower decrease in calcein-signal upon hypoosmotic chock, confirming our previous results (see chapter 3). Interestingly, the co-treatment of laminin with Ro 31-8220 led to an increased cell swelling compared to laminin alone (Fig. 5.7K). The cell swelling rescue was partial compared to the untreated control (Fig. 5.7J). Together these results suggest that laminin treatment induced PKC activation which may be a regulator of the laminin-induced clustering of AQP4 as well as AQP4-mediated water transport.

5.4 Discussion

In the present study, we show that the effect of laminin on the clustering of GM1, β-DG and AQP4 is time-dependent and reaches a "plateau" at 2h for β-DG and laminin and 3h for GM1 and AQP4 following the addition of laminin. These data indicate that laminin co-assembles with β-DG prior to the GM1-containing lipid raft and AQP4 clustering. It is noteworthy that the surface area of all these clusters reaches a maximum at the same time (5h) which suggests that even though the formation of β-DG and laminin clusters precedes that of lipid rafts, the coalescence and stabilization of β-DG and laminin clusters may be regulated by lipid raft.

Lipid rafts have received much attention in the past few years and are known to be enriched for cholesterol and sphingolipids and form liquid-ordered islands at the plasma membrane, which is composed mainly of phospholipids in liquid-disorder. Proteins that concentrate in lipid raft domains include doubly acylated proteins such as a subunits of heterotrimeric G-proteins and Src-family kinases (67). The concentration of such signalling proteins in lipid raft domains may provide a platform for a better interaction between these proteins which is necessary for coordinated signal transduction. Interestingly, it has been proposed that Src-dependent phosphorylation of β-DG on tyrosine 890 regulates SH2-SH3-mediated signalling that plays a role in membrane protrusion (68-71).

We therefore asked whether the laminin and DG-mediated clustering of lipid rafts in astrocytes was associated with specific signalling events. First, we investigated whether laminin

induces a change in tyrosine phosphorylation and found that not only it increases the level of phosphorylation on tyrosine-containing proteins but induces the formation of phosphotyrosine-rich clusters some of which colocalized with laminin clusters. We have previously shown that laminin induces the clustering of α- and β-DG but not β1-integrin (23,72) suggesting that the binding of laminin to α-DG triggers the increase in tyrosine phosphorylation.

In this study, we also show that the tyrosine kinase inhibitor, genistein, led to a decrease in laminin-induced DG and AQP4 clustering. These implicate tyrosine kinases in the clustering of the DAP complex and AQP4. Indeed, we identified the protein-serine kinase C delta (PKCδ) as one of the main kinases that undergoes a high increase in the level of tyrosine phosphorylation upon laminin treatment using the Kinexus antibody KAM-1.1 microarray chip. Using selective inhibitors of PKCδ, we found that it differentially regulates the laminin-induced clustering of β-DG and AQP4. Indeed, while PKCδ inhibition decreases the surface area of both β-DG and AQP4 clusters, it increases the number of β-DG clusters and decreases that of AQP4. A possible explanation would be that the size of β-DG clusters is a determinant factor for the formation and stabilization of AQP4 clusters at the cell surface. Interestingly, it has been shown in various studies that lipid rafts were critical for PKC activity in T cells (73-75) to mediate apoptosis-resistance (76) or contribute to inflammatory signalling (77). It has also been suggested that ceramide recruits PKC into lipid rafts (78) and that its activation can induce changes in the composition of detergent-resistant membrane domains that are representative of lipid rafts (79). Together, these data suggest that the reorganization of lipid rafts mediated by laminin is associated with the activation of PKC.

Several studies have reported the implication of protein kinases such as protein kinase A (80), Ca^{2+}/calmodulin-dependent kinase II (60) or casein kinase II (81,82) in water transport. Moreover, PKC has been shown to be a regulator of the AQP4-mediated water transport (51,61,64,65,83). Indeed, it has been suggested that phosphorylation of serine 180 (S180) inhibits AQP4-mediated water transport whereas phosphorylation of serine 111 (S111) activates it (66). Interestingly, we found that laminin-induced activation of PKC was associated with a decrease in AQP4-mediated water transport upon laminin treatment. On the contrary, the inhibition of PKC activity results in an increase in water transport in laminin-treated astrocytes. The specific mechanism regulating AQP4-mediated water transport via PKC remains unclear. It has been proposed that PKC down-regulates water transport by increasing AQP4 internalization

(63,84-86). In our case, this hypothesis seems unlikely because laminin-induces a clear cell surface clustering of AQP4. The only possibility would be that the pool of AQP4 expressed in the areas outside of the clusters may be internalized which could impede the apparent water permeability. The other hypothesis involves a differential regulation of both M1 and M23 isoforms of AQP4 by laminin (62,87-89).

In conclusion, we show in the present study that laminin regulates AQP4 clustering by facilitating the lipid raft-mediated signalling possibly associated with PKCδ. Using selective inhibitors of PKCδ, we found a dramatic disruption of β-DG and AQP4 clustering associated with an increase in AQP4-mediated water transport in astrocytes treated with laminin. These findings indicate that PKCδ not only regulates AQP4 clustering but also its role in water permeability in astrocytes.

5.5 References

1.   Petrof, B. J., Shrager, J. B., Stedman, H. H., Kelly, A. M., and Sweeney, H. L. (1993) *Proc Natl Acad Sci U S A* **90**, 3710-3714

2.   Ibraghimov-Beskrovnaya, O., Ervasti, J. M., Leveille, C. J., Slaughter, C. A., Sernett, S. W., and Campbell, K. P. (1992) *Nature* **355**, 696-702

3.   Henry, M. D., and Campbell, K. P. (1996) *Current Opinion in Cell Biology* **8**, 625-631

4.   Gee, S. H., Blacher, R. W., Douville, P. J., Provost, P. R., Yurchenco, P. D., and Carbonetto, S. (1993) *The Journal of Biological Chemistry* **268**, 14972-14980

5.   Gee, S. H., Montanaro, F., Lindenbaum, M. H., and Carbonetto, S. (1994) *Cell* **77**, 675-686.

6.   Henry, M. D., and Campbell, K. P. (1998) *Cell* **95**, 859-870

7.   Sugita, S., Saito, F., Tang, J., Satz, J., Campbell, K., and Sudhof, T. C. (2001) *J Cell Biol* **154**, 435-445

8.   Way, M., Pope, B., Cross, R. A., Kendrick-Jones, J., and Weeds, A. G. (1992) *FEBS Lett* **301**, 243-245

9.   Jung, D., Yang, B., Meyer, J., Chamberlain, J. S., and Campbell, K. P. (1995) *J Biol Chem* **270**, 27305-27310

10.   Ehmsen, J., Poon, E., and Davies, K. (2002) *J Cell Sci* **115**, 2801-2803

11.   Hayashi, Y. K., Ogawa, M., Tagawa, K., Noguchi, S., Ishihara, T., Nonaka, I., and Arahata, K. (2001) *Neurology* **57**, 115-121

12.   Kano, H., Kobayashi, K., Herrmann, R., Tachikawa, M., Manya, H., Nishino, I., Nonaka, I., Straub, V., Talim, B., Voit, T., Topaloglu, H., Endo, T., Yoshikawa, H., and Toda, T. (2002) *Biochem Biophys Res Commun* **291**, 1283-1286

13.   Beltran-Valero de Bernabe, D., Currier, S., Steinbrecher, A., Celli, J., van Beusekom, E., van der Zwaag, B., Kayserili, H., Merlini, L., Chitayat, D., Dobyns, W. B., Cormand, B., Lehesjoki, A. E., Cruces, J., Voit, T., Walsh, C. A., van Bokhoven, H., and Brunner, H. G. (2002) *Am J Hum Genet* **71**, 1033-1043

14.   Longman, C., Brockington, M., Torelli, S., Jimenez-Mallebrera, C., Kennedy, C., Khalil, N., Feng, L., Saran, R. K., Voit, T., Merlini, L., Sewry, C. A., Brown, S. C., and Muntoni, F. (2003) *Hum Mol Genet* **12**, 2853-2861

15.   Blake, D. J., Hawkes, R., Benson, M. A., and Beesley, P. W. (1999) *J Cell Biol* **147**, 645-658

16.   Moukhles, H., and Carbonetto, S. (2001) *J Neurochem* **78**, 824-834

17.   Zaccaria, M. L., Di Tommaso, F., Brancaccio, A., Paggi, P., and Petrucci, T. C. (2001) *Neuroscience* **104**, 311-324

18.   Nielsen, S., Nagelhus, E. A., Amiry-Moghaddam, M., Bourque, C., Agre, P., and Ottersen, O. P. (1997) *J Neurosci* **17**, 171-180

19.   Nicchia, G. P., Nico, B., Camassa, L. M., Mola, M. G., Loh, N., Dermietzel, R., Spray, D. C., Svelto, M., and Frigeri, A. (2004) *Neuroscience* **129**, 935-945

20.   Nico, B., Frigeri, A., Nicchia, G. P., Corsi, P., Ribatti, D., Quondamatteo, F., Herken, R., Girolamo, F., Marzullo, A., Svelto, M., and Roncali, L. (2003) *Glia* **42**, 235-251

21.   Neely, J. D., Amiry-Moghaddam, M., Ottersen, O. P., Froehner, S. C., Agre, P., and Adams, M. E. (2001) *Proc Natl Acad Sci U S A* **98**, 14108-14113

22.   Guadagno, E., and Moukhles, H. (2004) *Glia* **47**, 138-149

23.   Noel, G., Tham, D. K., and Moukhles, H. (2009) *J Biol Chem* **284**, 19694-19704

24. Campanelli, J. T., Roberds, S. L., Campbell, K. P., and Scheller, R. H. (1994) *Cell* **77**, 663-674

25. Grady, R. M., Zhou, H., Cunningham, J. M., Henry, M. D., Campbell, K. P., and Sanes, J. R. (2000) *Neuron* **25**, 279-293.

26. Jacobson, C., Cote, P. D., Rossi, S. G., Rotundo, R. L., and Carbonetto, S. (2001) *J Cell Biol* **152**, 435-450.

27. Peng, H. B., Ali, A. A., Daggett, D. F., Rauvala, H., Hassell, J. R., and Smalheiser, N. R. (1998) *Cell Adhes Commun* **5**, 475-489

28. Langenbach, K. J., and Rando, T. A. (2002) *Muscle Nerve* **26**, 644-653

29. Marangi, P. A., Wieland, S. T., and Fuhrer, C. (2002) *J Cell Biol* **157**, 883-895.

30. Sadasivam, G., Willmann, R., Lin, S., Erb-Vogtli, S., Kong, X. C., Ruegg, M. A., and Fuhrer, C. (2005) *J Neurosci* **25**, 10479-10493

31. Spence, H. J., Dhillon, A. S., James, M., and Winder, S. J. (2004) *EMBO Rep* **5**, 484-489

32. Weston, C. A., Teressa, G., Weeks, B. S., and Prives, J. (2007) *J Cell Sci* **120**, 868-875

33. Zhou, Y., Jiang, D., Thomason, D. B., and Jarrett, H. W. (2007) *Biochemistry* **46**, 14907-14916

34. Zhou, Y. W., Thomason, D. B., Gullberg, D., and Jarrett, H. W. (2006) *Biochemistry* **45**, 2042-2052

35. Sotgia, F., Bonuccelli, G., Bedford, M., Brancaccio, A., Mayer, U., Wilson, M. T., Campos-Gonzalez, R., Brooks, J. W., Sudol, M., and Lisanti, M. P. (2003) *Biochemistry* **42**, 7110-7123

36. Stetzkowski-Marden, F., Gaus, K., Recouvreur, M., Cartaud, A., and Cartaud, J. (2006) *J Lipid Res* **47**, 2121-2133

37. Stetzkowski-Marden, F., Recouvreur, M., Camus, G., Cartaud, A., Marchand, S., and Cartaud, J. (2006) *J Mol Neurosci* **30**, 37-38

38. Campagna, J. A., and Fallon, J. (2006) *Neuroscience* **138**, 123-132

39. Zhu, D., Xiong, W. C., and Mei, L. (2006) *J Neurosci* **26**, 4841-4851

40. Brenman, J. E., Chao, D. S., Gee, S. H., McGee, A. W., Craven, S. E., Santillano, D. R., Wu, Z., Huang, F., Xia, H., Peters, M. F., Froehner, S. C., and Bredt, D. S. (1996) *Cell* **84**, 757-767

41. Hasegawa, M., Cuenda, A., Spillantini, M. G., Thomas, G. M., Buee-Scherrer, V., Cohen, P., and Goedert, M. (1999) *J Biol Chem* **274**, 12626-12631.

42. Hogan, A., Shepherd, L., Chabot, J., Quenneville, S., Prescott, S. M., Topham, M. K., and Gee, S. H. (2001) *J Biol Chem* **276**, 26526-26533

43. Lumeng, C., Phelps, S., Crawford, G. E., Walden, P. D., Barald, K., and Chamberlain, J. S. (1999) *Nat Neurosci* **2**, 611-617

44. Oak, S. A., Russo, K., Petrucci, T. C., and Jarrett, H. W. (2001) *Biochemistry* **40**, 11270-11278

45. Okumura, A., Nagai, K., and Okumura, N. (2008) *FEBS J* **275**, 22-33

46. Adams, M. E., Mueller, H. A., and Froehner, S. C. (2001) *The Journal of Cell Biology* **155**, 113-122

47. Yakubchyk, Y., Abramovici, H., Maillet, J. C., Daher, E., Obagi, C., Parks, R. J., Topham, M. K., and Gee, S. H. (2005) *Mol Cell Biol* **25**, 7289-7302

48. Luo, S., Chen, Y., Lai, K. O., Arevalo, J. C., Froehner, S. C., Adams, M. E., Chao, M. V., and Ip, N. Y. (2005) *J Cell Biol* **169**, 813-824

49. Abramovici, H., Hogan, A. B., Obagi, C., Topham, M. K., and Gee, S. H. (2003) *Mol Biol Cell* **14**, 4499-4511

50. Benfenati, V., Nicchia, G. P., Svelto, M., Rapisarda, C., Frigeri, A., and Ferroni, S. (2007) *J Neurochem* **100**, 87-104

51. Han, Z., Wax, M. B., and Patil, R. V. (1998) *J Biol Chem* **273**, 6001-6004
52. Hibino, H., and Kurachi, Y. (2007) *Eur J Neurosci* **26**, 2539-2555
53. Huber, V. J., Tsujita, M., and Nakada, T. (2008) *Bioorg Med Chem*
54. Huber, V. J., Tsujita, M., Yamazaki, M., Sakimura, K., and Nakada, T. (2007) *Bioorg Med Chem Lett* **17**, 1270-1273
55. Baron, W., Decker, L., Colognato, H., and ffrench-Constant, C. (2003) *Curr Biol* **13**, 151-155
56. del Pozo, M. A., Alderson, N. B., Kiosses, W. B., Chiang, H. H., Anderson, R. G., and Schwartz, M. A. (2004) *Science* **303**, 839-842
57. Ichikawa, N., Iwabuchi, K., Kurihara, H., Ishii, K., Kobayashi, T., Sasaki, T., Hattori, N., Mizuno, Y., Hozumi, K., Yamada, Y., and Arikawa-Hirasawa, E. (2009) *J Cell Sci* **122**, 289-299
58. Ramseger, R., White, R., and Kroger, S. (2009) *J Biol Chem* **284**, 7697-7705
59. Cavaldesi, M., Macchia, G., Barca, S., Defilippi, P., Tarone, G., and Petrucci, T. C. (1999) *J Neurochem* **72**, 1648-1655
60. Gunnarson, E., Axehult, G., Baturina, G., Zelenin, S., Zelenina, M., and Aperia, A. (2005) *Neuroscience* **136**, 105-114
61. Zelenina, M., Zelenin, S., Bondar, A. A., Brismar, H., and Aperia, A. (2002) *Am J Physiol Renal Physiol* **283**, F309-318
62. Fenton, R. A., Moeller, H. B., Zelenina, M., Snaebjornsson, M. T., Holen, T., and Macaulay, N. (2009) *Cell Mol Life Sci*
63. Moeller, H. B., Fenton, R. A., Zeuthen, T., and Macaulay, N. (2009) *Neuroscience* **164**, 1674-1684
64. McCoy, E. S., Haas, B. R., and Sontheimer, H. (2009) *Neuroscience*
65. Okuno, K., Taya, K., Marmarou, C. R., Ozisik, P., Fazzina, G., Kleindienst, A., Gulsen, S., and Marmarou, A. (2008) *Acta Neurochir Suppl* **102**, 431-436
66. Yukutake, Y., and Yasui, M. (2009) *Neuroscience*
67. Resh, M. D. (1999) *Biochim Biophys Acta* **1451**, 1-16
68. Thompson, O., Kleino, I., Crimaldi, L., Gimona, M., Saksela, K., and Winder, S. J. (2008) *PLoS One* **3**, e3638
69. Sotgia, F., Lee, H., Bedford, M. T., Petrucci, T., Sudol, M., and Lisanti, M. P. (2001) *Biochemistry* **40**, 14585-14592
70. James, M., Nuttall, A., Ilsley, J. L., Ottersbach, K., Tinsley, J. M., Sudol, M., and Winder, S. J. (2000) *J Cell Sci* **113** (**Pt 10**), 1717-1726
71. Vogtlander, N. P., Visch, H. J., Bakker, M. A., Berden, J. H., and van der Vlag, J. (2009) *PLoS One* **4**, e5979
72. Noel, G., Belda, M., Guadagno, E., Micoud, J., Klocker, N., and Moukhles, H. (2005) *J Neurochem* **94**, 691-702
73. Fakhry, Y. E., Alturaihi, H., Diallo, D., Merhi, Y., and Mourad, W. (2009) *Eur J Immunol*
74. Jin, Z. X., Huang, C. R., Dong, L., Goda, S., Kawanami, T., Sawaki, T., Sakai, T., Tong, X. P., Masaki, Y., Fukushima, T., Tanaka, M., Mimori, T., Tojo, H., Bloom, E. T., Okazaki, T., and Umehara, H. (2008) *Int Immunol* **20**, 1427-1437
75. Liu, Y., Belkina, N. V., Graham, C., and Shaw, S. (2006) *J Biol Chem* **281**, 12102-12111
76. zum Buschenfelde, C. M., Wagner, M., Lutzny, G., Oelsner, M., Feuerstacke, Y., Decker, T., Bogner, C., Peschel, C., and Ringshausen, I. *Leukemia* **24**, 141-152
77. Shin, D. M., Yang, C. S., Lee, J. Y., Lee, S. J., Choi, H. H., Lee, H. M., Yuk, J. M., Harding, C. V., and Jo, E. K. (2008) *Cell Microbiol* **10**, 1893-1905

78. Fox, T. E., Houck, K. L., O'Neill, S. M., Nagarajan, M., Stover, T. C., Pomianowski, P. T., Unal, O., Yun, J. K., Naides, S. J., and Kester, M. (2007) *J Biol Chem* **282**, 12450-12457
79. Botto, L., Masserini, M., and Palestini, P. (2007) *J Neurosci Res* **85**, 443-450
80. Carmosino, M., Procino, G., Tamma, G., Mannucci, R., Svelto, M., and Valenti, G. (2007) *Biol Cell* **99**, 25-36
81. Madrid, R., Le Maout, S., Barrault, M. B., Janvier, K., Benichou, S., and Merot, J. (2001) *EMBO J* **20**, 7008-7021
82. Kadohira, I., Abe, Y., Nuriya, M., Sano, K., Tsuji, S., Arimitsu, T., Yoshimura, Y., and Yasui, M. (2008) *Biochem Biophys Res Commun* **377**, 463-468
83. Yamamoto, T., Kuramoto, H., and Kadowaki, M. (2007) *Life Sci* **81**, 115-120
84. Zhu, S. M., Xiong, X. X., Zheng, Y. Y., and Pan, C. F. (2009) *Anesth Analg* **109**, 1493-1499
85. Fazzina, G., Amorini, A. M., Marmarou, C., Fukui, S., Okuno, K., Glisson, R., Marmarou, A., and Kleindienst, A. (2009) *J Neurotrauma*
86. Tang, Y., Cai, D., and Chen, Y. (2007) *J Mol Neurosci* **31**, 83-93
87. Jung, J. S., Bhat, R. V., Preston, G. M., Guggino, W. B., Baraban, J. M., and Agre, P. (1994) *Proc Natl Acad Sci U S A* **91**, 13052-13056
88. Neely, J. D., Christensen, B. M., Nielsen, S., and Agre, P. (1999) *Biochemistry* **38**, 11156-11163
89. Silberstein, C., Bouley, R., Huang, Y., Fang, P., Pastor-Soler, N., Brown, D., and Van Hoek, A. N. (2004) *Am J Physiol Renal Physiol* **287**, F501-511

6 A HIGH THROUGHPUT SCREEN IDENTIFIES CHEMICAL MODULATORS OF THE LAMININ-INDUCED CLUSTERING OF DYSTROGLYCAN AND AQUAPORIN-4 IN PRIMARY ASTROCYTES[5]

6.1 Introduction

Cerebral edema with excess accumulation of water and cellular swelling is a common consequence of stroke, traumatic brain injury, brain tumor and meningitis. In the normal brain, water is distributed between cerebrospinal fluid, blood, intracellular and interstitial compartments and moves between these compartments in response to osmotic gradients. In pathological conditions, the abnormal accumulation of water in brain parenchyma gives rise to either cytotoxic or vasogenic edema (1). Cytotoxic edema is seen in early cerebral ischemia and is primarily characterized by an increase in astrocyte volume due to enhanced water flux from the bloodstream into these cells. Vasogenic edema is often seen following brain tumor formation and is characterized by enhanced water entry in the interstitial compartment of the brain due to disruption of the blood-brain barrier (1).

Aquaporin-4 (AQP4), the principal water channel in the brain, is mainly expressed at the interface between the brain tissue and the blood at the perivascular astrocyte endfeet (2). Recent studies in the AQP4 knockout or overexpressing mice demonstrated a dual role for AQP4 in the pathophysiology of brain edema (1,3-7). Indeed, there is increasing evidence that AQP4 deficiency is associated with reduced water entry into the brain and reduced water outflow from the brain parenchyma in edema models that include water intoxication, focal cerebral ischemia, bacterial meningitis, cortical freeze-injury and brain tumor (1,4). Because AQP4 permits bidirectional water transport it has been shown that it plays a role not only in the early accumulation of water in cytotoxic edema (4) but also in the removal of excess water in vasogenic edema (1,8-10). Therefore, blocking AQP4 or inhibiting its clustering around blood vessels would reduce water entry which may be beneficial in preventing cytotoxic edema at early stages of stroke. On the contrary, activating AQP4 or increasing its clustering around blood vessels would promote the extrusion of the excess water from the brain preventing thereby vasogenic edema.

[5]A version of this chapter has been submitted for publication. Noel G., Stevenson S. and Moukhles H. (2010) A high throughput screen identifies chemical modulators of the laminin-induced clustering of dystroglycan and aquaporin-4 in primary astrocytes.

Several studies have focused their effort in designing drugs that specifically inhibit AQP4 function (11-17). To date, only three drugs, tetraethylammonium (TEA), 6-ethoxybenzothiazole-2-sulfamide (EZA) and acetazolamide (AZA) have been identified as potential inhibitors of AQP4 activity. However, the ability of these candidate blockers to inhibit cell swelling upon hypo-osmotic chock has been disputed (18). In an attempt to identify other drugs that inhibit the function of AQP4 in water transport, Mola et al (15) developed a functional high-throughput assay based on the measurement of osmotically-induced cell volume changes to screen several libraries of drugs and identified four blockers of AQP4-mediated water transport.

Multiple lines of evidence suggest that the integrity of the dystroglycan-associated complex (DAP) is essential for the proper localization and function of AQP4. This multiprotein complex includes numerous intracellular proteins such as syntrophin, dystrobrevin and dystrophin downstream of dystroglycan (DG) (19,20). DG is post-translationally cleaved into a transmembrane protein, β-DG, and an extracellular protein, α-DG. α-DG binds non-covalently to the short extracellular domain of β-DG as well as to the ECM proteins laminin, agrin and perlecan as well as neurexin (21-24). Intracellularly, β-DG binds directly dystrophin, which in turn binds dystrobrevin and syntrophin. Interestingly, DG, dystrophin, dystrobrevin and syntrophin are co-clustered with AQP4 at perivascular astrocyte endfeet (25,26). We have shown in astrocyte cultures that this co-clustering is mediated by the interaction of DG with extracellular laminin-1 (27,28). Likewise, we have demonstrated that α-DG interaction with perivascular laminin is key to the polarized distribution of AQP4 at astrocyte endfeet in brain (25). Furthermore, the deletion of α-syntrophin or mutations of dystrophin result in the loss of AQP4 clustering, relocating it away from astrocyte endfeet (29-31). Most importantly, the loss of AQP4 polarized distribution in these mice resulted in a beneficial effect as it delayed the onset of brain edema (32,33). Therefore, treatments using drugs capable of disrupting the clustered distribution of the DAP complex at astrocyte endfeet will ultimately lead to the disruption of AQP4 distribution as well.

In the present study we used a well established assay of laminin-induced clustering of the DAP complex and AQP4 in primary astrocyte cultures to screen a library of >3,500 chemicals and identified 5 enhancers and 6 inhibitors of this clustering. Here, we focused our analysis on chloranil, one the inhibitory drugs, and demonstrate that it causes cell surface cleavage of the 43 kDa β-DG to a 31 kDa form via a metalloproteinase-mediated mechanism. Chemical variants of

chloranil also induce β-DG shedding leading to the loss of cell surface tethering of α-DG and subsequent severance of laminin binding, resulting in the inhibition of DG and AQP4 clustering. This study provides evidence that the DAP complex is a valuable target for the disruption of laminin-induced AQP4 clustering and validates the high-throughput screen on primary astrocyte cultures as a powerful tool in the discovery of potential therapeutic drugs for both cytotoxic and vasogenic edema that occur in brain disorders including stroke, tumour, hydrocephalus, infection and traumatic brain injury.

6.2 Materials and methods

6.2.1 Chemicals

The 3,594 chemicals used in the screen were from the Pretswick, Sigma LOPAC, Microsource Spectrum and Biomol natural products collections, and were provided by the Canadian Chemical Biology Network (www.ccbn-rbc.ca). P-chloranil (referred to as chloranil in the rest of the text), benzoquinone and flunarizine were purchased from Sigma-Aldrich and Hoechst 33342 was from Invitrogen. Prinomastat (AG3340) was purchased from Agouron Pharmaceuticals, the tissue inhibitors of metallo-proteinases TIMP1 and TIMP2 were a generous gift from Dr. C.M. Overall (University of British Columbia, Vancouver) and N-acetyl-L-cysteine (NAC) was purchased from Sigma-Aldrich.

6.2.2 Antibodies

The following antibodies were used: rabbit anti-AQP4 raised against rat GST-AQP4 residues 249–323 (Alomone Laboratories, Jerusalem, Israel), mouse anti-β-DG, 43DAG1/8D5, raised against 15 of the last 16 C-terminal amino acids of human dystroglycan (Novocastra Laboratories, Newcastle-upon-tyne, UK), mouse anti- syntrophin, SYN1351, raised against *Torpedo* syntrophin (Affinity Bioreagents, USA), rabbit anti-MMP-2 (anti-gelatinase A βIV), raised against a synthetic peptide of human gelatinase A (34) and mouse anti-β-actin raised against a mouse synthetic peptide (Sigma, USA).

6.2.3 Chemical screen for modulators of laminin-induced dystroglycan clustering in astrocytes

Experiments were performed using postnatal day 1 Sprague-Dawley rats (Charles River) in accordance with the protocols of the animal care committee of University of British Columbia. Primary hippocampal astrocyte cultures were prepared from postnatal day 1 Sprague-Dawley rats (Charles River). Hippocampi were dissected, and meninges and choroid plexus were removed. They were then cut into small pieces and incubated for 25 min with trypsin (3.0 mg/ml; Gibco, Burlington, Canada). Dissociated hippocampi were then plated in culture flasks and grown in Dulbecco's modified Eagle's medium (DMEM) supplemented with 10% fetal bovine serum, 1% penicillin-streptomycin and 1 mM L-glutamine (Gibco) for 2-3 weeks. To remove microglia and oligodendrocyte progenitors, the flasks were shaken the day following the plating.

The culture medium was changed every 3 days. After trypsinization, the cells were plated in PerkinElmer View 96-well plates at 8000 cells per well. One day after seeding, the cells were treated for 7 h with 20 nM Engelbreth-Holm-Swarm Sarcoma laminin-1 (Sigma-Aldrich), washed with warn PBS and fixed with 4% (w/v) paraformaldehyde in 0.1 M phosphate buffer for 20 min followed by rinsing in PBS, 3 x 15 min. Four hours before fixation, chemicals were transferred from stock plates (5 mM in DMSO) to each well for a final concentration of ≈15 μM using a Biorobotics Biogrid II robot equipped with a 0.7 mm diameter 96-pin tool that adds ~20 nl per well. Fixed cells were incubated for 1 h at room temperature (20-22°C) in a solution containing 2% bovine serum albumin (Sigma) and 0.25% Triton X-100. Immunolabelling was performed by incubating the cells at room temperature for 1 h in the presence of primary antibodies against β-DG (1/100). Subsequently, cells were rinsed with PBS (3 x 15 min) and incubated with Alexa Fluor 568 goat anti-mouse IgG (1/200; Molecular Probes, USA). After three 15 min washes with PBS, the cells were incubated with PBS containing 500 ng/ml Hoechst 33342 for 15 min at room temperature. Plates were read in a Cellomics^{TM} Arrayscan V^{TI} automated fluorescence imager. Cells were photographed using a 20x objective in the Hoechst and TRITC (XF-100 filter) channels. The compartment analysis algorithm was used to identify the nuclei, apply a cytoplasmic mask and quantitate TRITC spots in the TRITC channel fixed at 250 pixel intensity units. Fluorescence intensity in the TRITC channel was gated at 10 average

pixel intensity units inside the cytoplasmic mask to select against diffuse β-DG staining. The total pixel intensity for clustered β-DG was acquired as 'circ spot total intensity ch2'.

Compounds inducing an increase or decrease greater than 1.5 in clustered β-DG staining were considered as active. Wells showing 3-fold or higher increase in clustered β-DG staining over control were re-examined to eliminate any false positives resulting from precipitation of fluorescent compounds. Similarly, compounds causing a decrease in cell number were disregarded as toxic chemicals. The Z-factor of the assay was determined from clustered β-DG measured in cells treated with DMSO (negative control) or laminin (positive control). Effective drugs identified in the screening assay were further evaluated in a dose-response curve where DMSO concentration was kept at 0.1% in all wells for all experiments.

6.2.4 Cell viability assay

Cells were seeded in 96-well plates at 8000 cells per well and grown for 24 h prior to the treatment with the drugs for 4h as described above. The drugs and media were then removed and cell viability was measured using the 3-[4,5-dimethylthiazol-2-yl]-2.5-diphenyl-tetrazolium bromide (MTT) assay (Sigma, USA). Cells were incubated for 2 h at 37°C with MTT, then 20% sodium dodecyl sulfate was added and the absorbance at 570 nm was measured after overnight incubation.

6.2.5 Immunoblotting

Treated astrocytes were harvested and suspended in 0.5 ml of ice-cold extraction buffer (25 mM Tris pH 7.4, 25 mM glycine and 150 mM NaCl) containing 1% Triton X-100, 1x complete protease inhibitor cocktail and 5 mM EDTA. After 20 min incubation on ice, the lysates were centrifuged at 800 g for 10 min. Supernatant was collected and protein was quantified using a BCA protein assay kit (Pierce, USA). Extracted proteins were denatured by boiling for 4 min in reducing sample buffer and then loaded on 10% sodium dodecyl sulfate-polyacrylamide electrophoresis gels. The gels were electrotransferred to nitrocellulose membranes (Bio-Rad, Mississauga, ON, Canada) and the blots were probed with antibodies to β-DG (1/300), AQP4 (1/1000), syntrophin (1/1000) and β-actin (1/10000. Bound antibodies were

171

detected using horseradish peroxidase-conjugated goat anti-rabbit IgG or goat anti-mouse IgG (1/2000; Jackson ImmunoResearch, USA). Signals were visualized on Bioflex econo films (Interscience, Markham, ON, Canada) using chemiluminescence (Amersham Biosciences, Buckinghamshire, UK).

6.2.6 Gelatin zymography

Media from treated astrocytes were collected and 10 µl aliquots per well were applied to 10% SDS-PAGE gels co-polymerized with 1% gelatin (Fisher, USA). After electrophoresis under non-reducing conditions, the gels were washed in 2.5% Triton X-100 for 1 h to remove SDS and then incubated for 16 h at 37°C in 20 mM Tris, 150 mM NaCl, 5 mM $CaCl_2$ and stained with SimplyBlue[TM] Safestain (Invitrogen, USA). For the standards, we used the pre-stained protein ladder from Bio-Rad as well as purified gelatinase A (MMP-2) and B (MMP-9). Regions of gelatinolytic activity regions were observed as clear bands against a blue background.

6.3 Results

6.3.1 Development of an automated microscopy screen for chemical modulators of the laminin-induced dystroglycan clustering in primary astrocyte cultures

To screen libraries of compounds for modulators of the laminin-induced clustering of β-DG in primary astrocyte cultures, we used an automated microscopy assay. The high-content screening instrument programmed to detect and quantify fluorescent spots enabled the automatic imaging of β-DG fluorescent clusters on a Cellomics ArrayScan V[TI] HCS Reader and analysis by the Compartmental Analysis BioApplication. Representative images obtained with this automated image analysis system are shown in Figure 6.1A in which each cell is outlined in red and nuclei of each live cell overlaid in blue. Individual clusters associated with each cell are shown in yellow (Fig. 6.1A). To determine the most suitable conditions for optimum detection of β-DG clustering in astrocytes cultured in 96 well plates using the Cellomics reader, we treated these cultures with increasing concentrations of laminin-1 for 7 h. In the absence of laminin-1,
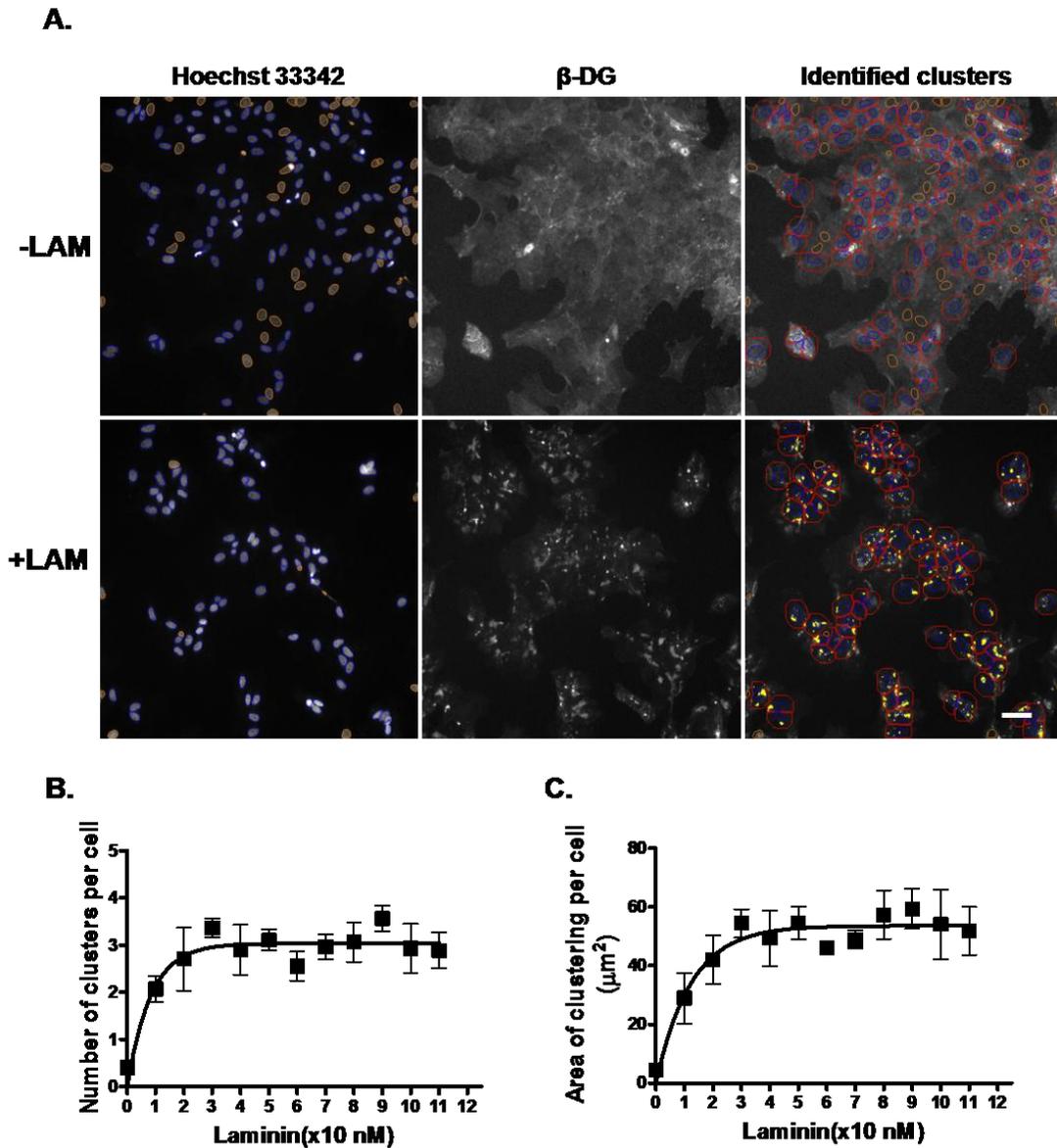
Figure 6.1 Validation of the Cellomics^{TM} Arrayscan V^{TI} automated fluorescence imaging of the laminin-induced clustering of β-dystroglycan in primary astrocyte cultures. A. Images of untreated astrocytes and astrocytes treated with 20 nM laminin-1 were acquired on the ArrayScan V^{TI} HCS Reader. The right panels are merged images of Hoechst 33342 (left panels) and β-DG labeled astrocytes (middle panels). Automatic identification of the cytoplamic mask of individual astrocytes (red) and detected spots (yellow) by the Compartmental Analysis BioApplication. **B, C.** Dose-response curve of laminin-induced β-DG clustering in astrocytes grown in 96 well-plates. Each point represents the mean number of clusters or areas of clusters ± S.E. from three different experiments. Scale bar, 30 μm.

β-DG labelling was largely diffuse at the cell surface (Fig. 6.1A), however in the presence of laminin a dose-dependent response both in the number and area of the clusters was observed reaching a plateau at 20 nM of laminin-1 as previously reported in Muller glial cells (Fig. 6.1A-C; 21).

Evaluating assay performance: The values from untreated negative control and treated (20 nM laminin) positive control wells were used to assess the Z' factor for the number of clusters and the total area covered by the clusters per cell. The values of 0.54 and 0.62 for the number of clusters and the total area of clustering per cell, respectively, are greater than 0.5, indicating that the criteria tested in this assay (i.e. number and area of the clusters) are appropriate for use in screening (Table. 1). As demonstrated by the automated assay, the addition of laminin-1 for 7 h caused a 9.11 to 18.35-fold increase in the number and area of β-DG clusters, respectively (Table 1). Other criteria shown in Table 1 include the assay's signal/noise and signal window, both of which are greater than 2-fold, further demonstrating the robustness of this assay (35).

Screening of compound collections: A collection of 3,584 drugs and pharmaceutically active chemicals was tested at a concentration of 15 μM for the final 4 h of the 7 h laminin incubation. In addition to automatically reporting the number of clusters and their total area, the number of cells (i.e., number of nuclei) and the nuclear area were simultaneously measured. Chemicals causing 80% reduction in cell number were considered cytotoxic and were eliminated from our analysis. Compounds causing over 1.6-fold increase or decrease in the clustering of β-DG without causing cell death were considered as active (Fig. 6.2 C and D). Examples of these are illustrated in Figure 6.2A and B in which data compiled from three 96-well plates corresponding to approximately 200 compounds are shown. Twelve active chemicals were initially identified as inhibitors of the clustering, but subsequent testing by dose-response proved that only 6 of these were true inhibitors inducing a reduction of β-DG clustering ranging from 2.2 to 17.1-fold (data not shown). To our knowledge, none of these 6 compounds have been previously reported to reduce laminin-DG interaction or laminin-induced clustering of the DAP complex. Subsequent analysis has shown that two of these inhibitors, namely chloranil and flunarizine, induce a dose-dependent decrease in β-DG clustering (Fig. 6.3).

Subsequent experiments were done to determine the most efficient concentration of chloranil and flunarizine required to induce a 50% inhibition (EC_{50}) of laminin-induced

174

	Number of clusters per cell	Area of clustering per cell (μm^2)
Z' factor	0.54302	0.62
Signal to background	9.115798017	18.35
Signal to noise	28.62252524	35.39
Signal window	4.625771126	6.42

Table 6.1 β-dystroglycan clustering is a suitable assay for detection using the Cellomics^{TM} Arrayscan V^{TI} automated fluorescence imager. β-DG clustering in laminin-treated astrocytes was used as the positive control and the spontaneous clustering occurring in the absence of exogenous laminin was used as the negative control. Z' = 1 − (($3s_{max}$+ $3\sigma_{min}$)/|μ_{max} − μ_{min}|), where μ_{max} is the mean positive control signal, σ_{max} is the standard deviation of the positive control signal, μ_{min} is the mean negative control signal, and σ_{min} is the standard deviation of the negative control signal. Signal/background (fold increase) = μ_{max}/μ_{min}. Signal/noise = (μ_{max} − μ_{min})/σ_{min}. Signal window= (μ_{max} − μ_{min}− 3(s_{max}+ σ_{min}))/ s_{max} (35).
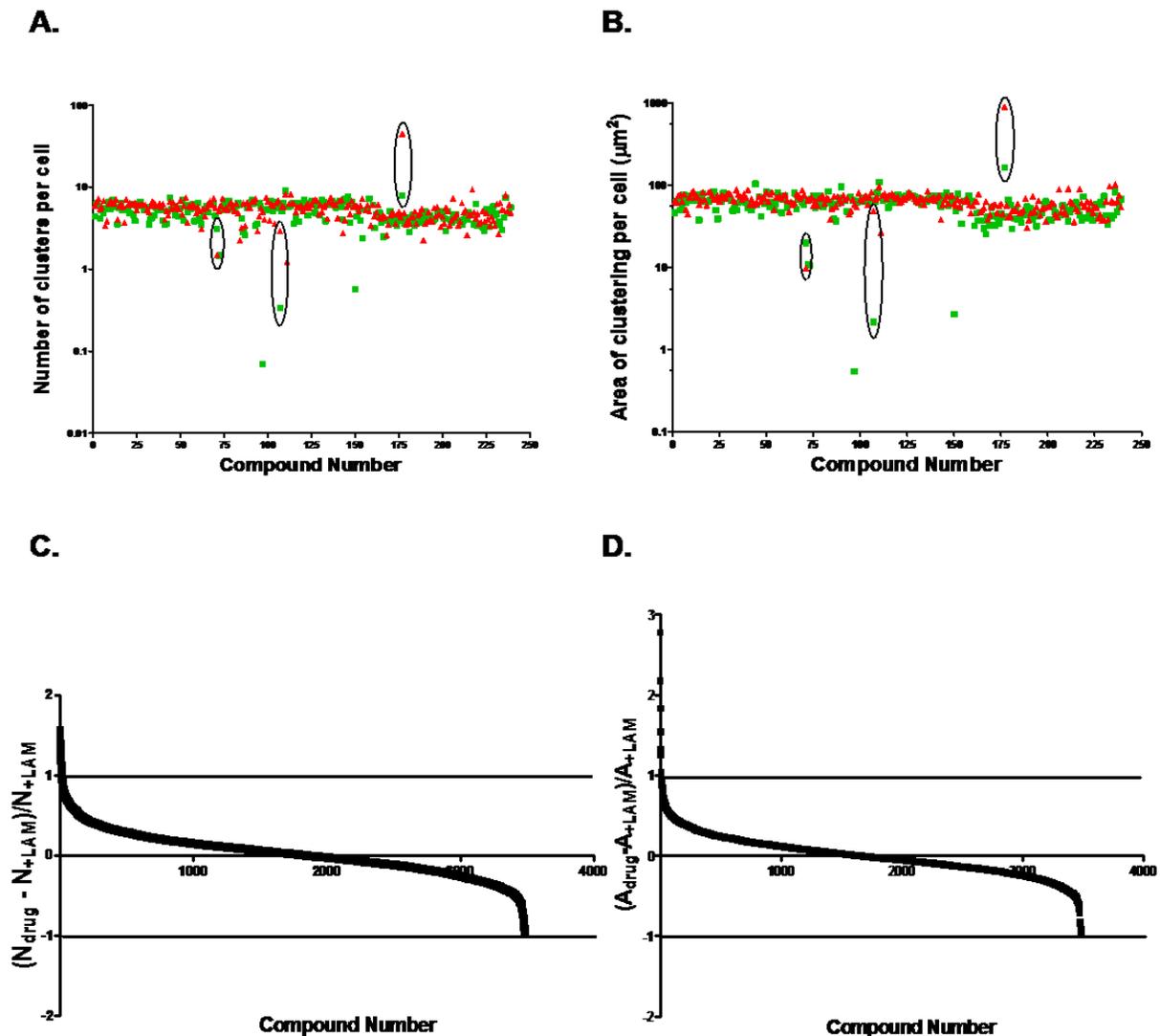
Figure 6.2 Identification of modulators of β-dystroglycan clustering using a high throughput screen of a library containing 3,594 drugs. A, B. Duplicate experiments (red and green) from three 96-well plates corresponding to approximately 200 drugs are represented. Drugs inducing a change greater than 1.6 fold in β-DG clustering in laminin-treated compared to untreated astrocytes in both experiments (as circled in black) were considered effective and used for subsequent testing. **C, D.** Normalized fold differences in the number and area of the clusters plotted for each of the 3,594 compounds tested.

Figure 6.3 Dystroglycan clustering in cells treated chloranil and flunarizine dihydrochloride. A. Primary astrocytes were treated for 7 h with 20 nM laminin-1 alone, 20 nM laminin-1 and 15 µM chloranil or 20 nM laminin-1 and 15 µM flunarizine during the last 4 h. The chemical structures of chloranil and flunarizine are represented. **B, C.** Dose-response curve of laminin-induced β-DG clustering in astrocytes treated with increasing concentrations of chloranil or flunarizine (2.5 to 100 µM). Clustered staining was automatically quantified using the Cellomics ArrayScan V^TI HCS Reader. Scale bar, 30 µm.

A.

+LAM

+Flunarizine Dihydrochloride

+Chloranil

Hoechst 3342

β-DG

B.

C.

- ■ Chloranil
- ○ Flunarizine
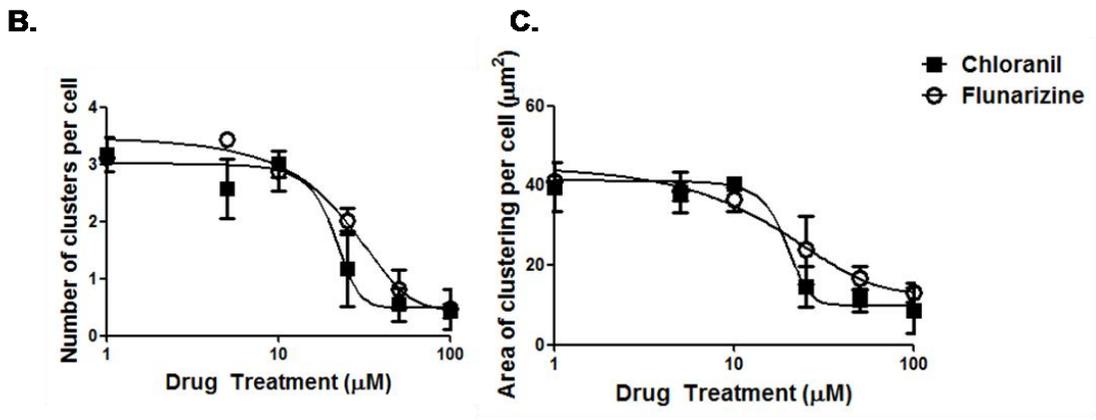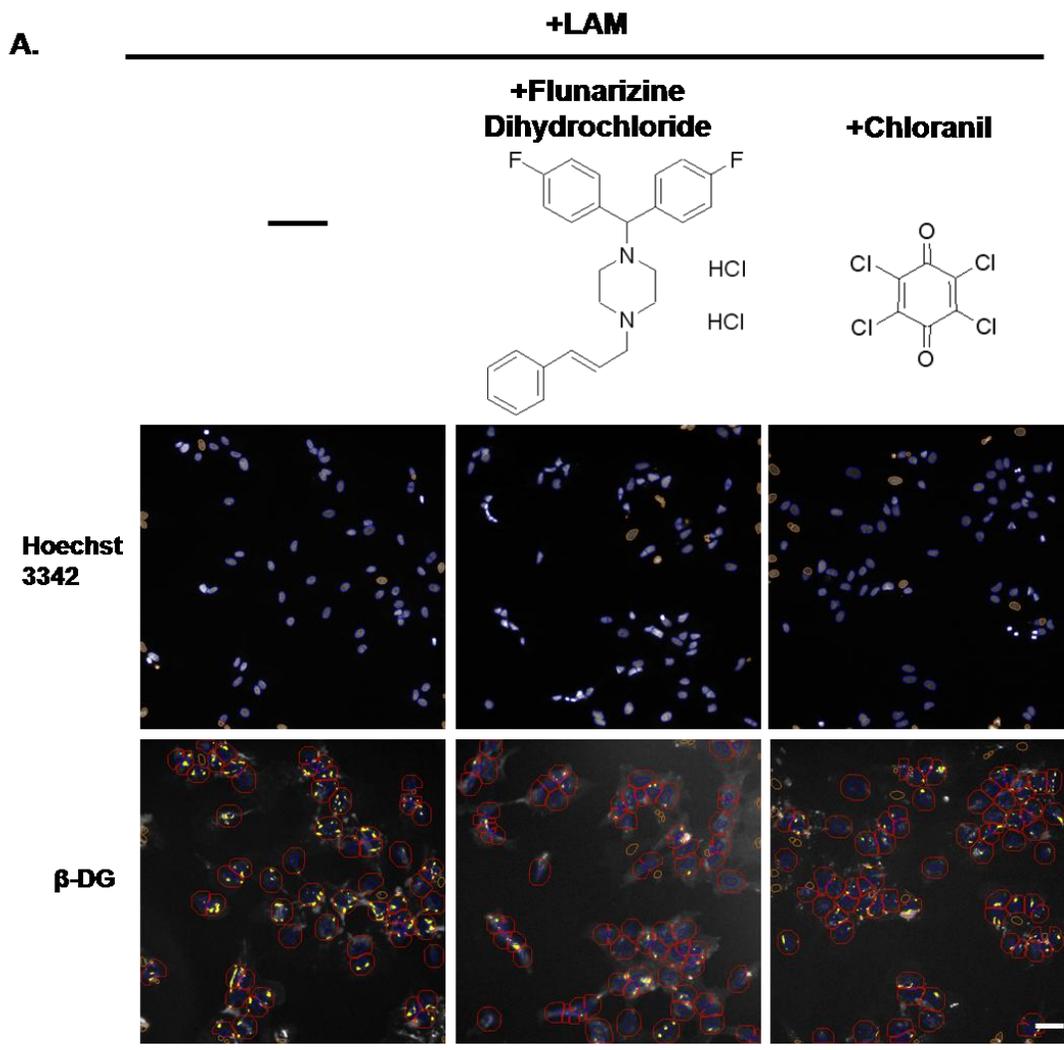
clustering. Astrocytes were incubated with 20 nM laminin-1 and either chloranil of flunarizine at concentrations ranging from 1 to 100 μM (Fig. 6.3B). The data from this dose-response experiment are represented as curves that were fitted using a sigmoidal function allowing the determination of the EC_{50}. Figure 6.3B shows a dose-dependent inhibition of the laminin-induced β-DG clustering by both drugs, however chloranil presents an EC_{50} (~20 μM) lower than that of flunarizine (~30 μM) indicating that chloranil is more potent than flunarizine.

6.3.2 Characterization of the effect of chloranil and flunarizine on β-dystroglycan and AQP4 clustering

To assess whether AQP4 clustering is also reduced in the presence of chloranil and flunarizine, β-DG and AQP4 clusters were examined at higher resolution by laser confocal microscopy. The data show that chloranil significantly inhibits the laminin-induced AQP4 clustering and as for β-DG, this inhibition is dose-dependent (Fig. 6.4). Similar results were found for flunarizine (data not shown).

To ensure that the reduction in β-DG and AQP4 clustering was not due to either cytotoxicity or reduction in β-DG or AQP4 expression levels, we assessed cell viability using the MTT assay and β-DG and AQP4 levels by immunoblotting. Figure 6.5 shows that while β-DG expression level remains unchanged in the presence of flunarizine that of AQP4 is slightly decreased. Interestingly, chloranil causes the cell surface cleavage of full length 43kDa β-DG and consequent formation of the 31 kDa fragment of β-DG (Fig. 6.5A). The size of this fragment is consistent with the cleavage of the short extracellular domain of β-DG that has been reported to be mediated by metallo-proteinases. We next investigated the effect of increasing concentrations of chloranil and flunarizine on astrocyte survival. Four hours following the treatment, we subjected the astrocytes to the MTT cell viability assay and found that chloranil caused a slight reduction in the total number of actrocytes but only at a very high concentration (100 μM; Fig. 6.5B). These results demonstrate that the inhibition of β-DG and AQP4 clustering observed with <100 μM chloranil is not due to adverse effects on cell survival (Fig. 6.3 and 4).

Figure 6.4 Effect of chloranil on the laminin-induced coclustering of β-DG and AQP4. Primary astrocytes were treated for 7 h with 20 nM laminin and 15 μM chloranil during the last 4 h. The concentration of chloranil varied from 0 (**A, B, C**), 6 (**D, E, F**), 12 (**G, H, I**), 25 (**J, K, L**), 50 (**M, N, O**) to 100 μM (**P, Q, R**). The cells were fixed and labeled for β-DG (**A, D, G, J, M** and **P**) and AQP4 (**B, E, H, K, N** and **Q**). Clustered staining was quantified using confocal microscopy. Scale bar, 30 μm.
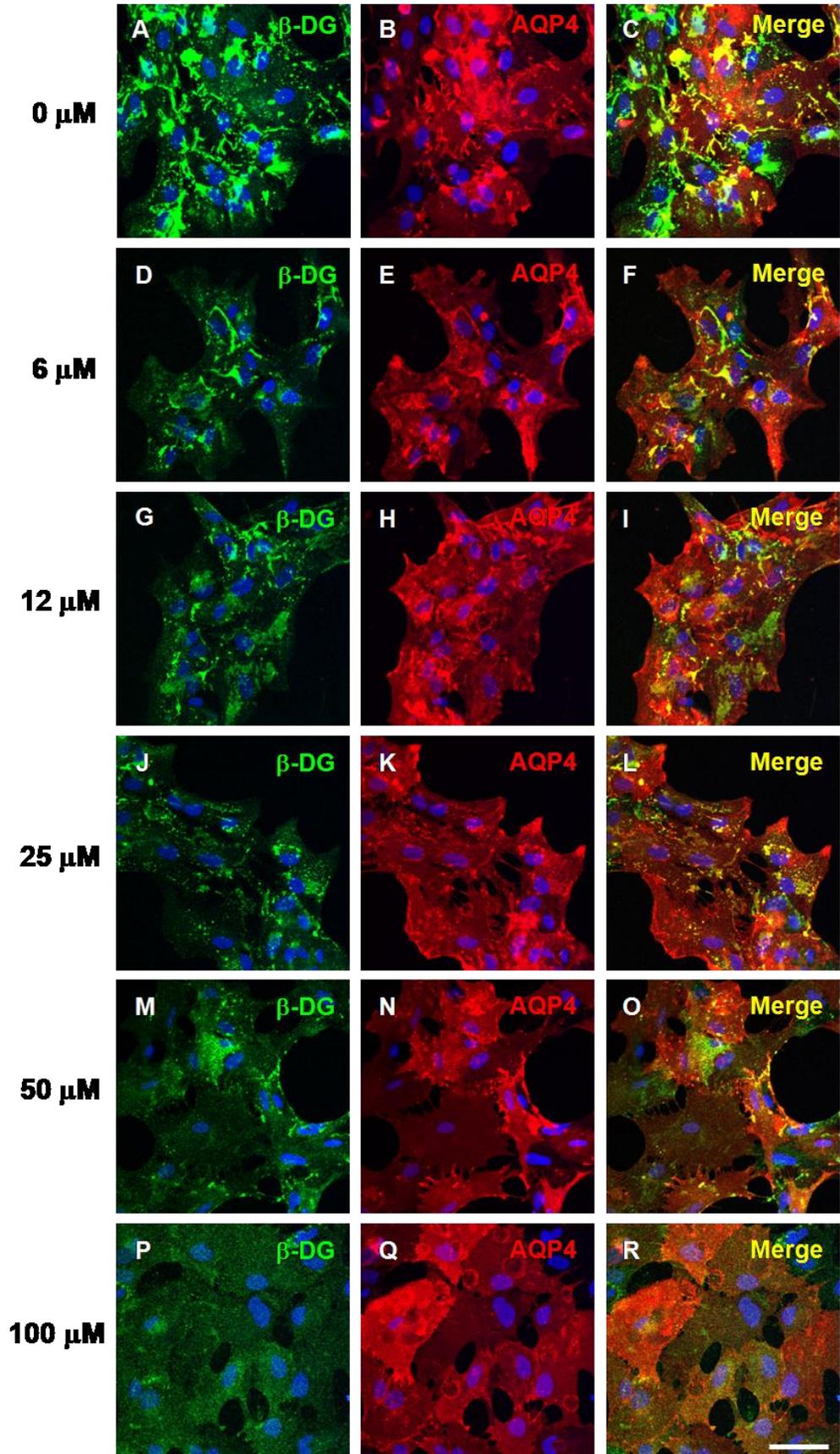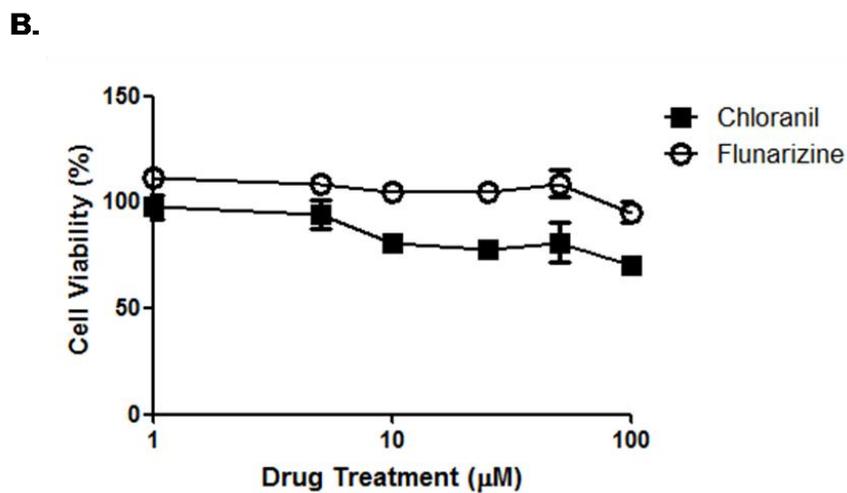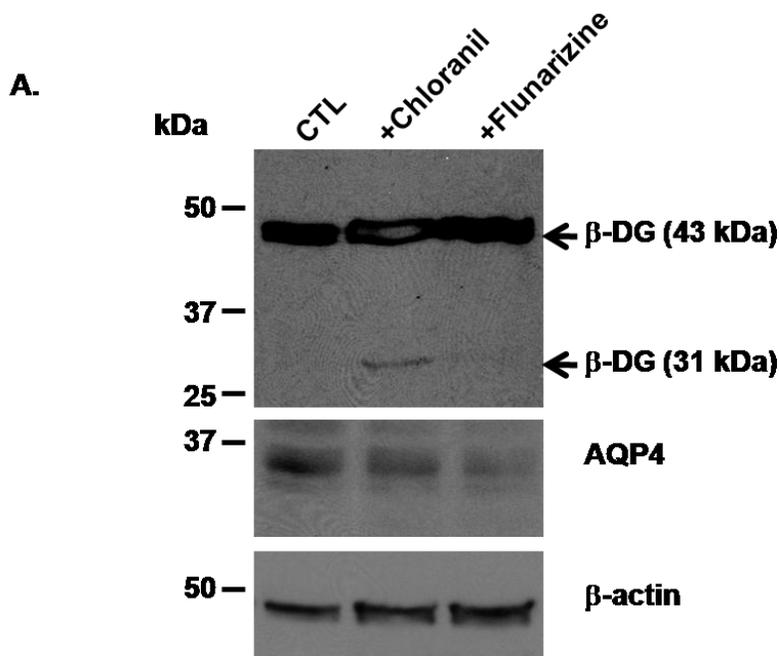
Figure 6.5 Effect of chloranil and flunarizine on astrocyte survival and β-dystroglycan, and AQP4 expression. A. Primary astrocytes were incubated for 4 h with 15 μM of active chemicals. Extracted proteins were loaded (30 μg/lane) and analyzed for β-DG, syntrophin and AQP4 expression levels by western blot analysis. Note the 31 kDa band under the 43 kDa band corresponding to the cleaved form of β-dystroglycan upon chloranil treatment. **B.** Primary astrocytes were incubated for 4 h with different concentrations of the active chemicals. Chemicals and media were washed away and the cells were assayed for cell viability by MTT assay.

6.3.3 Chloranil-induced β-dystroglycan shedding is mediated by metalloproteinases other than MMP-2 and MMP-9

Since the formation of the 31 kDa β-DG fragment in chloranil-treated astrocytes is consistent with a proteolytic cleavage of β-DG possibly implicating metalloproteinases, we tested whether longer exposure to chloranil results in increased accumulation of the 31kDa β-DG. The data show a more intense 31 kDa band and weaker 43 kDa band at 7 h compared to 4 h post-treatment (Fig. 6.6). This time-dependent accumulation of the proteolytic 31 kDa β-DG fragment is consistent with proteolytic activity. Increasing accumulation of the 31kDa β-DG fragment was also seen with chloranil concentrations raging from 15 μM to 50 μM (data not shown).

We next evaluated the role of metallo-proteinases in the chloranil-induced β-DG cleavage using the metalloproteinase inhibitor, Prinomastat at 15 and 30 μM. Immunoblots of protein extracts of astrocytes co-incubated for 7 h with 15 μM chloranil and 15 or 30 μM prinomastat show that prinomastat inhibits the chloranil-induced β-DG cleavage partially when applied at 15 μM and completely at 30 μM (Fig. 6.6). These data show conclusively that the chloranil-induced cleavage of β-DG is mediated by metalloproteinases.

Shedding of β-DG at the cell surface has been studied in many cell types including tumor cells and glial cells. Several studies have reported that the two metalloproteinases, MMP-2 and MMP-9 are involved in this process in brain (36,37). To determine whether chloranil-induced shedding of β-DG in astrocytes is mediated by these two metalloproteinases, we investigated their activity and expression via gelatin zymography and immunoblotting, respectively. Culture media from untreated astrocytes and chloranil-treated astrocytes were collected and analyzed by gelatin zymography. As standards, we used a mix of gelatinase A (MMP-2) and B (MMP-9) from CHO cells or purified gelatinase A. The gelatinolytic regions observed on both untreated and chloranil-treated astrocytes culture media corresponded to MMP-9 and the pro-form of MMP-2, as revealed by the clear bands at 92 and 72 kDa, respectively (Fig. 6.7A). No difference in intensity or activation state of either one of these MMPs was observed between the untreated and chloranil-treated astrocytes (Fig. 6.7A). To evaluate the possible implication of membrane associated MMP-2, membrane protein extracts from untreated and chloranil-treated astrocytes were analyzed by immunoblotting. The results confirm that MMP-2 is indeed present

183
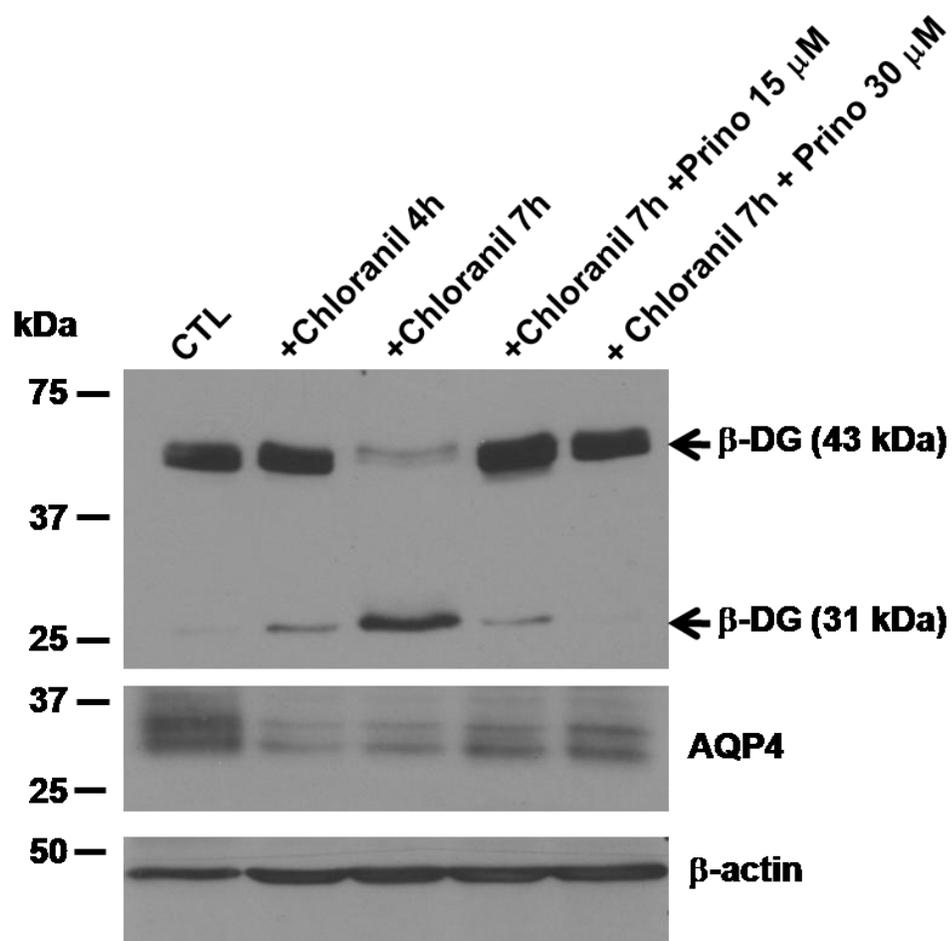
Figure 6.6 Time-dependent shedding of β-dystroglycan by chloranil is blocked by the metalloproteinase inhibitor, prinomastat. Primary astrocytes were incubated with 25 mM chloranil for 4 or 7 h with or without addition of prinomastat 15 μM or 30 μM. Extracted proteins were loaded (30 μg/lane) and analyzed for β-DG and AQP4 expression levels by western blot analysis. Note the increase in signal intensity of the 31 kDa β-DG band after extended incubation with chloranil and its disappearance with prinomastat co-incubation.

Figure 6.7 Gelatin zymography and the effect of tissue inhibitors of metalloproteinases on the chloranil-induced shedding of dystroglycan. A. Primary astrocytes were incubated in the absence or the presence of 25 μM chloranil for 7 h. Media samples were collected and analyzed by SDS-PAGE gelatin zymography. Note the clear bands against the blue background with an apparent molecular weight of 92 and 72 kDa, representing gelatinolytic activity of pro-MMP-9 and pro-MMP-2, respectively. The chloranil does not modulate the amount of MMP-2 and 9 or their activation state. **B.** Primary astrocytes were incubated for 4 h with 25 μM chloranil alone, 25 μM chloranil with 30 μM prinomastat, 25 μM chloranil with 110 nM TIMP1 or 25 μM chloranil with 100 nM TIMP2. Protein extracts were loaded (30 μg/lane) and analyzed for β-DG expression levels by western blot analysis. Note that the chloranil-mediated shedding of β-DG is inhibited by prinomastat but not TIMP1 or 2.

A.

B.
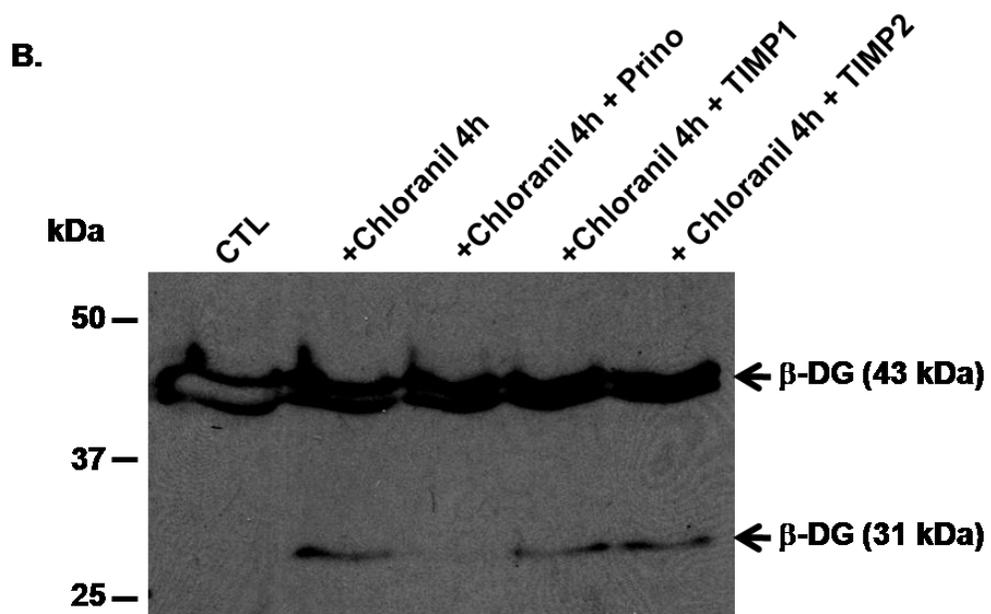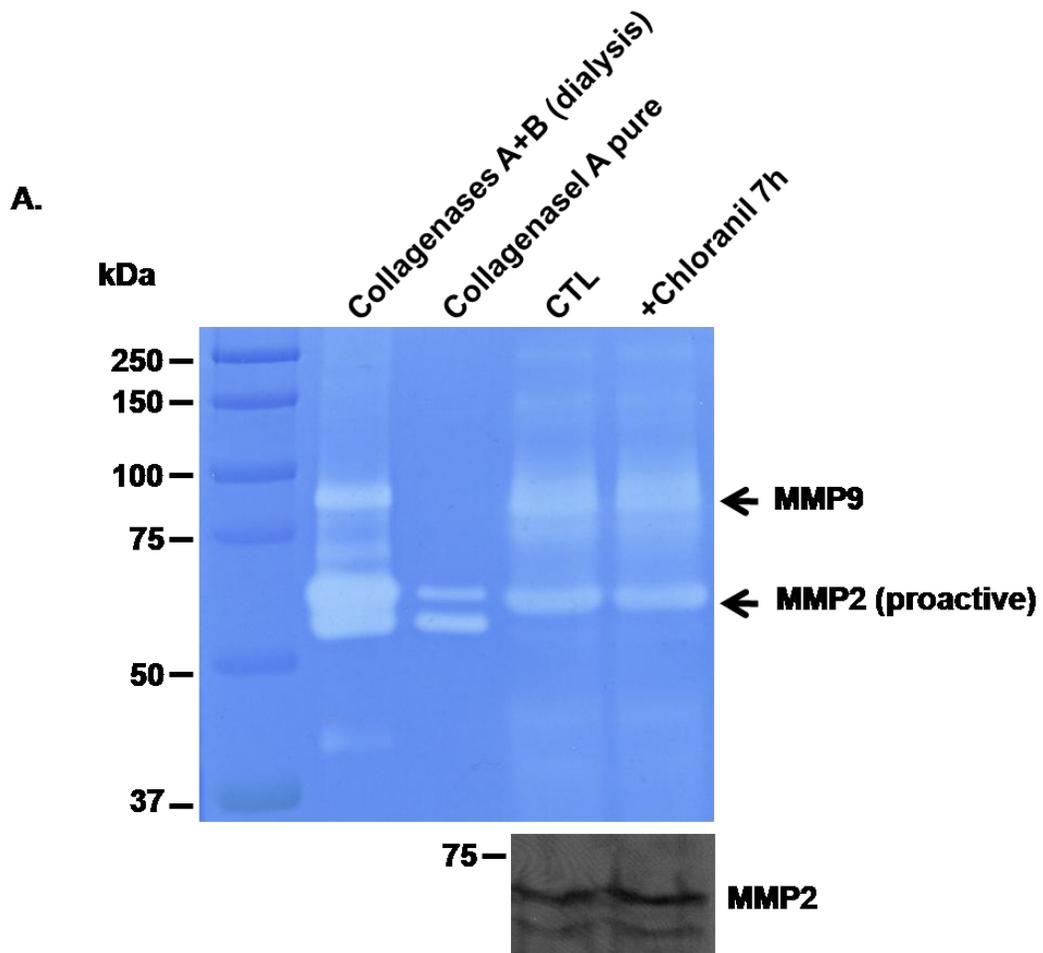
predominantly in its pro-form as shown on the zymogram and that levels do not change in the chloranil-treated compared to untreated astrocytes (Fig. 6.7A). Further analysis was conducted using the tissue inhibitors of metalloproteinases, TIMP1 (110 nM) and TIMP2 (100 nM) that inhibit selectively MMP-2 and MMP-9 but not the ADAMs (a disintegrin and a metalloproteinase). Astrocytes treated for 4 h with chloranil alone, chloranil with prinomastat or chloranil with TIMP1 or TIMP2 were analyzed by immunoblotting. Unlike prinomastat, neither TIMP1 nor TIMP2 were capable of preventing the chloranil-induced cleavage of β-DG (Fig. 6.7B), suggesting that metalloproteinases other than MMP-2 and MMP-9, possibly ADAMs, may be involved.

6.3.4 β-dystroglycan shedding by chloranil and its chemical variants is mediated by reactive oxygen species

Chloranil is a general electron acceptor that has a role in radical ion formation and has been shown to be most effective at producing reactive oxygen species (ROS) by accepting electrons from oxygen (38). Based on this property of chloranil, its reported inability to interact or regulate collagenase activity (39) and the fact that metalloproteinases can be activated by ROS, we hypothesized that choranil induces β-DG shedding by producing ROS that in turn activate specific metalloproteinases. To test this hypothesis, astrocytes were incubated either with chloranil alone or chloranil plus the ROS scavenger, N-acetyl-cysteine (NAC). Interestingly, NAC completely inhibited the proteolytic cleavage of β-DG by chloranil (Fig. 6.8A).

Similar to chloranil, chemical variants of chloranil such as 2,3-dichloro-5,6-dimethyl (1,4)benzoquinone and benzoquinone, induced β-DG cell surface cleavage and a significant and dose-dependent decrease both in the number and area of β-DG clusters as assessed by immunblotting and immunofluorescence (Fig. 6.8). The effect of chloranil and its variants is most likely mediated by the benzoquinone which is common to these three aromatic compounds. The observation that these variants induce a similar effect to chloranil and that chloranil acts via the production of ROS suggest strongly that chloranil variants increase ROS production as well leading to the activation of metalloproteinases.

Figure 6.8 Effect of chloranil, 2,3-dichloro-5,6-dimethyl-(1,4)benzoquinone and benzoquinone on β-dystroglycan shedding and laminin-mediated clustering. A. Primary astrocytes were incubated for 4 h with 15 μM of active chemicals. Protein extracts were loaded (30 μg/lane) and analyzed for β-DG expression levels by western blot analysis. Note the 31 kDa band corresponding to the cleaved form of β-DG upon chloranil as well as 2,3-dichloro-5,6-dimethyl-(1,4)benzoquinone or benzoquinone treatment. The chloranil induced shedding of β-dystroglycan is prevented by co-incubation of the cells with 15 μM of chloranil and 1 mM of the ROS scavenger, N-Acetylcysteine (NAC). **B, C.** Primary astrocytes were treated for 7 h with 20 nM laminin and chloranil, 2,3-dichloro-5,6-dimethyl-(1,4)benzoquinone or benzoquinone during the last 4 h. The concentration of the compounds varied from 2.5 to 100 μM. Clustered staining was quantified using the automated microscopy assay.

A.

kDa	CTL	+Chloranil 4h	+2, 3-dichloro-5,6-dimethyl-(1,4)benzoquinone 4h	+Benzoquinone 4h	+Chloranil 4h + NAC

50 —   ← β-DG (43 kDa)

37 —

    ← β-DG (31 kDa)

25 —

50 —   β-actin

B.

Number of clusters per cell vs *Drug Treatment (μM)*

C.

Area of clustering per cell (μm²) vs *Drug Treatment (μM)*

■ Chloranil
△ 2,3-dichloro-5,3-dimethyl-(1,4)benzoquinone
◆ Benzoquinone

189
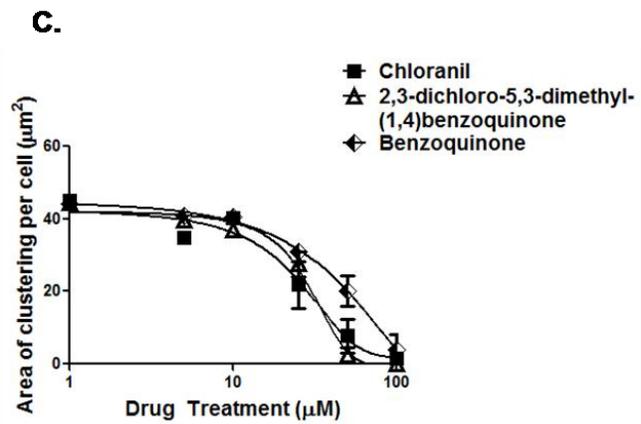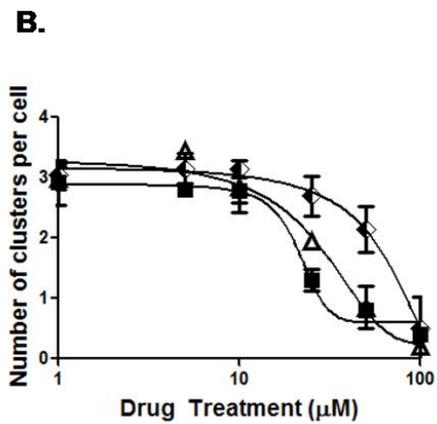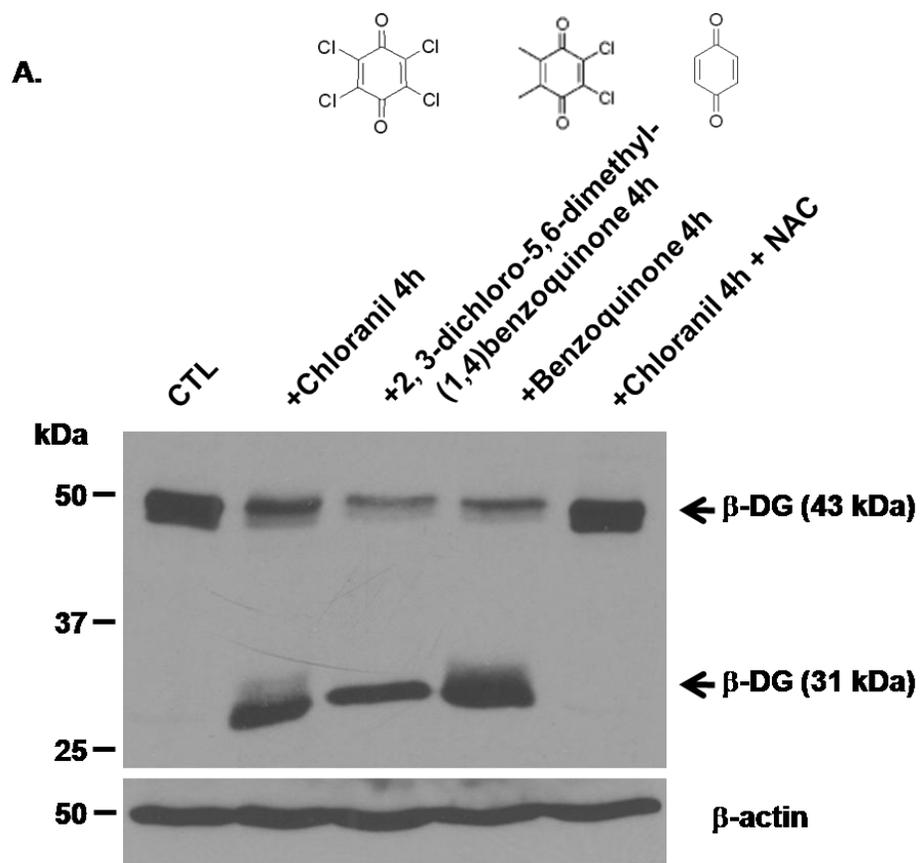
6.4 Discussion

Several studies have supported the role of the DAP complex and its interaction with extracellular laminin in the polarized distribution of AQP4 at astrocyte endfeet abutting blood vessels. Indeed, the severance of the DG interaction with laminin in the DG-glycosylation deficient mouse, Large^{myd}, results in the loss of AQP4 localization at astrocyte endfeet without affecting its expression level (25). We have also shown that the laminin-induced clustering of AQP4 in astrocyte cultures requires DG (27,28). In addition, the deletion of α-syntrophin or mutations in the dystrophin gene result in the mislocalization of AQP4, distributing it away from astrocyte endfeet (29-31). It is noteworthy that AQP4 mislocalization in these mice results in a better outcome as it delays the onset of brain edema (32,40). A study in the AQP4-null mouse reported brain swelling in models of vasogenic edema where excess fluid accumulates in the extracellular space, due to impairment of the AQP4-dependent water clearance in the AQP4 null mouse (41). On the contrary, another study in the AQP4 null mouse reported reduced brain swelling and improved neurological outcome following water intoxication and focal cerebral ischemia. This defines a role for AQP4 in the development of cytotoxic (cellular) cerebral edema where excess fluid accumulates mainly in the astrocyte foot processes (4). Modulators of AQP4 expression or perivascular clustering may therefore have a therapeutic application to reduce cytotoxic edema by blocking water influx in astrocytes at early stages of stroke and recent studies have identified potential inhibitors of AQP4-mediated water transport *in vitro* (12,14,15), although the data by Huber et al (12,14) have been disputed (18).

In the present study we implemented a high-throughput screen in primary astrocyte cultures to identify compounds that modulate the laminin-induced clustering of β-DG and AQP4. First, we showed that the Cellomics^{TM}Arrayscan VTI automated fluorescence imager is suitable for efficient detection of the laminin-induced clustering of β-DG (Fig. 6.1). Indeed, the Z' factor (0.54), signal/background, signal/noise and signal window values of this assay are appropriate for use in screening (Table. 6.1). Screening of the Pretswick, Sigma LOPAC, Microsource Spectrum and Biomol natural products collections identified a number of chemically active molecules, 6 of which inhibited β-DG clustering. Here, we focused our study on flunarizine and chloranil, two inhibitors of the clustering, and show based on the EC$_{50}$ that chloranil (EC$_{50}$~20 μM) is more potent than flunarizine (EC$_{50}$~30 μM). The effect of these drugs

on β-DG clustering was reversible (data not shown) and neither of them compromised astrocyte viability at the concentration used throughout the experiments (15 μM). These are generally considered favourable properties for drugs with a therapeutic potential.

Flunarizine has been reported to increase the rate of recovery in a rat model of cerebral ischemia (42) and spinal cord contusion injury (43). Flunarizine plays the role of a calcium channel blocker in astrocytes (44,45) and protects rats from severe ischemic cell death without disrupting the blood-brain barrier (46). Its role on brain edema has been investigated by (42) and despite a remarkable functional recovery, flunarizine did not induce a significant change in brain swelling and blood brain barrier damage. However, conflicting results on ischemia showed that flunarizine can be used in humans to treat both ischemia and epilepsy (47). Further *in vivo* experiments aiming at investigating the role of flunarizine in models of brain edema addressing particularly its effect on DG and AQP4 perivascular distribution are warranted.

Chloranil is commonly used as an oxidizing agent in organic syntheses. Here we show that it induces the shedding of β-DG ectodomain resulting in formation of 31 kDa β-DG and a similar effect is seen with other oxidizing agents such as 2,3-dichloro-5,6-dimethyl-(1,4)benzoquinone and benzoquinone, suggesting that the effect of chloranil and its variants on β-DG is due to ROS production. This is further substantiated by the observation that chloranil-induced β-DG cleavage is prevented by the anti-oxidant, NAC (Fig. 6.8). β-DG shedding is typical of a metalloproteinase-mediated cell surface cleavage of β-DG as previously reported (37,48,49). Indeed, our data show that prinomastat, an inhibitor with selectivity for MMP-2, MMP-9, MMP-13, and MMP-14, completely blocks the chloranil-induced cell surface cleavage of β-DG (Fig. 6.7B). These findings together with the established role of ROS in MMP activation (50-52) indicates that the chloranil induces the production of ROS that in turn activate metalloproteinases leading to the cleavage of β-DG ectodomain. This is in accordance with the report that cerebral ischemia seen after oxygen-glucose deprivation leads to a metalloproteolytic cleavage of β-DG in astrocytes (53) and that prinomastat protects against ischemic brain injury as shown in hippocampal organotypic slices (54). The observation that MMP-2 and MMP-9 expression remains unchanged in the chloranil-treated astrocytes as detected by zymography analysis and the absence of reversal of the chloranil effect by the inhibitors of metalloproteinases, TIMP1 and TIMP2 argue against an MMP-2 or MMP-9 mediated β-DG shedding in astrocytes (Fig. 6.7). Although a number of studies have shown in various cells that

191

β-DG is a substrate for MMP-2 and MMP-9 but not MMP-3, MMP-8 or MMP-13 (37,48,55-57), our data eliminate MMP-2 and MMP-9 as possible targets for chloranil.

There is evidence that β-DG is a substrate of the disintegrin and metalloproteinase family, ADAMs, including ADAMTS-4, ADAMTS1 or TACE (58-60). TIMP2 does not inhibit ADAMS and TIMP1 inhibits ADAM10 but not ADAM17 (TACE). Thus, we hypothesize that ADAMS in particular ADAM17 could be involved in β-DG shedding induced by chloranil. Several ADAMs including ADAM-10, ADAM-17 as well as ADAMTS-1 and ADAMTS-4 are expressed in astrocytes (61,62). Furthermore, up-regulation ADAMTS-1 and ADAMTS-4 has been shown in transient middle cerebral artery occlusion in rat (62).

In light of the fact that ROS-induced activation of MMPs is involved in BBB disruption leading to vasogenic edema after stroke (63), the use of chloranil would be detrimental as it would result in the breakdown of the BBB. While the detailed analysis of chloranil allows its elimination as a potential drug that could be used in models of brain edema, several other drugs that inhibit both β-DG and AQP4 clustering in a metalloproteinase-independent manner have been identified using the high throughput screen on primary astrocyte cultures. It remains to be determined whether these drugs are capable of reducing the clustering of β-DG and AQP4 at perivascular astrocyte endfeet and whether this is beneficial in models of cytotoxic brain edema.

6.5 References

1. Manley, G. T., Binder, D. K., Papadopoulos, M. C., and Verkman, A. S. (2004) *Neuroscience* 129, 983-991
2. Nielsen, S., Nagelhus, E. A., Amiry-Moghaddam, M., Bourque, C., Agre, P., and Ottersen, O. P. (1997) *J Neurosci* 17, 171-180
3. Auguste, K. I., Jin, S., Uchida, K., Yan, D., Manley, G. T., Papadopoulos, M. C., and Verkman, A. S. (2007) *FASEB J* 21, 108-116
4. Manley, G. T., Fujimura, M., Ma, T., Noshita, N., Filiz, F., Bollen, A. W., Chan, P., and Verkman, A. S. (2000) *Nat Med* 6, 159-163
5. Feng, X., Papadopoulos, M. C., Liu, J., Li, L., Zhang, D., Zhang, H., Verkman, A. S., and Ma, T. (2009) *J Neurosci Res* 87, 1150-1155
6. Ma, T., Yang, B., Gillespie, A., Carlson, E. J., Epstein, C. J., and Verkman, A. S. (1997) *J Clin Invest* 100, 957-962
7. Yang, B., Zador, Z., and Verkman, A. S. (2008) *J Biol Chem* 283, 15280-15286
8. Bloch, O., Auguste, K. I., Manley, G. T., and Verkman, A. S. (2006) *J Cereb Blood Flow Metab* 26, 1527-1537
9. Bloch, O., Papadopoulos, M. C., Manley, G. T., and Verkman, A. S. (2005) *J Neurochem* 95, 254-262
10. Tait, M. J., Saadoun, S., Bell, B. A., Verkman, A. S., and Papadopoulos, M. C. *Neuroscience* 167, 60-67
11. Detmers, F. J., de Groot, B. L., Muller, E. M., Hinton, A., Konings, I. B., Sze, M., Flitsch, S. L., Grubmuller, H., and Deen, P. M. (2006) *J Biol Chem* 281, 14207-14214
12. Huber, V. J., Tsujita, M., Kwee, I. L., and Nakada, T. (2009) *Bioorg Med Chem* 17, 418-424
13. Huber, V. J. (2009) *Bioorg Med Chem* 17, 425-426
14. Huber, V. J., Tsujita, M., Yamazaki, M., Sakimura, K., and Nakada, T. (2007) *Bioorg Med Chem Lett* 17, 1270-1273
15. Mola, M. G., Nicchia, G. P., Svelto, M., Spray, D. C., and Frigeri, A. (2009) *Anal Chem* 81, 8219-8229
16. Tanimura, Y., Hiroaki, Y., and Fujiyoshi, Y. (2009) *J Struct Biol* 166, 16-21
17. Dibas, A., Yang, M. H., He, S., Bobich, J., and Yorio, T. (2008) *Mol Vis* 14, 1770-1783
18. Yang, B., Zhang, H., and Verkman, A. S. (2008) *Bioorg Med Chem* 16, 7489-7493
19. Mehler, M. F. (2000) *Brain Res Brain Res Rev* 32, 277-307
20. Worton, R. (1995) *Science* 270, 755-756
21. Gee, S. H., Blacher, R. W., Douville, P. J., Provost, P. R., Yurchenco, P. D., and Carbonetto, S. (1993) *J Biol Chem* 268, 14972-14980
22. Gee, S. H., Montanaro, F., Lindenbaum, M. H., and Carbonetto, S. (1994) *Cell* 77, 675-686
23. Peng, H. B., Ali, A. A., Daggett, D. F., Rauvala, H., Hassell, J. R., and Smalheiser, N. R. (1998) *Cell Adhes Commun* 5, 475-489

24. Sugita, S., Saito, F., Tang, J., Satz, J., Campbell, K., and Sudhof, T. C. (2001) *J Cell Biol* 154, 435-445

25. Rurak, J., Noel, G., Lui, L., Joshi, B., and Moukhles, H. (2007) *J Neurochem* 103, 1940-1953

26. Bragg, A. D., Amiry-Moghaddam, M., Ottersen, O. P., Adams, M. E., and Froehner, S. C. (2006) *Glia* 53, 879-890

27. Guadagno, E., and Moukhles, H. (2004) *Glia* 47, 138-149

28. Noel, G., Tham, D. K., and Moukhles, H. (2009) *J Biol Chem* 284, 19694-19704

29. Amiry-Moghaddam, M., Otsuka, T., Hurn, P. D., Traystman, R. J., Haug, F. M., Froehner, S. C., Adams, M. E., Neely, J. D., Agre, P., Ottersen, O. P., and Bhardwaj, A. (2003) *Proc Natl Acad Sci U S A* 100, 2106-2111

30. Neely, J. D., Amiry-Moghaddam, M., Ottersen, O. P., Froehner, S. C., Agre, P., and Adams, M. E. (2001) *Proc Natl Acad Sci U S A* 98, 14108-14113

31. Nico, B., Frigeri, A., Nicchia, G. P., Corsi, P., Ribatti, D., Quondamatteo, F., Herken, R., Girolamo, F., Marzullo, A., Svelto, M., and Roncali, L. (2003) *Glia* 42, 235-251

32. Amiry-Moghaddam, M., Frydenlund, D. S., and Ottersen, O. P. (2004) *Neuroscience* 129, 999-1010

33. Vajda, Z., Pedersen, M., Fuchtbauer, E. M., Wertz, K., Stodkilde-Jorgensen, H., Sulyok, E., Doczi, T., Neely, J. D., Agre, P., Frokiaer, J., and Nielsen, S. (2002) *Proc Natl Acad Sci U S A* 99, 13131-13136

34. Overall, C. M., King, A. E., Sam, D. K., Ong, A. D., Lau, T. T., Wallon, U. M., DeClerck, Y. A., and Atherstone, J. (1999) *J Biol Chem* 274, 4421-4429

35. Inglese, J., Johnson, R. L., Simeonov, A., Xia, M., Zheng, W., Austin, C. P., and Auld, D. S. (2007) *Nat Chem Biol* 3, 466-479

36. Yamada, H., Saito, F., Fukuta-Ohi, H., Zhong, D., Hase, A., Arai, K., Okuyama, A., Maekawa, R., Shimizu, T., and Matsumura, K. (2001) *Hum Mol Genet* 10, 1563-1569

37. Agrawal, S., Anderson, P., Durbeej, M., van Rooijen, N., Ivars, F., Opdenakker, G., and Sorokin, L. M. (2006) *J Exp Med* 203, 1007-1019

38. Siraki, A. G., Chan, T. S., and O'Brien, P. J. (2004) *Toxicol Sci* 81, 148-159

39. Makinen, P. L., and Makinen, K. K. (1988) *Biochem Biophys Res Commun* 153, 74-80

40. Vajda, Z., Promeneur, D., Doczi, T., Sulyok, E., Frokiaer, J., Ottersen, O. P., and Nielsen, S. (2000) *Biochem Biophys Res Commun* 270, 495-503

41. Papadopoulos, M. C., Manley, G. T., Krishna, S., and Verkman, A. S. (2004) *FASEB J* 18, 1291-1293

42. Abiko, H., Mizoi, K., Suzuki, J., Oba, M., and Yoshimoto, T. (1988) *Neurol Res* 10, 145-150

43. Leybaert, L., and De Ley, G. (1994) *Exp Brain Res* 100, 369-375

44. Fischer, R., Schliess, F., and Haussinger, D. (1997) *Glia* 20, 51-58

45. Kim-Lee, M. H., Stokes, B. T., and Yates, A. J. (1992) *Glia* 5, 56-64

46. Zumkeller, M., and Dietz, H. (1996) *Neurosurg Rev* 19, 253-260

47. Hartmann, A. (1986) *Eur Neurol* 25 Suppl 1, 7-26

48. Michaluk, P., Kolodziej, L., Mioduszewska, B., Wilczynski, G. M., Dzwonek, J., Jaworski, J., Gorecki, D. C., Ottersen, O. P., and Kaczmarek, L. (2007) *J Biol Chem* 282, 16036-16041

49. Singh, J., Itahana, Y., Knight-Krajewski, S., Kanagawa, M., Campbell, K. P., Bissell, M. J., and Muschler, J. (2004) *Cancer Res* 64, 6152-6159

50. Haorah, J., Ramirez, S. H., Schall, K., Smith, D., Pandya, R., and Persidsky, Y. (2007) *J Neurochem* 101, 566-576

51. Pun, P. B., Lu, J., and Moochhala, S. (2009) *Free Radic Res* 43, 348-364

52. Meli, D. N., Christen, S., and Leib, S. L. (2003) *J Infect Dis* 187, 1411-1415

53. Milner, R., Hung, S., Wang, X., Spatz, M., and del Zoppo, G. J. (2008) *J Cereb Blood Flow Metab* 28, 812-823

54. Leonardo, C. C., Hall, A. A., Collier, L. A., Gottschall, P. E., and Pennypacker, K. R. (2009) *Neuroscience* 160, 755-766

55. Paggi, P., De Stefano, M. E., and Petrucci, T. C. (2006) *J Physiol Paris* 99, 119-124

56. Leone, L., De Stefano, M. E., Del Signore, A., Petrucci, T. C., and Paggi, P. (2005) *J Neuropathol Exp Neurol* 64, 1007-1017

57. Zhong, D., Saito, F., Saito, Y., Nakamura, A., Shimizu, T., and Matsumura, K. (2006) *Biochem Biophys Res Commun* 345, 867-871

58. Wimsey, S., Lien, C. F., Sharma, S., Brennan, P. A., Roach, H. I., Harper, G. D., and Gorecki, D. C. (2006) *Osteoarthritis Cartilage* 14, 1181-1188

59. Canals, F., Colome, N., Ferrer, C., Plaza-Calonge Mdel, C., and Rodriguez-Manzaneque, J. C. (2006) *Proteomics* 6 Suppl 1, S28-35

60. Herzog, C., Has, C., Franzke, C. W., Echtermeyer, F. G., Schlotzer-Schrehardt, U., Kroger, S., Gustafsson, E., Fassler, R., and Bruckner-Tuderman, L. (2004) *J Invest Dermatol* 122, 1372-1380

61. Bandyopadhyay, S., Hartley, D. M., Cahill, C. M., Lahiri, D. K., Chattopadhyay, N., and Rogers, J. T. (2006) *J Neurosci Res* 84, 106-118

62. Cross, A. K., Haddock, G., Stock, C. J., Allan, S., Surr, J., Bunning, R. A., Buttle, D. J., and Woodroofe, M. N. (2006) *Brain Res* 1088, 19-30

63. Gursoy-Ozdemir, Y., Can, A., and Dalkara, T. (2004) *Stroke* 35, 1449-1453

7. CONCLUSION

As the extent of cell swelling in the brain is constrained by the encasing skull, pathological conditions that disturb cell volume homeostasis can severely compromise neural function and survival. Water accumulation in the brain is characteristic of many pathological situations such as stroke, trauma, neoplasm, infection or metabolic disorders. In an attempt to counteract the osmolarity disturbance generated during those conditions and restore normal cell volume, neural cells initiate volume regulatory mechanisms by modifying the concentration of active osmolytes (1) but these mechanisms are rapidly altered by the lack of ATP and the acidosis which results from those conditions. Therefore, it seems that one primary target to prevent brain swelling early on during its onset or even to accelerate its dissipation could be the water channel AQP4. Although the general characteristics of AQPs have been extensively studied, only recently has evidence emerged to indicate that both AQP4 activity and distribution in the brain are crucial for water homeostasis and brain swelling evolution.

At the initiation of this thesis only two distinct factors had been described to regulate AQP4 distribution; the necessity of DAP complex integrity for its proper localization as well as the role of laminin in its cell surface organization. Studies reported in this dissertation highlight the role of post-translational modifications of DG, ECM cooperation between laminin and agrin, lipid rafts and signalling cascade in the control of DG-dependent AQP4 distribution.

In chapter 2, we focused on the defective O-glycosylation of α-DG which severs its binding to laminin and is associated with muscular dystrophies, named dystroglycanopathies. These conditions are characterized not only by muscle degeneration but also by brain and ocular defects. When we used the Large^{myd} mouse, an animal model with a hypoglycosylated form of α-DG, to determine the impact of the Large^{myd} mutation on the perivascular localization of Kir4.1 and AQP4 in brain and retina, we found that both Kir4.1 and AQP4 were lost from astrocyte endfeet in brain. However significant labeling for these channels was detected at similar cell domains in retina. Furthermore, while both α- and β1-syntrophins were lost from perivascular astrocytes in brain, labeling for β1-syntrophin was found in retina of the Large^{myd} mouse. Together, these results have revealed many findings seminal to the understanding of the brain

and retinal pathologies secondary to α-DG hypoglycosylated muscular dystrophies and it has simultaneously unveiled a large number of questions that remain to be elucidated. Indeed, these findings show that while ligand-binding to the highly glycosylated isoform of α-DG in concert with α- and β1-syntrophins is crucial for the polarized distribution of Kir4.1 and AQP4 to functional domains in brain, distinct mechanisms may contribute to their localization in retina.

The differences in the anchoring mechanisms could reflect a different complex entirely, perhaps relying on another transmembrane protein capable of binding to proteins of the basal lamina. The presence of integrin receptors in the retina (2) could account for these results. Integrins are transmembrane proteins composed of an αb-heterodimer that bind matrix proteins such as fibronectin and laminin (3). In the CNS, α1β1, α3β1, α6β1, α6β4 integrins have been localized around the microvasculature (4,5). Our previous results in the laboratory showed that unlike α-DG, β1-integrin is not clustered upon laminin treatment suggesting a differential implication of α-DG compared to β1-integrin in the clustering of Kir4.1 and AQP4. In addition, both α6 and β4 were not found in the primary astrocytes cultures and assessment of integrin activation state by use of tagged fragment of fibronectin did not show any activated integrin capable of interacting with ECM molecules at the surface of our glial cell culture system (data not shown). These results suggest that even though integrins might play a role *in vivo*, in our *in vitro* system it appears that they are not expressed or responsive and therefore rule out their potential implication in our findings.

In chapter 3, we focused on the blood-brain barrier which is characterized by the interposition of endothelial cells, astrocytes and a rich basal lamina composed of collagens perlecan, agrin, fibronectin and laminins. Interestingly, both agrin and laminins are known for organizing the post-synaptic differentiation of the neuromuscular junction and for binding to DG. In our laboratory, we demonstrated that exogenous laminin-1 but not exogenous agrin can induce the coclustering of DG and AQP4 in both Müller cell and astrocyte cultures. In addition, among the channels and receptors specifically concentrated at astrocyte endfeet *in vivo*, we assessed the distribution of ClC2, Kv1.5 and P2Y4 (Appendix M) and found that, even if Kv1.5 presents a PDZ-binding motif in its C-terminal, only AQP4, Kir4.1 and DG cluster upon laminin treatment, suggesting a specificity of the DAP vis a vis of AQP4 and Kir4.1 channels.

Here we describe the effects of endogenous agrin as well as exogenous laminin-1, collagen IV and Matrigel^{TM}, an artificial basal lamina mixture, on the distribution and expression of AQP4. We also investigated the role of those ECM molecules on the swelling capacity of cultured astrocytes. We found that upon laminin treatment, endogenous agrin was enhanced at the cell surface and was coclustered with β-DG. In addition, the silencing of agrin using siRNA led to an altered laminin-mediated clustering of AQP4 and DG suggesting a crucial role for endogenous agrin in the laminin-induced clustering of AQP4, most likely in the coalescence of the clusters. Among the other ECM molecules tested, Matrigel^{TM} induces a laminin-like clustering which could be reduced by both incubation with laminin-blocking antibodies, directed against LE1 domain of laminin-γ1, and DG silencing suggesting that laminin molecules contained in the Matrigel^{TM} mixture and capable of binding to DG are responsible for the effect of Matrigel^{TM} on AQP4 distribution in astrocytes.

The discovery that endogenous but not exogenous agrin is translocated and coclusters with DG upon laminin treatment and that agrin is crucial for the stabilization and extent of the clusters adds to the growing list of cooperative components necessary for basal membrane assembly with perlecan, nidogen, DG and integrins (6-8). Although only a limited amount of information is available about the role of agrin in astrocytes, its role in process formation and membrane domain polarity is well documented. Indeed, efforts to understand the role of agrin have yielded multiple mechanisms that contribute to potentiating synapse and filopodia-like processes formation which actually involves the membrane fluidity characteristics of the plasma membrane (9-12). In addition, the properties of agrin to bind both laminin-γ1 and DG simultaneously have been used to treat muscular dystrophy (13-15). This dissertation provides evidence that agrin can enhance DG-laminin co-assembly by bridging the two partners together, via its laminin LG4-5 domains binding to α-DG and its N-terminal Agrin (NtA) domain binding to laminin γ1 (16,17). Depending on the agrin forms present in our *in vitro* system, either the secreted or transmembrane form, another hypothesis could involve the transmembrane form bridging lipid rafts to DG, by its transmembrane domain located in lipid rafts and its LG4-5 domains binding to DG (18,19). In any case, since laminin can also binds to GM1 a major component of lipid rafts, agrin, laminin, DG and lipid rafts co-assembly would stabilize and extent the degree of clustering of DG and AQP4. Studies investigating the mechanism and the nature of agrin involved in the clustering remains to be investigated further.

Therefore, in chapter 4, we investigated the nature of astrocyte endfeet and focused on the mechanism underlying the compartmentalization of membrane domains involved in water and potassium ion transport. We found that AQP4 resided in Triton X-100-insoluble fraction, whereas DG was recovered in the soluble fraction in astrocytes. Cholesterol depletion resulted in the translocation of a pool of AQP4 to the soluble fraction indicating that its distribution is indeed associated with cholesterol-rich membrane domains. Upon laminin treatment, AQP4 and the DAP complex reorganized into laminin-associated clusters enriched for the lipid raft markers GM1 and flotillin-1 but not caveolin-1. Reduced diffusion rates of FITC-CTX, a marker for lipid rafts, in the laminin-induced clusters was indicative of the regulation of the dynamic of lipid rafts at the plasma membrane by laminin. In addition, both cholesterol depletion and DG silencing reduced the number and area of laminin-induced clusters of GM1, AQP4, and DG. These findings demonstrate the interdependence between laminin binding to DG and GM1-containing lipid raft reorganization and provide novel insight into the dystrophin complex regulation of AQP4 polarization in astrocytes. They also represent a new line of investigation on the role of cholesterol in modulating AQP4 distribution. Cholesterol is one of the major lipid components of mammalian membranes. An increase in cholesterol content restricts the motion of phospholipids resulting in lipid ordering and decreases in membrane fluidity, whereas a reduction in cholesterol content increases this fluidity (20). Previous studies suggest that AQP4 activity is not dependent on cholesterol but that AQP4 was certainly present in lipid rafts and that changes in the physical properties of the membrane would have an impact on AQP4 function in the brain (21). My study, which demonstrates a reduction of laminin-induced clustering of AQP4 with decreasing cholesterol content, is consistent with this proposal and further investigated the propensity of different inhibitors of cholesterol synthesis, called statins, on laminin-induced clustering of AQP4. Appendix N presents the rank order of efficacy for 4 commercially available and FDA approved statins (atorvastatin > mevastatin > simvastatin > lovastatin). It is noteworthy that, among those inhibitors, it has been shown that the lipophilicity of simvastatin, lovastatin and atorvastatin allows them to cross the blood-brain barrier (22-24), and could therefore be suitable to study their effect on astrocyte endfeet properties. Interestingly atorvastatin dramatically reduced brain water content after MCAO (25) and both lovastatin and simvastatin have protective effects after ischemia (26).

To identify the different components of the lipid rafts recruited in the AQP4 clusters upon laminin treatment, we also initiated a proteomic analysis by light chromatography-mass spectrometry following lipid rafts isolation and resuspension in either formaldehyde (control astrocytes) or deuterated formaldehyde (laminin treated astrocytes) as previously described (27). In Appendix O (collaboration with Dr. Foster at University of British Columbia), we can notice the recruitment in lipid rafts of proteins such as phospholipase D3 and the exclusion of protein kinase 7, AHNAK, membrane-associated progesterone receptor or Rap-1A, upon laminin treatment. These different proteins have been shown to be related to signalling events or signalling platform formation. Indeed, phospholipase D3 has been shown to be activated upon PMA in a manner similar to PKC (28), AHNAK has been shown to interact with DG (29) and Rap-1A is known to associate with NAPDH oxidase in mitochondria and participate in integrin activation (30,31).

In the following chapter (chapter 5), we were interested in the signalling events triggered upon laminin treatment since lipid rafts have been extensively associated with the recruitment of signalling proteins and, in muscle, laminin binding to DG has been shown to induce the tyrosine phosphorylation of syntrophin and the activation of Rac, PAK1-JNK and PI3K/AKT pathways. We found that, concomitant to the sudden increase in DG, AQP4 and GM1 clustering between 3-4 hours of laminin treatment, tyrosine phosphorylation labeling increased at 3 hours, both by western blot and immmunofluorescence analyses. In addition, immunofluorescence data show that laminin induces the formation of phosphotyrosine-rich clusters that are reminiscent of laminin clusters. When co-treated with laminin and the tyrosine kinase inhibitor, genistein, we subsequently found that DG and AQP4 clusters are significantly reduced in number and surface area. Antibody-based microarrays identified a number of signalling molecules which expression was altered following laminin treatment, In the present thesis, I chose to focus on the protein-serine kinase C delta (PKCδ) exhibiting a high level of tyrosine phosphorylation following laminin treatment. Using selective inhibitors of PKCδ, we found that PKCδ is involved in the laminin-induced clustering of AQP4 (Appendix Q). Since PKC activation has been extensively studied to be associated with release of intracellular stores of Ca^{2+}, one possibility is that laminin-binding to DG is linked to changes in $[Ca^{2+}]_i$ via an activation of phospholipase C. Interestingly, calcium has been shown to bind to both syntrophin and dystrophin and regulate their protein-protein interactions (32-34) in addition to having role in the laminin-DG interaction

(35-37). This hypothesis is supported by the fact that among the inhibitors of the laminin-induced clustering of DG, flunarizine is a calcium-channel blocker (38).

When the water transport capacity was assessed in the laminin-treated astrocytes, we observed that laminin delays significantly the onset of cell swelling upon hypoosmotic stress. These results could have two implications. The first possibility is that laminin may be decreasing the threshold "set-point" of the volume-sensing and regulatory processes such that the cells respond immediately to the stress. The second one is that laminin may be decreasing the AQP4-dependent water entry. Since the experiments in this study also provide evidence for the involvement of PKC activity in the laminin-induced reduction of cell swelling upon hypoosmotic shock, both hypotheses could occur. Indeed, an increased mobilization of Ca^{2+} and PKC activity have been shown to be pre-requisite for the release of organic osmolyte in RVD (39-44) and a PKC-dependent phosphorylation of AQP4 on serine 180 has also been shown to down regulate AQP4-mediated water transport after PMA (45), vasopressin (46,47), thrombin (48), propofol (49) or dopamine treatments (50). However, it is important to note that RVD has been shown to normally take 20-60 min in order to reach a steady-state cell volume (51,52) and in this thesis short hypoosmotic stresses (120 sec) were applied. Caution in interpretation is still warranted due to the lack of knowledge of VSOAC identity and its mode of activation. Nevertheless, together these data suggest that the processes whereby cells regulate volume may be under neuro-humoral control and are more dynamic than previously considered. Interestingly, we could hypothesize that laminin targets AQP4 at the astrocytes endfeet but in parallel downregulates its water transport in a protective manner to avoid any excessive water influx following changes in blood osmolarity. However, changes in brain activity could trigger signalling event that would unleash AQP4-mediated water transport. This remains to be elucidated using mutants of AQP4. Overall, these findings define a novel role for laminin-induced signalling in AQP4-mediated water transport in astrocytes.

In chapter 6, we were interested in the major importance of AQP4 distribution as it renders the channel capable of increasing water fluxes between the neuropil and the bloodstream, thereby playing an important role in handling water accumulation characteristic of brain edema. The quest to identify inhibitors of AQP4 has been increasingly popular in the last two years with new screening assays (53-55). To date, no AQP4 modulators that are suitable candidates for

clinical development have been discovered. The new approaches to block or down-regulate AQP4 activity and expression, *in vitro* and *in vivo*, have led to the identification of erythropoietin (56), progesterone (57), zinc (58), tetraethylammonium (59), edaravone (60), sulforaphane (61), tributyl-chloroplumbane and tributyl-(2,3,5-trichlorophenoxy) stannane (54) or antiepileptic (62-64) and arylsulfonamides (55), although many have been subject to controversy (65). The mechanisms involved in the observed effects on AQP4 expression and activity following treatment with these compounds remain unknown and the use of antiepileptic seems even contradictory with the fact that AQP4 deficiency is associated with longer durations of epileptic seizures (66). In addition, none of the precedent compounds target the up-regulation of AQP4 which is now believed to accelerate the absorption of vasogenic brain edema. Interestingly, mice lacking components of the DAP complex show a delayed onset of cytotoxic edema or an accentuated vasogenic edema due to a redistribution of AQP4 away from astrocyte endfeet. It is therefore important to identify modulatory drugs of laminin-dependent AQP4 clustering which may prevent or reduce brain edema. In the present study we used primary astrocyte cultures to screen a library of >3,500 chemicals and identified so far 6 drugs that inhibit the laminin-induced clustering of DG and AQP4. Detailed analysis of the inhibitory drug, chloranil, revealed that its inhibition of the clustering is due to the activation of metalloproteinase which in turn leads to shedding of β-dystroglycan and subsequent loss of laminin interaction with DG. Furthermore, chemical variants of chloranil induced a similar effect on β-dystroglycan and this was prevented by the antioxidant N-acetylcysteine. These findings reveal the mechanism of action of chloranil in preventing the laminin-induced clustering of DG and AQP4, and offer an excellent proof of principle regarding the disruption of the BBB with concomitant loss of AQP4 and DG perivascular distribution after stroke (67). Most importantly, this study validates the use of high-throughput screening as a tool to identify drugs that modulate AQP4 clustering and that could be tested in models of brain edema. We have indeed identified and characterized 3 other compounds (A, B and C) that we are in the process of testing *in vivo* (Appendix P).

7.1 Relevance and future directions

The relevance of these studies needs to be considered in terms of both therapeutic and pathological implications in the brain. Understanding the issues regarding the physiological, pathophysiological and pharmacological factors that either impair or enhance astrocyte cell volume can help in the design of therapies that alleviate the neurological manifestations accompanying brain edema.

In order to further characterize the dissimilarities in the effects of the Large^{myd} mutation between the brain and retina, a more detailed investigation of integrins *in vivo* will be carried out. The availability of integrin knock-out mice will be used to assess whether specific integrin are crucial for Kir4.1 and AQP4 in retina.

It will also be important to carry out 2D Native/Denaturing SDS Polyacrylamide Gel Electrophoresis separation that allows the analysis of stable multiprotein complexes ranging from few kDa up to 10 MDa, to identify the proteins associated with either AQP4M1 or AQP4M23. In 2008 and 2010, Nicchia GP. et al. (68,69) showed that dystrophin is important for the formation of the M23-containing OAPs. It is therefore interesting to determine a preferential association of some of the DAP members with either AQP4M1 or AQP4M23 and the modification in the composition of these complexes during laminin-induced clustering. In addition, to investigate the effect of laminin on the assembly of OAPs and the formation of large clusters, astrocytes treated with laminin will be analyzed by freeze-fracture and electron microscopy.

Experiments in this dissertation outline mechanisms involving PKC in the laminin-induced reduction of cell swelling upon hypoosmotic chock, therefore studies investigating an activation of RVD or alternatively a reduction of AQP4 activity need to be conducted. The release of the inorganic osmolyte, Cl$^-$, as well as the organic osmolyte, taurine, upon laminin treatment and hypoosmotic chock will need to be measured. The use of VSOAC inhibitor 5-nitro-(3-phenyl-propylamino)-benzoic acid (NPPB) will also help in demonstrating potential activation of RVD. Alternatively, future studies using AQP4 phosphomimetic or missense mutants for serine 180 conjugated with cell volume measurement will demonstrate the potential correlation of laminin-induced decrease in cell swelling with AQP4 downregulation. Real time imaging of the changes in cell volume may not only contribute to distinguish between the two

hypotheses but may also unveil possible new kinetics of volume correction involving both AQP4 downregulation and subsequent RVD activation. The main motive underlying such investigation would be that in spite of more than a 30 year history on the study of cell volume regulatory mechanisms, the nature of the primary volume sensor as well as the identity of VSOAC remains elusive. To accelerate the progress in the field of osmoregulation and delineate the proper role of VSOAC and AQP4 activity in cell swelling, it seems critical to solve this issue. The fact that both swelling activated Cl^- channels as well as AQP4 have been suggested to play a role in tumour cell migration further emphasize the importance of studying the relation between these two channels (70-72).

In addition to narrow down the full signalling cascade involved in AQP4 clustering and concomitant decrease in cell swelling, another approach would be to study the distribution and activity of nNOS with release of NO since NO has been shown to play a important role in signalling pathways in addition to the finding that nNOS interact with syntrophin (73,74).

To evaluate further the effects of the modulators identified in chapter 6, I will undertake *in vivo* studies. Compounds identified *in vitro* as inhibitors, including the statins, or potentiators of AQP4 clustering will be administered at different concentrations either by intravenous or intraventricular injections in rats. The ability of the relevant compounds to disrupt or potentiate DG and AQP4 distribution will be assessed by immunofluorescence and confocal microscopy. We will also evaluate the integrity of the blood-brain barrier permeability using Evans blue dye. Since the basal lamina of Large^{myd} mouse cerebral vessels remains intact despite the loss of α-DG binding to perivascular laminin, we could expect an intact BBB in the drug treated rats. This study will validate *in vivo* the effect of the characterized compounds on the distribution of AQP4 at the perivascular astrocyte endfeet.

Interestingly, alterations in cholesterol content occur not only under conditions of dietary modification (75) but also in conditions associated with disorders of cholesterol metabolism or intracellular cholesterol transport, such as Niemann-Pick type C, Smith-Lemli-Opitz syndrome or Tangier disease (76). My results raise the possibility that changes in cholesterol content could further serve an important modulatory role in AQP4 distribution around the brain blood vessels. Studies investigating the distribution of AQP4 after statin treatment or in Niemann-Pick type C, Smith-Lemli-Opitz syndrome or Tangier patients would be carried out in a manner analogous to the one presented above.

The discovery that hypoglycosylation of α-DG, depletion of cholesterol or shedding of β-DG disrupt the laminin-mediated distribution of AQP4 (Appendix R) substantiates the role of the DAP complex defects in the mislocalization of both Kir4.1 and AQP4. It also lays the ground for future experiments to study the role of such defects in altering the electrical activity of the brain and in reducing brain swelling after stroke, brain trauma or brain tumor.

With respect to the redistribution of Kir4.1 and AQP4 in Large[myd] brain, genetic linkage studies have identified correlations between deficiency of Kir4.1 and AQP4 genes and increased seizure susceptibility in humans (77,78). Since the DAP complex confers a specialized organization of AQP4 and Kir4.1 at perivascular astrocyte endfeet to allow their proper activity, a disruption in this organization would compromise potassium clearance and lead to seizure susceptibility. In light of this, it is reasonable to speculate that the Large[myd] mouse would suffer from an increased propensity towards chemoconvulsant pentylenetetrazol (PTZ) or hyperthermia induced behaviour. In order to ascertain whether the Large[myd] mutation is associated with deficits similar to the ones encountered in AQP4 and Kir4.1 null mice, Large[myd] mice will be tested for the incidence of febrile seizures, as well as their duration and severity by by injecting them PTZ (66) or immersing them in a warm water bath (79).

In addition, since both perivascular and glia limitans localization of AQP4 is disrupted in the brain of the Large[myd] mouse, it is also reasonable to speculate a possible alteration of water extrusion in the Large[myd] mouse. To determine whether the mislocalization of AQP4 in the Large[myd] mouse could prevent cytotoxic edema, I will induce such edema by transient middle cerebral artery occlusion and determine the hemispheric enlargement reflecting the water exchange after ischemic stroke. Together these studies could offer valuable insights into the water and potassium handling abilities of these animals when submitted to physiological stresses and may shed light on the way humans with dystroglycanopathy type muscular disease handle water and potassium imbalances secondary to stroke, trauma or kindling.

Similar studies investigating the susceptibility to seizure or brain edema of animal treated with the different statins identified in Appendix M and the inhibitors identified in Appendix O will be carried out. In parallel, since we also need to investigate the role of potentiators of DG and AQP4 clustering in the treatment of vasogenic edema, I will determine their effects in rat models of vasogenic edema using tumor implant and brain injury. The identified potentiators should not only reinforce the BBB, but also facilitate the role of AQP4 in the absorption of the

edema. Furthermore, since new studies investigating the loss of AQP4 in neuromyletis optica (also known as Devic's disease) revealed a common development of brain edema (80,81), attention needs to be given not only to the efficiency of the AQP4 inhibitors but also to AQP4 potentiators in preventing both cytotoxic and vasogenic edema.

The paucity of effective drugs to be used in brain edema reflects, in part, the incomplete understanding of cellular and molecular mechanisms involving AQP4 in brain edema formation and resolution. Investigations into the molecular deficits that underlie the cognitive and ocular abnormalities associated with muscular dystrophies gave us the tools to study the mechanisms underlying the functional distribution of AQP4 around blood vessels. This polarized concentration of AQP4 at astrocyte endfeet appears to be crucial to determine AQP4 role in water homeostasis in the brain. The tools that we have developed present great possibilities through which a comprehensive understanding of alternatives therapeutic targets can be delineated.

7.2 References

1. Mulligan, S. J., and MacVicar, B. A. (2006) *Sci STKE* **2006**, pe42
2. Hering, H., Koulen, P., and Kroger, S. (2000) *J Comp Neurol* **424**, 153-164
3. Hynes, R. O. (1992) *Cell* **69**, 11-25
4. del Zoppo, G. J., and Milner, R. (2006) *Arterioscler Thromb Vasc Biol* **26**, 1966-1975
5. Wagner, S., Tagaya, M., Koziol, J. A., Quaranta, V., and del Zoppo, G. J. (1997) *Stroke* **28**, 858-865
6. Jones, J. C., Lane, K., Hopkinson, S. B., Lecuona, E., Geiger, R. C., Dean, D. A., Correa-Meyer, E., Gonzales, M., Campbell, K., Sznajder, J. I., and Budinger, S. (2005) *J Cell Sci* **118**, 2557-2566
7. Kanagawa, M., Michele, D. E., Satz, J. S., Barresi, R., Kusano, H., Sasaki, T., Timpl, R., Henry, M. D., and Campbell, K. P. (2005) *FEBS Lett* **579**, 4792-4796
8. Henry, M. D., Satz, J. S., Brakebusch, C., Costell, M., Gustafsson, E., Fassler, R., and Campbell, K. P. (2001) *J Cell Sci* **114**, 1137-1144
9. Porten, E., Seliger, B., Schneider, V. A., Woll, S., Stangel, D., Ramseger, R., and Kroger, S. *J Biol Chem* **285**, 3114-3125
10. Ramseger, R., White, R., and Kroger, S. (2009) *J Biol Chem* **284**, 7697-7705
11. Ferreira, A. (1999) *J Cell Sci* **112 (Pt 24)**, 4729-4738
12. Bose, C. M., Qiu, D., Bergamaschi, A., Gravante, B., Bossi, M., Villa, A., Rupp, F., and Malgaroli, A. (2000) *J Neurosci* **20**, 9086-9095
13. Meinen, S., Barzaghi, P., Lin, S., Lochmuller, H., and Ruegg, M. A. (2007) *J Cell Biol* **176**, 979-993
14. Moll, J., Barzaghi, P., Lin, S., Bezakova, G., Lochmuller, H., Engvall, E., Muller, U., and Ruegg, M. A. (2001) *Nature* **413**, 302-307
15. Bentzinger, C. F., Barzaghi, P., Lin, S., and Ruegg, M. A. (2005) *FASEB J* **19**, 934-942
16. Denzer, A. J., Brandenberger, R., Gesemann, M., Chiquet, M., and Ruegg, M. A. (1997) *J Cell Biol* **137**, 671-683
17. Kammerer, R. A., Schulthess, T., Landwehr, R., Schumacher, B., Lustig, A., Yurchenco, P. D., Ruegg, M. A., Engel, J., and Denzer, A. J. (1999) *EMBO J* **18**, 6762-6770
18. Burgess, R. W., Skarnes, W. C., and Sanes, J. R. (2000) *J Cell Biol* **151**, 41-52
19. Neumann, F. R., Bittcher, G., Annies, M., Schumacher, B., Kroger, S., and Ruegg, M. A. (2001) *Mol Cell Neurosci* **17**, 208-225
20. Xu, X., and London, E. (2000) *Biochemistry* **39**, 843-849
21. Hibino, H., and Kurachi, Y. (2007) *Eur J Neurosci* **26**, 2539-2555
22. Saheki, A., Terasaki, T., Tamai, I., and Tsuji, A. (1994) *Pharm Res* **11**, 305-311
23. Tsuji, A., Saheki, A., Tamai, I., and Terasaki, T. (1993) *J Pharmacol Exp Ther* **267**, 1085-1090
24. Guillot, F., Misslin, P., and Lemaire, M. (1993) *J Cardiovasc Pharmacol* **21**, 339-346
25. Cui, L., Zhang, X., Yang, R., Wang, L., Liu, L., Li, M., and Du, W. *Brain Res* **1325**, 164-173
26. Shabanzadeh, A. P., Shuaib, A., and Wang, C. X. (2005) *Brain Res* **1042**, 1-5
27. Rogers, L. D., and Foster, L. J. (2007) *Proc Natl Acad Sci U S A* **104**, 18520-18525
28. Bradshaw, C. D., Ella, K. M., Qi, C., Sansbury, H. M., Wisehart-Johnson, A. E., and Meier, K. E. (1996) *Immunol Lett* **53**, 69-76
29. Salim, C., Boxberg, Y. V., Alterio, J., Fereol, S., and Nothias, F. (2009) *Glia* **57**, 535-549

30. Quinn, M. T., Parkos, C. A., and Jesaitis, A. J. (1995) *Methods Enzymol* **255**, 476-487
31. Jenei, V., Deevi, R. K., Adams, C. A., Axelsson, L., Hirst, D. G., Andersson, T., and Dib, K. (2006) *J Biol Chem* **281**, 35008-35020
32. Jung, D., Yang, B., Meyer, J., Chamberlain, J. S., and Campbell, K. P. (1995) *J Biol Chem* **270**, 27305-27310
33. Rentschler, S., Linn, H., Deininger, K., Bedford, M. T., Espanel, X., and Sudol, M. (1999) *Biol Chem* **380**, 431-442
34. Newbell, B. J., Anderson, J. T., and Jarrett, H. W. (1997) *Biochemistry* **36**, 1295-1305
35. Hohenester, E., Tisi, D., Talts, J. F., and Timpl, R. (1999) *Mol Cell* **4**, 783-792
36. Wizemann, H., Garbe, J. H., Friedrich, M. V., Timpl, R., Sasaki, T., and Hohenester, E. (2003) *J Mol Biol* **332**, 635-642
37. Gee, S. H., Blacher, R. W., Douville, P. J., Provost, P. R., Yurchenco, P. D., and Carbonetto, S. (1993) *J Biol Chem* **268**, 14972-14980
38. Solomon, G. D. (1982) *Lancet* **2**, 162
39. Pasantes-Morales, H., Cardin, V., and Tuz, K. (2000) *Neurochem Res* **25**, 1301-1314
40. Mongin, A. A., Cai, Z., and Kimelberg, H. K. (1999) *Am J Physiol* **277**, C823-832
41. Mongin, A. A., Reddi, J. M., Charniga, C., and Kimelberg, H. K. (1999) *Am J Physiol* **276**, C1226-1230
42. Mongin, A. A., and Kimelberg, H. K. (2005) *Am J Physiol Cell Physiol* **288**, C204-213
43. Rudkouskaya, A., Chernoguz, A., Haskew-Layton, R. E., and Mongin, A. A. (2008) *J Neurochem*
44. Nilius, B., Eggermont, J., Voets, T., Buyse, G., Manolopoulos, V., and Droogmans, G. (1997) *Prog Biophys Mol Biol* **68**, 69-119
45. Okuno, K., Taya, K., Marmarou, C. R., Ozisik, P., Fazzina, G., Kleindienst, A., Gulsen, S., and Marmarou, A. (2008) *Acta Neurochir Suppl* **102**, 431-436
46. Liu, X., Nakayama, S., Amiry-Moghaddam, M., Ottersen, O. P., and Bhardwaj, A. *Neurocrit Care* **12**, 124-131
47. Moeller, H. B., Fenton, R. A., Zeuthen, T., and Macaulay, N. (2009) *Neuroscience* **164**, 1674-1684
48. Tang, Y., Cai, D., and Chen, Y. (2007) *J Mol Neurosci* **31**, 83-93
49. Zhu, S. M., Xiong, X. X., Zheng, Y. Y., and Pan, C. F. (2009) *Anesth Analg* **109**, 1493-1499
50. Zelenina, M., Zelenin, S., Bondar, A. A., Brismar, H., and Aperia, A. (2002) *Am J Physiol Renal Physiol* **283**, F309-318
51. Lang, F., Busch, G. L., Ritter, M., Volkl, H., Waldegger, S., Gulbins, E., and Haussinger, D. (1998) *Physiol Rev* **78**, 247-306
52. Ateya, D. A., Sachs, F., Gottlieb, P. A., Besch, S., and Hua, S. Z. (2005) *Anal Chem* **77**, 1290-1294
53. Heo, J., Meng, F., and Hua, S. Z. (2008) *Anal Chem* **80**, 6974-6980
54. Mola, M. G., Nicchia, G. P., Svelto, M., Spray, D. C., and Frigeri, A. (2009) *Anal Chem* **81**, 8219-8229
55. Huber, V. J., Tsujita, M., Yamazaki, M., Sakimura, K., and Nakada, T. (2007) *Bioorg Med Chem Lett* **17**, 1270-1273
56. Gunnarson, E., Song, Y., Kowalewski, J. M., Brismar, H., Brines, M., Cerami, A., Andersson, U., Zelenina, M., and Aperia, A. (2009) *Proc Natl Acad Sci U S A* **106**, 1602-1607
57. Guo, Q., Sayeed, I., Baronne, L. M., Hoffman, S. W., Guennoun, R., and Stein, D. G. (2006) *Exp Neurol* **198**, 469-478

58. Yukutake, Y., Hirano, Y., Suematsu, M., and Yasui, M. (2009) *Biochemistry* **48**, 12059-12061

59. Detmers, F. J., de Groot, B. L., Muller, E. M., Hinton, A., Konings, I. B., Sze, M., Flitsch, S. L., Grubmuller, H., and Deen, P. M. (2006) *J Biol Chem* **281**, 14207-14214

60. Kikuchi, K., Tancharoen, S., Matsuda, F., Biswas, K. K., Ito, T., Morimoto, Y., Oyama, Y., Takenouchi, K., Miura, N., Arimura, N., Nawa, Y., Meng, X., Shrestha, B., Arimura, S., Iwata, M., Mera, K., Sameshima, H., Ohno, Y., Maenosono, R., Tajima, Y., Uchikado, H., Kuramoto, T., Nakayama, K., Shigemori, M., Yoshida, Y., Hashiguchi, T., Maruyama, I., and Kawahara, K. (2009) *Biochem Biophys Res Commun* **390**, 1121-1125

61. Zhao, J., Moore, A. N., Clifton, G. L., and Dash, P. K. (2005) *J Neurosci Res* **82**, 499-506

62. Huber, V. J., Tsujita, M., Kwee, I. L., and Nakada, T. (2009) *Bioorg Med Chem* **17**, 418-424

63. Huber, V. J., Tsujita, M., and Nakada, T. (2009) *Bioorg Med Chem* **17**, 411-417

64. Tanimura, Y., Hiroaki, Y., and Fujiyoshi, Y. (2009) *J Struct Biol* **166**, 16-21

65. Yang, B., Zhang, H., and Verkman, A. S. (2008) *Bioorg Med Chem* **16**, 7489-7493

66. Binder, D. K., Oshio, K., Ma, T., Verkman, A. S., and Manley, G. T. (2004) *Neuroreport* **15**, 259-262

67. Milner, R., Hung, S., Wang, X., Spatz, M., and del Zoppo, G. J. (2008) *J Cereb Blood Flow Metab* **28**, 812-823

68. Nicchia, G. P., Rossi, A., Mola, M. G., Pisani, F., Stigliano, C., Basco, D., Mastrototaro, M., Svelto, M., and Frigeri, A. *Neuroscience*

69. Nicchia, G. P., Rossi, A., Nudel, U., Svelto, M., and Frigeri, A. (2008) *Glia* **56**, 869-876

70. Saadoun, S., Papadopoulos, M. C., Watanabe, H., Yan, D., Manley, G. T., and Verkman, A. S. (2005) *J Cell Sci* **118**, 5691-5698

71. Kong, H., Fan, Y., Xie, J., Ding, J., Sha, L., Shi, X., Sun, X., and Hu, G. (2008) *J Cell Sci* **121**, 4029-4036

72. Auguste, K. I., Jin, S., Uchida, K., Yan, D., Manley, G. T., Papadopoulos, M. C., and Verkman, A. S. (2007) *FASEB J* **21**, 108-116

73. Adams, M. E., Tesch, Y., Percival, J. M., Albrecht, D. E., Conhaim, J. I., Anderson, K., and Froehner, S. C. (2008) *J Cell Sci* **121**, 48-54

74. Adams, M. E., Mueller, H. A., and Froehner, S. C. (2001) *J Cell Biol* **155**, 113-122

75. Foot, M., Cruz, T. F., and Clandinin, M. T. (1982) *Biochem J* **208**, 631-640

76. Maxfield, F. R., and Tabas, I. (2005) *Nature* **438**, 612-621

77. Buono, R. J., Lohoff, F. W., Sander, T., Sperling, M. R., O'Connor, M. J., Dlugos, D. J., Ryan, S. G., Golden, G. T., Zhao, H., Scattergood, T. M., Berrettini, W. H., and Ferraro, T. N. (2004) *Epilepsy Res* **58**, 175-183

78. Binder, D. K., Yao, X., Verkman, A. S., and Manley, G. T. (2006) *Acta Neurochir Suppl* **96**, 389-392

79. Amiry-Moghaddam, M., Williamson, A., Palomba, M., Eid, T., de Lanerolle, N. C., Nagelhus, E. A., Adams, M. E., Froehner, S. C., Agre, P., and Ottersen, O. P. (2003) *Proc Natl Acad Sci U S A* **100**, 13615-13620

80. Matsushita, T., Isobe, N., Matsuoka, T., Ishizu, T., Kawano, Y., Yoshiura, T., Ohyagi, Y., and Kira, J. (2009) *Mult Scler* **15**, 1113-1117

81. Saadoun, S., and Papadopoulos, M. C. (2009) *Neuroscience*
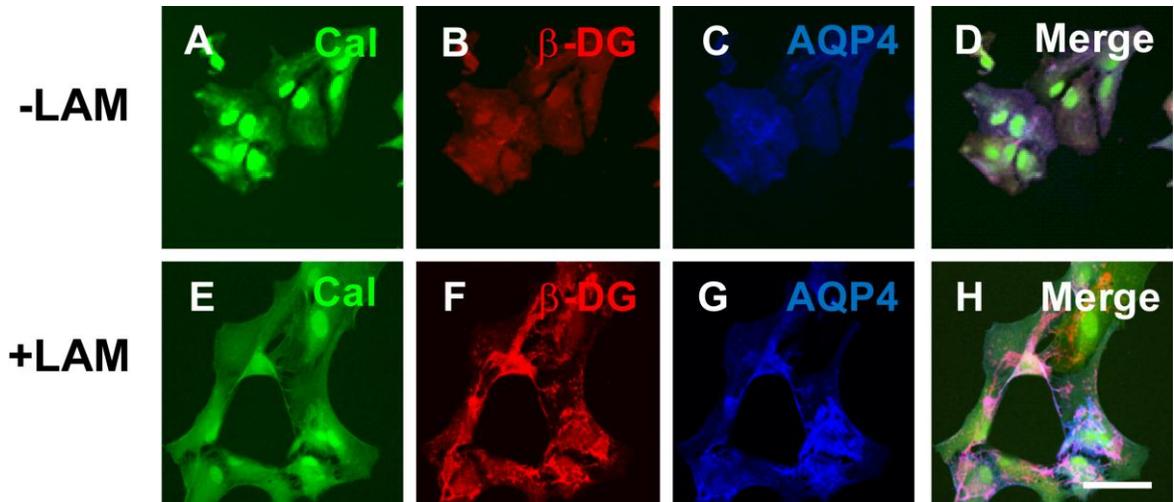
Appendix A: Supplemental Figure 3.1 Laminin-induced clustering of β-DG and AQP4 persists after calcein loading and live-imaging measurement. (A-T) Rat hippocampal astrocytes incubated in the absence (**A-D**) or (**E-T**) the presence of 15 nM laminin were first loaded with calcein, submitted to live imaging water measurements and then double immunolabeled for β-DG (**B** and **F**) and AQP4 (**C** and **G**). Scale bar, 30 μm.

Appendix B: Supplemental Figure 3.2 Astrocyte volume remains unchanged upon laminin treatment. **(A** and **F)** Live 3D-reconstruction of calcein signal from untreated and laminin-treated astrocytes. The same astrocytes incubated in the absence (**A-E**) or (**F-J**) the presence of 15 nM laminin were then double immunolabeled for β-DG (**C** and **H**) and AQP4 (**D** and **I**). Scale bar, 30 μm.

A. -LAM

F. +LAM

B Cal

G Cal
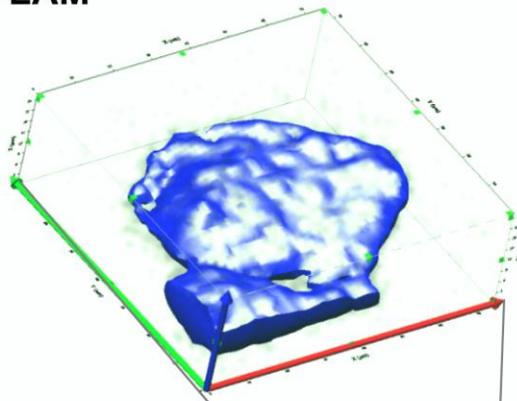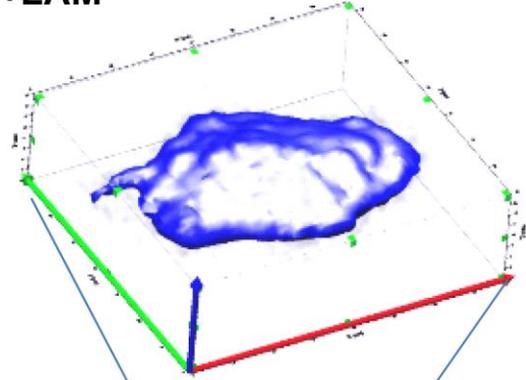
Volume average=
17835 ± 946 μm³
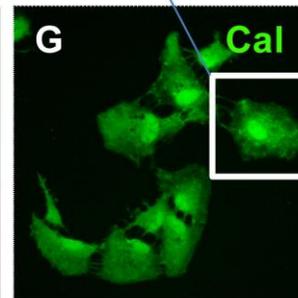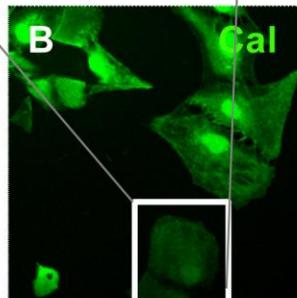
Volume average=
19221 ± 789 μm³

C β-DG

H β-DG

D AQP4

I AQP4

E Merge

J Merge

212
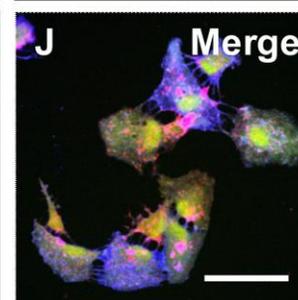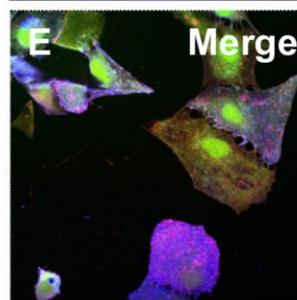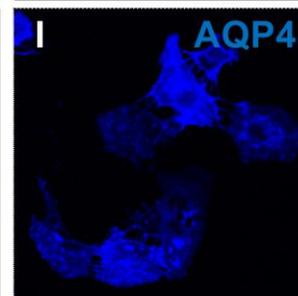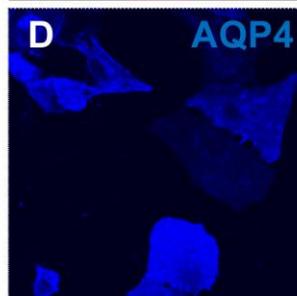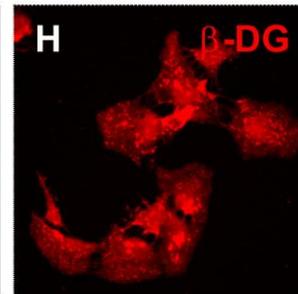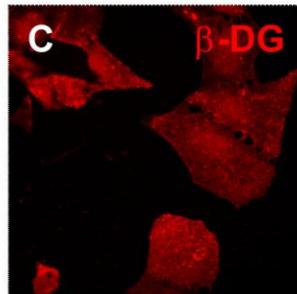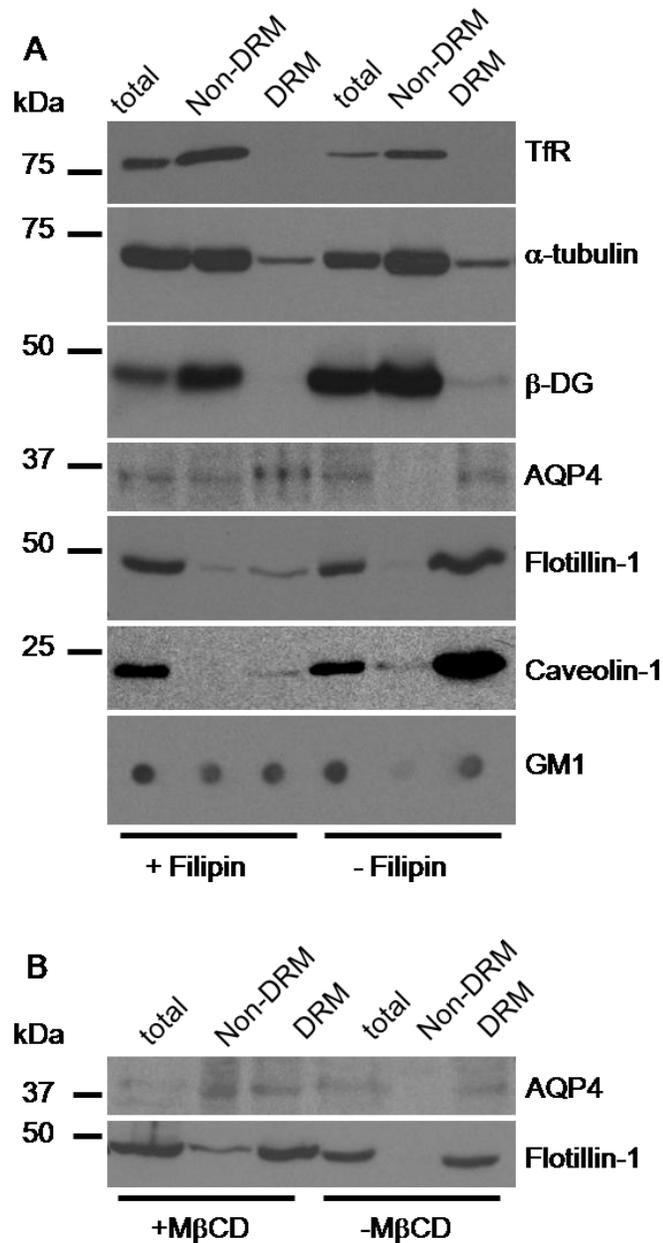
Appendix C: Supplemental Figure 4.1 The association of AQP4 with the detergent-resistant membranes (DRM) is dependent on cholesterol in astrocytes. **(A)** Detergent resistant membranes **(DRM)** and non-detergent resistant membranes **(Non-DRM)** were harvested from astrocytes incubated for 8h with 0.5 μg/ml of the cholesterol-sequestering agent, filipin. Immunoblots were probed for the transferrin receptor (TfR), α-tubulin, β-DG, AQP4, flotillin-1 and caveolin-1 and the dot blot labeled for GM1. **(B)** Proteins from astrocytes incubated for 1h with 20 mM of the cholesterol-extracting agent, methyl β-cyclodextrin **(MβCD)**, were harvested in DRM and Non-DRM and immunoblotted for AQP4 and flotillin-1.
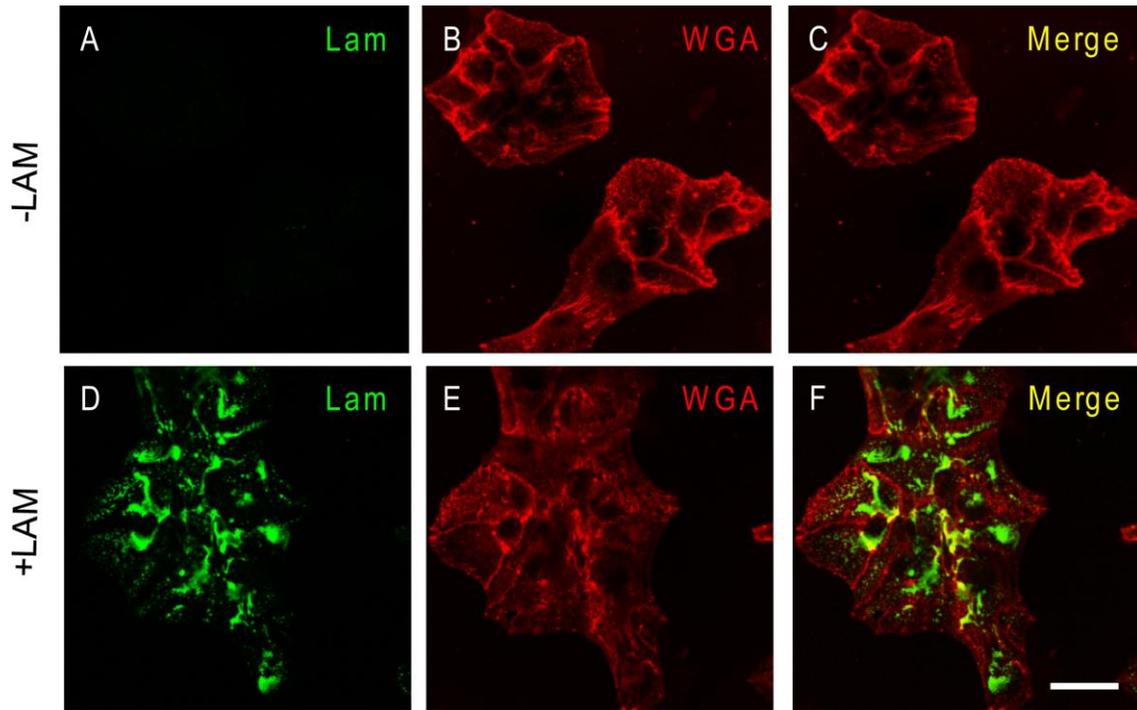
Appendix D: Supplemental Figure 4.2 The morphology of astrocytes remains unchanged after laminin treatment. (**A**-**C**) Astrocytes were incubated in the absence or (**D**-**F**) the presence of 30 nM laminin and labeled for laminin (**A** and **D**). The plasma membrane of these cells was labeled using wheat germ agglutinin conjugated to Alexa Fluor 568 (WGA; B and E). Scale bar, 45 µm.
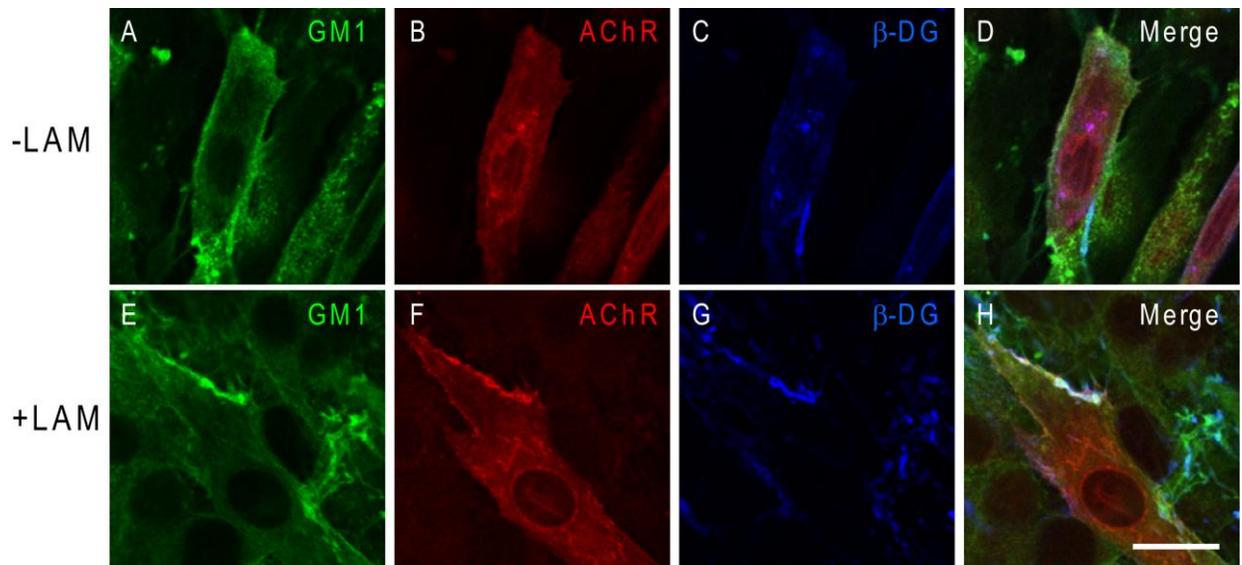
Appendix E: Supplemental Figure 4.3 Laminin induces the coclustering of GM1-containing lipid rafts with AChR and β-DG in C2C12 myotubes. (**A-D**) Differentiated C2C12 myotubes were incubated in the absence or (**E-H**) the presence of 30 nM laminin overnight and labeled for GM1 using FITC-conjugated cholera toxin subunit B (**A** and **E**), acetylcholine receptors (AChR) using RITC-conjugated α-bungarotoxin (**B** and **F**) and β-DG (**C** and **G**). Scale bar, 8 μm.
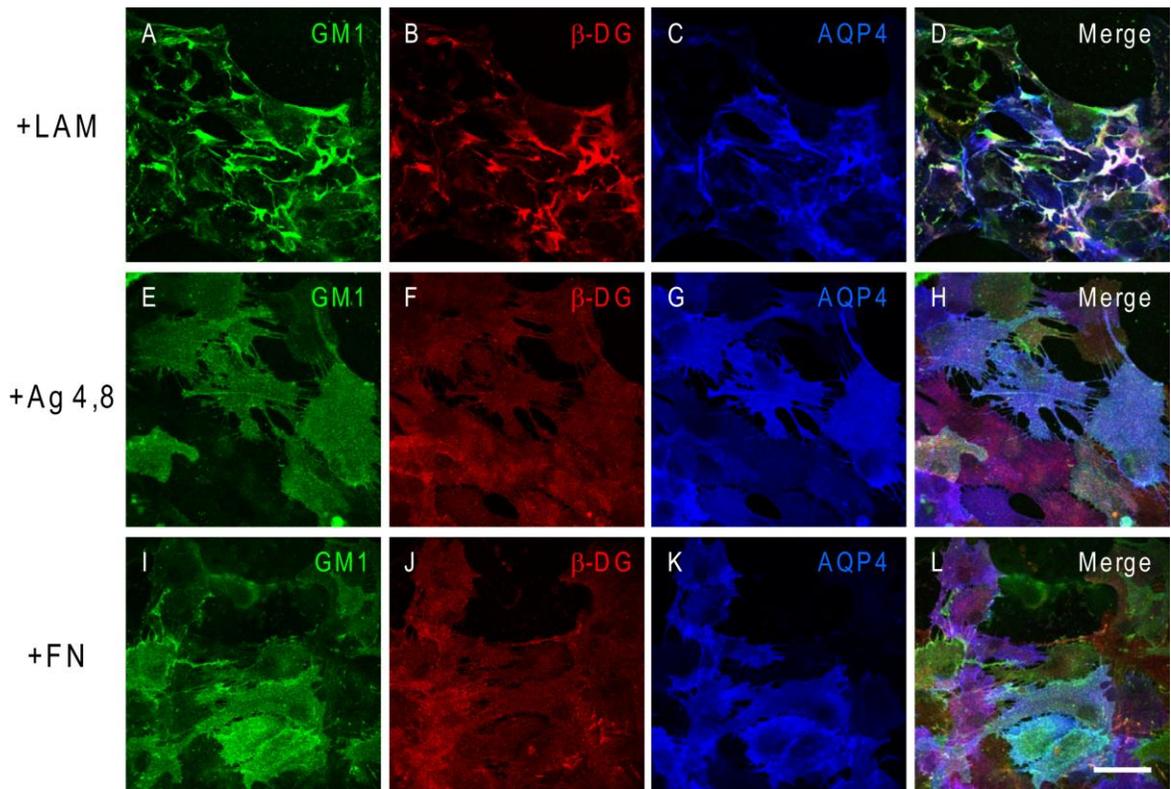
Appendix F: Supplemental Figure 4.4 Laminin but not agrin or fibronectin clusters the the GM1-containing lipid rafts in astrocytes. (**A**-**D**) Astrocytes were incubated with 30 nM laminin, (**E**-**H**) 10 nM C-agrin 4,8 or (**I**-**L**) 100 nM fibronectin and labeled for GM1 (**A**, **E** and **I**), β-DG (**B**, **F** and **J**) and AQP4 (**C**, **G** and **K**). Scale bar, 45 μm.
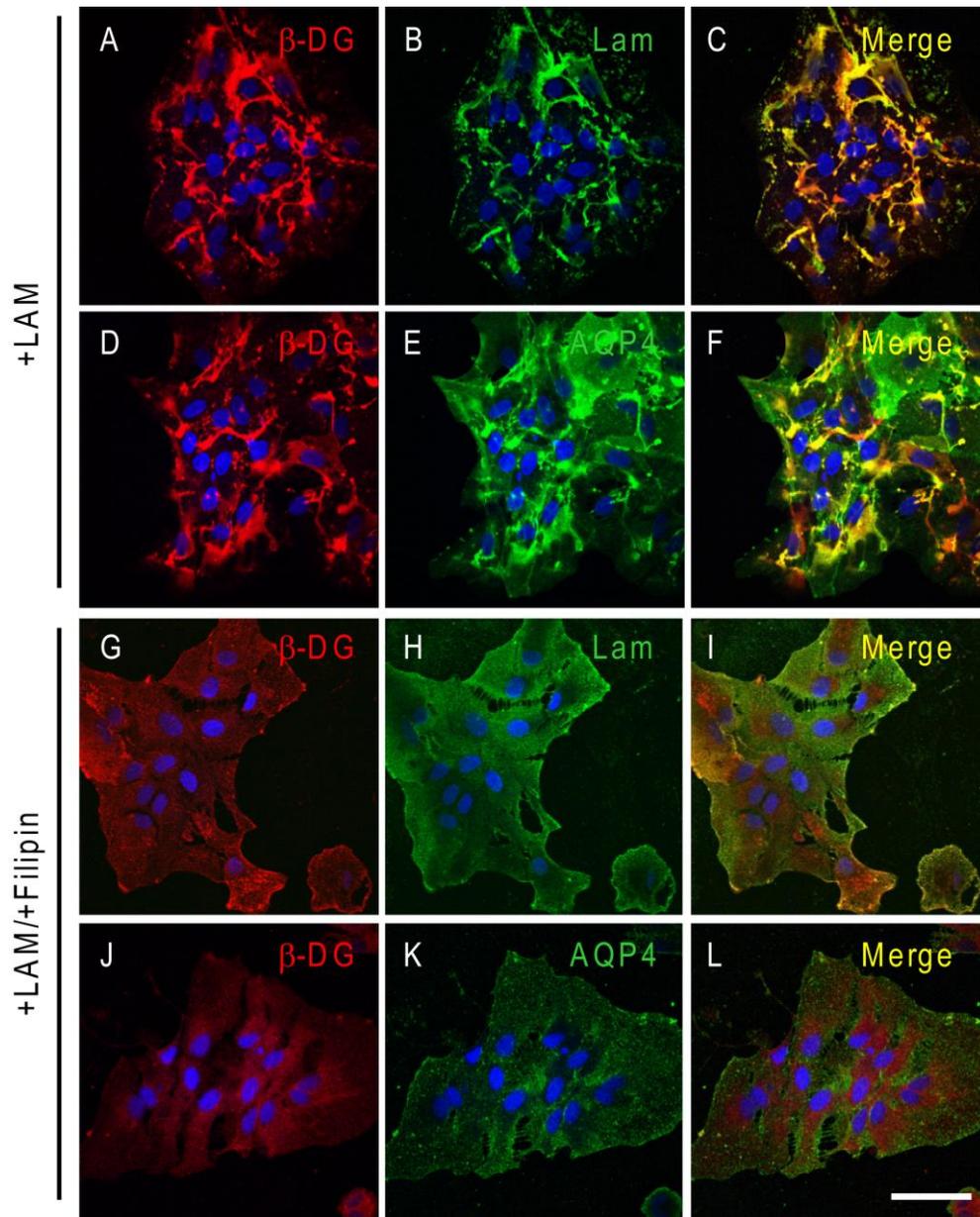
Appendix G: Supplemental Figure 4.5. The disruption of lipid rafts with the cholesterol-sequestering agent, filipin, inhibits β-DG, AQP4 and laminin clustering. (**A**-**F**) Astrocytes incubated with 30 nM laminin or (**G**-**L**) 30 nM laminin and 0.5 μg/ml of filipin were double immunolabeled for β-DG (**A**, **G**) and laminin (**B**, **H**) or β-DG (**D**, **J**) and AQP4 (**E**, **K**). Scale bar, 50 μm.
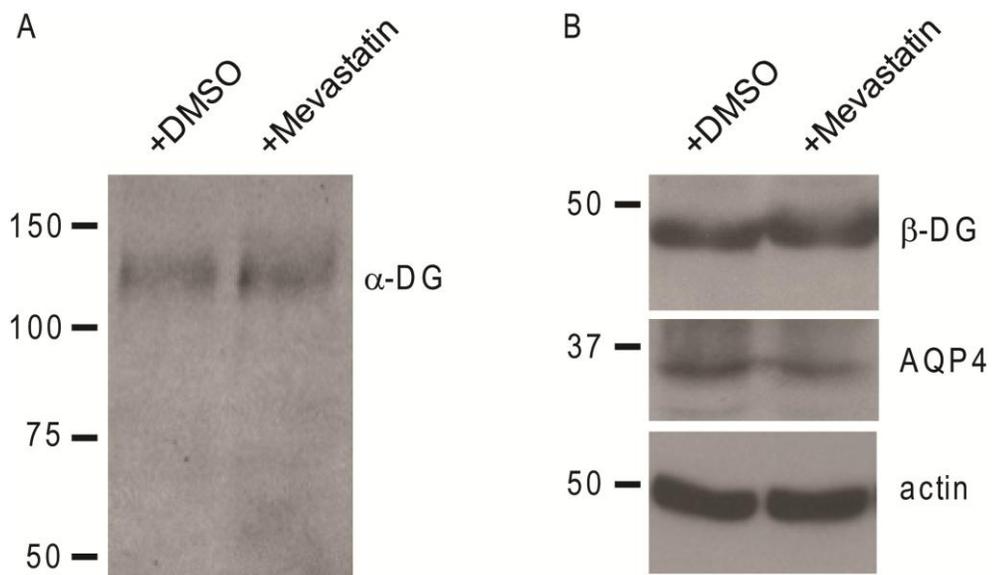
Appendix H: Supplemental Figure 4.6 Cholesterol depletion does not alter dystroglycan and AQP4 expression levels in astrocytes. Western blot analysis of α-DG, β-DG and AQP4 total expression levels was performed in astrocytes treated with 10 μM (+Mevastatin) and control astrocytes (+DMSO).

	siCTL	siDAG1	siAQP4
GFAP	A	B	C
DIC	D	E	F
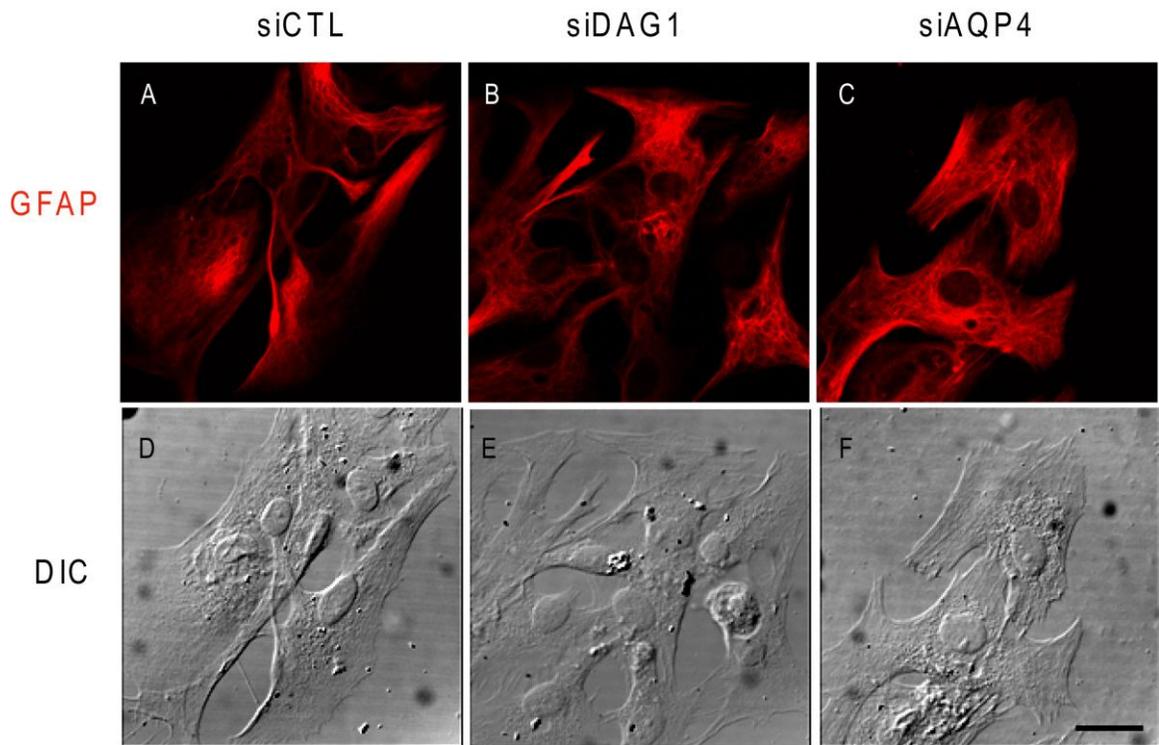
Appendix I: Supplemental Figure 4.7 The morphology of astrocytes remains unchanged after dystroglycan and AQP4 silencing. (**A-C**) Astrocytes transfected with siCTL, si*Dag1* and si*Aqp4* were immunolabeled for the glial fibrillary acidic protein (GFAP) and (**D-F**) corresponding differential interference contrast photomicrographs are shown (DIC). Scale bar, 30 μm.
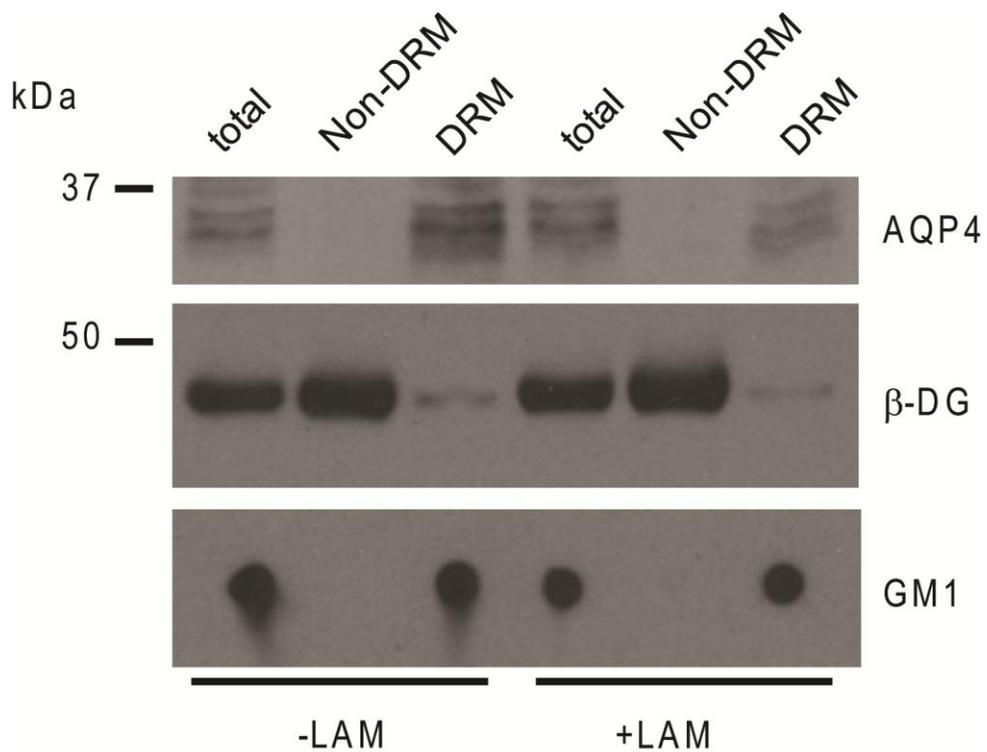
Appendix J : Supplemental Figure 4.8 β-DG remains associated with non-detergent-resistant membranes in laminin-treated astrocytes. Proteins from astrocytes incubated with (+LAM) or without 30 nM laminin (-LAM) were harvested in detergent resistant membranes (DRM) and non-detergent resistant membranes (Non-DRM) and blotted for AQP4, β-DG and GM1.
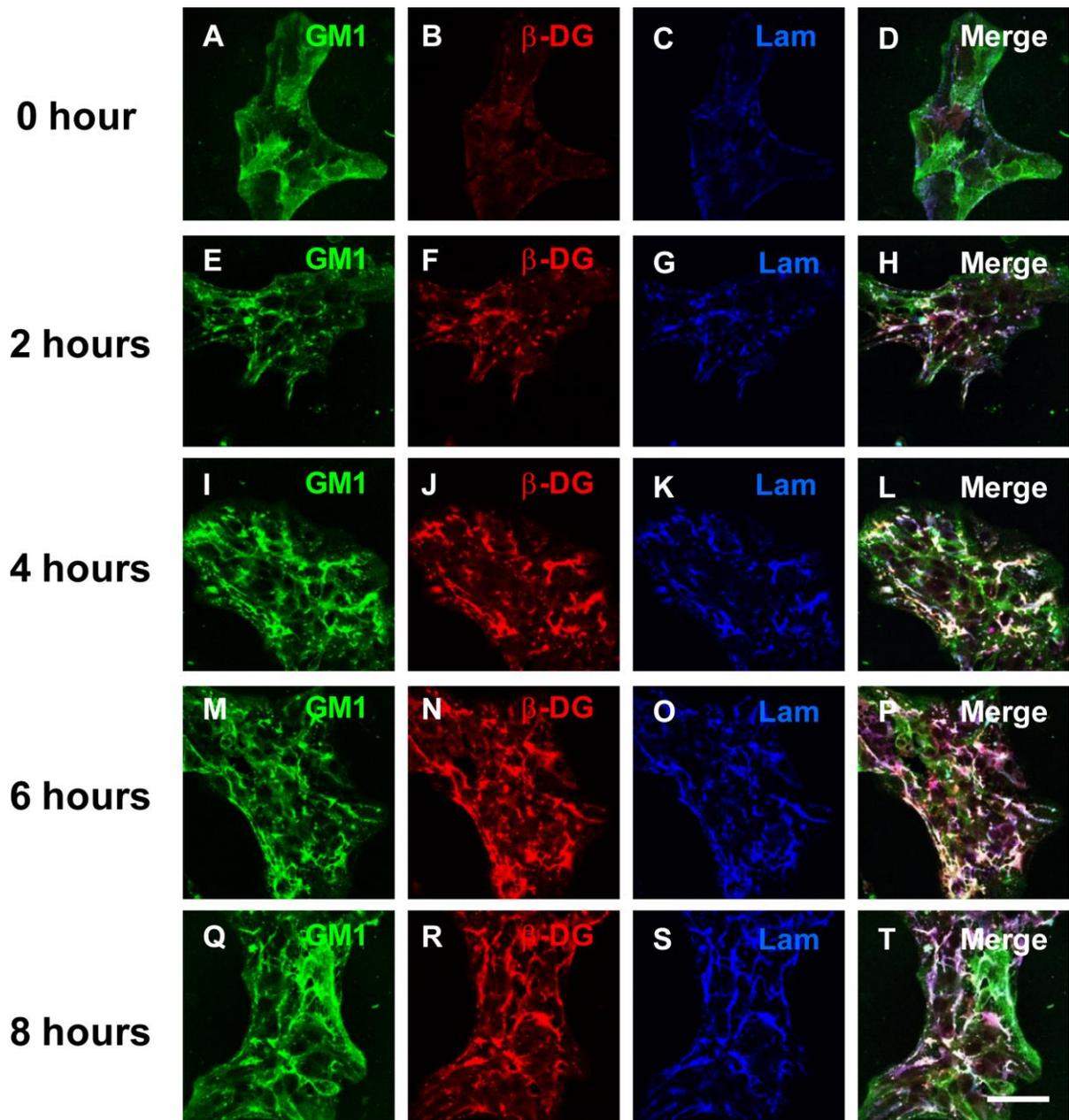
Appendix K: Supplemental Figure 5.1 Laminin-induced clustering of GM1 and β-DG is time-dependent. Rat hippocampal astrocytes incubated in the absence (**A-D**) or the presence of 15 nM laminin (**E-T**) were first labeled for GM1 using FITC-CtxB (**A, E, I, M** and **Q**) and then double immunolabeled for β-DG (**B, F, J, N** and **R**) and laminin (**C, G, K, O** and **S**). Scale bar, 30 μm.

Appendix L: Supplemental Figure 5.2 Laminin-induced increase in Pyk2 tyrosine phosphorylation is reduced by staurosporine, genistein and siPyk2 but is not involved in the laminin-induced clustering of AQP4. Astrocytes were incubated in the presence (+**LAM**) or in the absence (-**LAM**) of 15 nM laminin-1 for 3 hours. Protein extracts were immunobloted for phospho-Pyk2, Pyk2 and β-actin (**A**).. Astrocytes were incubated for 3 hours with 15 nM laminin1 alone (+**LAM**) or laminin plus 5 nM staurosporin (+**Stau**) or plus 0.5 μg/ml herbimycin (+**Herb**) or plus 50 μM genistein (+**Gen**). Protein extracts were immunobloted for phospho-Pyk2, β-DG, AQP4 and β-actin (**B**). Astrocytes were transfected with siCTL or siPyk2. Protein extracts were immunoblotted for phospho-Pyk2, Pyk2, FAK and β-actin (**C**). A representative blot from three independent experiments is shown (**A**, **B** and **C**). Quantitative analysis of the laminin-induced clustering of AQP4. The histograms represent the mean number of clusters ±SE and surface area of clusters ±SE in astrocyte cultures transfected with siCTL or siPyk2 and treated with laminin from three different experiments (**D**). All quantifications were performed on 15 fields acquired randomly from each experiment.

A.

B.

C.

D.
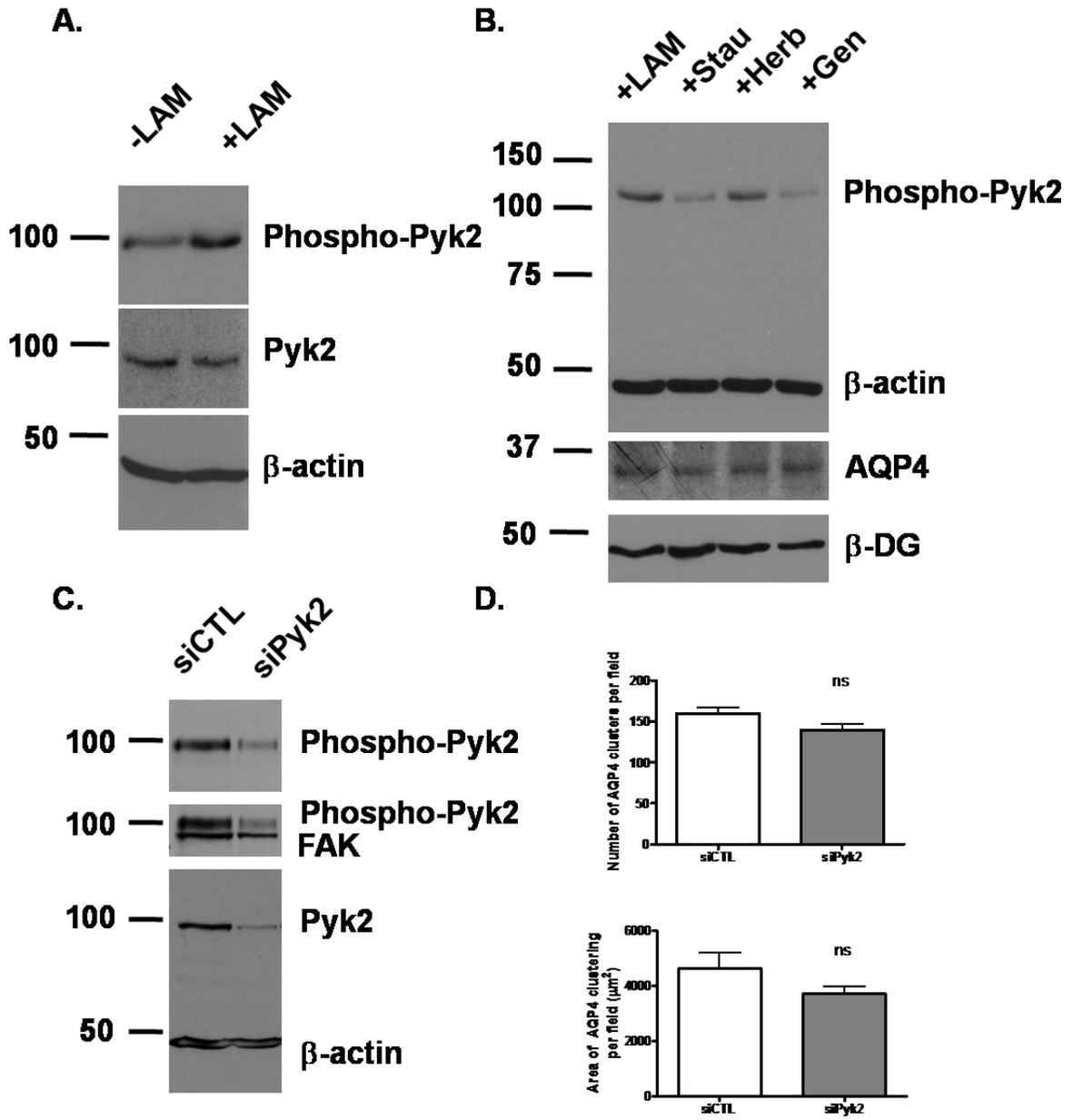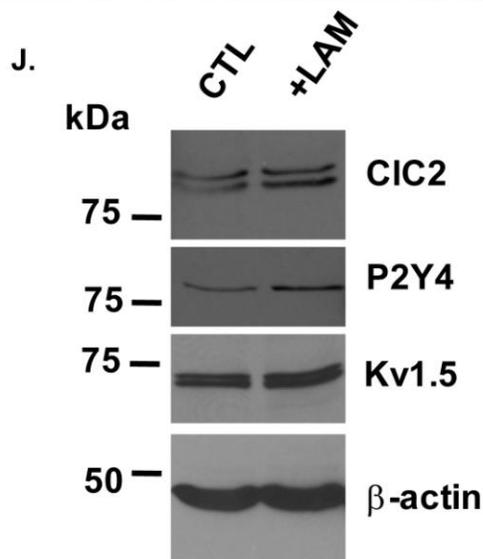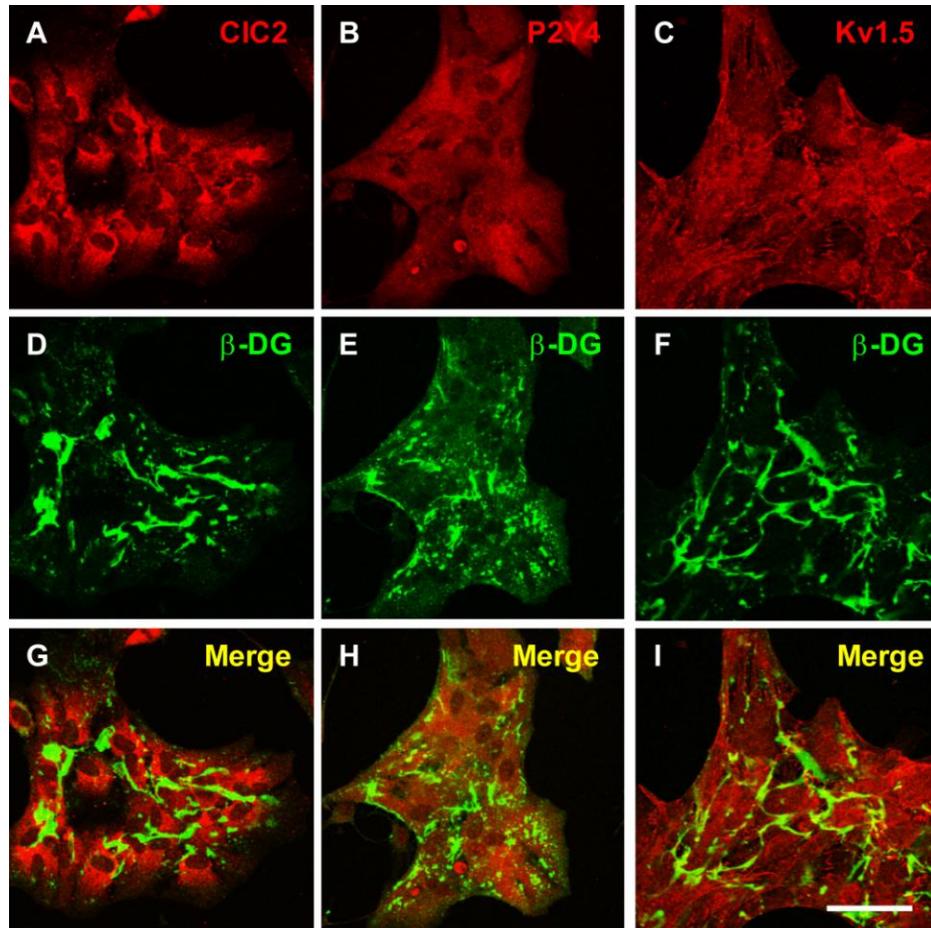
Appendix M. Distribution and expression of β-DG, ClC2, P2Y4 and Kv1.5 upon laminin treatment. Astrocytes incubated in the presence of 30 nM laminin were labeled for β-DG (**D**, ,**E**, and **F**) and ClC2 (**A**), P2Y4 (**B**) or Kv1.5 (**C**). Scale bar, 30 μm. (**J**) Western blot analysis of ClC2, P2Y4, Kv1.5 and β-actin was performed in laminin treated and untreated astrocytes.
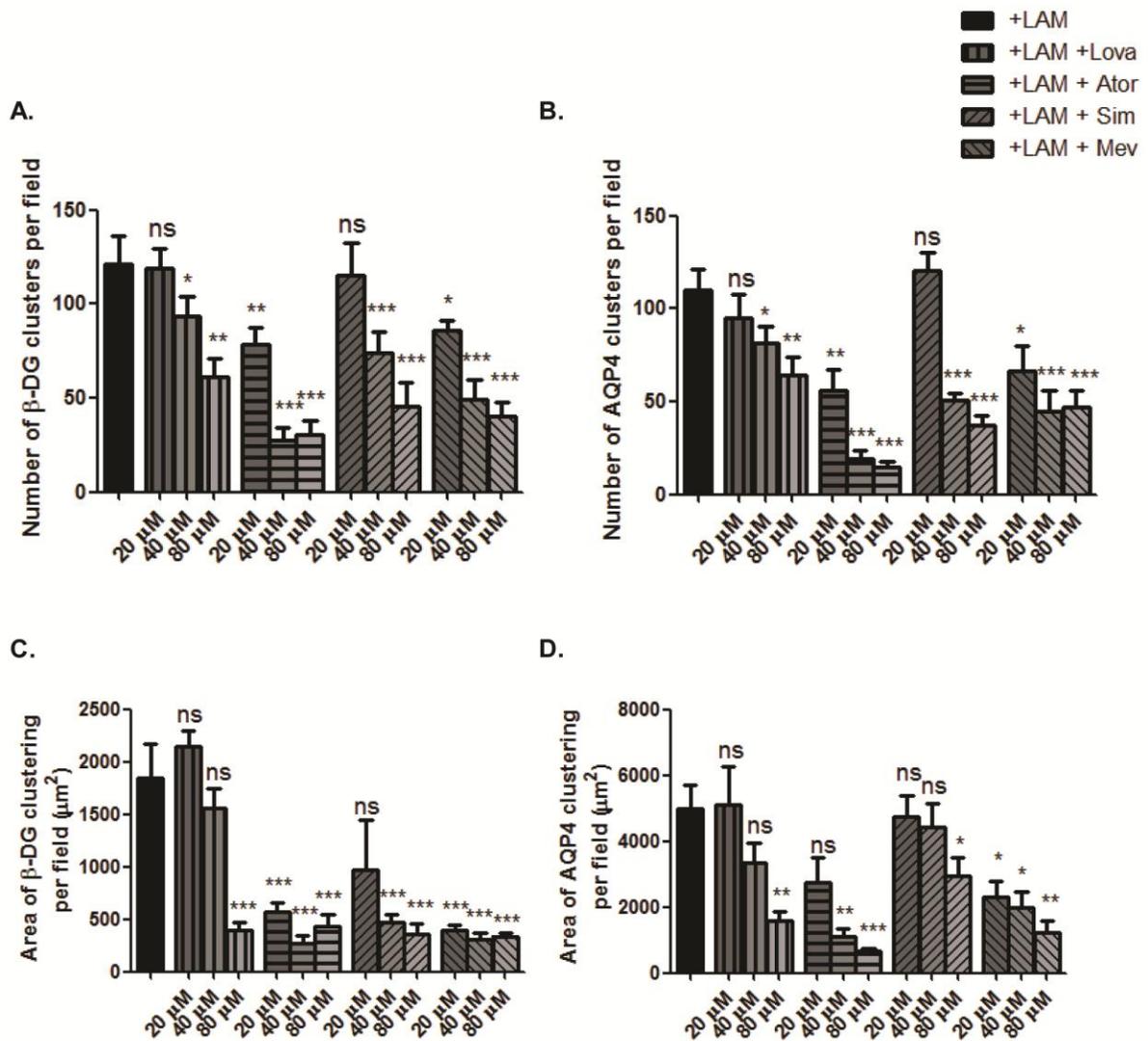
Appendix N. Quantitative analysis of the laminin-induced clustering of β-DG and AQP4 upon treatment with lovastatin, atorvastatin, simvastatin or mevastatin. The histograms represent the mean number of clusters ±S.E. (**A** and **B**) and surface area of clusters ±S.E. (**C** and **D**) of β-DG (**A** and **C**) and AQP4 (**B** and **D**) in astrocyte cultures treated with laminin alone (+LAM) or with laminin plus lovastatin (+LAM +Lova), plus atorvastatin (+LAM +Ator), plus simvastatin (+LAM +Sim) or mevastatin (+LAM +Mev) from three different experiments. The asterisks represent statistically significant differences from control (+LAM) as assessed by Student's t test (***p<0.0001; **p<0.001).

Number of peptides	Average ratio	Standart Deviation	Fold change	Description
1	22.551	0	22.551	Sfrs11 Splicing factor, arginine/serine-rich 11
3	13.693	7.67	13.693	Rbm39 RNA binding motif protein 39
1	11.691	0	11.691	Lrrc59 Leucine-rich repeat-containing protein 59
2	9.51	8.15	9.51	U2af2;LOC690372 similar to U2 (RNU2) isoform b
1	9.099	0	9.099	Pld3 Phospholipase D3
5	8.638	9.84	8.638	Gpnmb Transmembrane glycoprotein NMB
3	8.456	0.08	8.456	LOC682649 similar to Histone H2A type 1
2	7.243	5.31	7.243	Actn4 Alpha-actinin-4
2	7.107	7.71	7.107	Prpf38b Pre-mRNA-splicing factor 38B
7	7.067	1.84	7.067	Itih3 99 kDa protein
1	5.883	0	5.883	Tomm40 Mitochondrial import receptor subunit
2	5.032	0	5.032	RGD1565117 similar to 40S ribosomal protein S26
2	4.625	3.43	4.625	8 kDa protein
2	4.162	0.17	4.162	Gja1 Gap junction alpha-1 protein
1	3.629	0	3.629	Cct2 T-complex protein 1 subunit beta
2	3.338	3.1	3.338	Cct8 chaperonin subunit 8
2	3.327	0	3.327	Serpine2 Glia-derived nexin
1	3.113	0	3.113	Rps25 40S ribosomal protein S25
6	3.043	1.04	3.043	28 kDa protein
2	2.776	0	2.776	Fkbp11 Peptidyl-prolyl cis-trans isomerase
10	2.6915	2.24	2.6915	Ppap2b Lipid phosphate phosphohydrolase 3
6	2.663	1.27	2.663	Fn1 Isoform 1 of Fibronectin
1	2.658	0	2.658	Ctgf Connective tissue growth factor
3	2.588	0.38	2.588	Atp8a1 128 kDa protein
2	2.581	3.33	2.581	Abcb10 ATP-binding cassette, sub-family B
1	2.511	0	2.511	Cct3 T-complex protein 1 subunit gamma
3	2.297	1.78	2.297	Sfxn3 Sideroflexin-3
2	2.297	1.56	2.297	Siahbp1 Isoform 2 of Poly(U)-binding-splicing factor
2	2.24	0	2.24	Anpep Aminopeptidase N
9	2.206667	1.046667	2.206667	Vdac2 Voltage-dependent anion-selective channel
3	2.171	1.055	2.171	Slc25a3 Slc25a3 protein (Solute carrier family 25)
2	2.168	0.51	2.168	RGD1560475 Vesicle transport t-SNAREs homolog
2	2.166	0	2.166	Anxa6 Annexin A6
14	2.122333	0.98	2.122333	Vdac3 31 kDa protein
2	2.02	1.605	2.02	45 kDa protein

Appendix O. Quantitative analysis of the lipid raft proteome in astrocytes treated with laminin. Listed are the proteins with a minimum of two fold change in lipid rafts isolated from astrocytes treated with laminin compared to untreated astrocytes.

| Number of peptides	Average ratio	Standart Deviation	Fold change	Description
5	0.499	0.07	-2.00401	Ptk7 PTK7 protein tyrosine kinase 7
2	0.494	0.11	-2.02429	Zmpste24 zinc metallopeptidase, STE24 homolog
171	0.492	0.176667	-2.03252	Ahnak similar to AHNAK nucleoprotein isoform 1
3	0.483	0.65	-2.07039	Rpl23a 60S ribosomal protein L23a
2	0.471	0.1	-2.12314	Cox5b Cytochrome c oxidase subunit 5B
24	0.4685	0.11	-2.13447	Ptrf Polymerase I and transcript release factor
3	0.466	0.02	-2.14592	Gria2 Isoform Flip of Glutamate receptor 2
4	0.458	0.18	-2.18341	Pgrmc1 Membrane-associated progesterone receptor
2	0.44	0	-2.27273	H13 43 kDa protein
1	0.433	0	-2.30947	Dld Dihydrolipoyl dehydrogenase, mitochondrial
2	0.425	0.05	-2.35294	Ndufv2 NADH dehydrogenase flavoprotein 2
1	0.422	0	-2.36967	Armc10 armadillo repeat containing 10
4	0.421	0.09	-2.3753	Sec22b Vesicle-trafficking protein SEC22b
5	0.406	0.12	-2.46305	Vcp Transitional endoplasmic reticulum ATPase
2	0.406	0.08	-2.46305	Mtch2 mitochondrial carrier homolog 2
5	0.404	0.27	-2.47525	Atp6v0a1 95 kDa protein
5	0.403	0.12	-2.48139	Pgrmc2 Membrane-associated progesterone receptor
2	0.403	0	-2.48139	Slc1a4 Neutral amino acid transporter ASCT1
2	0.401	0.06	-2.49377	Ssr4 Translocon-associated protein subunit delta
3	0.398	0.06	-2.51256	Stt3a similar to Oligosaccharyl transferase STT3
2	0.396	0.1	-2.52525	Rpn2 Dolichyl-diphosphooligosaccharide
4	0.39	0.1	-2.5641	Rap1a Ras-related protein Rap-1A
1	0.389	0	-2.57069	Scfd1 Sec1 family domain-containing protein 1
1	0.388	0	-2.57732	RGD1564709 ATP-binding cassette, sub-family G
2	0.387	0	-2.58398	Ssr1 Translocon-associated protein subunit alpha
1	0.379	0	-2.63852	46 kDa protein
1	0.371	0	-2.69542	Tmem85 transmembrane protein 85
1	0.361	0	-2.77008	Ap2m1 AP-2 complex subunit mu-1
2	0.36	0.05	-2.77778	Ttc35 Tetratricopeptide repeat protein 35
2	0.358	0.05	-2.7933	Anxa5 Annexin A5
2	0.356	0.04	-2.80899	Atp1b1 Sodium/potassium-transporting ATPase
4	0.355	0.19	-2.8169	Rrbp1 similar to Ribosome-binding protein 1
1	0.353	0	-2.83286	Ndufa10l NADH dehydrogenase 1 alpha subcomplex
6	0.347	0.1	-2.88184	Fads2 Fatty acid desaturase 2
5	0.499	0.07	-2.00401	Ptk7 PTK7 protein tyrosine kinase 7
1	0.343	0	-2.91545	LOC681252 similar to Myristoylated alanine
2	0.339	0	-2.94985	Rpsa 40S ribosomal protein SA
5	0.333	0.11	-3.003	Cp GPI-anchored ceruloplasmin
2	0.326	0.09	-3.06748	Sdha Succinate dehydrogenase flavoprotein subunit
1	0.325	0	-3.07692	Cdk5rap3 CDK5 regulatory subunit-associated protein

| Number of peptides	Average ratio	Standart Deviation	Fold change	Description
2	0.325	0.05	-3.07692	Slc25a4 ADP/ATP translocase 1
3	0.324	0.16	-3.08642	Dlat Dihydrolipoyllysine-residue
1	0.309	0	-3.23625	17 kDa protein
1	0.303	0	-3.30033	Ndufb6 NADH dehydrogenase 1 beta
1	0.303	0	-3.30033	Vcp 89 kDa protein
2	0.296	0	-3.37838	Cox7a2;Cytochrome c oxidase polypeptide 7A2
2	0.27	0.01	-3.7037	Vapa Vesicle-associated membrane protein
5	0.269	0.06	-3.71747	Bcap31 B-cell receptor-associated protein 31
5	0.267	0.1	-3.74532	Uqcrc2 Cytochrome b-c1 complex subunit 2
3	0.262	0.01	-3.81679	Ogdh 2-oxoglutarate dehydrogenase E1 component
6	0.26	0.11	-3.84615	Nnt Nicotinamide nucleotide transhydrogenase
2	0.2555	0	-3.91389	Ndufb4 NADH dehydrogenase 1 beta subcomplex 4
1	0.251	0	-3.98406	LOC681418;LOC681867 hypothetical protein LOC681418
4	0.25	0.02	-4	Dlst Dihydrolipoyllysine-residue succinyltransferase component of 2-oxoglutarate dehydrogenase complex, mitochondrial
2	0.249	0	-4.01606	Ktn1 55 kDa protein
2	0.245	0.05	-4.08163	mt-Co2;mt-Co3 Cytochrome c oxidase subunit 2
2	0.244	0.02	-4.09836	Lrpprc Leucine-rich PPR motif-containing protein
17	0.2395	0.095	-4.17537	Ckap4 cytoskeleton-associated protein 4
3	0.239	0.05	-4.1841	55 kDa protein
1	0.234	0	-4.2735	Slc25a1 Tricarboxylate transport protein
1	0.233	0	-4.29185	RGD1309846 similar to Charged multivesicular body
2	0.223	0.12	-4.4843	Clta Isoform Non-brain of Clathrin light chain A
1	0.218	0	-4.58716	Rpl14 60S ribosomal protein L14
1	0.217	0	-4.60829	Degs1 Sphingolipid delta(4)-desaturase DES1
3	0.215	0.04	-4.65116	Rpl10a 60S ribosomal protein L10a
2	0.21	0	-4.7619	RGD1565438 similar to ATP synthase, H+ transporting
1	0.208	0	-4.80769	Ndufs3 NADH dehydrogenase Fe-S protein 3
2	0.207	0.16	-4.83092	Marcksl1 MARCKS-related protein
1	0.205	0	-4.87805	Wfs1 WFS1
2	0.179	0	-5.58659	Ptdss2 Phosphatidylserine synthase 2
1	0.17	0	-5.88235	17 kDa protein
2	0.16	0	-6.25	Usmg5 Up-regulated during skeletal muscle growth
1	0.159	0	-6.28931	Hspg2 396 kDa protein
1	0.148	0	-6.75676	Ndufa7 Ndufa7 protein
1	0.131	0	-7.63359	Ndufa9 similar to NADH dehydrogenase 1 alpha
2	0.116	0	-8.62069	Atp5o ATP synthase subunit O, mitochondrial
2	0.087	0.06	-11.4943	RGD1307736 protein KIAA0152 homolog
1	0.05	0	-20	Flnb filamin, beta
2	0.047	0	-21.2766	Rps3a 40S ribosomal protein S3a
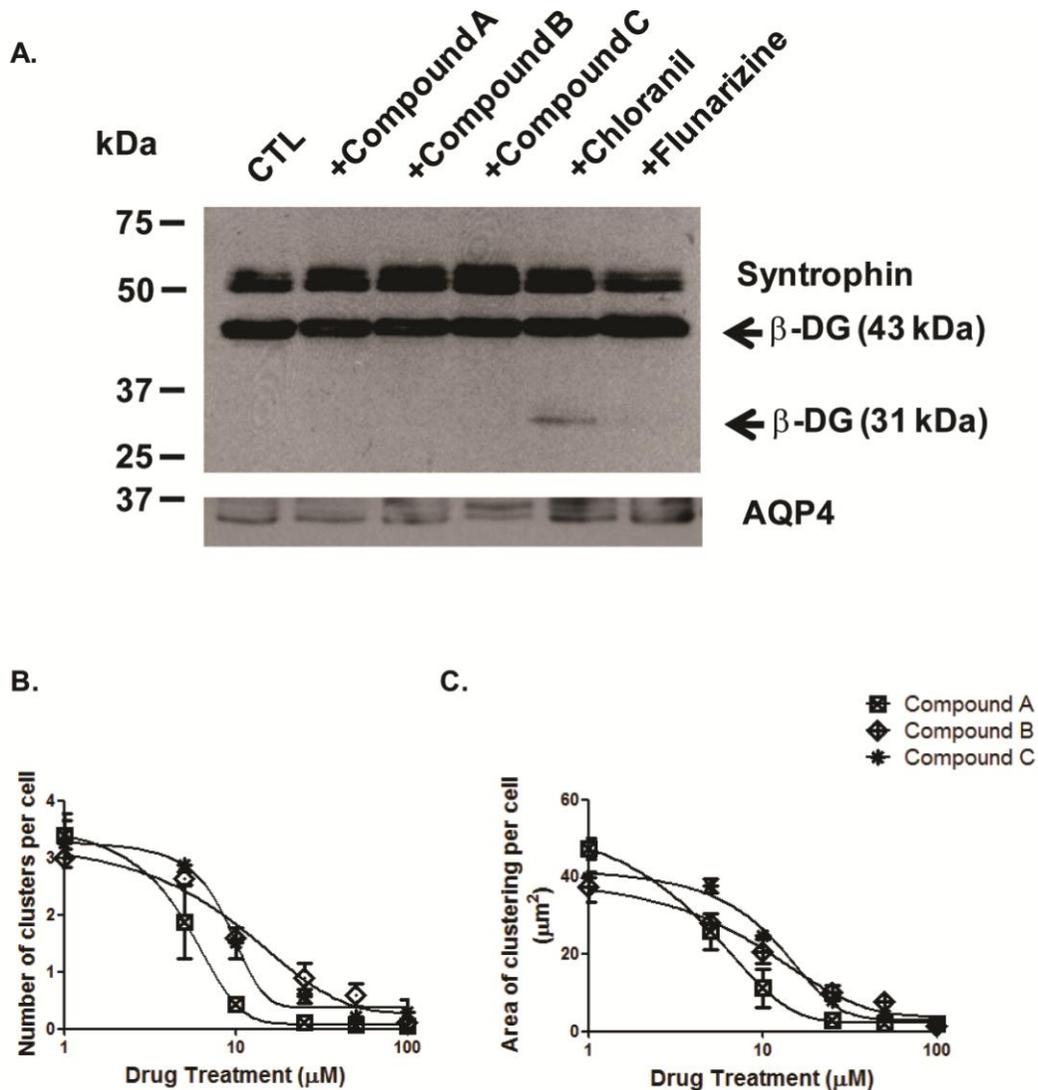
Appendix P. AQP4, β-DG and syntrophin expression as well as β-DG clustering in cells treated with the 3 different compounds A, B and C, chloranil or flunarizine. A. Primary astrocytes were incubated for 4 h with 15 μM of active chemicals. Extracted proteins were loaded (30 μg/lane) and analyzed for β-DG, syntrophin and AQP4 expression levels by western blot analysis. Note the 31 kDa band under the 43 kDa band corresponding to the cleaved form of β-DG upon chloranil treatment. **B, C.** Dose-response curve of laminin-induced β-DG clustering in astrocytes treated with increasing concentrations of compounds A, B and C (2.5 to 100 μM). Clustered staining was automatically quantified using the Cellomics ArrayScan V[TI] HCS Reader.
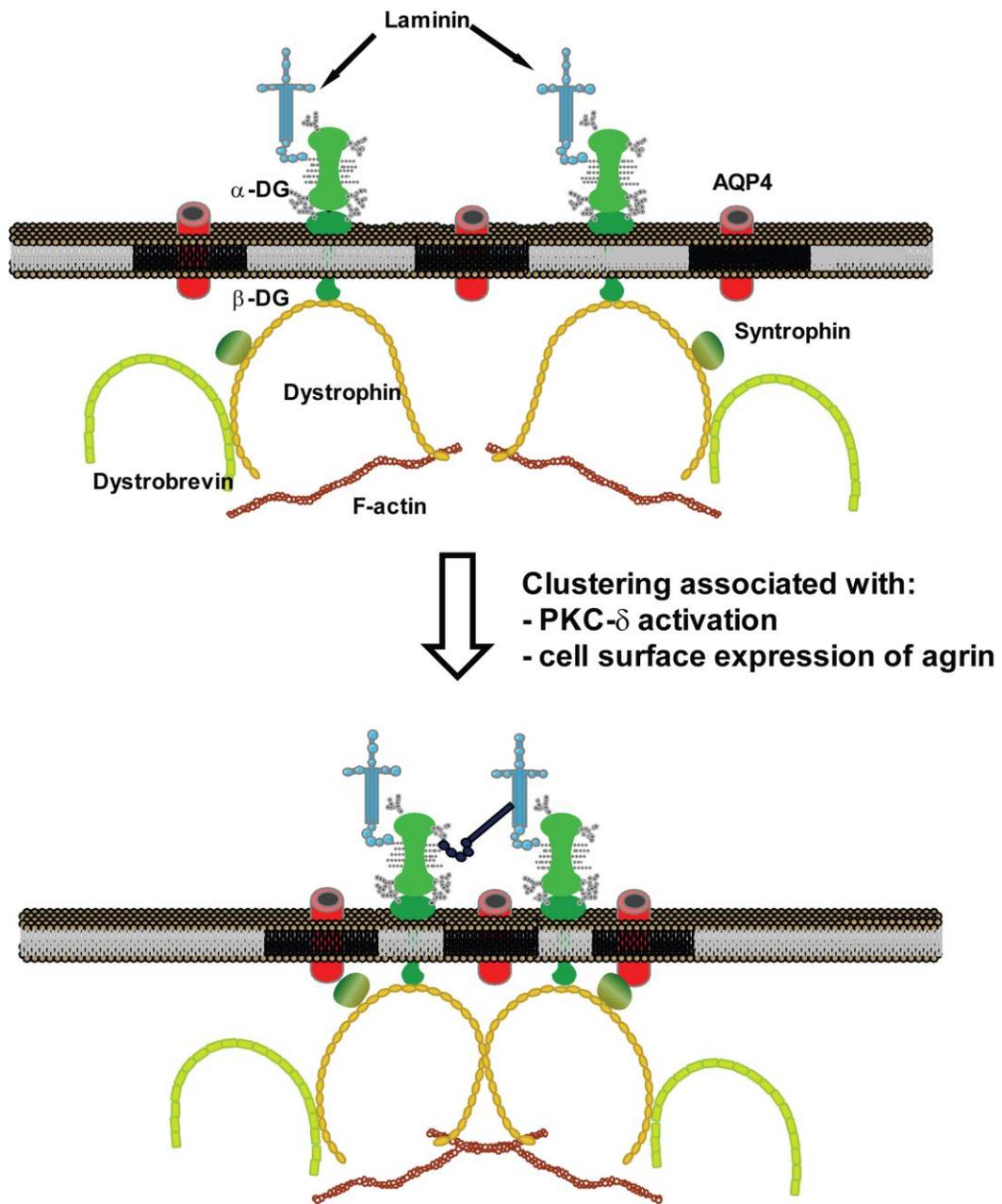
Appendix Q. Schematic representation of the molecular interactions within the DAP complex, the ECM, AQP4 and lipid rafts at the astrocyte cell surface during laminin treatment. Upon laminin treatment, the DAP complex, laminin, AQP4 and lipid rafts cocluster through a PKC-δ-dependent mechanism. In addition, an increased cell surface expression of agrin with a subsequent coenrichment within those clusters is crucial for the clustering.
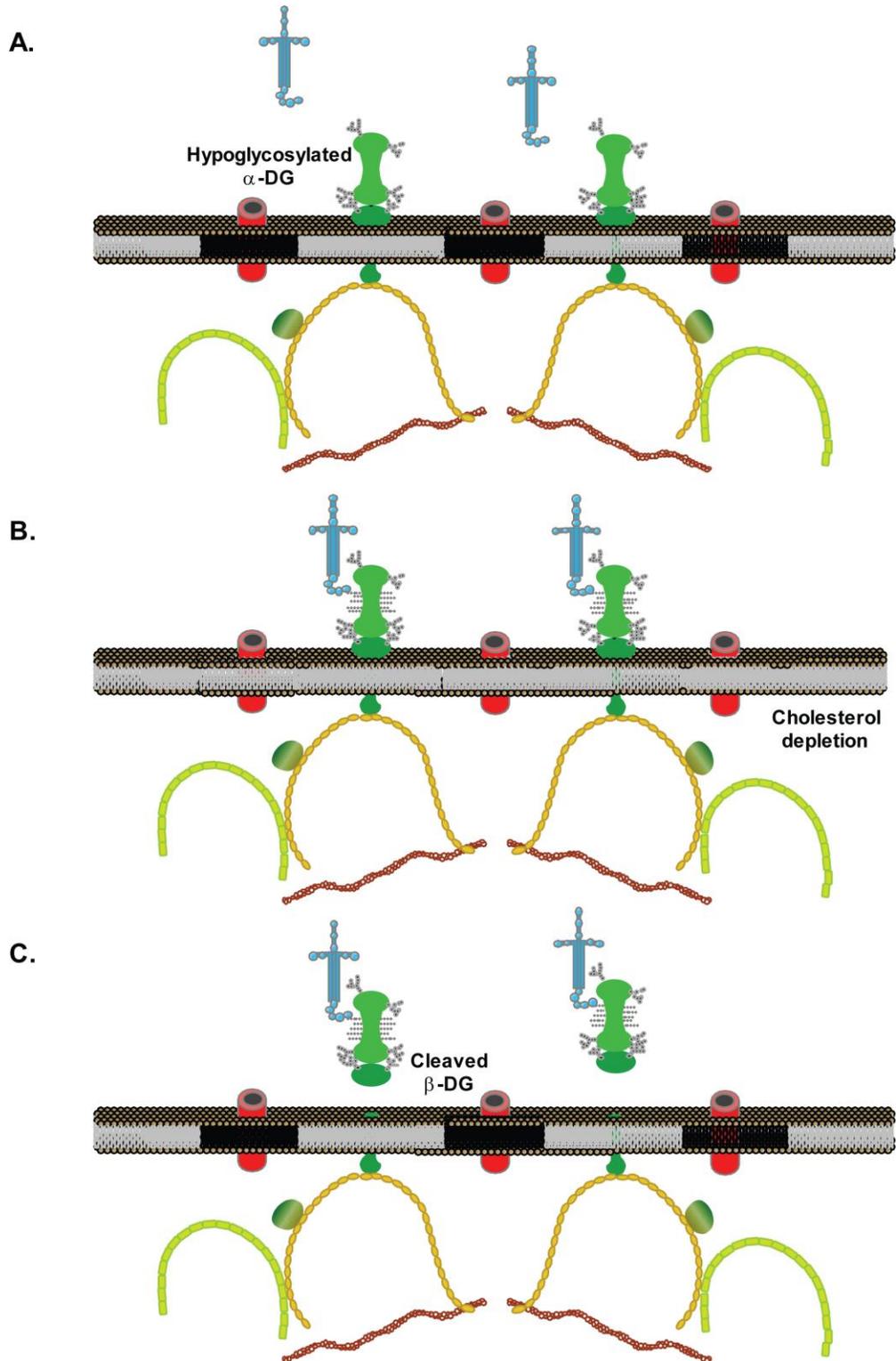
Appendix R. Schematic representations for the disruption of the laminin-dependent AQP4 distribution following α-DG hypoglycosylation (A), lipid rafts disruption (B) or β-DG shedding (C).

ANIMAL CARE CERTIFICATE

Application Number: A06-0319

Investigator or Course Director: Hakima Moukhles

Department: Cellular & Physiological Sc.

Animals:

| Rats Sprague Dawley 480 |
| Mice C57BL6 120 |

Start Date: April 15, 2007   **Approval Date:**   March 27, 2009

Funding Sources:

Funding Agency:	Muscular Dystrophy Association of Canada
Funding Title:	Dystroglycan function in glial cells
Funding Agency:	Amyotrophic Lateral Sclerosis Society of Canada
Funding Title:	Dystroglycan function in glial cells
Funding Agency:	Canadian Institutes of Health Research (CIHR)
Funding Title:	Dystroglycan function in glial cells

Unfunded title: N/A

The Animal Care Committee has examined and approved the use of animals for the above experimental project.

This certificate is valid for one year from the above start or approval date (whichever is later) provided there is no change in the experimental procedures. Annual review is required by the CCAC and some granting agencies.

A copy of this certificate must be displayed in your animal facility.

Appendix S. Animal care certificate